AD-756 854

# AERODYNAMIC STABILITY AND CONTROL, DATA, MODEL 844-2035

Boeing Company
Seattle, Washington

14 February 1972

[redacted]

BOEING AIRPLANE COMPANY

SEATTLE 24, WASHINGTON

AD735684

Details of illustrations in this document may be better studied on microfiche.

DOCUMENT NO. D2-8174

UNCLASSIFIED TITLE Aerodynamic Stability and Control Data, Model 844-2035

MODEL NO. ______ CONTRACT NO. AF 33(600)-41517

ISSUE NO. 17 ISSUED TO

CLASSIFIED TITLE ______
(STATE CLASSIFICATION)

PRELIMINARY INFORMATION

WORK ORDER NO. UNIT NO. ITEM NO.

SPECIAL ... ON ASTIA DISTRIBUTION





"Approved for public release; distribution unlimited"



PREPARED BY Flight Controls Group

SUPERVISED BY A. H. Lee 2-27-61

APPROVED BY L. E. Mason 2-28-61

CLASS. & DISTR. APPROVED BY J. S. Lesko (DATE)

NO. OF PAGES 164 (EXCLUDING TITLE AND REVISION AND ADDITION PAGES.)



[redacted]

DOCUMENT TITLE PAGE

## TABLE OF CONTENTS

TABLE OF CONTENTS - Cont'd

Page

## FIGURE INDEX

## FIGURE INDEX

## 6.1 LA[illegible] - DI[illegible] [illegible]

6.2 AILERON CHARACTERISTICS AND EFFECTIVENESS

## 6.3 RUDDER CHARACTERISTICS AND EFFECTIVENESS

## 6.4 ROLL AND YAW ROTARY DERIVATIVES

## FIGURE INDEX

## FORWARD

The glider configuration represented by the stability and control characteristics presented in this document is not current. Information derived from analysis and wind-tunnel tests as the document was being completed indicated the need for some configuration changes. However, the document is released for distribution to update the information being used by various agencies for stability and control analysis.

The most significant change to the configuration in a stability and control sense is a change in the incidence angle of the folding wing tip extensions. The tip extensions in the document are set at an incidence of -15° degrees relative to a water line. Currently, the tip extensions are considered at an incidence of zero degrees. This change principally affects the zero lift pitching moment with relatively little affect on longitudinal stability. However, it does affect the directional stability at transonic speeds favorably. With this change in tip incidence, the speed for tip extension must also be altered. Currently, tip extensions are considered retracted at speeds higher than Mach 1.2.

Other changes are being considered to correct some stability and control deficiencies evident in the document. The effects of these changes will be distributed in a revision of this document when they are available.

## ACKNOWLEDGEMENT

The following people contributed to the preparation of this document:

R. J. Montgomery
G. K. Dragseth
D. C. Leisy
M. A. Carter
J. L. Francis
P. M. Jacobsen
E. J. Hamilton
P. M. McGinnese
R. W. Meinke
D. E. Phillips
W. S. Cox
B. F. Ray
P. T. Victor
J. W. Ball
W. J. Moore
K. A. Noess
R. T. Barth
G. O. Mount
E. A. Piper
D. J. Rossini
L. A. Bodin
K. T. Underwood
R. K. Rice

1.0 INTRODUCTION

The aerodynamic stability and control characteristics of the 844-2035 Dyna Soar glider are presented in the following sections of this document. Data are presented for the glider and for the glider plus third stage.

These data are based on wind tunnel tests, where data are available. Where not available, theoretical estimates have been made for the vehicle characteristics.

This is the interim glider configuration. Some vehicle characteristics peculiar to this configuration are not satisfactory and will be modified for the final configuration. The wing tip extension configuration is subject to change. A good speed brake location is still to be defined. The vertical tail and rudder size may increase. The elevon configuration may change. The possibility of asymmetric deflection of the elevon for roll control to reduce couplings is being considered.

The data presented will be revised as additional wind tunnel data are received and better estimates of the vehicle characteristics are made.

Information presented in the document is estimated for an obsolete configuration, Model 844-2035. The document is being released to up-date data now in the possession of the customer and associates.

## 2.0 REFERENCES


Reference a BAC D2-6909-1 "Interim System Description of the Dyna Soar Step I", R. L. Campbell, November 29, 1960.

Reference b C119-ER-10440 "Dyna Soar I Configuration Evaluation Wind Tunnel Test Report Series II", Bell Aircraft Corporation, May 1959.

Reference c NACA TN 2409 "Summary of Methods for Calculating Dynamic Lateral Stability and Response and for Estimating Lateral Stability Derivatives", Campbell and Mc Kinney, July 1951.

Reference d NASA TM X - 287 "Theoretical Stability Derivatives for the X-15 Research Airplane at Supersonic and Hypersonic Speeds Including a Comparison with Wind Tunnel Results, Walker and Wolowicz, August 1960.

## 3.0 CONFIGURATION

3.1 The general arrangement of the 844-2035 configuration is shown on Figure 3.1.1. The configuration is shown in the manufactured shape (referred to as the "cold" shape).

A heat shield is shown covering the pilots wind shield. This is separated from the glider at supersonic speeds. The drag brake, shown on top the body, is actuated at subsonic and low supersonic speeds, only. The wing tip extensions, located on the vertical tails, are extended at supersonic speeds. The rudders are deflected outboard only.

The elevons are split in two panels. This was done to reduce the sensitivity of the elevons for roll control at transonic and supersonic speeds and at high dynamic pressures when the elevons have high effectiveness. In these flight conditions, roll commands are transmitted to the inboard panels only. If a continuous signal is required by the adaptive feature of the flight control system, it will be transmitted to the inboard panel only to conserve A.P.U. fuel.

The inboard elevon panel is shown to have a wedged section to eliminate possible "dead" zones in elevon effectiveness at small deflections at hypersonic speeds. This wedging is probably unnecessary. The elevon section of the inboard panel has been considered modified to the same as that outboard panel for the data in this document.

Elevon actuator housings, not shown on the drawing, are located on the upper wing surface. These are positioned at approximately midspan of the two elevon panels and extend forward of the elevon hinge line. Actuators for the rudders are located in the bottom section of the vertical tail.

A more complete configuration is presented in Reference 2.

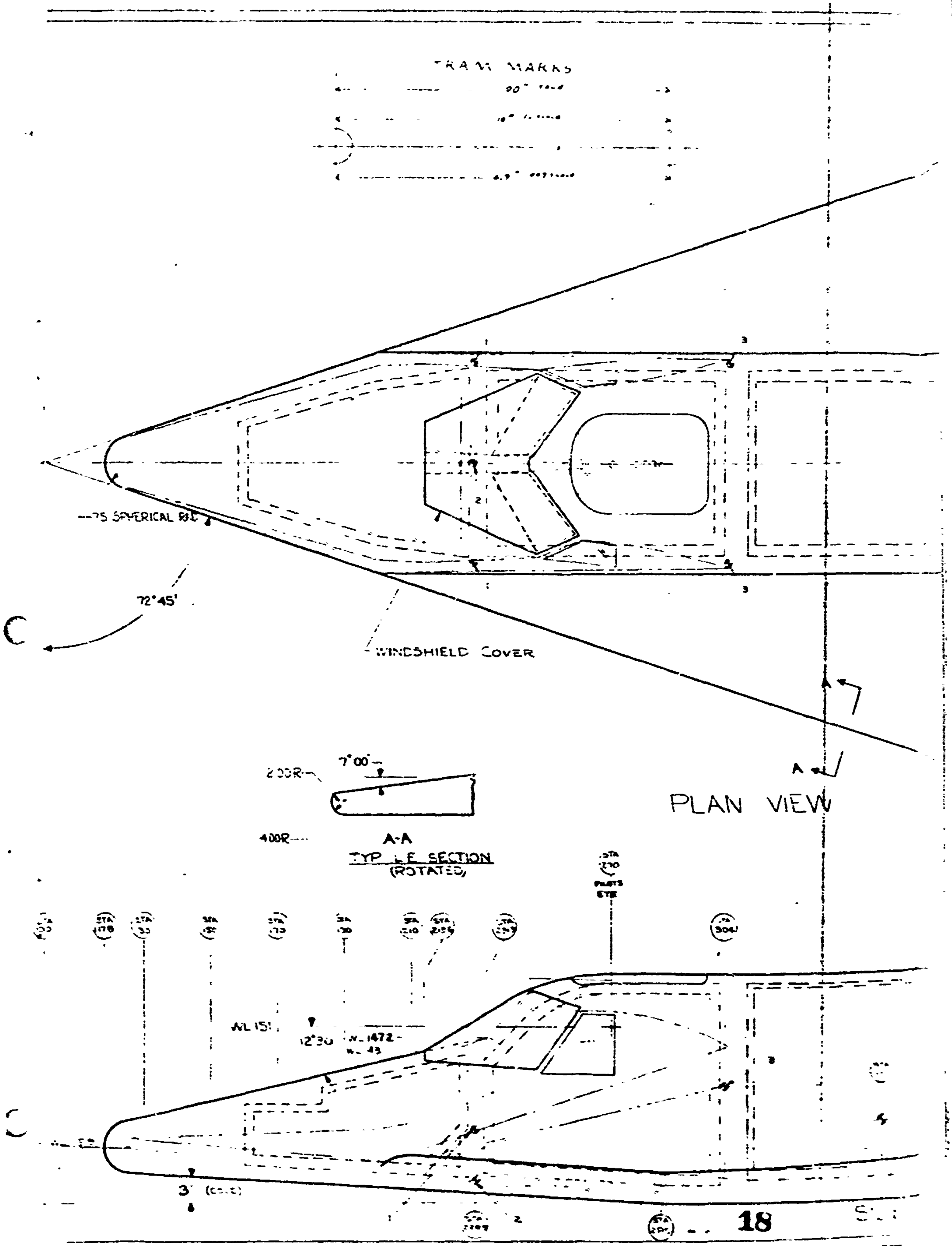
TRAM MARKS
WINDSHIELD COVER
72°45'
PLAN VIEW
7°00'
400R
A-A
TYP L.E. SECTION
(ROTATED)
PILOTS EYE
WL 151
12°30'
WL 147.2

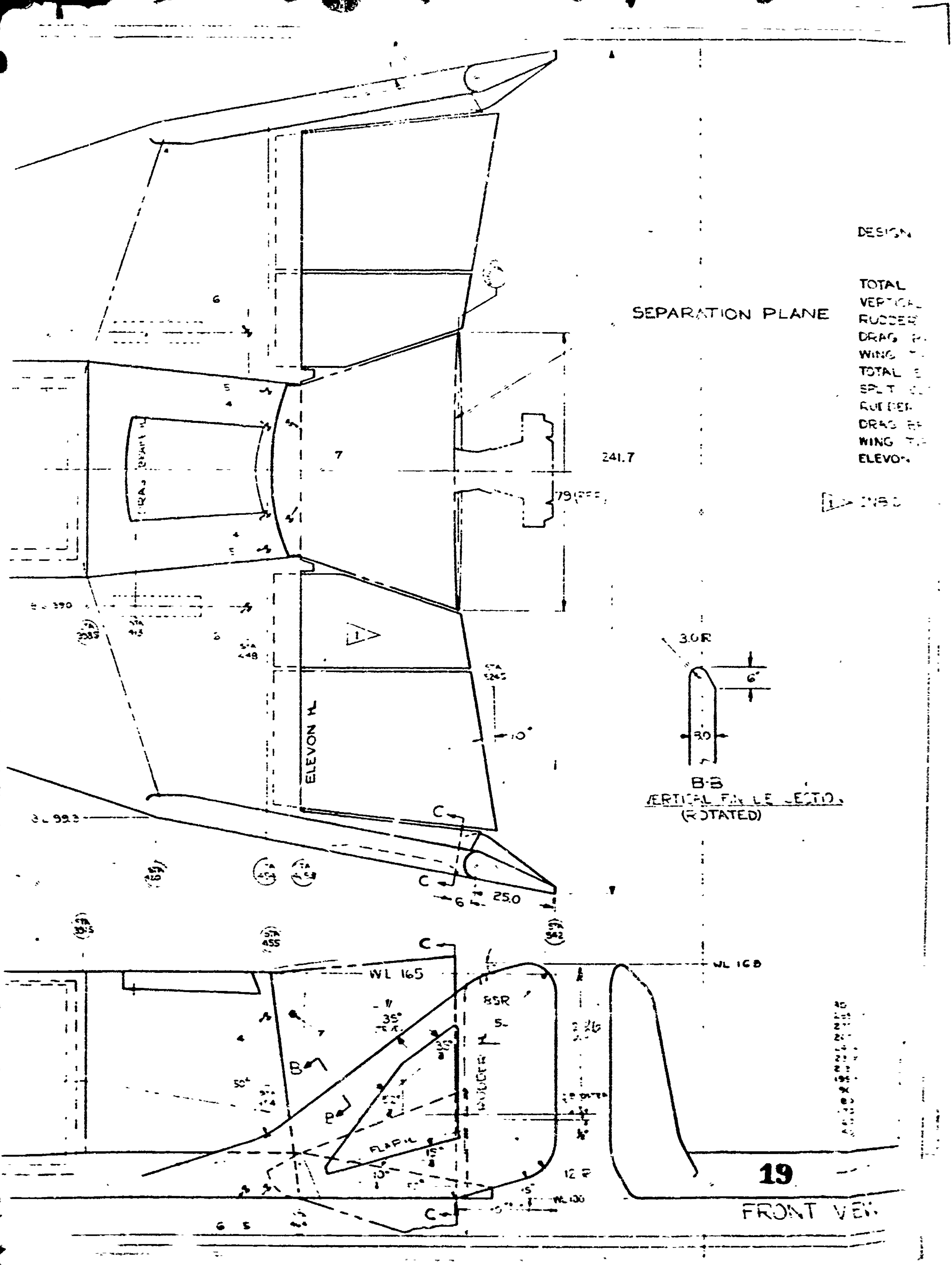

SEPARATION PLANE
DESIGN
TOTAL
ELEVON
241.7
79 (REF)
ELEVON
DRAG
3.0R
6"
3.0
B-B
(ROTATED)
WL 165
WL 168
RUDDER
FLAP
35°
15°
25.0
C
B

DESIGN LAUNCH GROSS WEIGHT — — — — — — 9600 LBS.

TOTAL LIFTING SURFACE AREA — — — — — — 343 SQ FT
VERTICAL FIN SURFACE AREA — — — — — — 3.0 SQ FT
RUDDER SURFACE AREA — — — — — — — 10.6 SQ FT
DRAG BRAKE AREA — — — — — — — 15 SQ FT
WING TIP EXTENSION AREA (TOTAL) — — — — — 11 SQ FT
TOTAL ELEVON SURFACE AREA — — — — — — 48.0 SQ FT
SPLIT ELEVON SURFACE AREA (TOTAL) — — — — 16.0 SQ FT
RUDDER ANGULAR MOVEMENT — — — — — — 25 OUTBD
DRAG BRAKE ANGULAR MOVEMENT — — — — — — 60°
WING TIP EXTENSION ANGULAR MOVEMENT — — — 90°
ELEVON ANGULAR MOVEMENT — — — — — 55° UP
22° DOWN

INBD SECTION OF ELEVON FIXED SPLIT ANGLE 20°

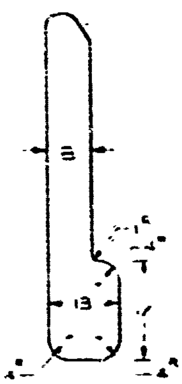

C-C

HOIST AND HANDLING POINTS

| CONDITION | ATTACHMENT POINTS |
|---|---|
| AIR TRANSPORT | 2 AND 4 |
| AIR LAUNCH | [illegible] AND 7, 3 AND 4 |
| SLING | [illegible] 4, AND 5 [illegible] AND 7 |
| DOLLY | 2 AND 4 |
| TRAILER | 2 AND 3 |
| [illegible] ATTACH | 4 AND 5 |
| [illegible] | 2 AND 3 |

[illegible] ADAPTER LIFTING PYLON

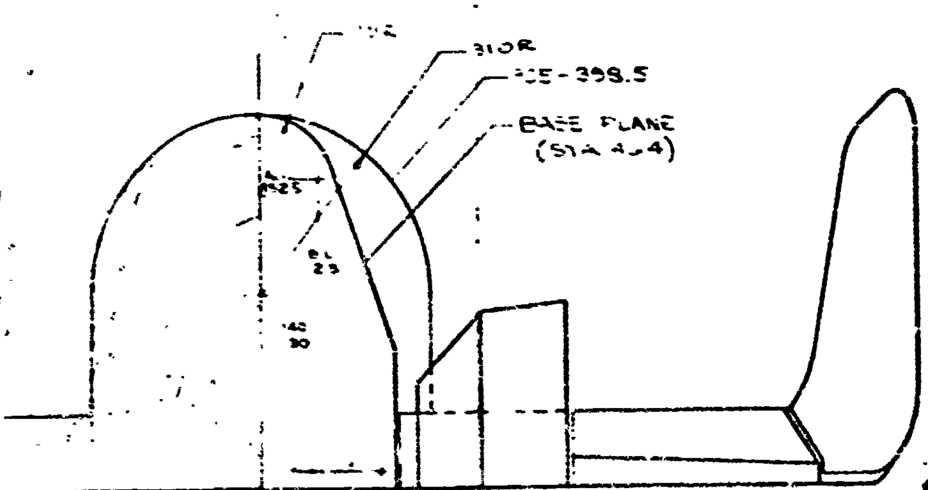

REAR VIEW

FIG 3.1.1
GENERAL ARRANGEMENT DYNA SOAR
MODEL 844-2035
DZ-8174

## 3.2 WEIGHTS AND MOMENTS OF INERTIA

The design weights and moments of inertia for the glider vehicle are presented below.

For the glider alone (transition section off):

Weight = 9600 lbs.

Principal Moments of Inertia about C.G.:

$I_y = 18{,}600$ slugs - ft$^2$ (pitch)

$I_x = 4{,}000$ slugs - ft$^2$ (roll)

$I_z = 21{,}000$ slugs - ft$^2$ (yaw)

The x principal axis is assumed parallel to glider water lines.

For the 9600 lb. glider plus the third stage, Figure 3.2.1 gives the moments of inertia during third stage burning, and the weights and the center of gravity locations at beginning and end of third stage burning.

The center of gravity location for the glider alone is shown on Figure 3.3.3 .

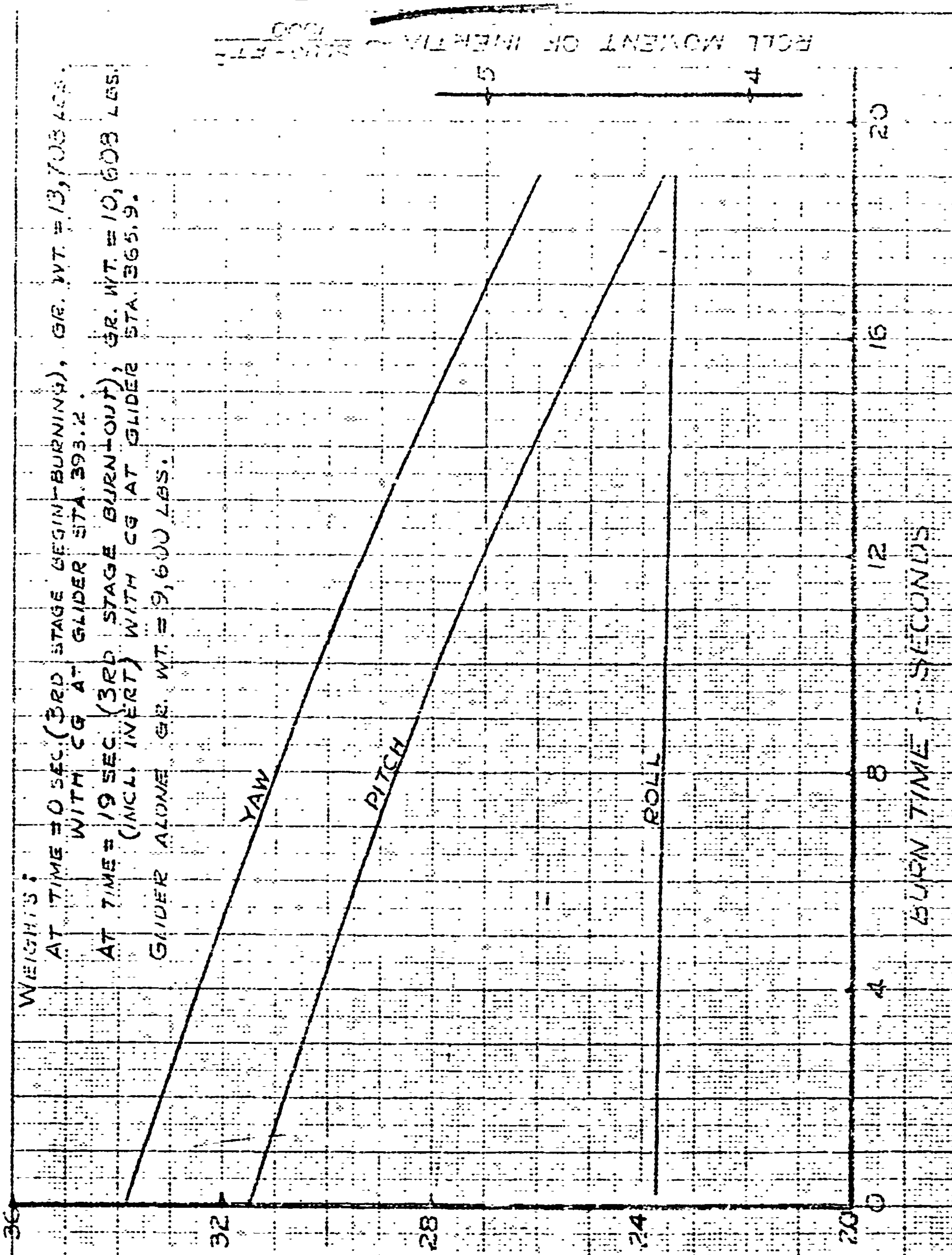


Fig 3.4

| | | |
|---|---|---|
| C.W. CANNON 12-21 ✓ 12-23 | MASS DATA FOR 9600 LB GLIDER AND THIRD STAGE | 844-2035 |
| REDRAWN M.A.C 12-23 | | D2-3174 |
| | BOEING AIRPLANE COMPANY | PAGE 3.4 |

## 3.3 AERODYNAMIC DATA AND REFERENCE CONSTANTS

Aerodynamic data in the document are presented on a fixed body axis system. The axis system is shown on Figure 3.3.1. Definition of angle of attack and sideslip and the sign convention for the force and moment coefficients are also shown. The sign conventions for control deflections are shown on Figure 3.3.2.

Reference constants and glider alone center of gravity location are shown on Figure 3.3.3. Some significant aerodynamic configuration constants are also presented.

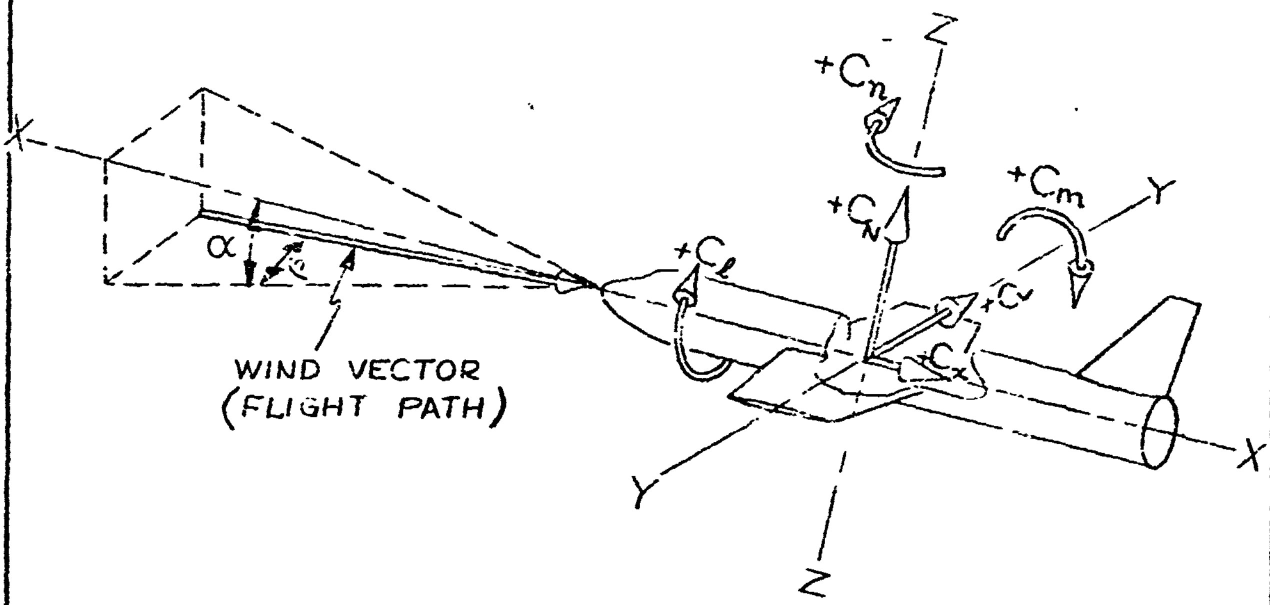


NOTES:

1.) THE MUTUALLY PERPENDICULAR X, Y, AND Z AXES ARE FIXED ON THE AIRPLANE, REGARDLESS OF FLIGHT ATTITUDE.

2.) ANGLE OF ATTACK IS MEASURED IN THE AIRPLANE PLANE OF SYMMETRY (X-Z PLANE), BETWEEN THE AIRPLANE X-AXIS AND THE PROJECTION OF THE WIND VECTOR INTO THE X-Z PLANE.

3.) ANGLE OF SIDESLIP IS MEASURED IN OR PARALLEL TO THE PLANE DEFINED BY THE AIRPLANE Y-AXIS AND THE WIND VECTOR, BETWEEN THE WIND VECTOR AND THE PROJECTION OF THE AIRPLANE X-AXIS INTO THE ABOVE-DEFINED PLANE.

4.) FOR THE DYNA SOAR 844-2035 CONFIGURATION, THE X-Y PLANE IS PARALLEL TO THE FLAT, AFT PART OF THE WING UNDERSURFACE.

FIG. 3.3.1

| CALC | | REVISED | DATE | BODY AXIS SYSTEM NOMENCLATURE ~ COMBINED ANGLE OF ATTACK & SIDESLIP | 844-2035 |
|---|---|---|---|---|---|
| CHECK | | | | | D2-8174 |
| APR | | | | BOEING AIRPLANE COMPANY | PAGE 3.6 |
| APR | | | | | |
| DWN. M. CARTER 12-23-0 | | | | | |

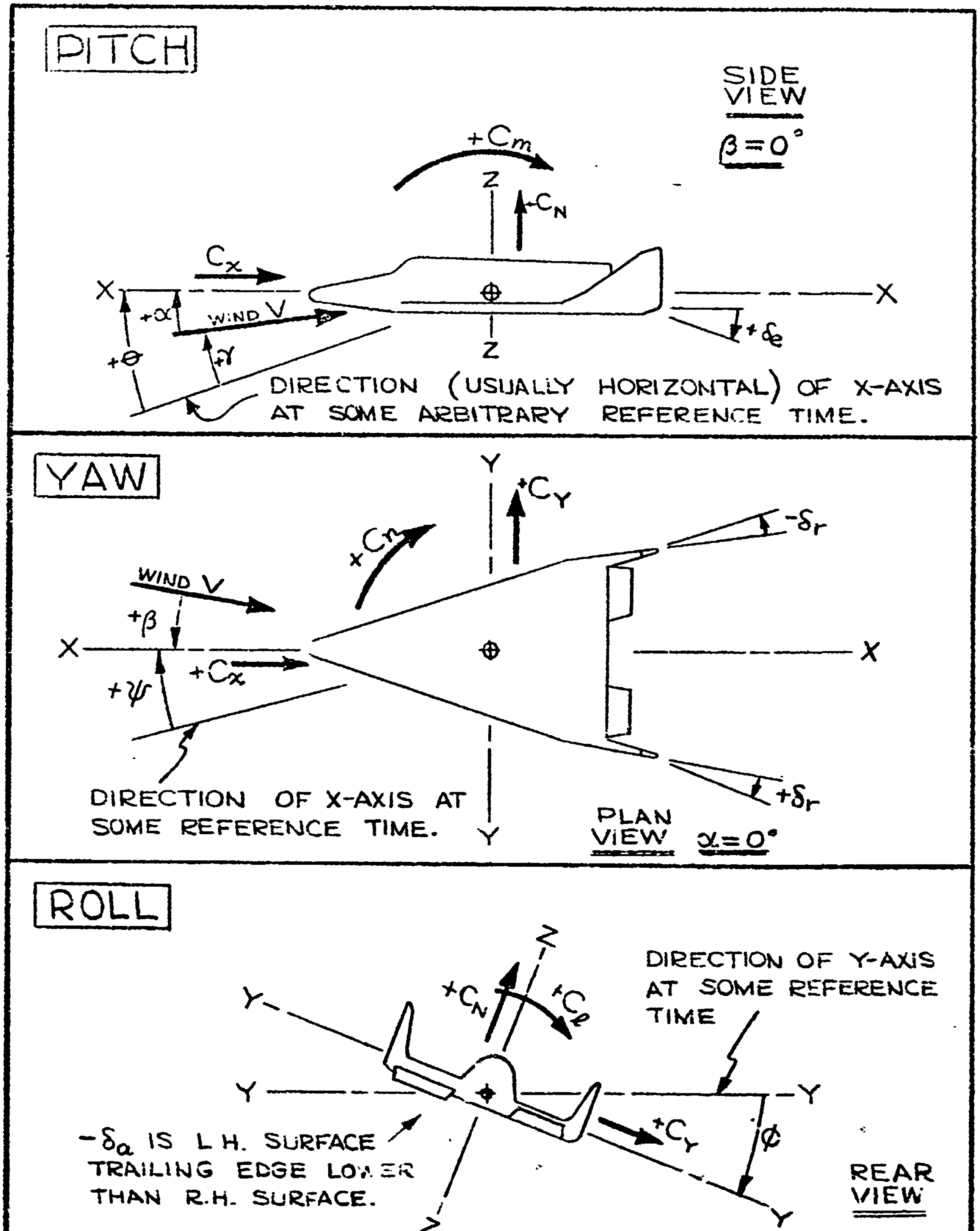


FIG. 3.3.2

| CALC | | REVISED | DATE | BODY AXIS SYSTEM ~ NOMENCLATURE | 844-2035 |
|---|---|---|---|---|---|
| CHECK | | | | | D2-8174 |
| APP | | | | | |
| APP | | | | BOEING AIRPLANE COMPANY 25 | PAGE 3.7 |
| DWN M. CARTER 12-27-60. | | | | | |

2-7000

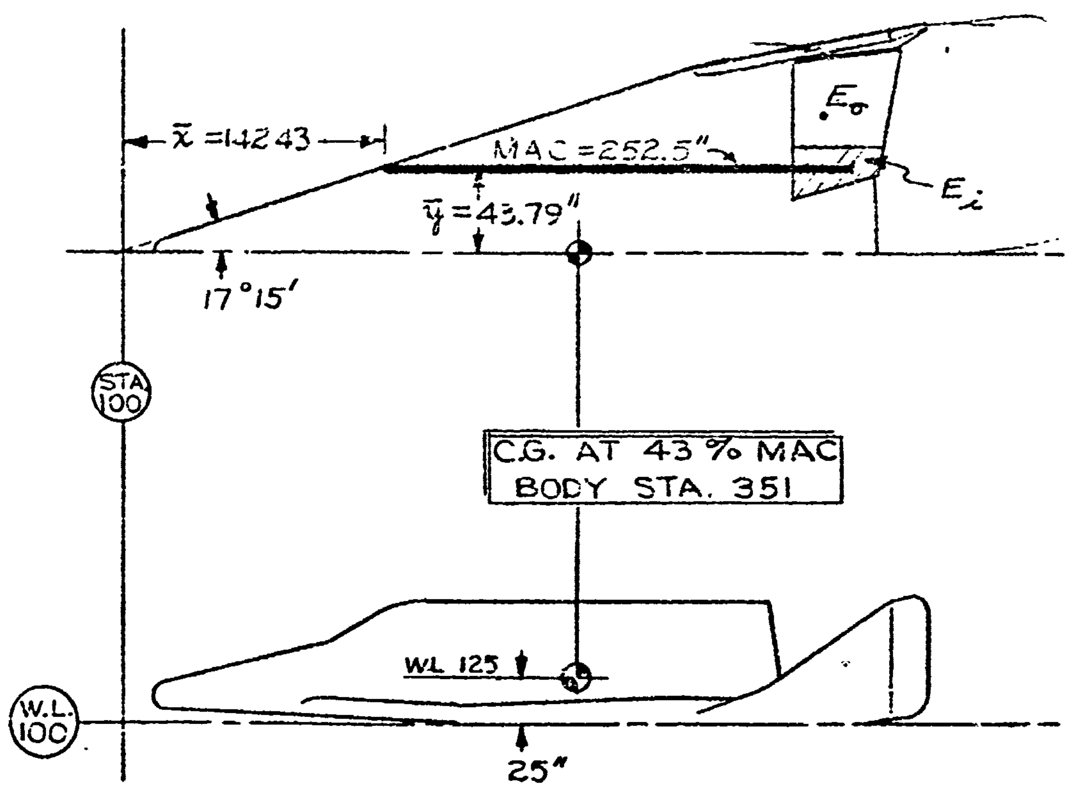


## AERODYNAMIC REFERENCE CONSTANTS:

WING AREA, $S_W = 343.24$ FT.$^2$
EFFECTIVE SPAN, $b = 236.7$ IN.
ASPECT RATIO, $\mathcal{R} = 1.13$
ROOT CHORD, $C_R = 406.1$ IN.
TIP CHORD, $C_T = 107.8$ IN.
$\lambda = C_T / C_R = .265$

## ELEVONS:

FULL ELEVON AREA, $S_E = .14\, S_W$
INBOARD PORTION AREA, $E_i = .047\, S_W$
OUTBOARD PORTION AREA, $E_\sigma = .093\, S_W$

FIG. 3.3.3

| | | REVISED | DATE | | |
|---|---|---|---|---|---|
| CALC | | | | AERODYNAMIC REFERENCE CONSTANTS & PERTINENT DIMENSIONS | 844-2035 |
| CHECK | | | | | D2-8174 |
| APR | | | | BOEING AIRPLANE COMPANY | 26 |
| APR | | | | | PAGE 3.8 |
| DAN M. CARTER 2-25-60 | | | | | |

## 4.0 DEFINITION OF SYMBOLS

| Symbol | Definition |
|---|---|
| a.c. | aerodynamic center |
| AR | aspect ratio |
| b | wing span |
| B.S. | body station |
| $\bar{c}$, m.a.c. or M.A.C. | mean aerodynamic chord |
| $c_e$ | elevon chord |
| c.g. or C.G. | center of gravity |
| $c_r$ | wing root chord |
| $c_t$ | wing tip chord |
| HM | hinge moment |
| $i_t$ | incidence angle of wing tip extensions |
| $I_x$ | moment of inertia in roll |
| $I_y$ | moment of inertia in pitch |
| $I_z$ | moment of inertia in yaw |
| $\ell$ | rolling moment |
| L | lift force |
| m | pitching moment |
| M | Mach number or pitching moment |
| n | yawing moment |
| N | normal force |
| p | roll rate |
| q | pitch rate or dynamic pressure in PSF |
| r | yaw rate |

| | |
|---|---|
| $S_e$ or $S_E$ | elevon area |
| $S_r$ or $S_R$ | rudder area |
| $S_t$ | wing tip extension area |
| $S_w$ | wing area |
| $V$ | velocity |
| $X$ | force along X (roll) axis |
| $Y$ | force along Y (pitch) axis |
| $\alpha$ | angle of attack |
| $\alpha_{OL}$ | angle of attack at zero lift |
| $\beta$ | angle of sideslip |
| $\delta_a$ | aileron deflection angle |
| $\delta_{e_L}$ | left elevon deflection angle |
| $\delta_{e_R}$ | right elevon deflection angle |
| $\delta_e$ OR $\delta_E$ | elevon deflection angle, elevons deflecting together |
| $\delta_R$ | rudder deflection angle |
| $\theta$ | pitch angle |
| $\phi$ | roll angle |
| $\psi$ | yaw angle |
| $\lambda$ | wing taper ratio $\frac{c_t}{c_r}$ |
| $C_l$ | rolling moment coefficient, $\frac{L}{qS_w b}$ |
| $C_{l_p}$ | $= \partial C_l / \partial (pb/2V)$ |
| $C_{l_r}$ | $= \partial C_l / \partial (rb/2V)$ |
| $C_{l_\beta}$ | $= \partial C_l / \partial \beta$ |
| $C_{l_{\dot\beta}}$ | $= \partial C_l / \partial (\dot\beta b/2V)$ |
| $C_{l_{\delta a}}$ | $= \partial C_l / \partial \delta_a$ |
| $C_{l_{\delta R}}$ | $= \partial C_l / \partial \delta_a$ |

| | |
|---|---|
| $C_L$ | lift coefficient, $\frac{L}{q S_w}$ |
| $C_m$ | pitching moment coefficient, $\frac{M}{q S_w \bar{c}}$ |
| $C_{m_o}$ | pitching moment coefficient at zero lift |
| $C_{m_q}$ | $= \partial C_m / \partial(q\bar{c}/2V)$ |
| $C_{m_\alpha}$ | $= \partial C_m / \partial \alpha$ |
| $C_{m_{\dot{\alpha}}}$ | $= \partial C_m / \partial(\dot{\alpha}\bar{c}/2V)$ |
| $C_{m_{\delta a}}$ | $= \partial C_m / \partial \delta a$ |
| $C_{m_{\delta e}}$ | $= \partial C_m / \partial \delta e$ |
| $C_n$ | yawing moment coefficient, $\frac{N}{q S_w b}$ |
| $C_{n_p}$ | $= \partial C_n / \partial(pb/2V)$ |
| $C_{n_r}$ | $= \partial C_n / \partial(rb/2V)$ |
| $C_{n_{\delta a}}$ | $= \partial C_n / \partial \delta a$ |
| $C_{n_{\delta R}}$ | $= \partial C_n / \partial \delta R$ |
| $C_{n_\beta}$ | $= \partial C_n / \partial \beta$ |
| $C_{n_{\dot{\beta}}}$ | $= \partial C_n / \partial(\dot{\beta} b/2V)$ |
| $C_N$ | normal force coefficient, $\frac{N}{q S_w}$ |
| $C_{N_\alpha}$ | $= \partial C_N / \partial \alpha$ |
| $C_{N_{\dot{\alpha}}}$ | $= \partial C_N / \partial(\dot{\alpha}\bar{c}/2V)$ |
| $C_{N_{\delta a}}$ | $= \partial C_N / \partial \delta a$ |
| $C_{N_{\delta e}}$ | $= \partial C_N / \partial \delta e$ |
| $C_{N_q}$ | $= \partial C_N / \partial(q\bar{c}/2V)$ |
| $C_x$ | axial force coefficient, $\frac{X}{q S_w}$ |
| $C_y$ | side force coefficient, $Y/q S_w$ |
| $C_{y_\beta}$ | $= \partial C_Y / \partial \beta$ |
| $C_{y_{\dot{\beta}}}$ | $\partial C_Y / \partial(\dot{\beta} b/2V)$ |

| | | |
|---|---|---|
| $C_{y_{\delta a}}$ | = | $\partial C_Y / \partial \delta_a$ |
| $C_{y_{\delta r}}$ | = | $\partial C_Y / \partial \delta_R$ |
| $C_{y_p}$ | = | $\partial C_Y / \partial (pb/2V)$ |
| $C_{y_r}$ | = | $\partial C_Y / \partial (rb/2V)$ |
| $C_h$ | | hinge moment coefficient, $\frac{HM}{q S_e C_e}$ |
| $C_{h_\alpha}$ | = | $\partial C_h / \partial \alpha$ |
| $C_{h_{\delta e}}$ | = | $\partial C_h / \partial \delta_e$ |

## 5.0 LONGITUDINAL STABILITY AND CONTROL (GLIDER)

### 5.1 SUMMARY

Longitudinal stability and control data are presented in the following sections for the 844-2035 glider configuration. Data are presented through the speed range of the glider. The elevon configuration of the glider has been modified from the 844-2035 such that the inboard panel has no wedging (same section as the outboard panel) for the data to be presented.

The glider aerodynamic configuration varies as a function of speed. At subsonic and supersonic speeds, wing tip extensions, located on the outboard surface of the vertical tails, are extended for increased stability. At hypersonic speeds, the glider is subjected to high temperatures resulting in structural deformation. Data are presented for these changes of configuration.

Normal force, axial force and pitching moment coefficients comprise the data presented in the following sections. The data are presented at the nominal center of gravity position of 43% of the M.A.C. and a vertical c.g. location at water line 125.

Summary curves of these coefficient data are presented on Figures 5.1.1 through 5.1.7. Trimmed aerodynamic center as a function of Mach number and trimmed lift coefficient is presented on Figures 5.1.1 and 5.1.2. Normal force curve slope, at trimmed elevon deflection for a given $C_L$, is presented on Figures 5.1.6 and 5.1.7. A minor amount of fairing was required to produce these curves from the basic data to be presented, except at $M = 0.7$. The data at $M = 0.7$ produce appreciable discontinuities in the curves and have been faired out of the summary data.

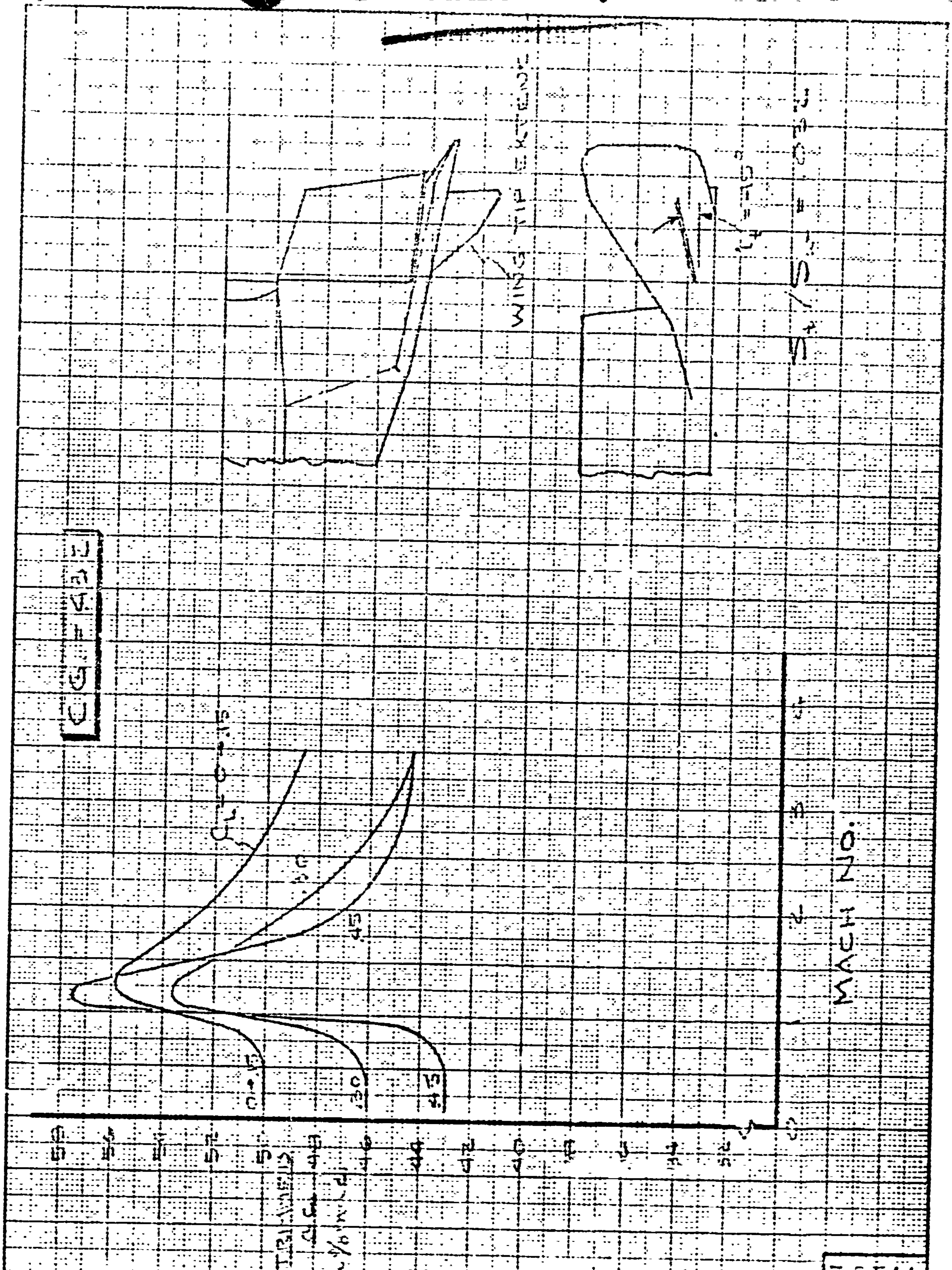


| | | | |
|---|---|---|---|
| CALC | D C L | 12/5/61 | REVISED / DATE |
| CHECK | | | |
| APR | | | |
| APR | | | |

FIG. 5.11

AERODYNAMIC CENTER
WING TIPS EXTENDED

844-2035

D2-8174

BOEING AIRPLANE COMPANY

PAGE 5.2

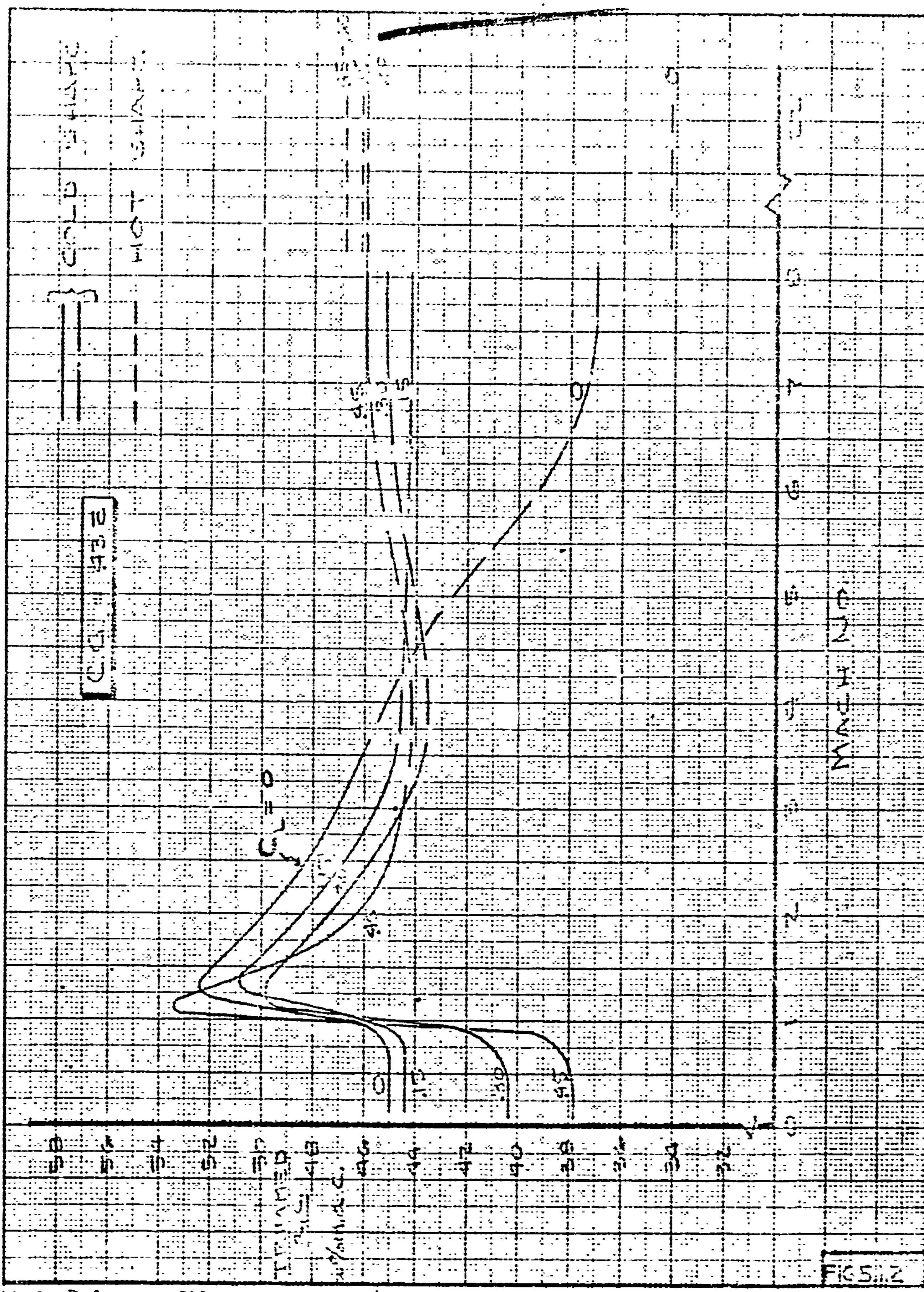

FIG 5.2

| CALC | D.C.L. | 12/15/5? | REVISED | DATE |
|---|---|---|---|---|
| CHECK | | | | |
| APR | | | | |
| APR | | | | |

AERODYNAMIC CENTER
WING TIPS RETRACTED

844-2035

D2-8174

BOEING AIRPLANE COMPANY **33**

PAGE 5.3

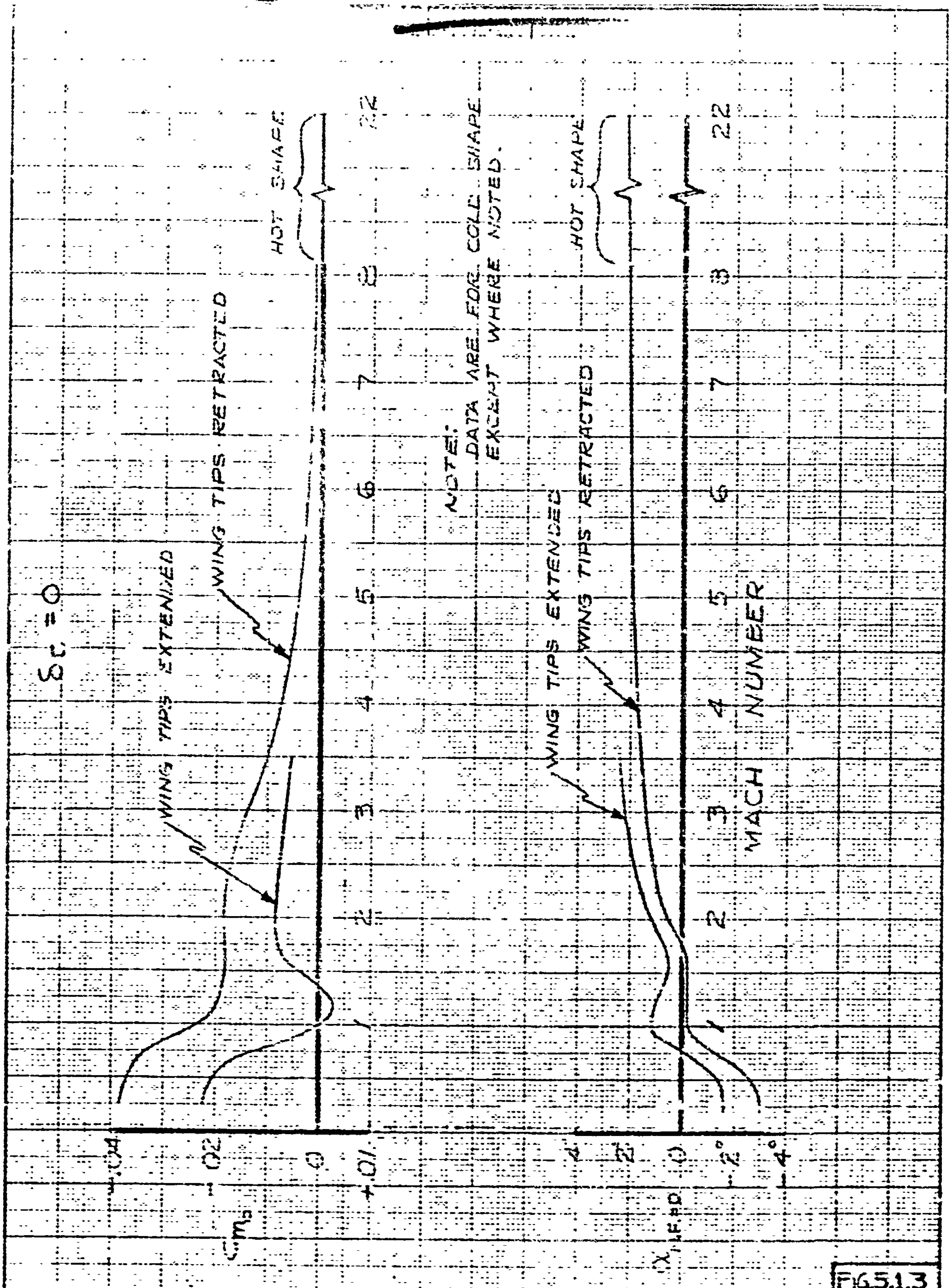


FIG 5.1.3

M. CARTER 12-16-60

ANGLE OF ATTACK
AND PITCHING MOMENT
AT ZERO NORMAL FORCE

S4-2035

D2-8174

BOEING AIRPLANE COMPANY 34

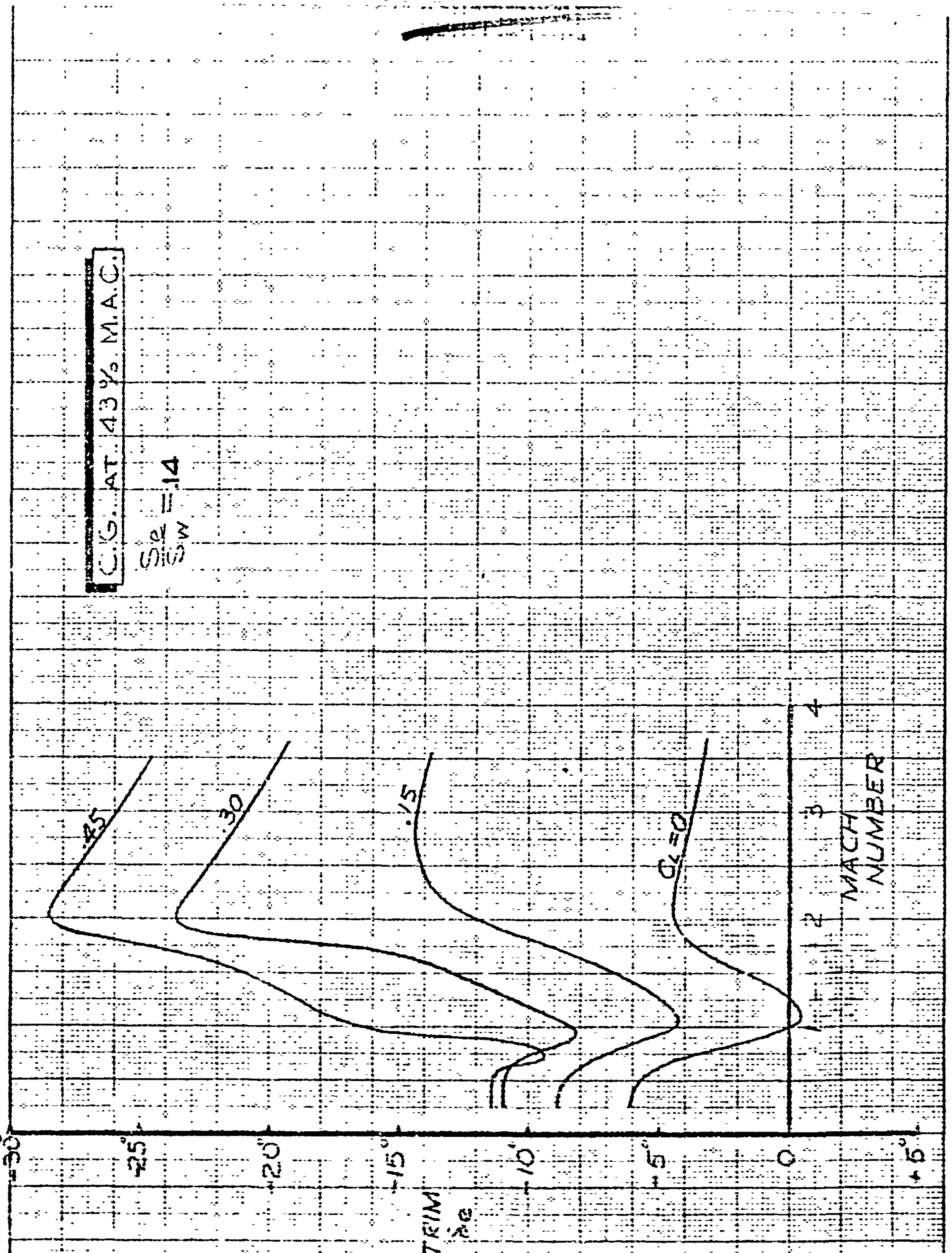


FIG.5.1.4

| | | |
|---|---|---|
| M. CARTER 12-16-60 | ELE ATOR REQUIRED TO ·RIM — WING TIPS EXTENDED | 844-2035 |
| | | D2-8174 |
| | BOEING AIRPLANE COMPANY **35** | PAGE 55 |

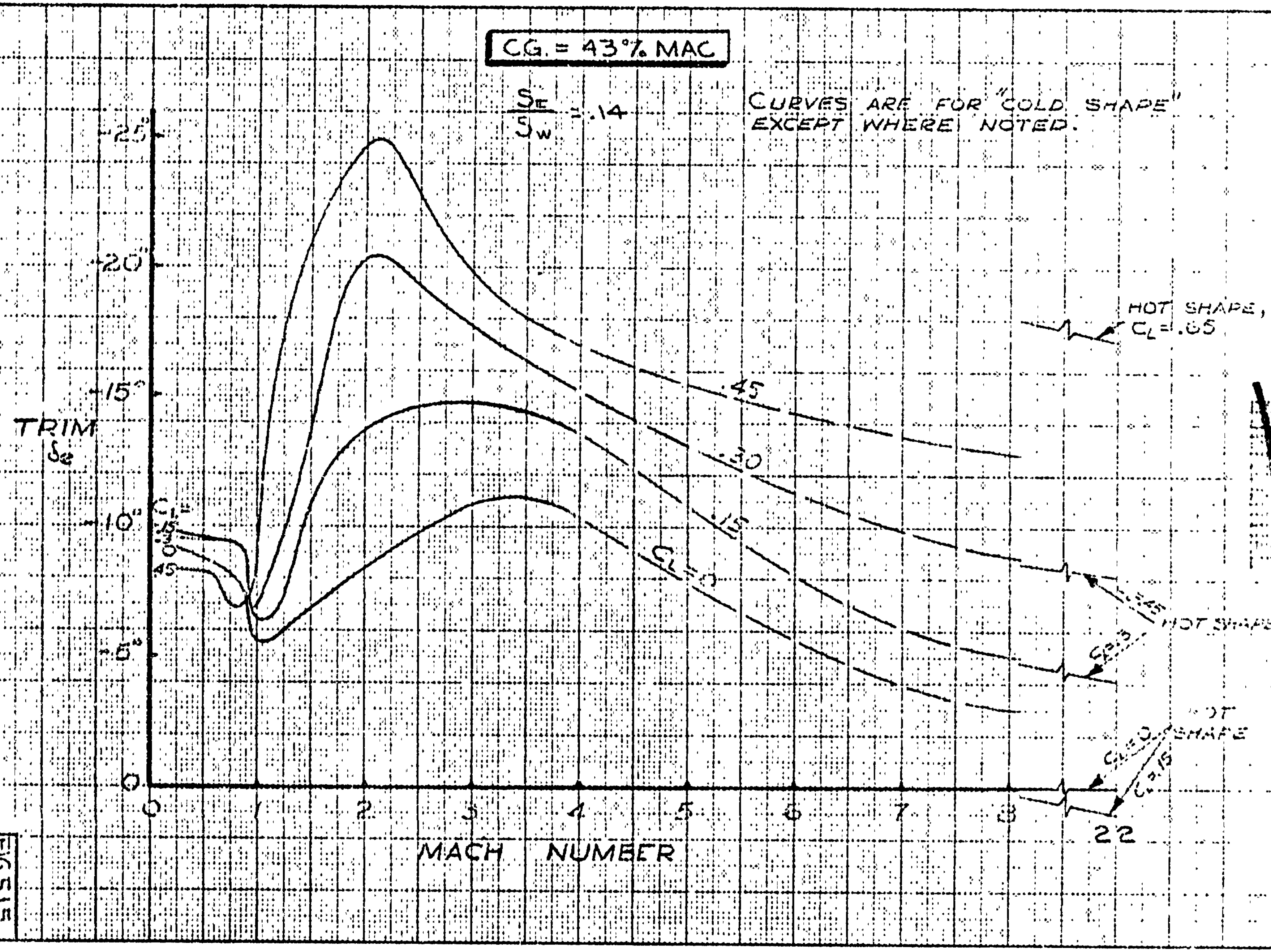


FIG. 5.15

844-2035

M. CARTER 12-16-60

ELEVATOR REQUIRED TO TRIM — WING TIP EXTENSIONS RETRACTED

D2-8174

BOEING AIRPLANE COMPANY

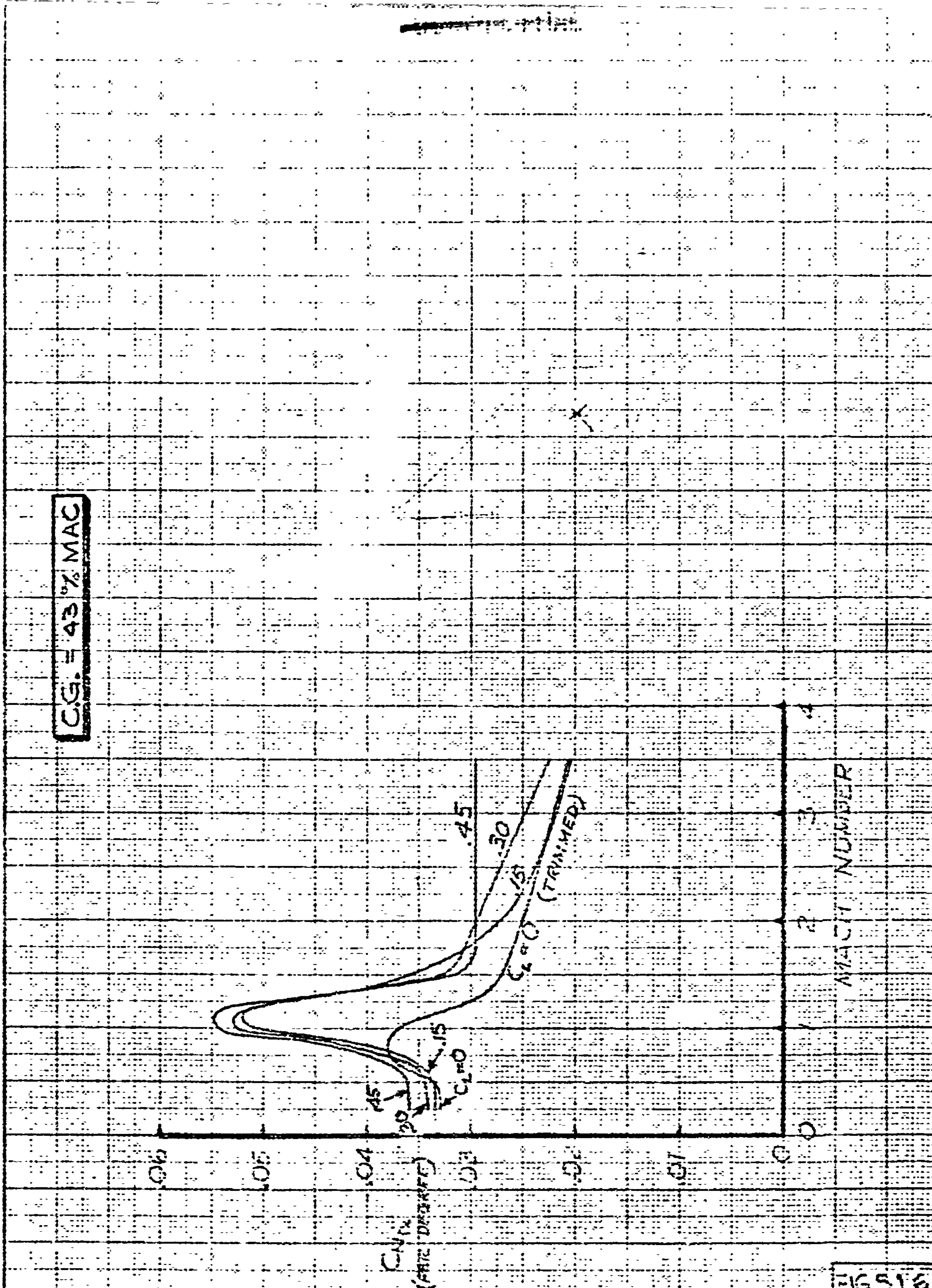


FIG. 5.16

M. CARTER 12-21-0

NORMAL FORCE CURVE SLOPE
WING TIPS EXTENDED

844-2035

D2-8174

BOEING AIRPLANE COMPANY 37

PAGE 5.7

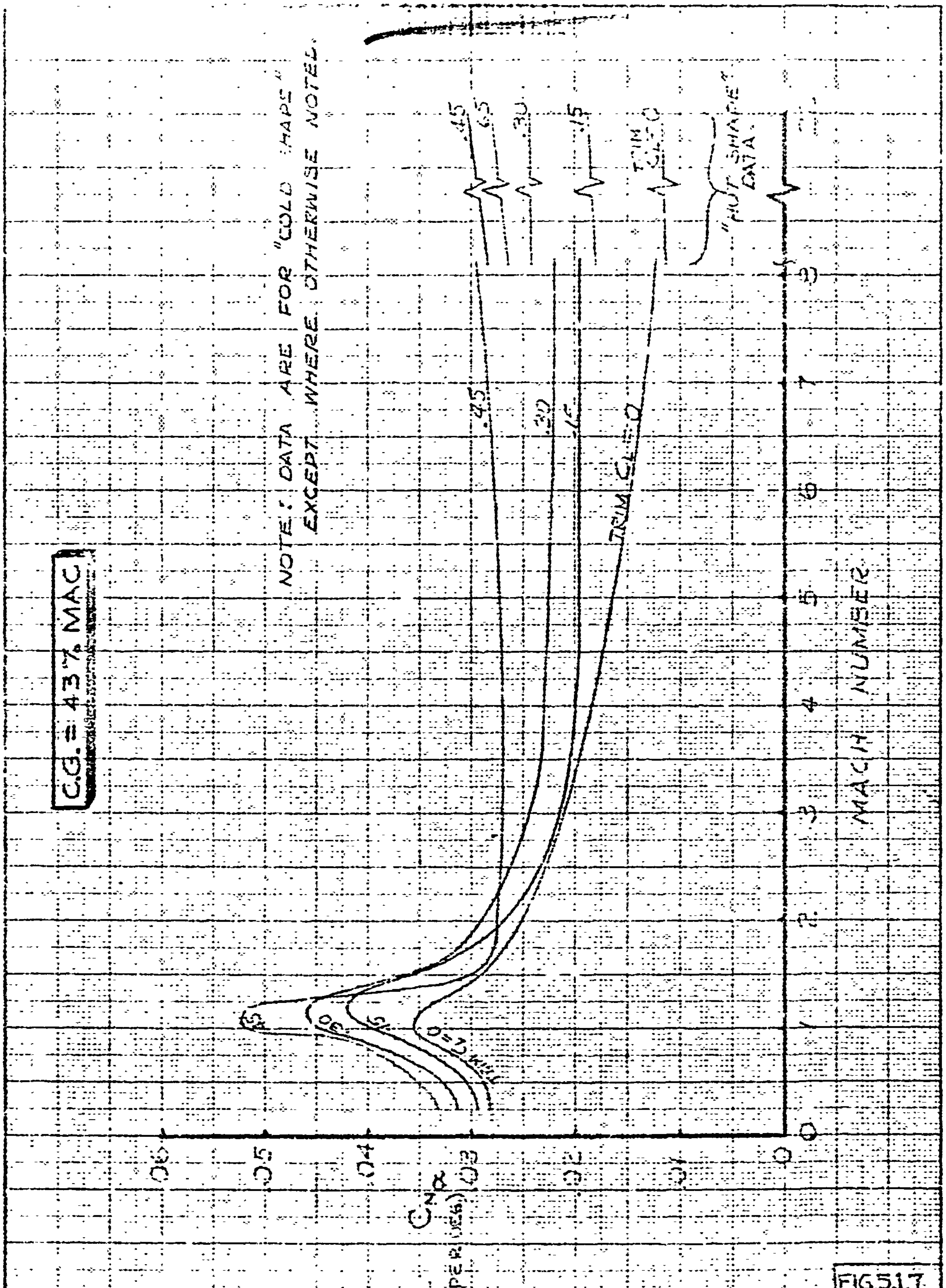


FIG.5.1.7

M. CARTER 12-20-0

NORMAL FORCE CURVE SLOPE
WING TIPS RETRACTED

844-2035

D2-8174

BOEING AIRPLANE COMPANY

## 5.2 LANDING SPEED

Basic stability and elevon effectiveness plots are presented on Figures 5.2.1 and 5.2.2 for the glider at a Mach number typical of landing speed. These data were determined from wind tunnel tests performed in the A.R.C. 12-Foot Pressure Wind Tunnel and the Boeing Transonic Wind Tunnel on a .15 scale model of the 844-2 05 configuration. These data have been modified to the 844-2035 configuration as required.

The change in stability and control effectiveness with landing gear extended and in close proximity to the ground is shown on Figure 5.2.3. These data were determined from wind tunnel tests in the Boeing Transonic Wind Tunnel on a similar configuration and modified for the present configuration. The incremental effect of extending the landing gear is shown on Figure 5.2.4. It was assumed that proximity to the ground would have little effect on these increments.

Axial force coefficients as a function of angle of attack are shown on Figures 5.3.11 and 5.3.12 at M = .26 which is typical of landing. The axial force increment due to landing gear extension is shown on Figure 5.2.5. Axial force is assumed to be unaffected by the presence of the ground.

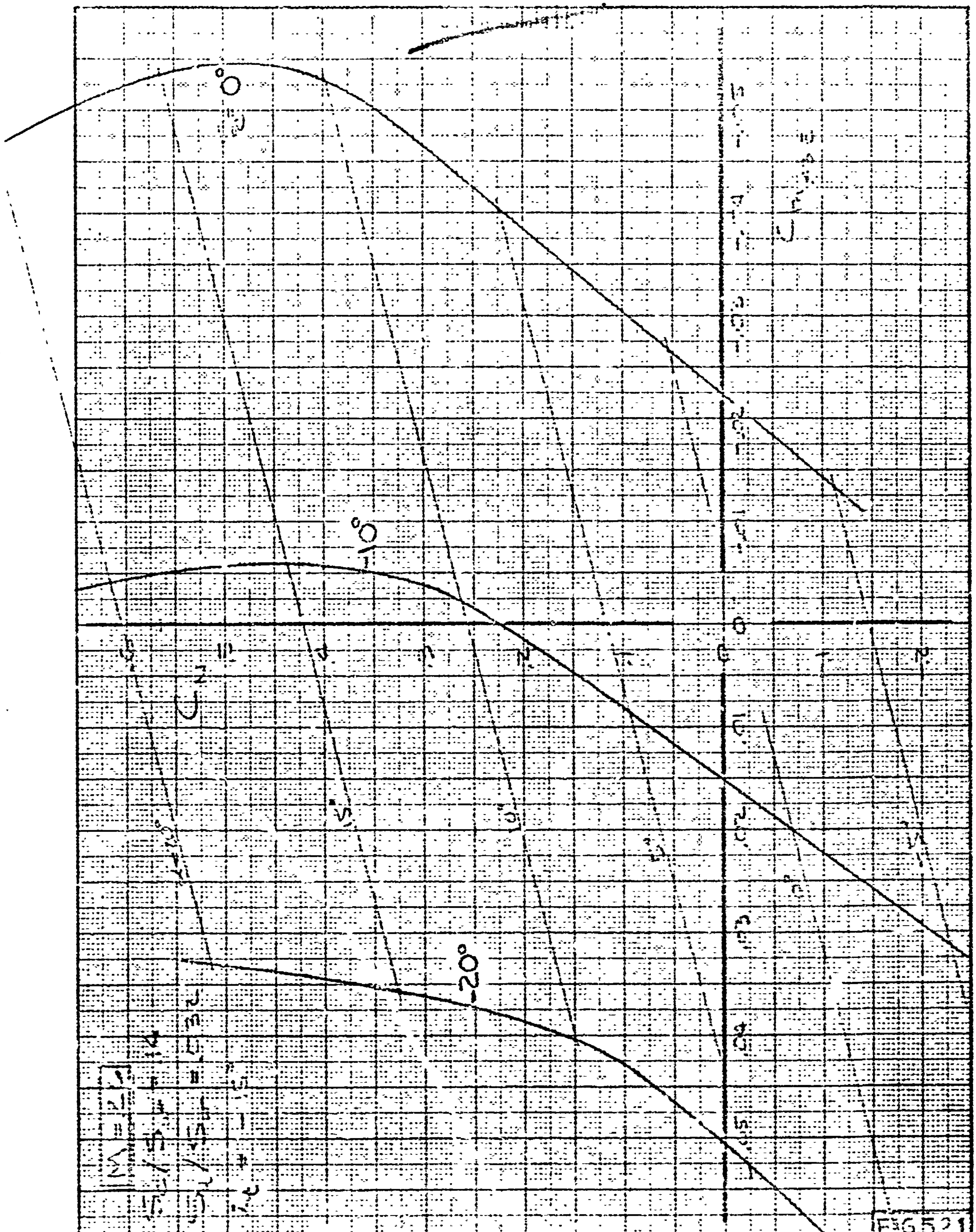


FIG. 5.2.1

| CALC | | | REVISED | DATE | LONGITUDINAL STABILITY<br>WING TIPS EXTENDED<br>M = .26 | 844-2035 |
|---|---|---|---|---|---|---|
| CHECK | | | | | | |
| APR | | | | | | D2-8174 |
| APR | | | | | BOEING AIRPLANE COMPANY **40** | PAGE 5.10 |

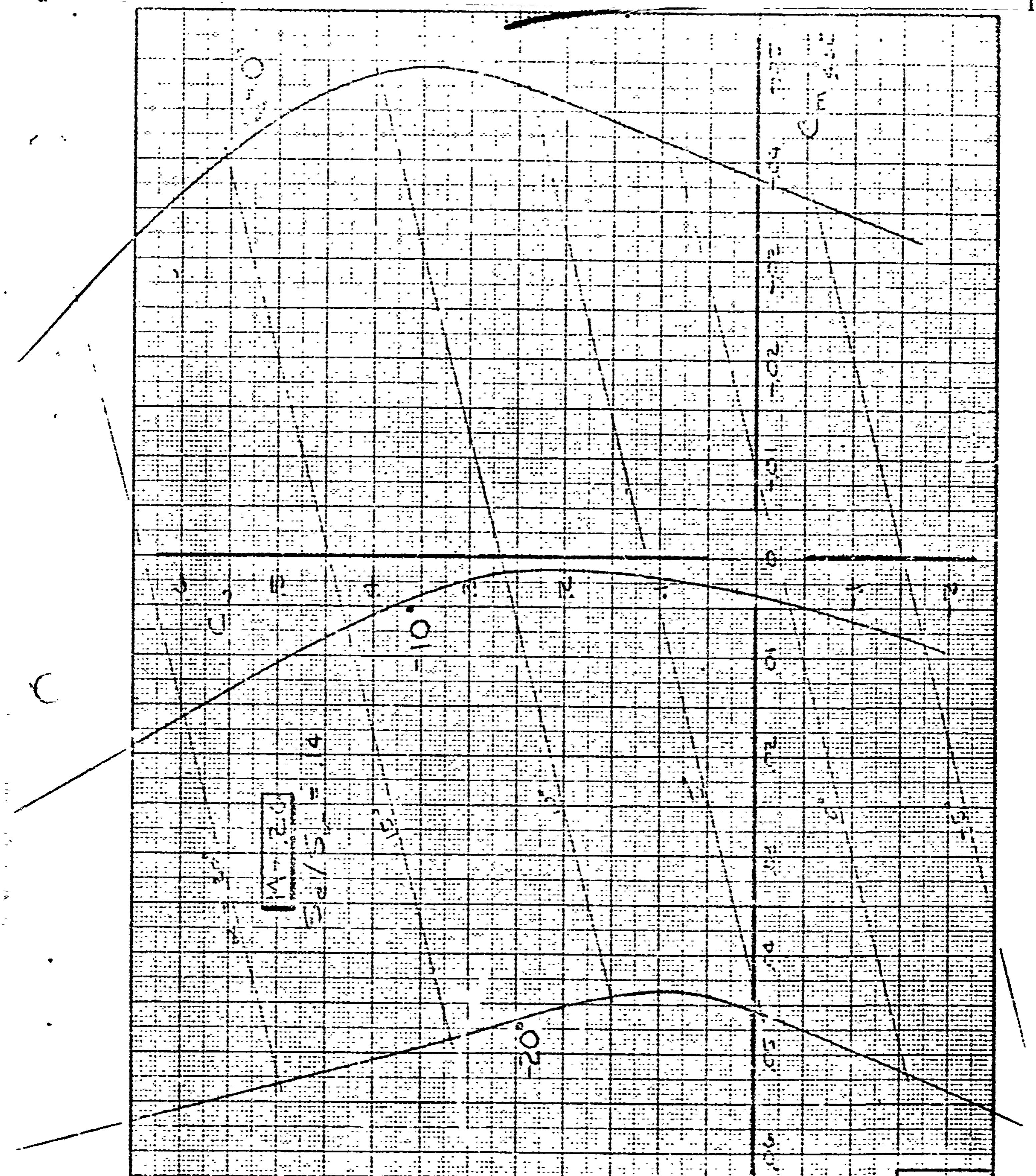

FIG 5.2.2

| CALC | LCL | 2-1-21 | REVISED | DATE | LONGITUDINAL STABILITY<br>WING TIPS RETRACTED<br>M = .26 | 644-2035 |
|---|---|---|---|---|---|---|
| CHECK | | | | | | |
| APR | | | | | | D2-8174 |
| APR | | | | | | |
| | | | | | BOEING AIRPLANE COMPANY **41** | PAGE 5.11 |

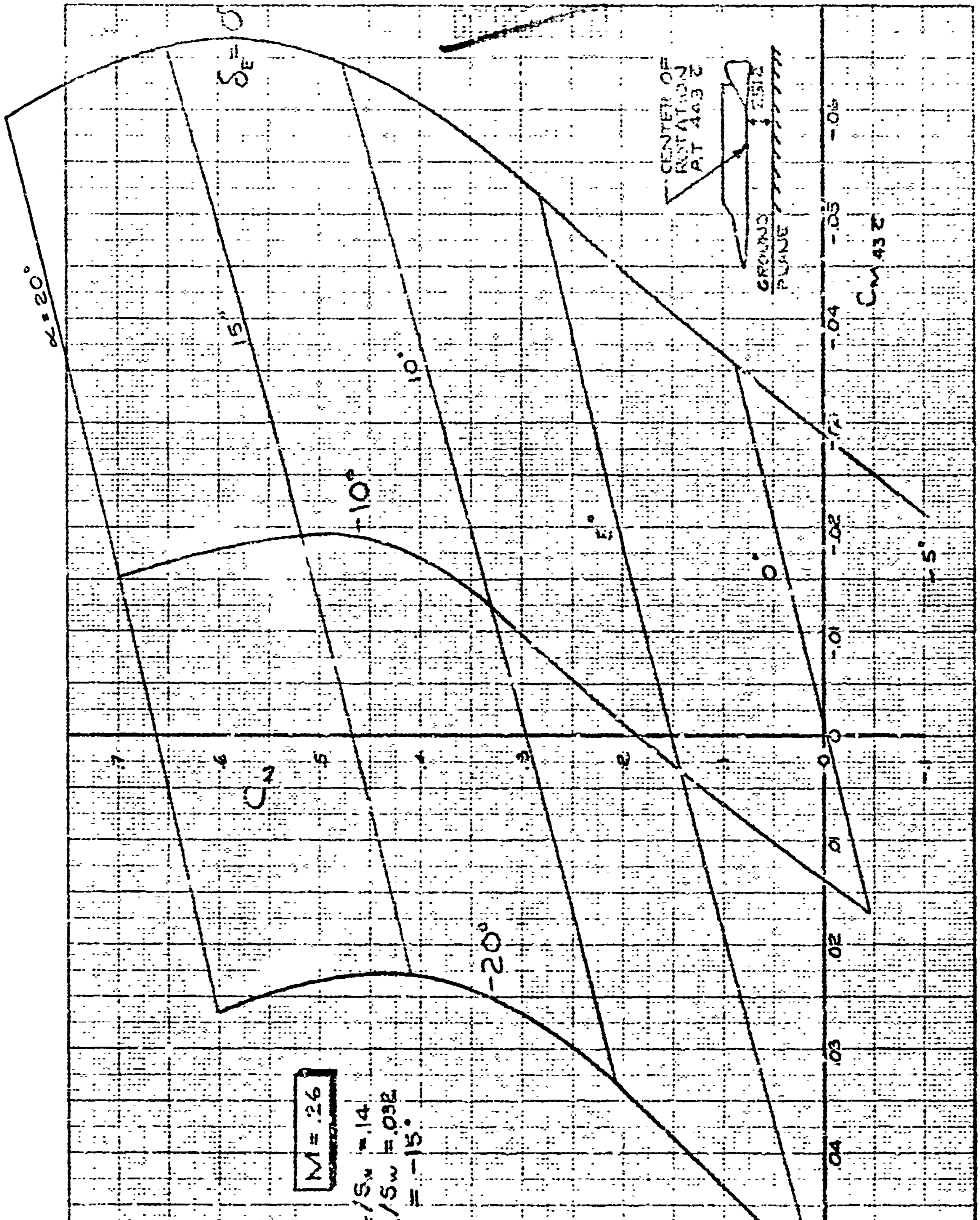


FIG 5.23

644-2035

J.L.FRANCIS 12/19/60

LONGITUDINAL STABILITY, WING TIPS & LANDING GEAR DOWN. IN PRESENCE OF GROUND PLANE

D2-8174

42

5.12

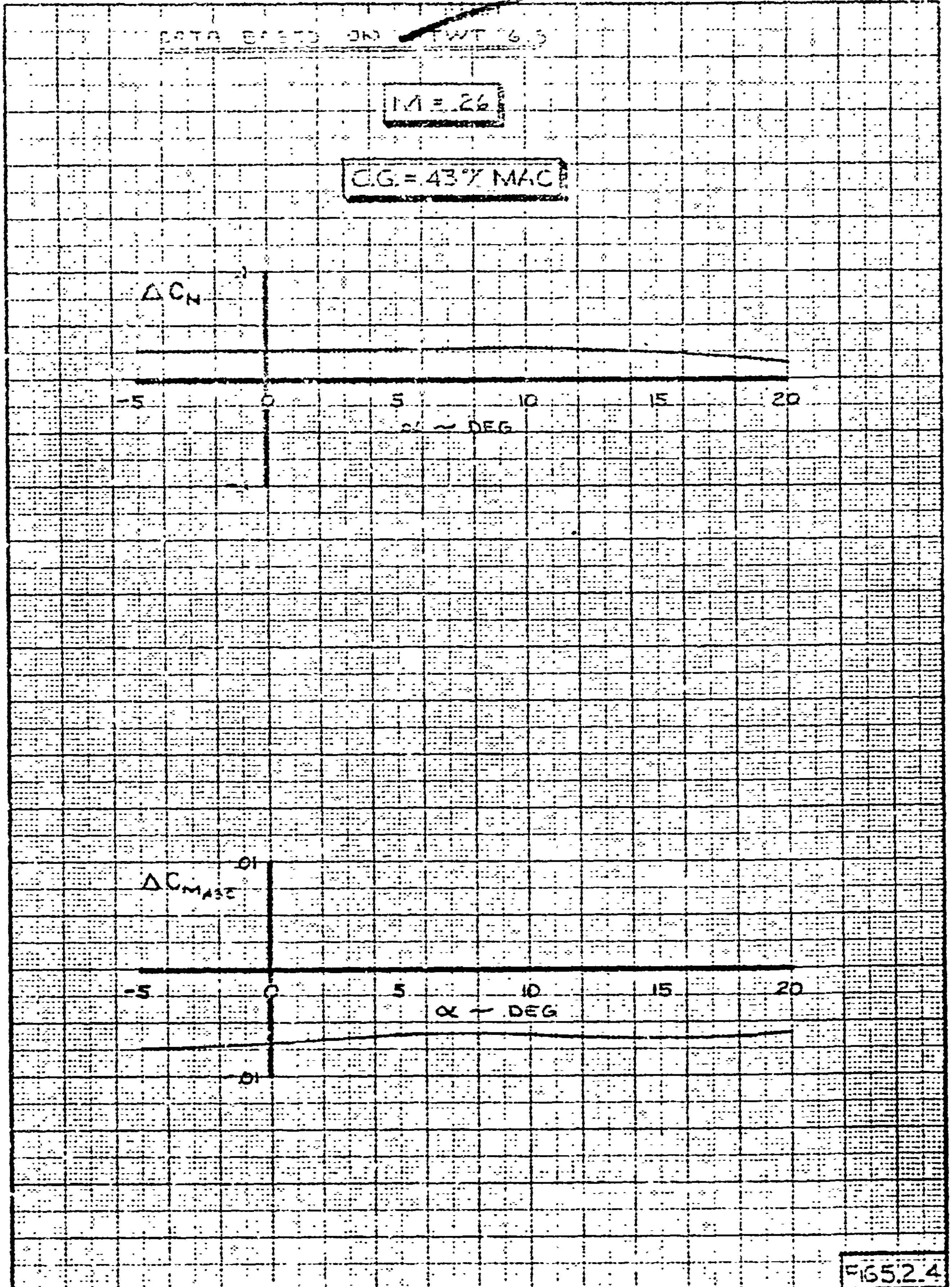


FIG 5.2.4

| | | | | | |
|---|---|---|---|---|---|
| CALC | J.L.FRANCIS | 12/19/60 | REVISED | DATE | EFFECT OF LANDING GEAR |
| CHECK | | | | | |
| APR | | | | | |
| APR | | | | | BOEING AIRPLANE COMPANY |

844-2035

D2-8174

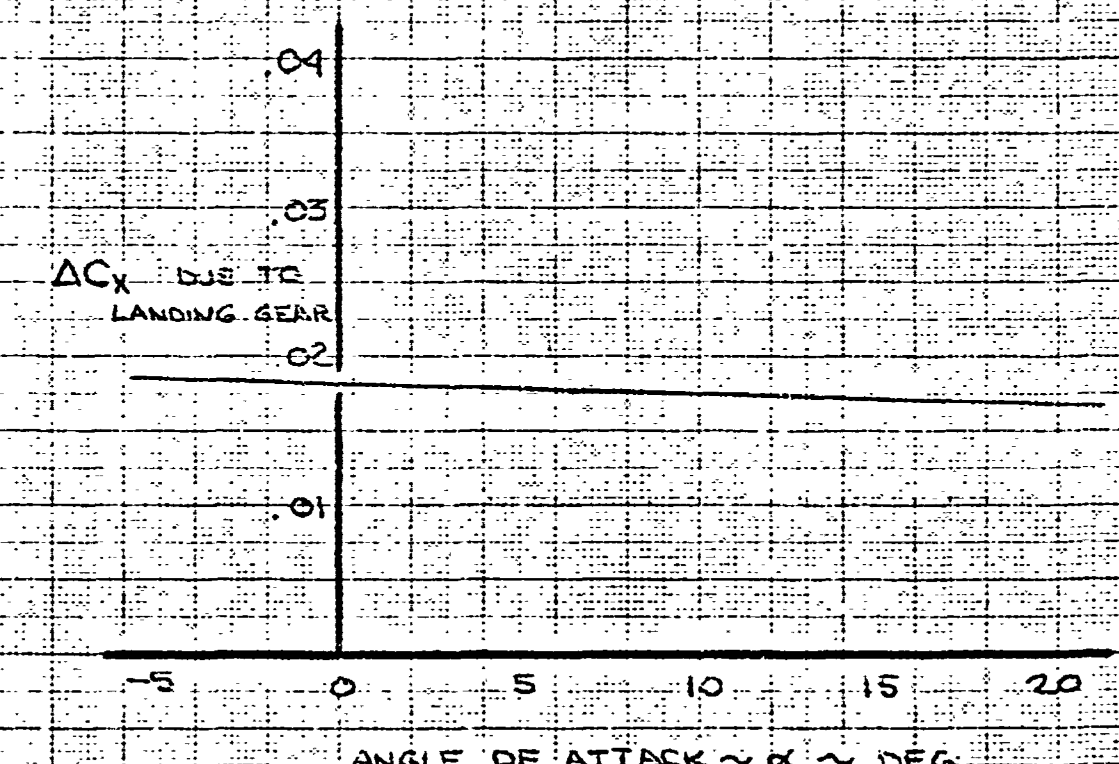


FIG. 5.2.5

WEJ 12-27-6

EFFECT OF LANDING GEAR ON CHORD FORCE
M = .26

844-2035

D2-8174

BOEING AIRPLANE COMPANY 44

## 5.3 SUBSONIC - TRANSONIC SPEEDS

Basic stability and control effectiveness data are presented on Figures 5.3.1 through 5.3.10. Data are shown at Mach numbers of 0.5, 0.7, 0.9, 0.95, and 1.05 for both the wing tip extensions retracted and extended. The data are presented in this fashion and for the various Mach numbers due to the appreciable non-linearities of the aerodynamics. The data are based on results of wind tunnel tests in the Boeing Transonic Wind Tunnel and preliminary results of tests in the L.R.C. 16-Foot Transonic Wind Tunnel. Due to the preliminary nature of some of these data, some modification to the characteristics shown can be anticipated. The tunnel data were modified to the current configuration by empirical and theoretical analysis.

Data shown at $M=0.7$ show discontinuity with the other data as a function of Mach number as discussed in the summary. These trends of the $M=0.7$ data were corroborated to some degree by the two tunnel tests mentioned. Further testing will be done to define these data better.

Axial force data as function of angle of attack are shown on Figure 5.3.11 for the glider with wing tips extended and on Figure 5.3.12 for wing tips retracted. These data are for the glider in trimmed flight.

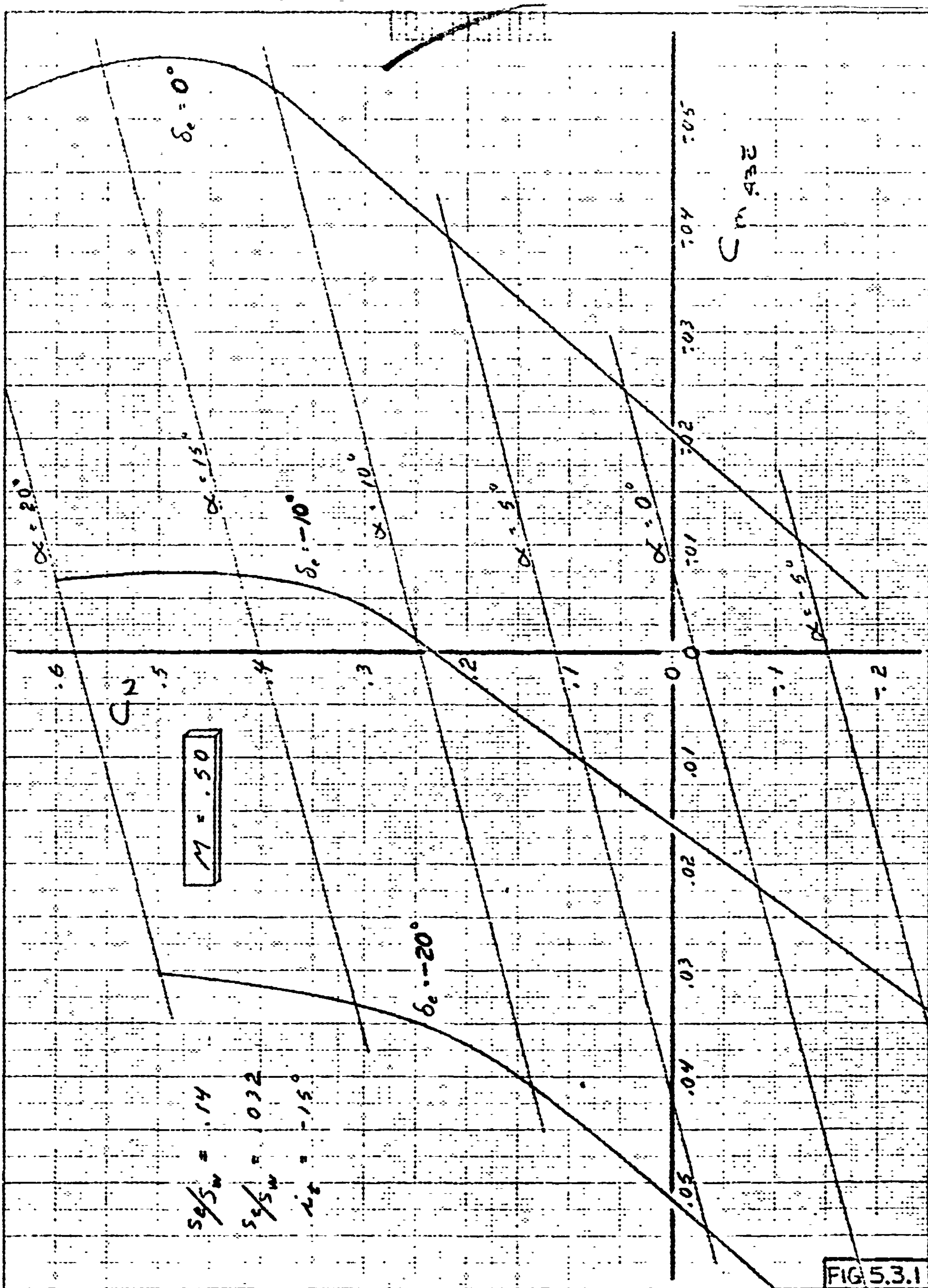

FIG 5.3.1

| | | |
|---|---|---|
| CALC DCL 12-9-60 | LONGITUDINAL STABILITY<br>WING TIPS EXTENDED<br>M = .50 | 844-2035 |
| CHECK | | D2-8174 |
| APD | | |
| APD | BOEING AIRPLANE COMPANY 46 | PAGE 5.16 |
| DWG. P.W | | |

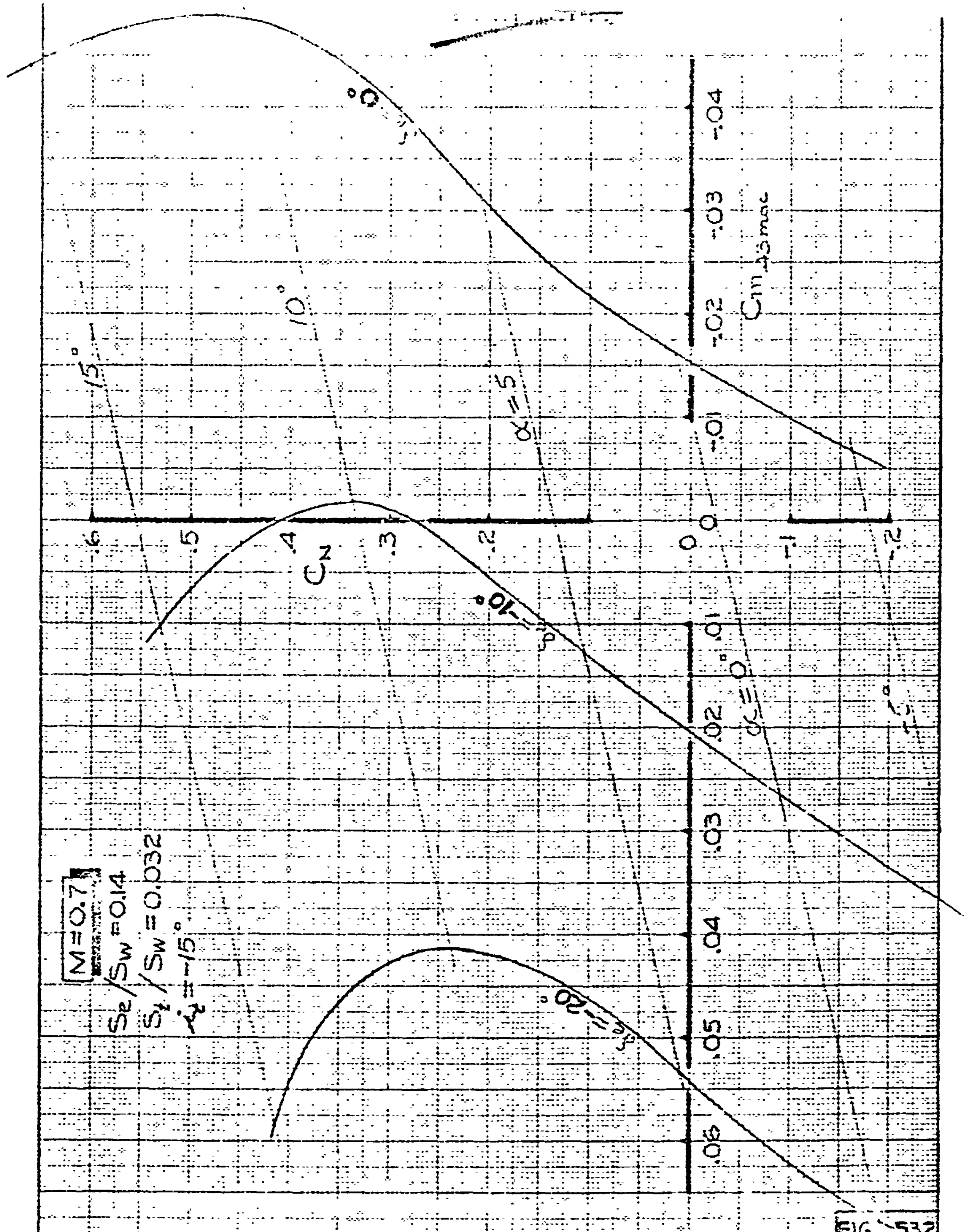


FIG 53.2

| | | | |
|---|---|---|---|
| M. CARTER 12-12-60 | | LONGITUDINAL STABILITY<br>WING TIPS EXTENDED<br>M = 0.7 | 844-2035 |
| CHECK | | | D2-8174 |
| | | BOEING AIRPLANE COMPANY 47 | PAGE 5/7 |

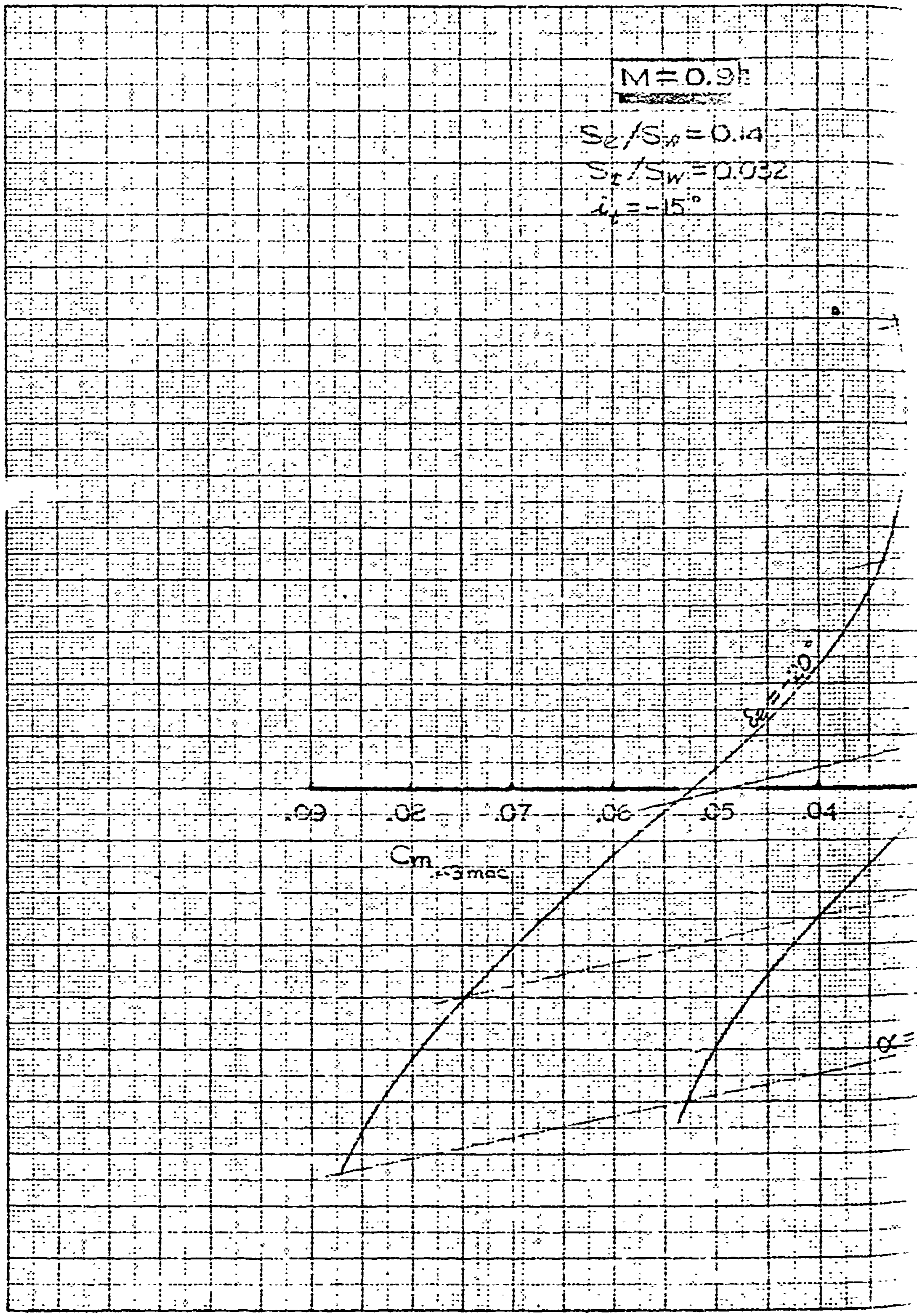
M = 0.9
Se/Sw = 0.14
St/Sw = 0.032
it = -15°
.09
.08
.07
.06
.05
.04

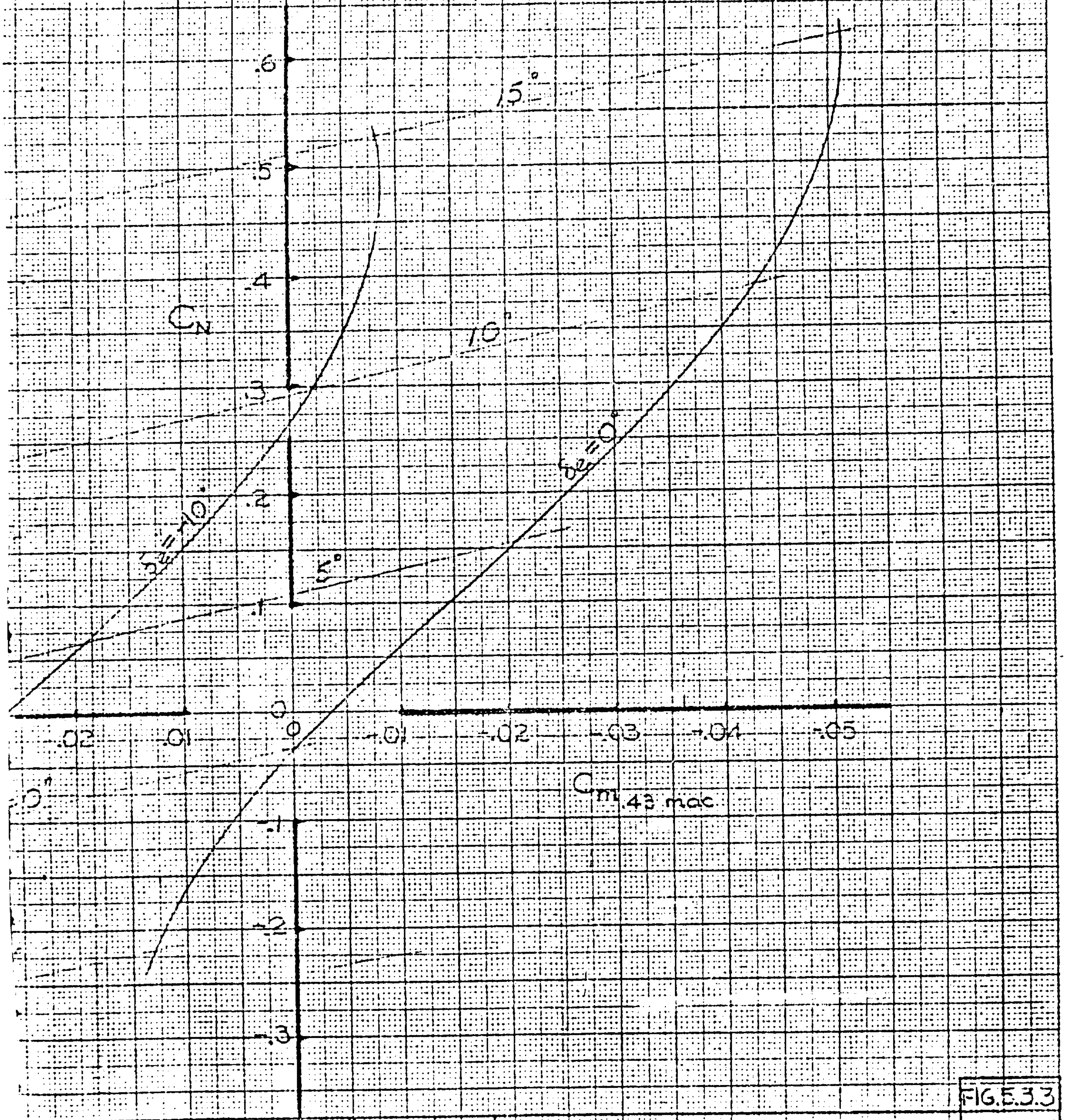


| | | | | |
|---|---|---|---|---|
| CALC | M. CARTER 12-12-60 | REVISED | DATE | LONGITUDINAL STABILITY WING TIPS EXTENDED M=0.9 |
| CHECK | | | | |
| APPD | | | | |
| APPD | | | | |

FIG. 5.3.3

844-2035

D2-8174

PAGE 5.18

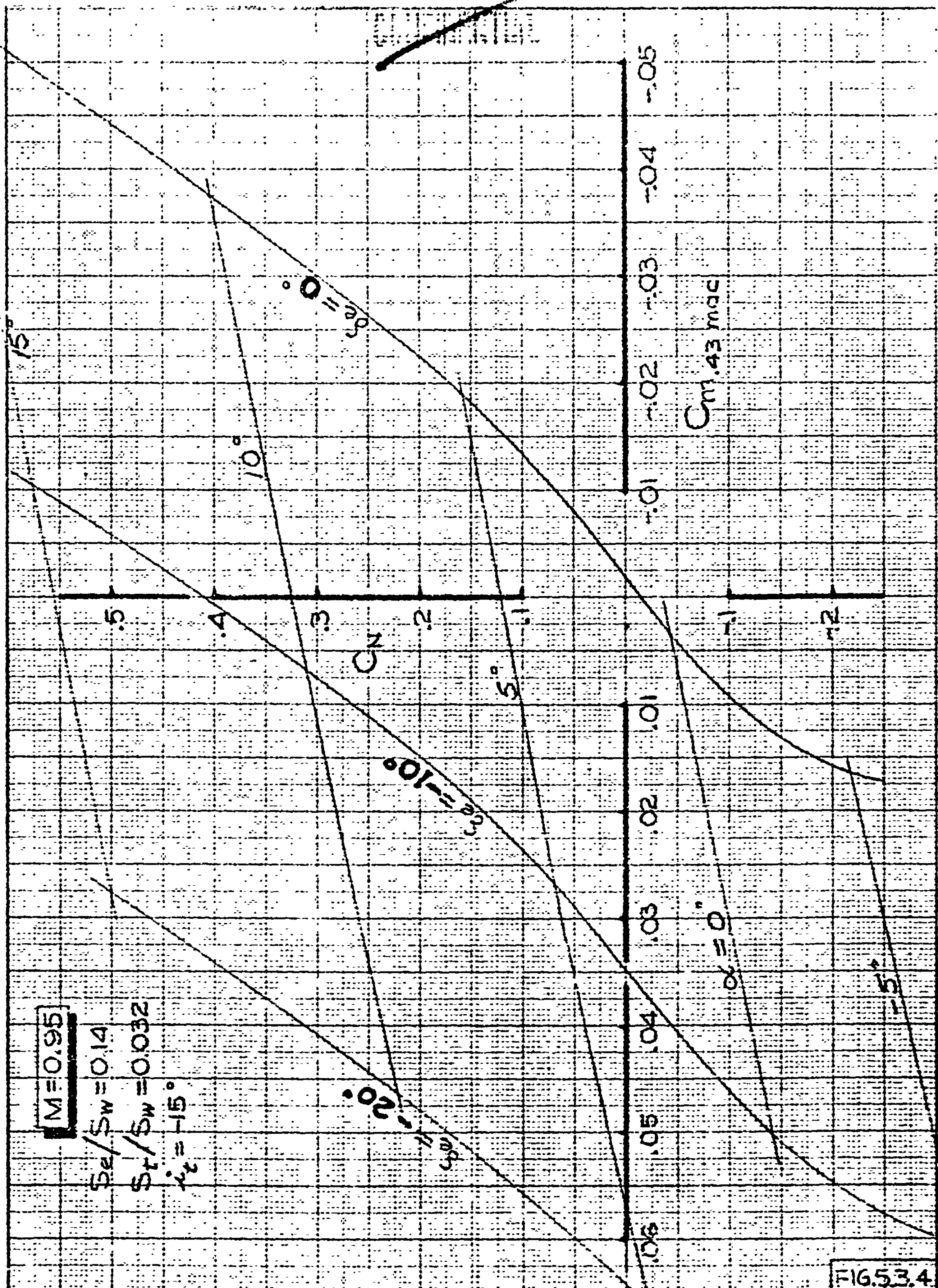


FIG 5.3.4

| | | | | | |
|---|---|---|---|---|---|
| CALC M. CARTER | 12-12-60 | REVISED | DATE | LONGITUDINAL STABILITY WING TIPS EXTENDED M = .95 | 844-2035 |
| CHECK | | | | | D2-8174 |
| APR | | | | | |
| APR | | | | BOEING AIRPLANE COMPANY 50 | PAGE 5.19 |

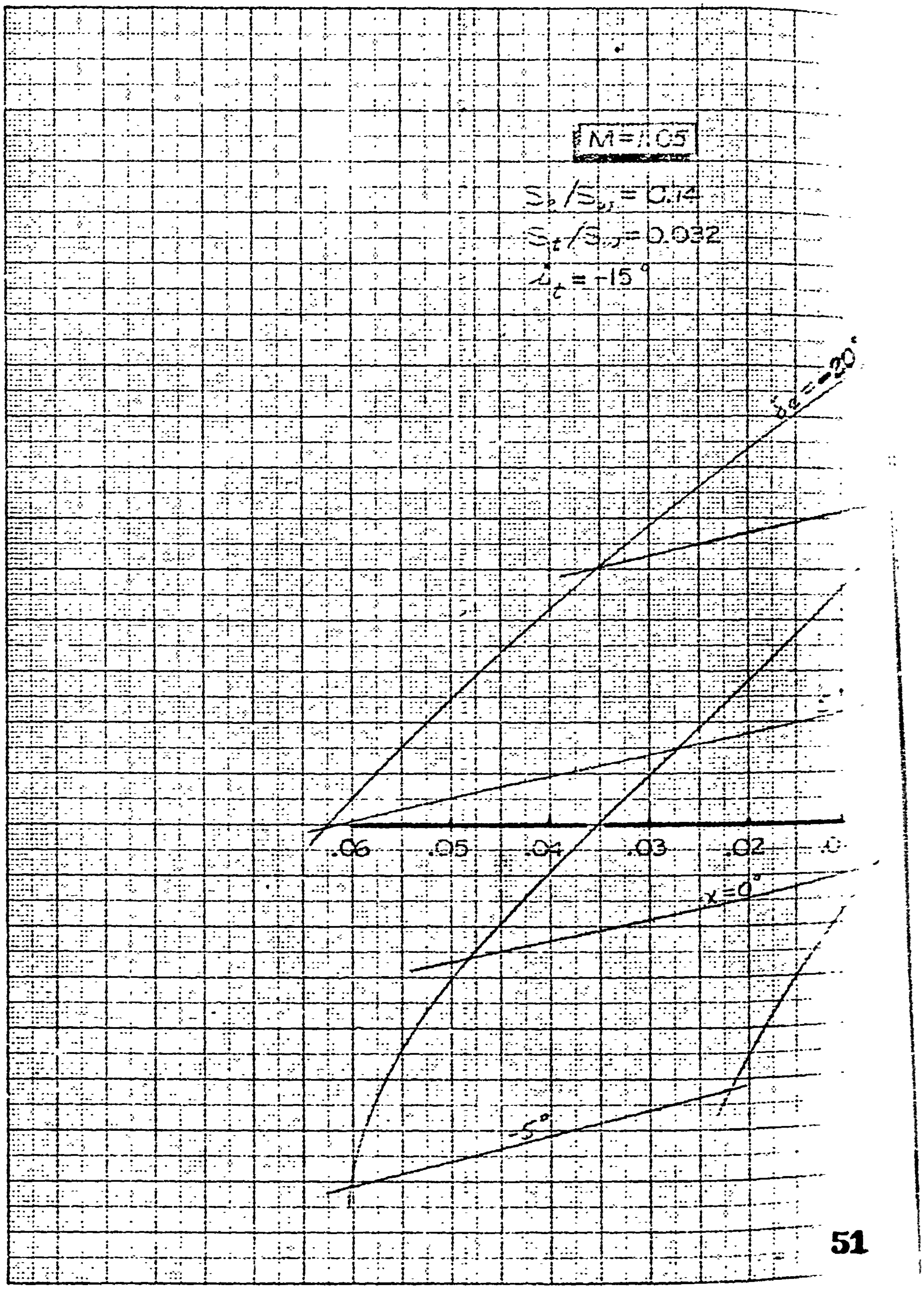
M = 1.05
$S_b/S_w = 0.14$
$S_t/S_w = 0.032$
$\delta_t = -15°$
$\delta_a = -20°$
.06
.05
.04
.03
.02
.01
$\alpha = 0°$
$-5°$

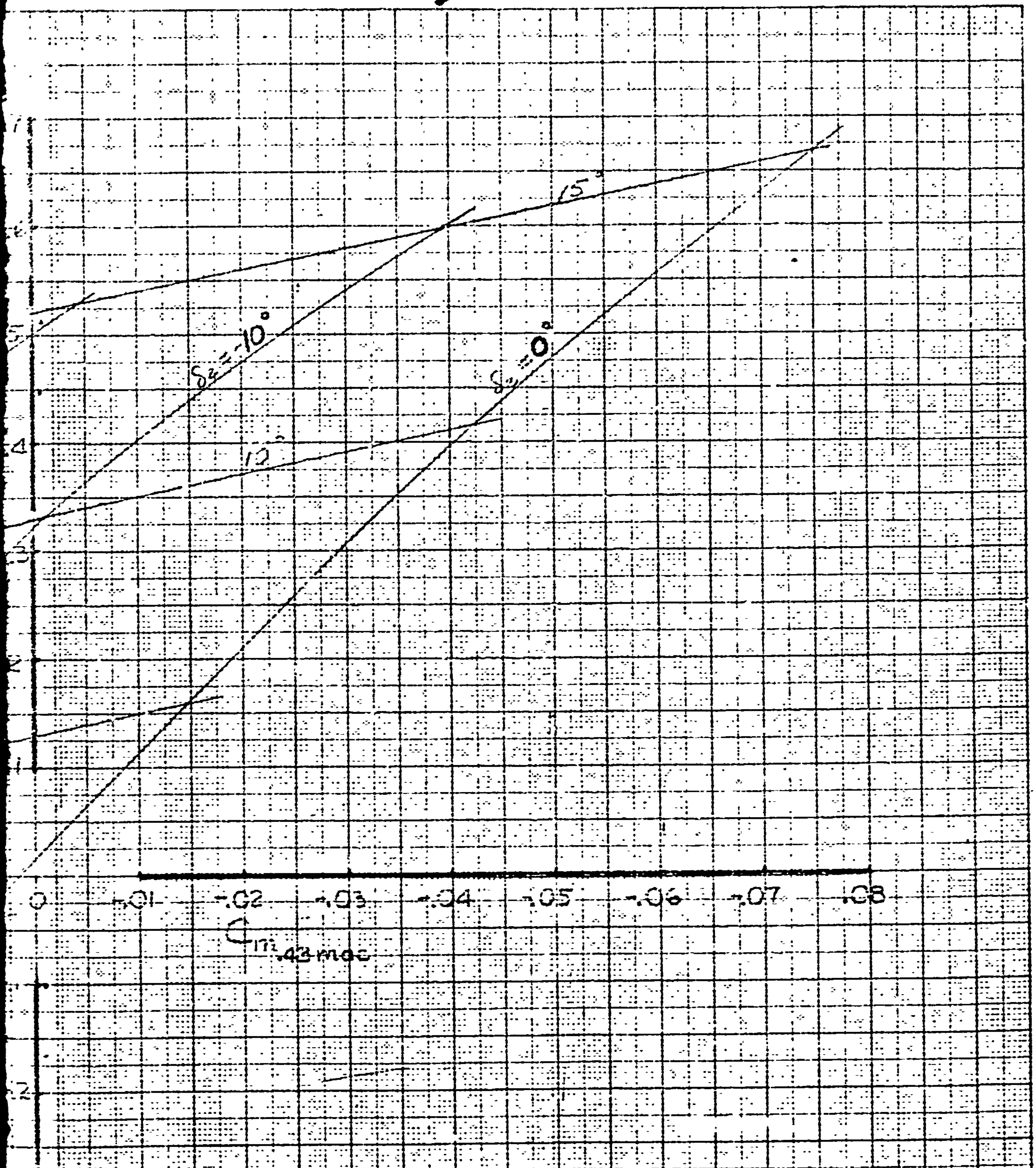


FIG 5.35

| CALC | M. Cor... | 12-9-60 | REVISED | DATE | LONGITUDINAL STABILITY WING TIPS EXTENDED M=1.05 | 844-2035 |
|---|---|---|---|---|---|---|
| CHECK | | | | | | D2-8174 |
| APPD | | | | | | PAGE 5.70 |
| APPD | | | | | | |

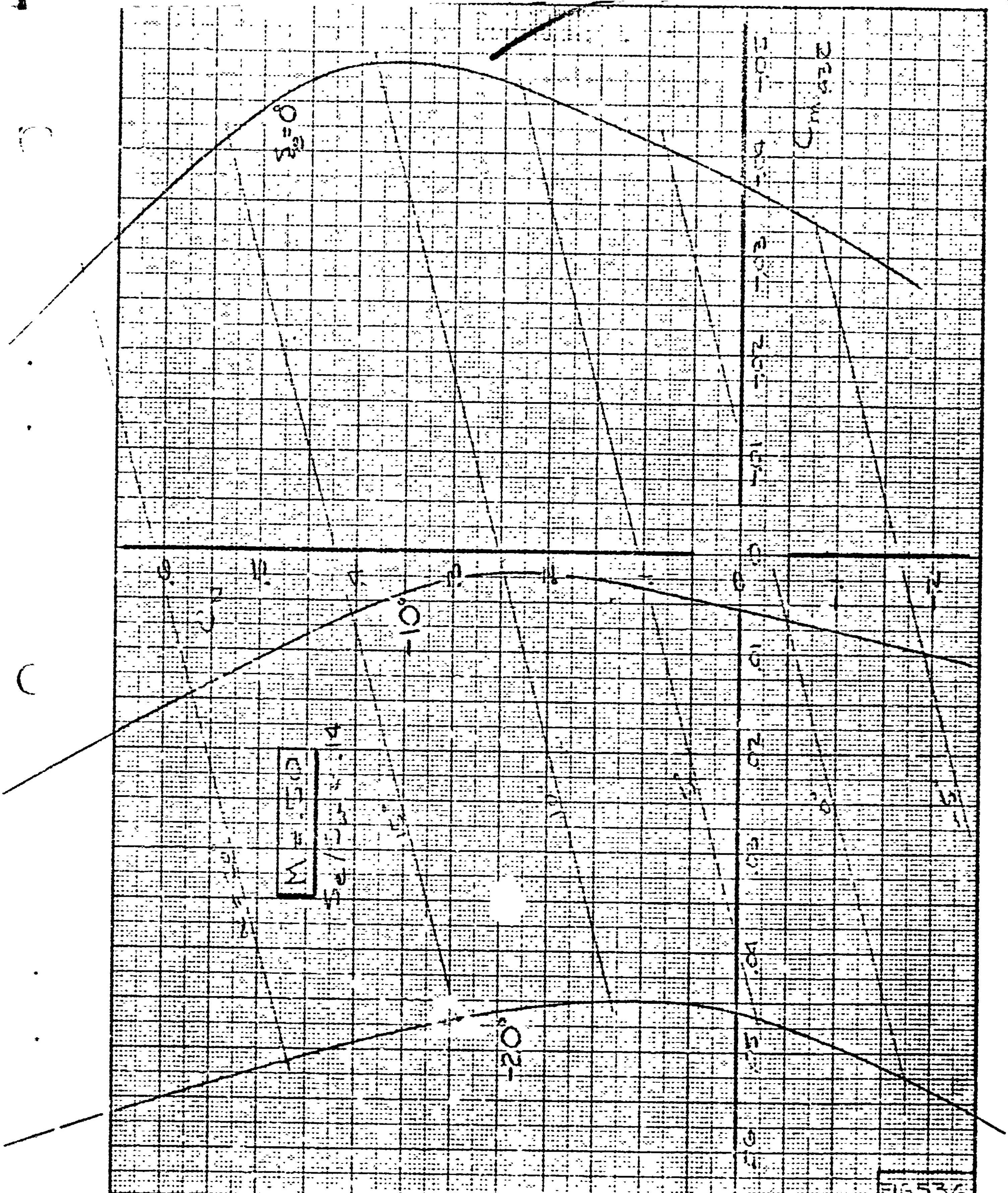

FIG. 53.6

| CALC | DCL | 2/9/0 | REVISED | DATE |
|---|---|---|---|---|
| CHECK | | | | |
| APR | | | | |
| APR | | | | |

LONGITUDINAL STABILITY
WING TIPS RETRACTED
M = .5

644-2035

D2-8174

BOEING AIRPLANE COMPANY

53

PAGE 521

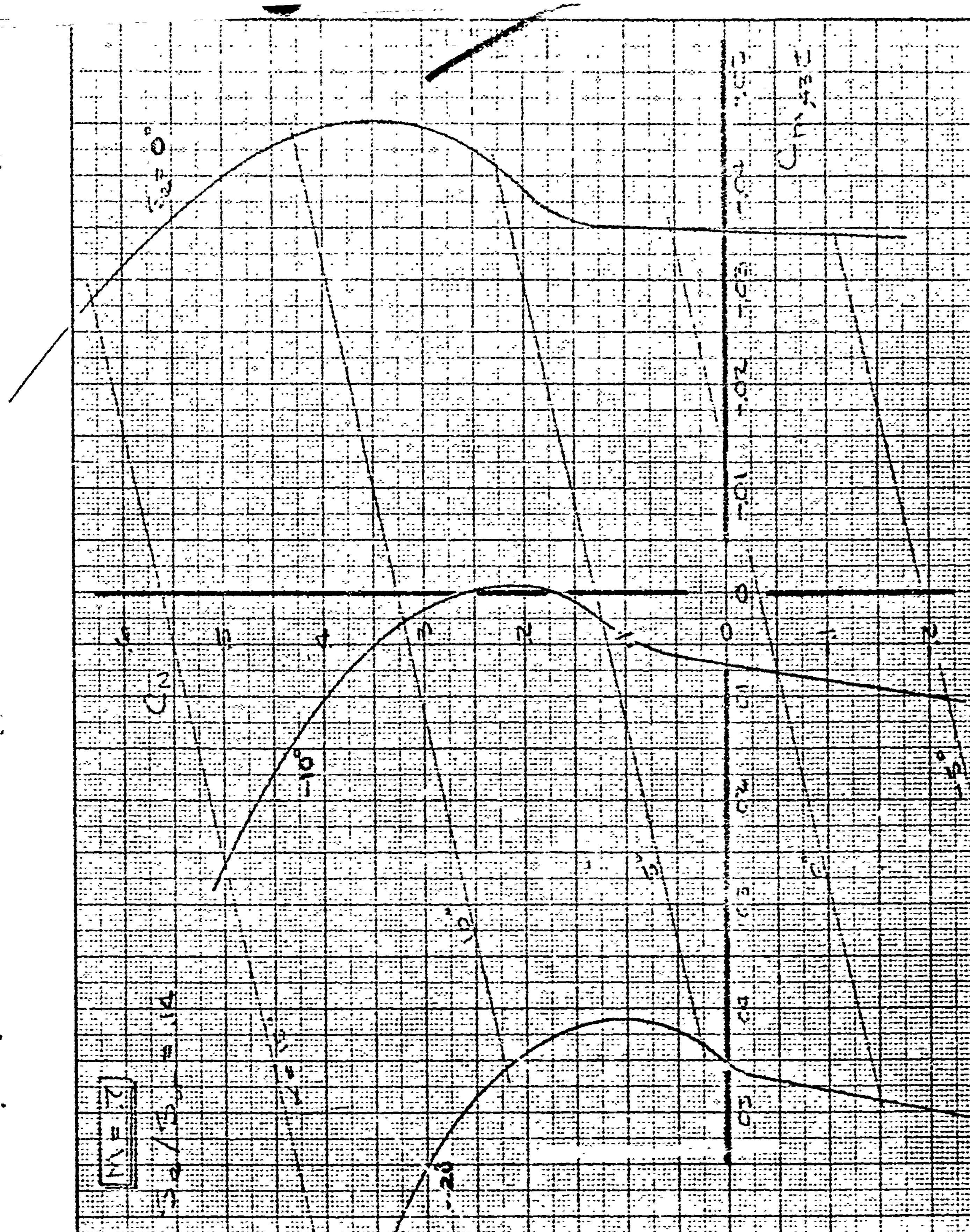

FIG 5.27

| CALC | DCL | 12/21/5? | REVISED | DATE | LONGITUDINAL STABILITY<br>WING TIPS RETRACTED<br>M = .7 | 844-2035 |
|---|---|---|---|---|---|---|
| CHECK | | | | | | D2-8174 |
| APR | | | | | BOEING AIRPLANE COMPANY | PAGE 5.22 |
| APR | | | | | | |

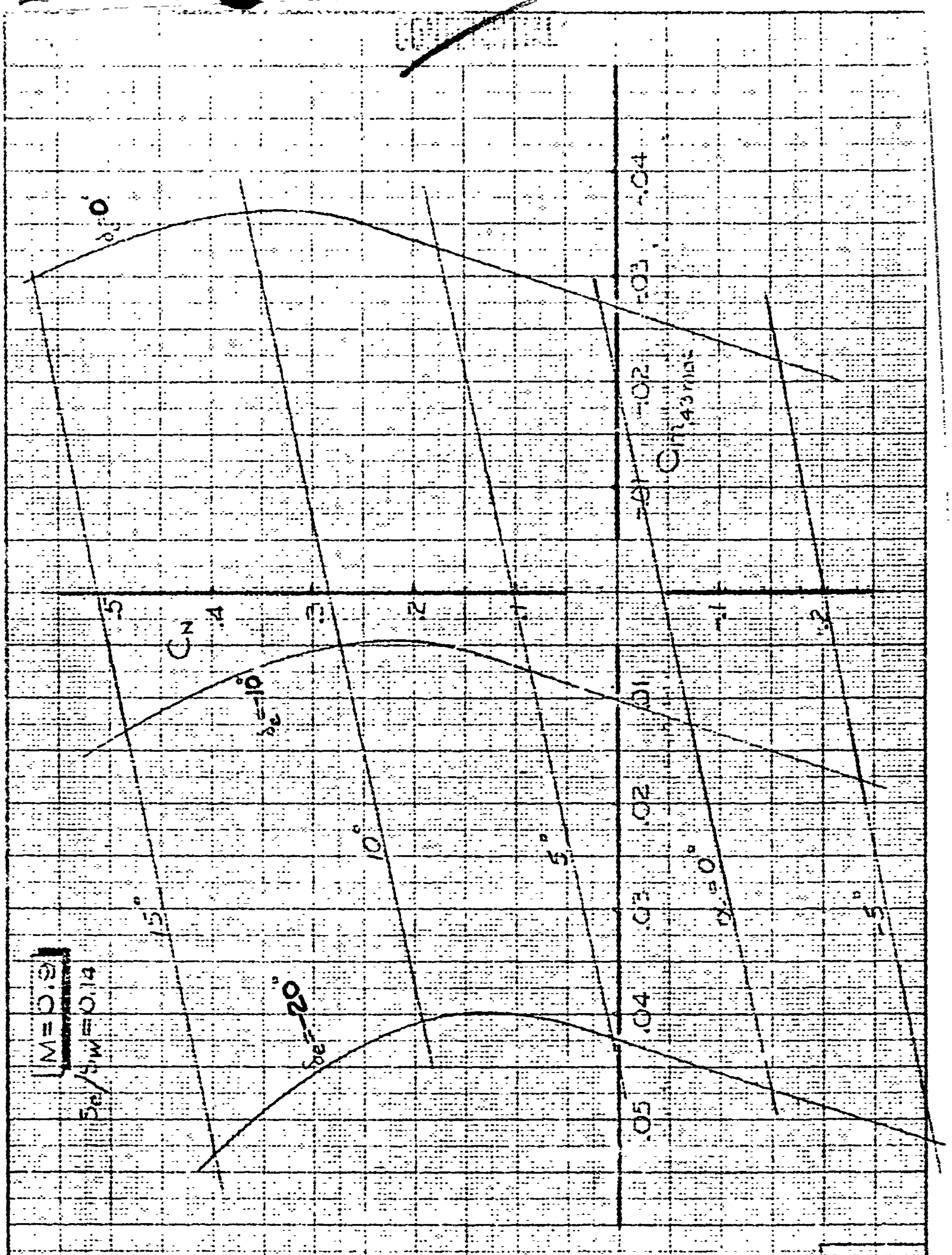


FIG.5.3.8

| | | |
|---|---|---|
| CA M. CARTER 12-7-60 | LONGITUDINAL STABILITY WING TIPS RETRACTED, M=.9 | 844-2035 |
| CHECK | | D2-8174 |
| APP | BOEING AIRPLANE COMPANY | 55 |
| APP | | PAGE 5.23 |

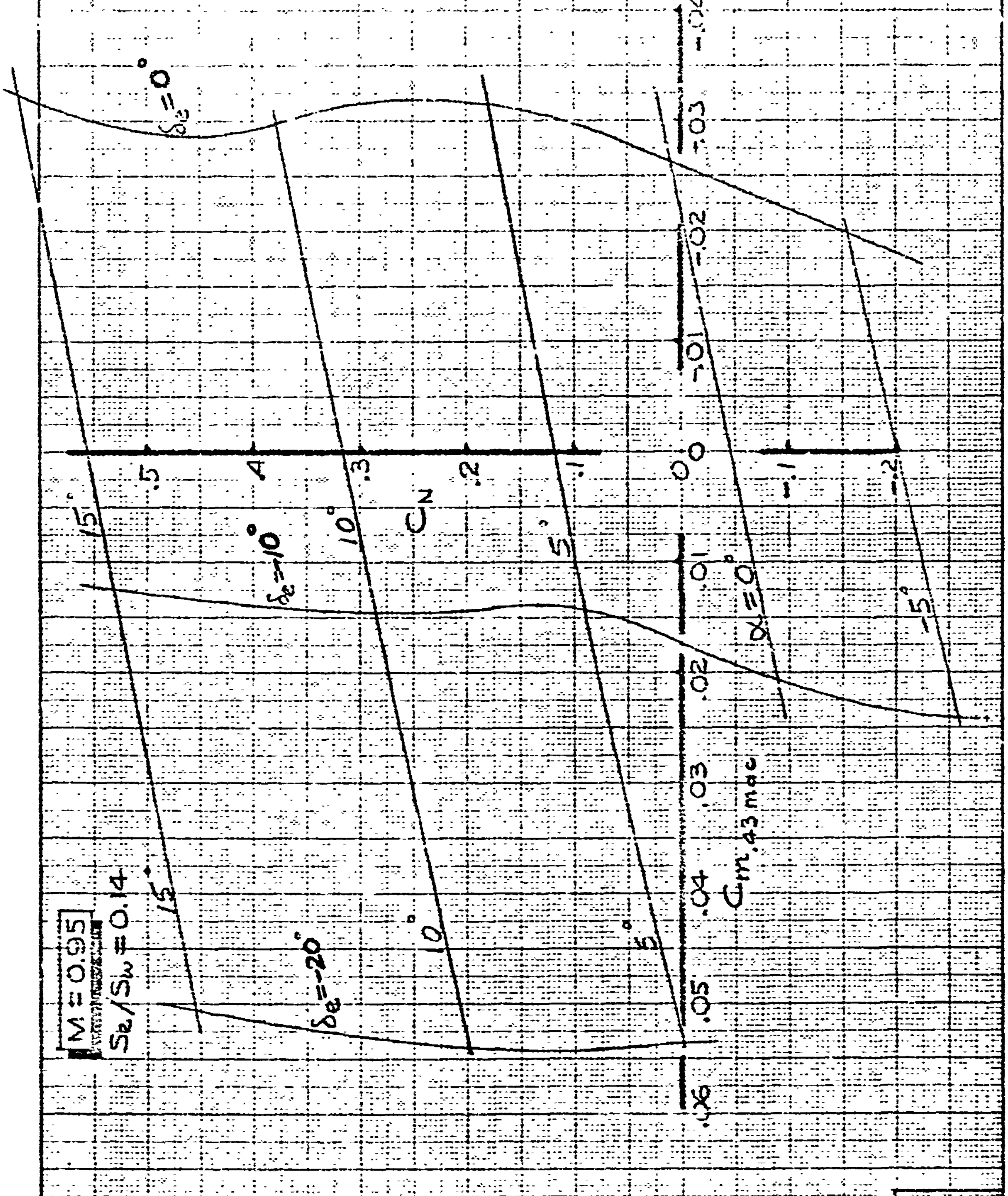


FIG 5.39

M. CARTER 12-9-60

LONGITUDINAL STABILITY
WING TIPS RETRACTED, M=.95

644-2035

D2-6174

BOEING AIRPLANE COMPANY 56

PAGE 5.24

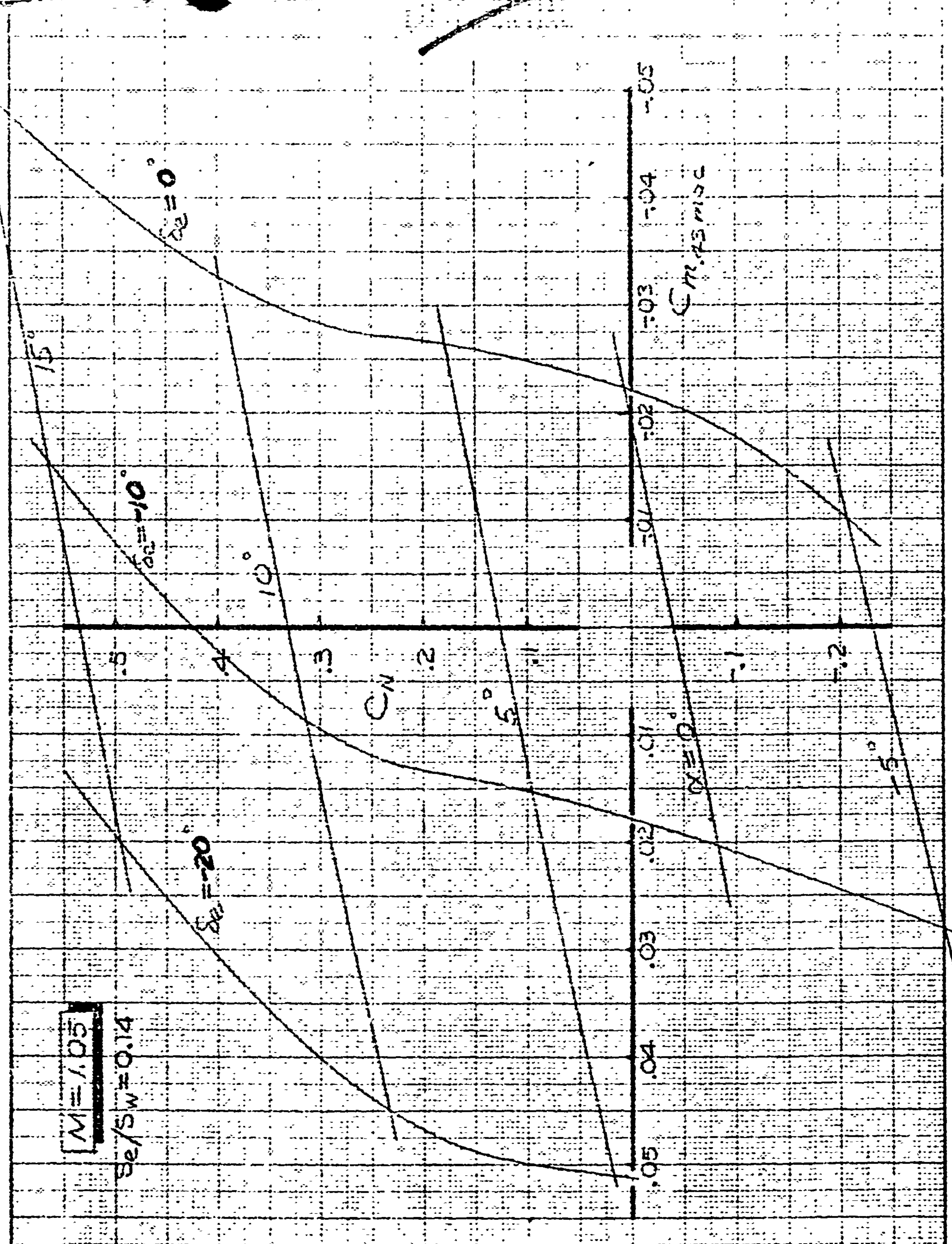


FIG 5.3.10

| CH | M. CARTER | 12-9-60 | REVISED | DATE | LONGITUDINAL STABILITY 844-2035 |
|---|---|---|---|---|---|
| CHECK | | | | | WING TIPS RETRACTED, M=1.05 D2-8174 |
| APP | | | | | |
| APP | | | | | BOEING AIRPLANE COMPANY 57 PAGE 5.25 |

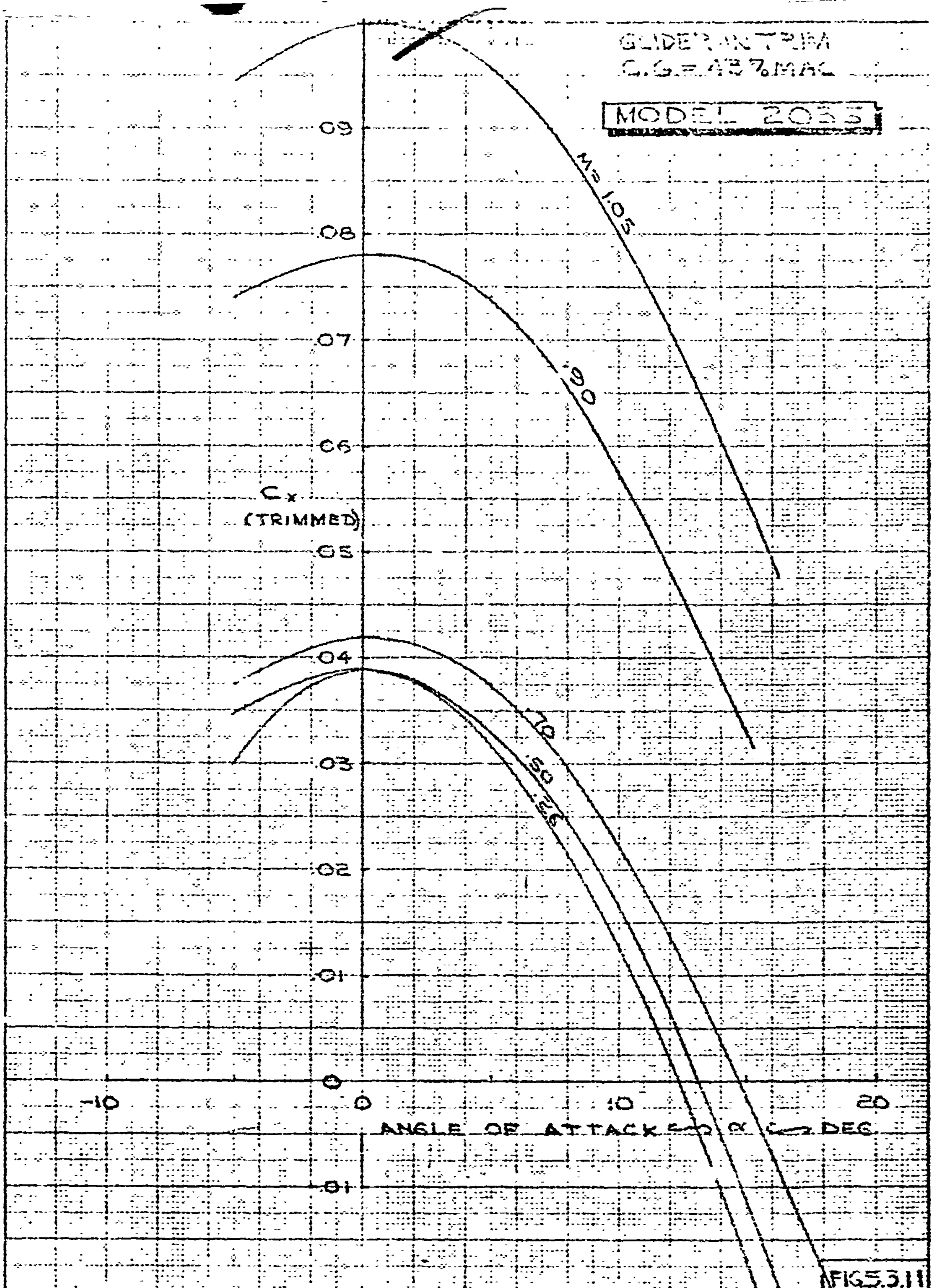


FIG 5.3.11

| | | |
|---|---|---|
| DEZ 12/22/60 | CHORD FORCE COEFFICIENT<br>WING TIPS EXTENDED | 844-2035 |
| | | D2-8174 |
| | BOEING AIRPLANE COMPANY **58** | PAGE 5.3.3 |

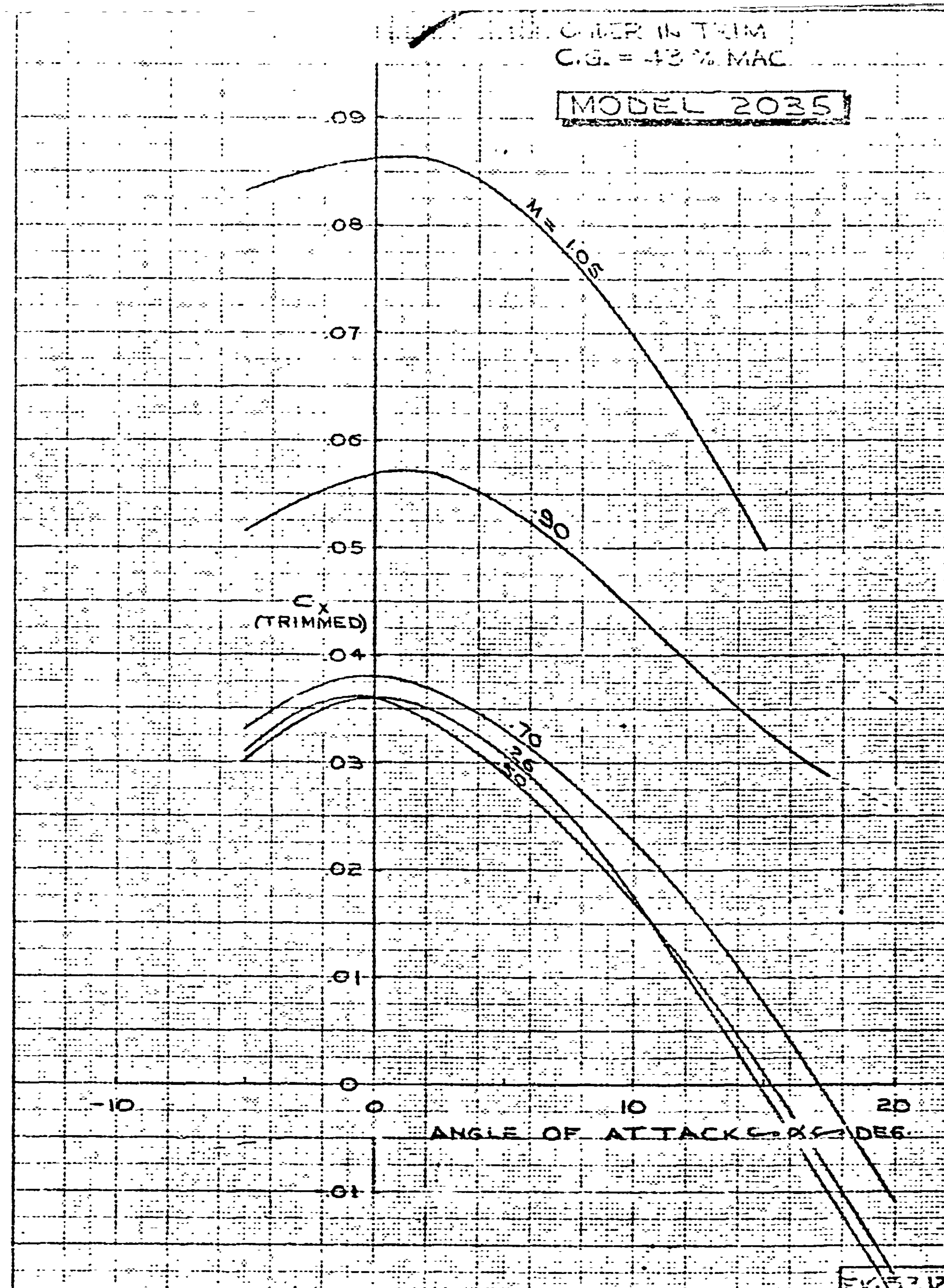


FIG 5.3.12

DEZ 12/22/60

CHORD FORCE COEFFICIENT
WING TIPS RETRACTED

BOEING AIRPLANE COMPANY

044-2035

D2-8174

PAGE 527

5.4 SUPERSONIC

Longitudinal stability and control characteristics at supersonic speeds for Mach numbers of 1.6, 2.0 and 3.5 are shown for wing tip extensions retracted, Figures 5.4.4 through 5.4.6 and for wing tip extensions extended, Figures 5.4.1 through 5.4.3. These curves were derived from wind tunnel tests performed in the Boeing Supersonic Wind Tunnel. The 814-1058 glider configuration was tested with variations in model components to give parametric data. The parametric data were corrected by theoretical methods to obtain predictions of pitch characteristics on the 844-2035 configuration.

Chord force coefficient data for the glider in trim and with wing tips extended are shown on Figure 5.4.7. Data with the tip extensions retracted are shown on Figure 5.4.8.

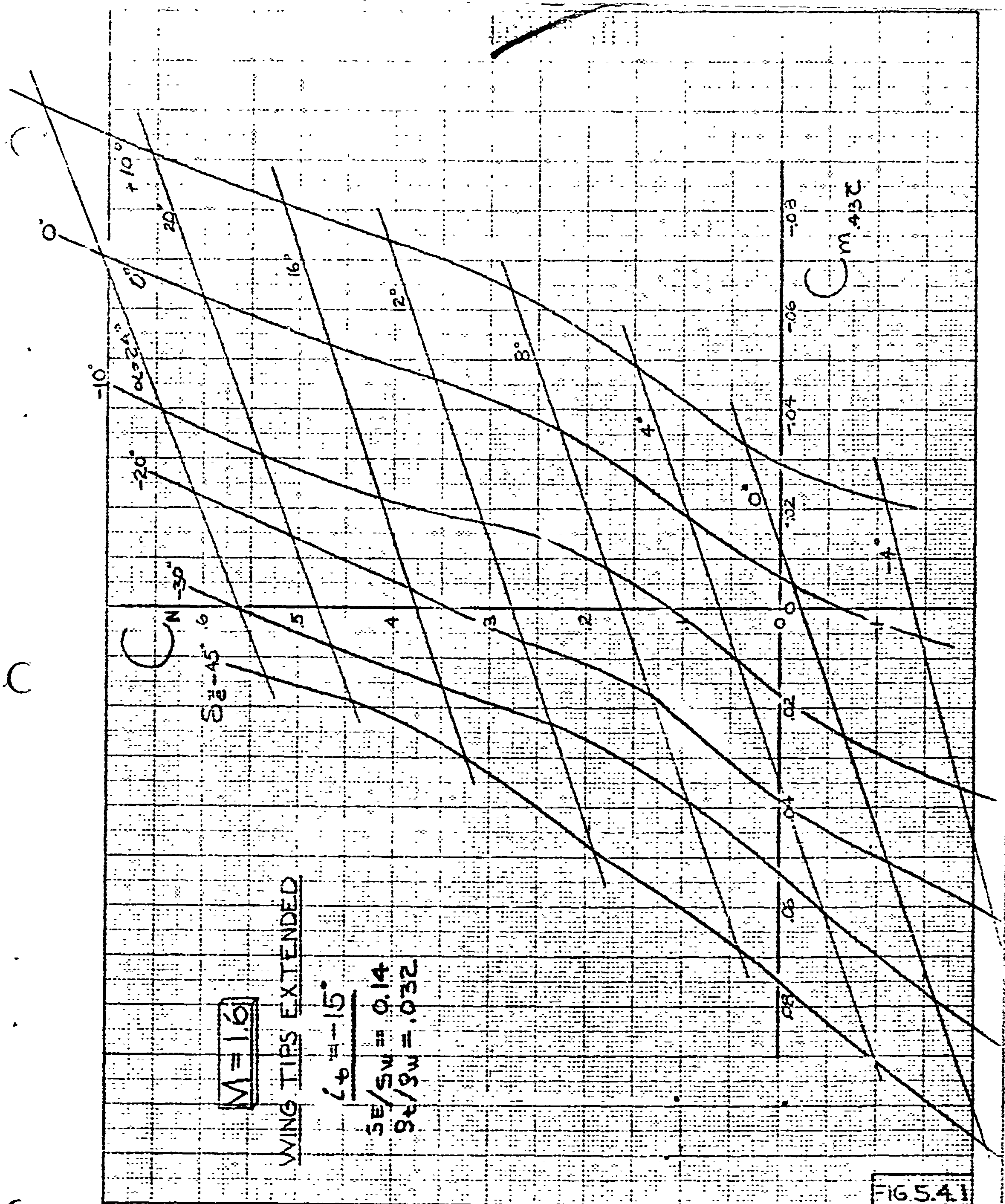


FIG. 5.4.1

DJR 12-8-61

LONGITUDINAL STABILITY
WING TIPS EXTENDED M=1.6

844-2035

D2-8174

BOEING AIRPLANE COMPANY

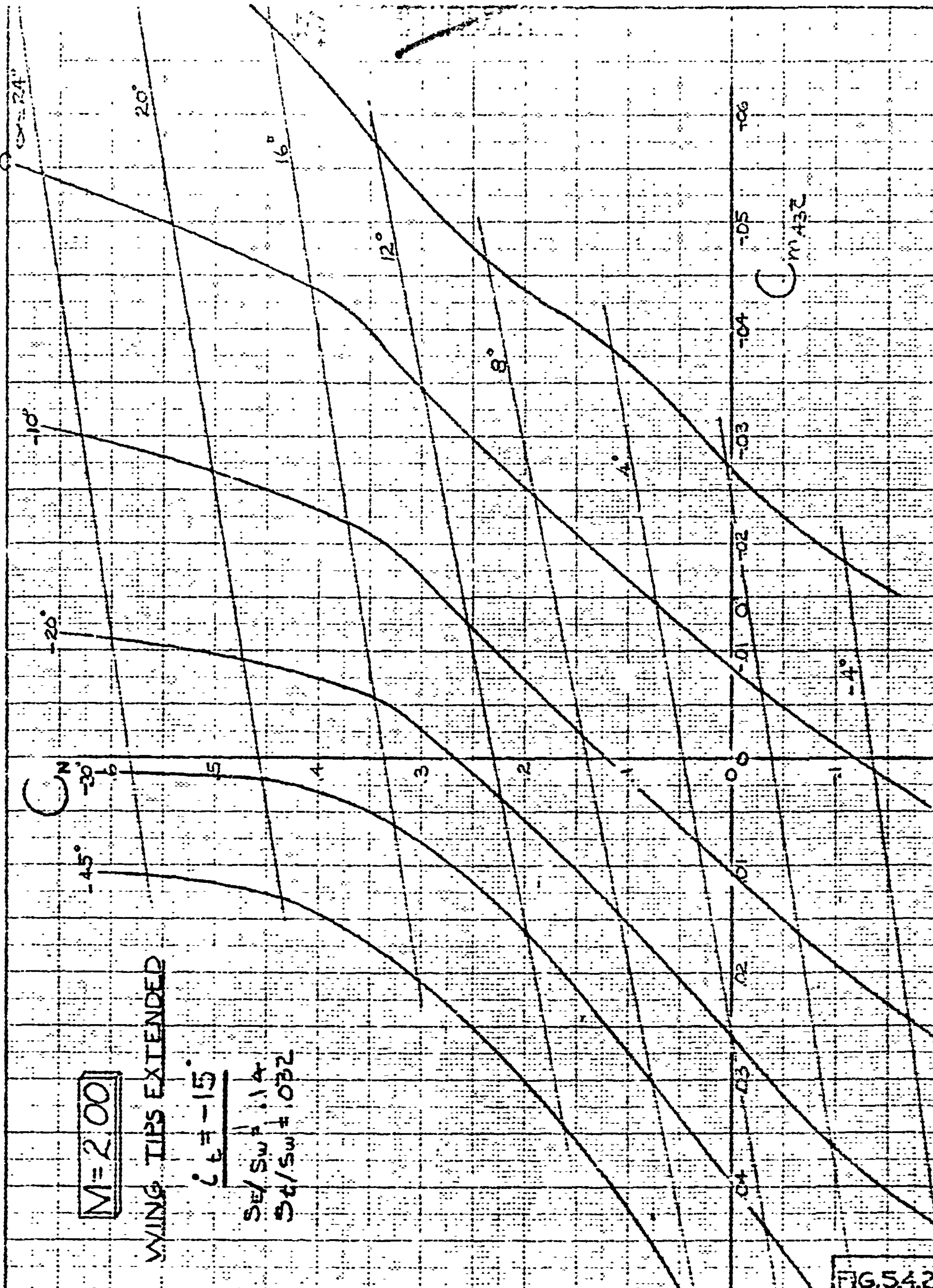


FIG. 5.4.2

| | | | |
|---|---|---|---|
| DJR | 12-7-0 | LONGITUDINAL STABILITY WING TIPS EXTENDED M=2.0 | 844-2035 |
| CHECK | | | D2-8174 |
| APR | | BOEING AIRPLANE COMPANY | 62 |
| APR | | | PAGE 5.30 |

CONFIDENTIAL

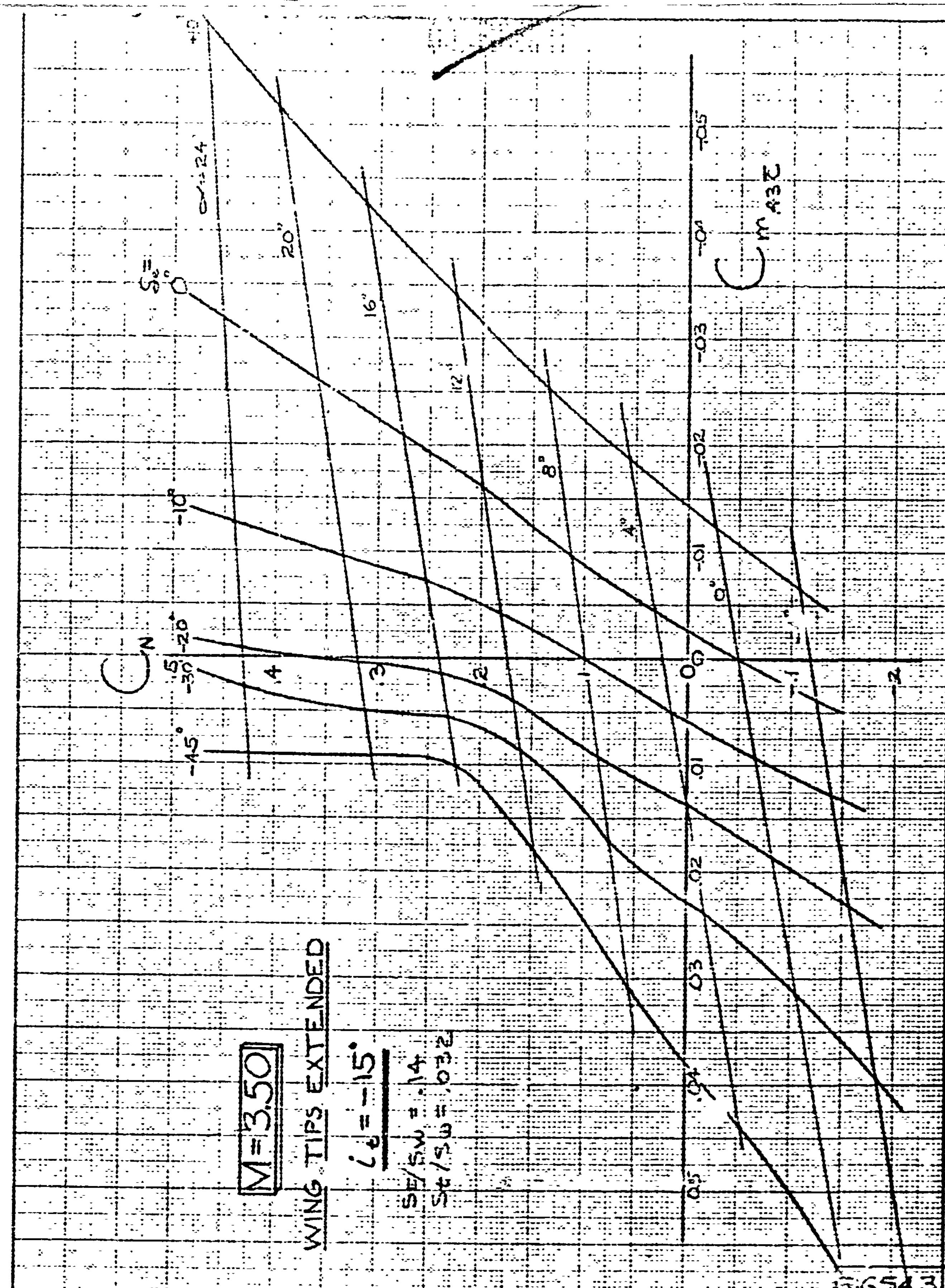


FIG 5.4.3

| DJR | R-7-0 | REVISED | DATE | LONGITUDINAL STABILITY WING TIPS EXTENDED M=3.5 | 844-2035 |
|---|---|---|---|---|---|
| CHECK | | | | | D2-8174 |
| APP | | | | BOEING AIRPLANE COMPANY 63 | PAGE 5.31 |
| APR | | | | | |

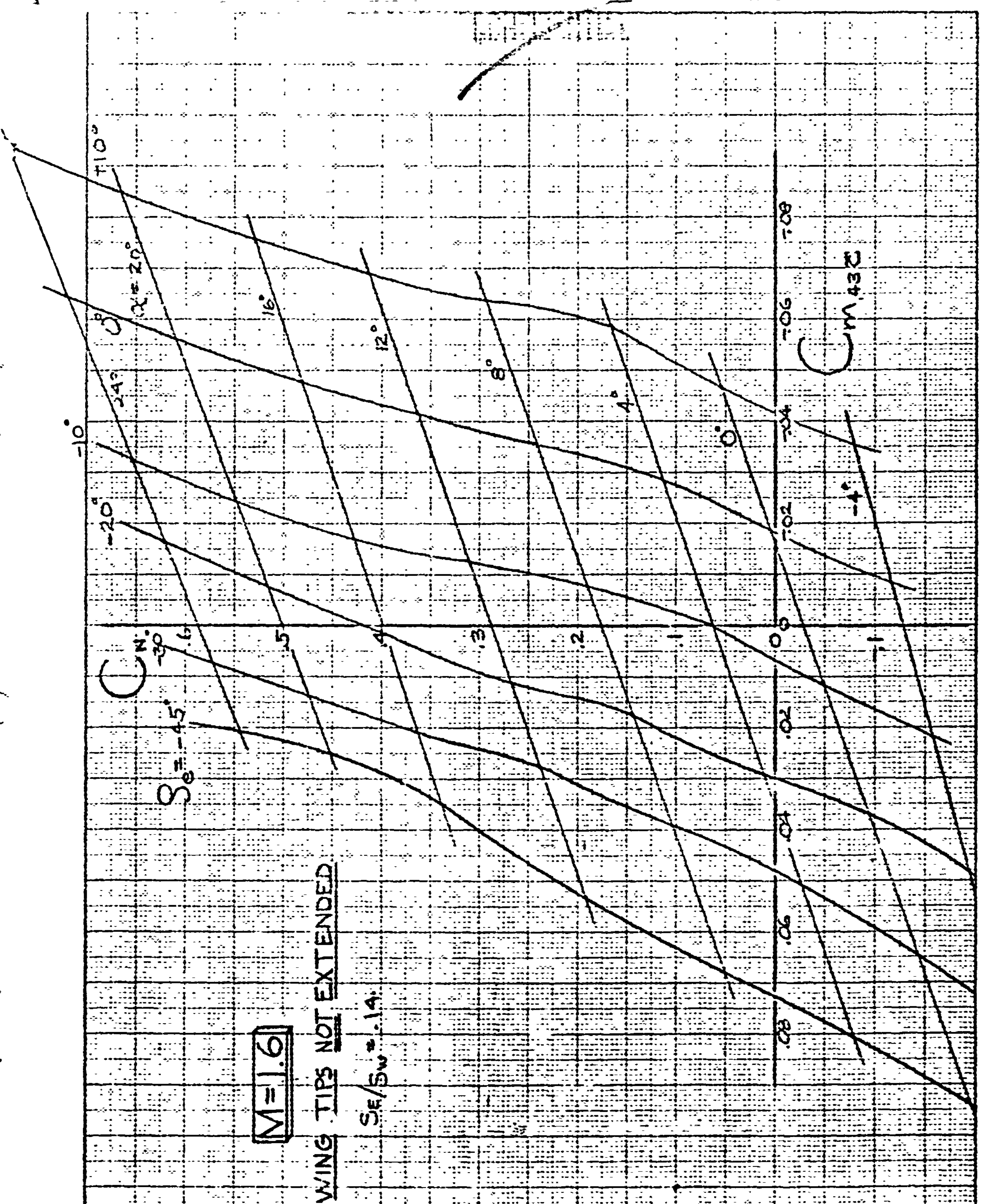


FIG. 5.4.4

| | | | |
|---|---|---|---|
| DJR | 12-2-0 | REVISED | DATE |
| CHECK | | | |
| APR | | | |
| APR | | | |

LONGITUDINAL STABILITY
WING TIPS RETRACTED M=1.6

844-2035

D2-8174

BOEING AIRPLANE COMPANY

**64** PAGE 5.32

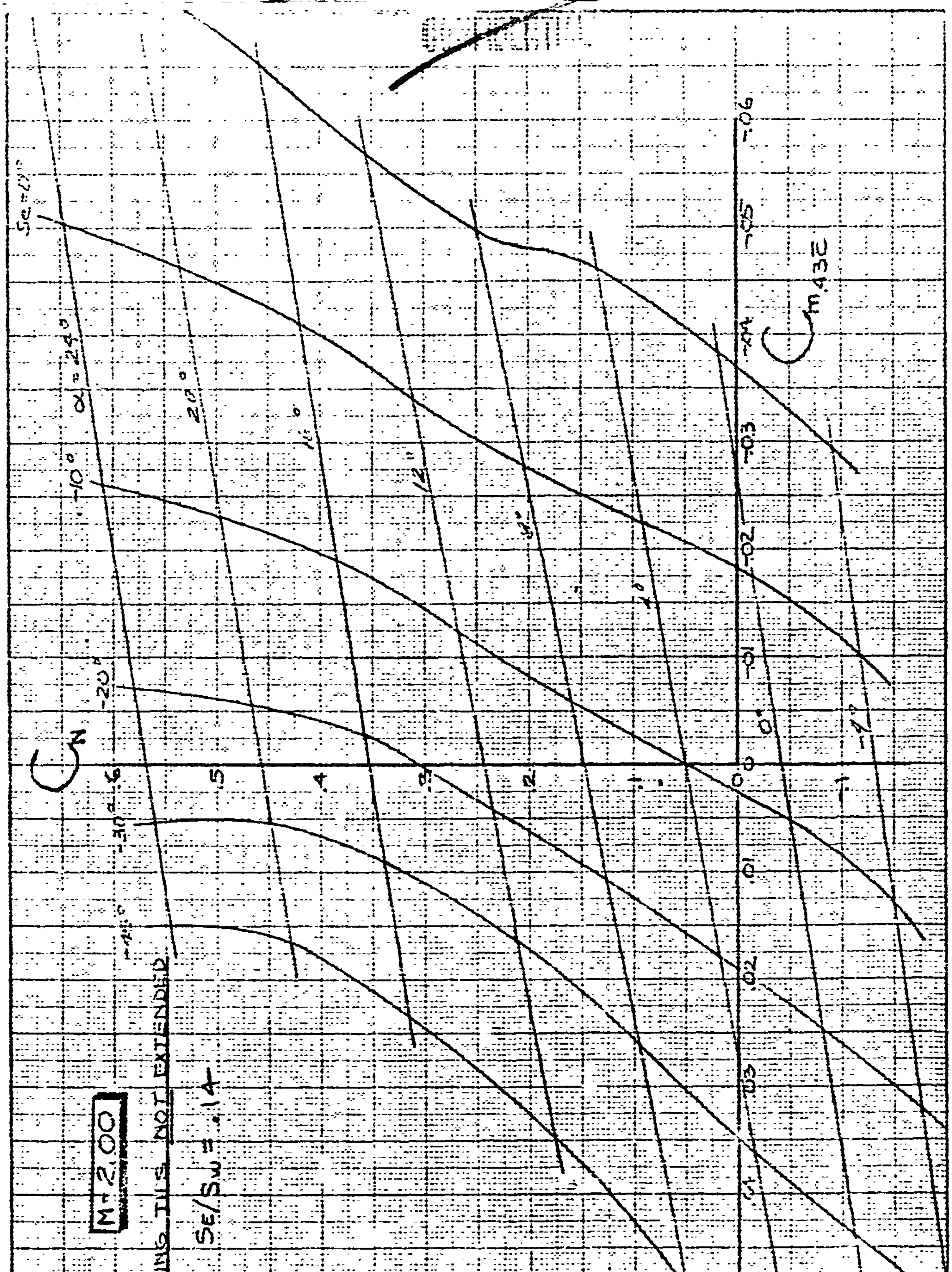


FIG 5.4.5

| | | | |
|---|---|---|---|
| CALC R.K.R. | 12-2-60 | REVISED | DATE |
| CHECK | | | |
| APR | | | |
| APR | | | |

**LONGITUDINAL STABILITY**
**WING TIPS RETRACTED M=2.0**

844-2035

D2-8174

BOEING AIRPLANE COMPANY

65 PAGE 5.33

~~CONFIDENTIAL~~

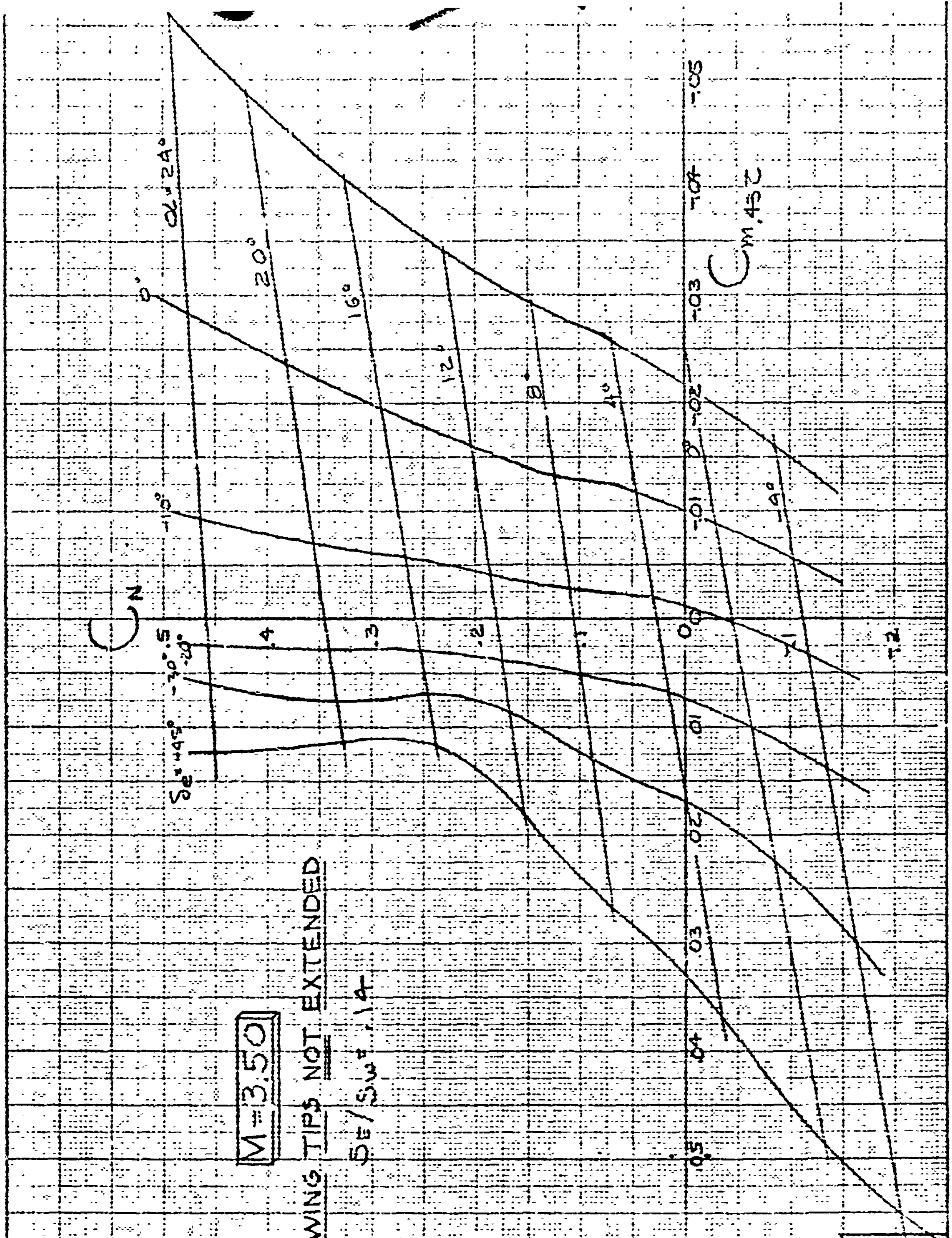


FIG. 5.4.6

| | | | |
|---|---|---|---|
| DJR 12-2-0 | REVISED DATE | LONGITUDINAL STABILITY | 844-2035 |
| CHECK | | WING TIPS RETRACTED M=3.5 | D2-8174 |
| APP | | | |
| APP | | BOEING AIRPLANE COMPANY **66** | PAGE 5.34 |

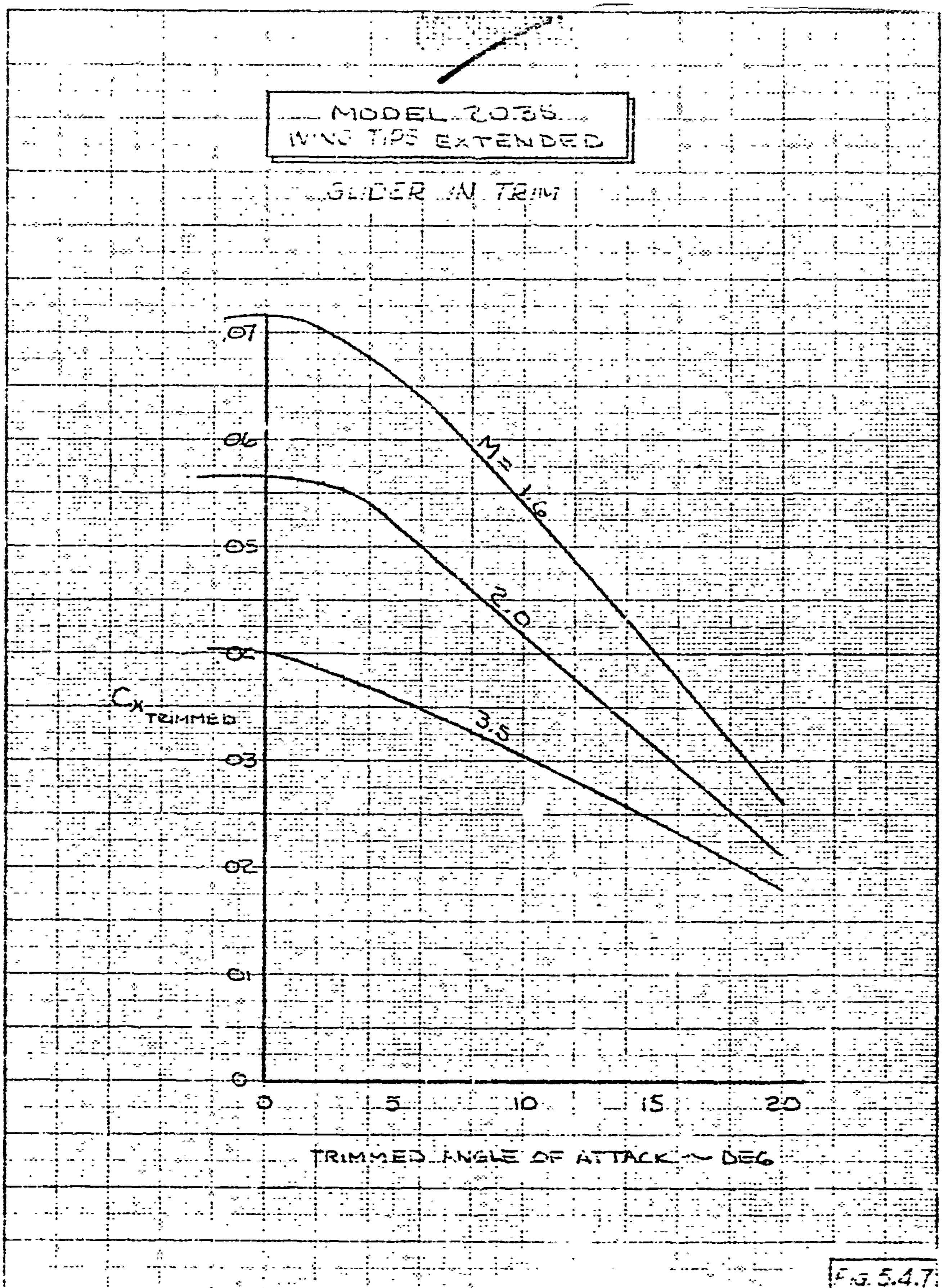


Fig. 5.4.7

WEJ 12/22/60

SUPERSONIC CHORD FORCE COEFFICIENT WING TIPS EXTENDED

D2-8174

BOEING AIRPLANE COMPANY

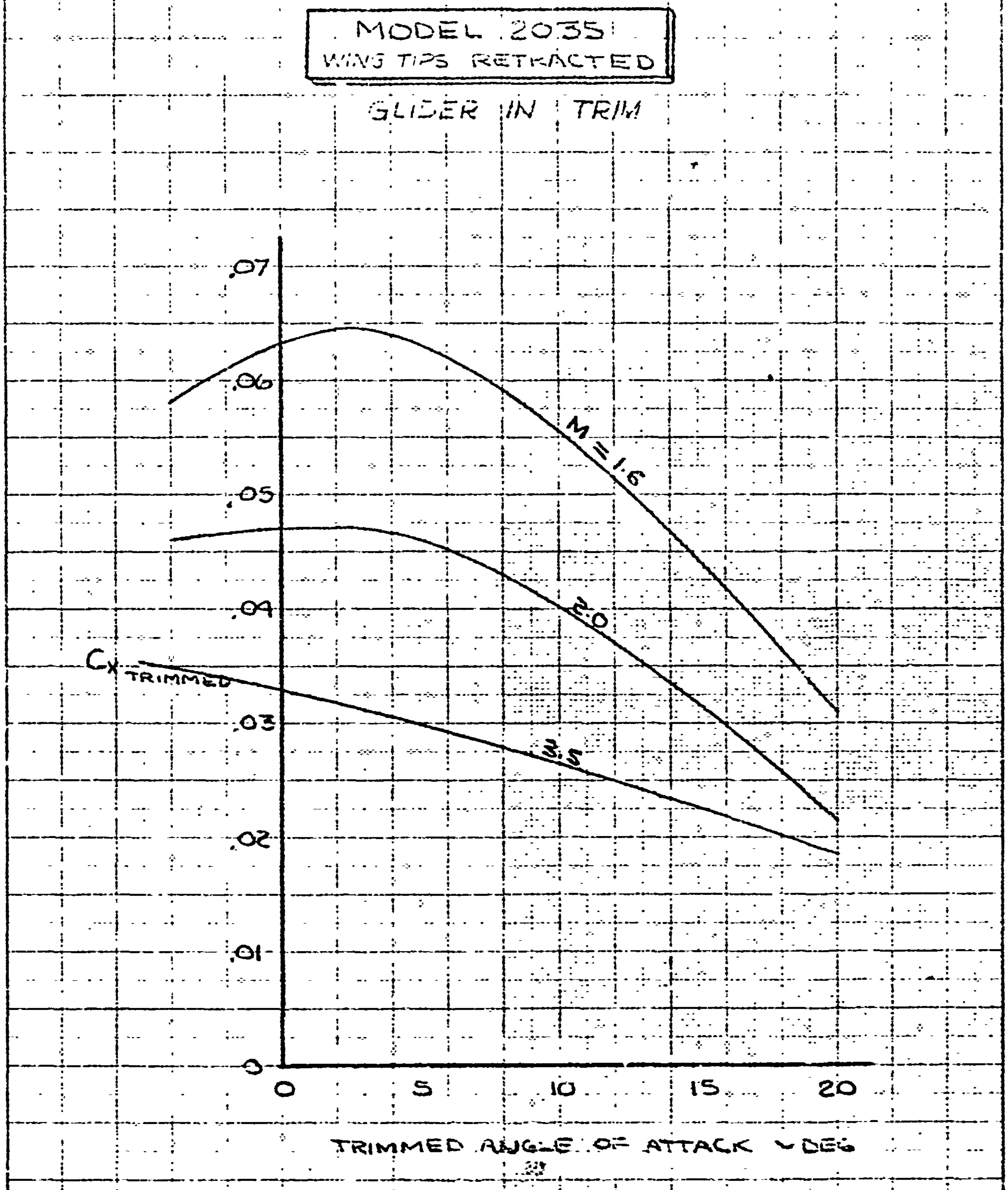


FIG. 5.4.8

WEJ 12/22/60

SUPERSONIC CHORD FORCE COEFFICIENT
WING TIPS RETRACTED

644-2035

D2-8174

BOEING AIRPLANE COMPANY

### 5.5 HYPERSONIC SPEEDS

Longitudinal stability and control characteristics for the 744-2035 glider configuration are shown on Figures 5.5.1 through 5.5.3. Data are shown on Figure 5.5.1 for a Mach number of 8 and the cold shape glider. This assumes the glider to have the manufactured, or jig shape, configuration. Data are shown on Figures 5.5.2 and 5.5.3 at a Mach number of 8.0 and 22.0 for the "hot shape" glider. This assumes that the glider has assumed its maximum structural deformation due to thermal effects.

The data presented are based on wind tunnel tests in the following facilities:

1) A.E.D.C. Tunnel B, M=8.08

2) J.P.L. 21-Inch Hypersonic Tunnel, M=9.5

3) L.R.C. 11-Inch Hypersonic Tunnel, M=9.6

4) Boeing 44-Inch Hotshot Tunnel, M=16 and 22

These data were corrected to the present configuration by theoretical methods (Modified Newtonian Flow Theory and Shock Expansion Theory, particularly for elevon effectiveness). The incremental effect of the "hot shape" glider was determined by Modified Newtonian Flow Theory.

The effect of altitude or Reynolds number change at a constant Mach number is not included. Work is currently in progress in this area. Some variation of characteristics between M=8 and 22 can also be anticipated. Wind tunnel tests are currently in progress to define this variation.

Chord force data as a function of angle of attack for Mach numbers of 8 and 22 are presented on Figure 5.5.4. These data are for the glider trimmed at the various angles of attack.

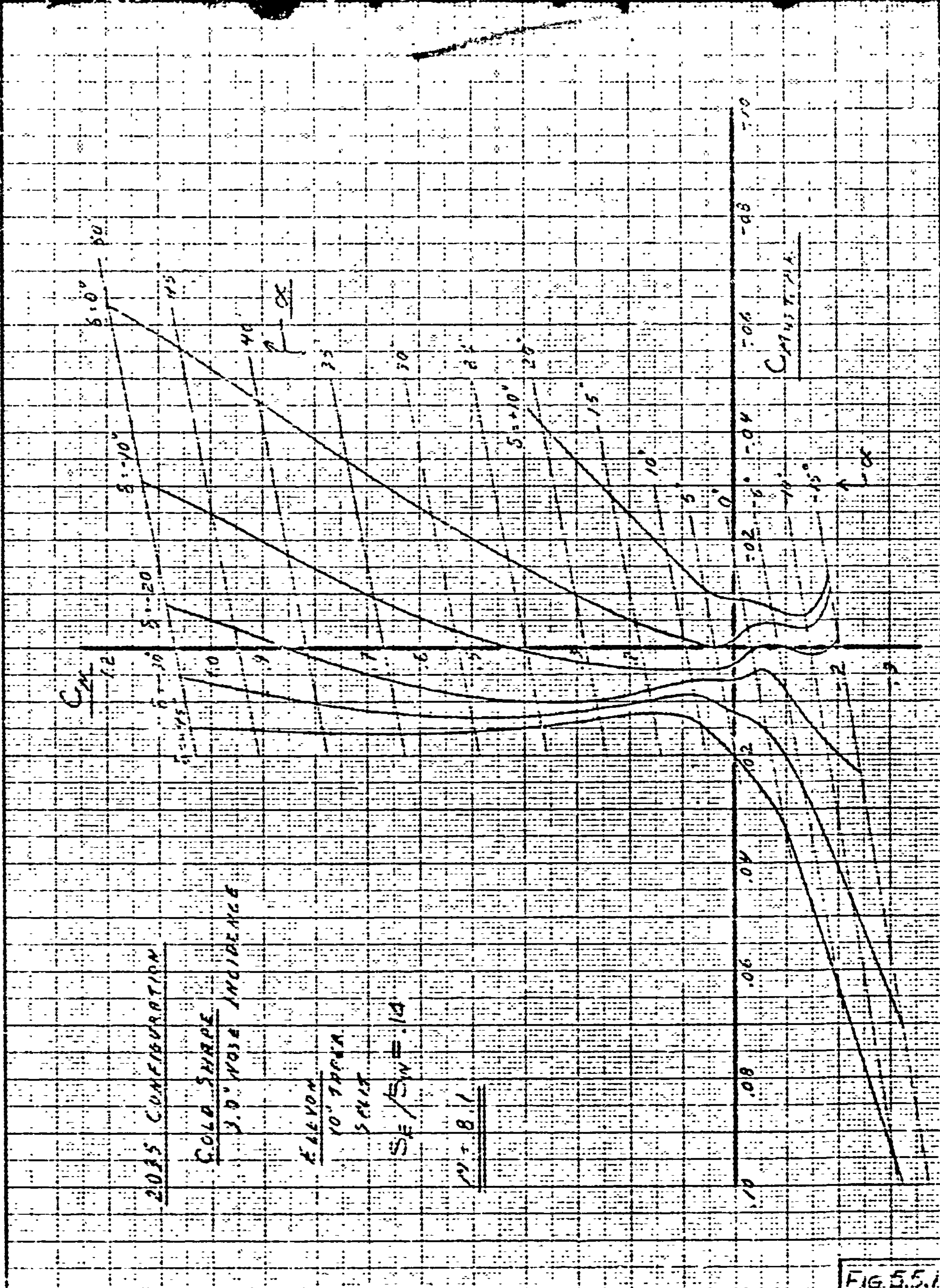


FIG. 5.5.1

| CALC | PW | 12-2-60 | REVISED | DATE | LONGITUDINAL STABILITY<br>COLD SHAPE<br>M = 3.1 | 70 | 844-2035 |
|---|---|---|---|---|---|---|---|
| CHECK | | | | | | | D2-8174 |
| APR | | | | | | | |
| APR | | | | | BOEING AIRPLANE COMPANY<br>SEATTLE 24, WASHINGTON | | PAGE 538 |

SAC 461 C-R4

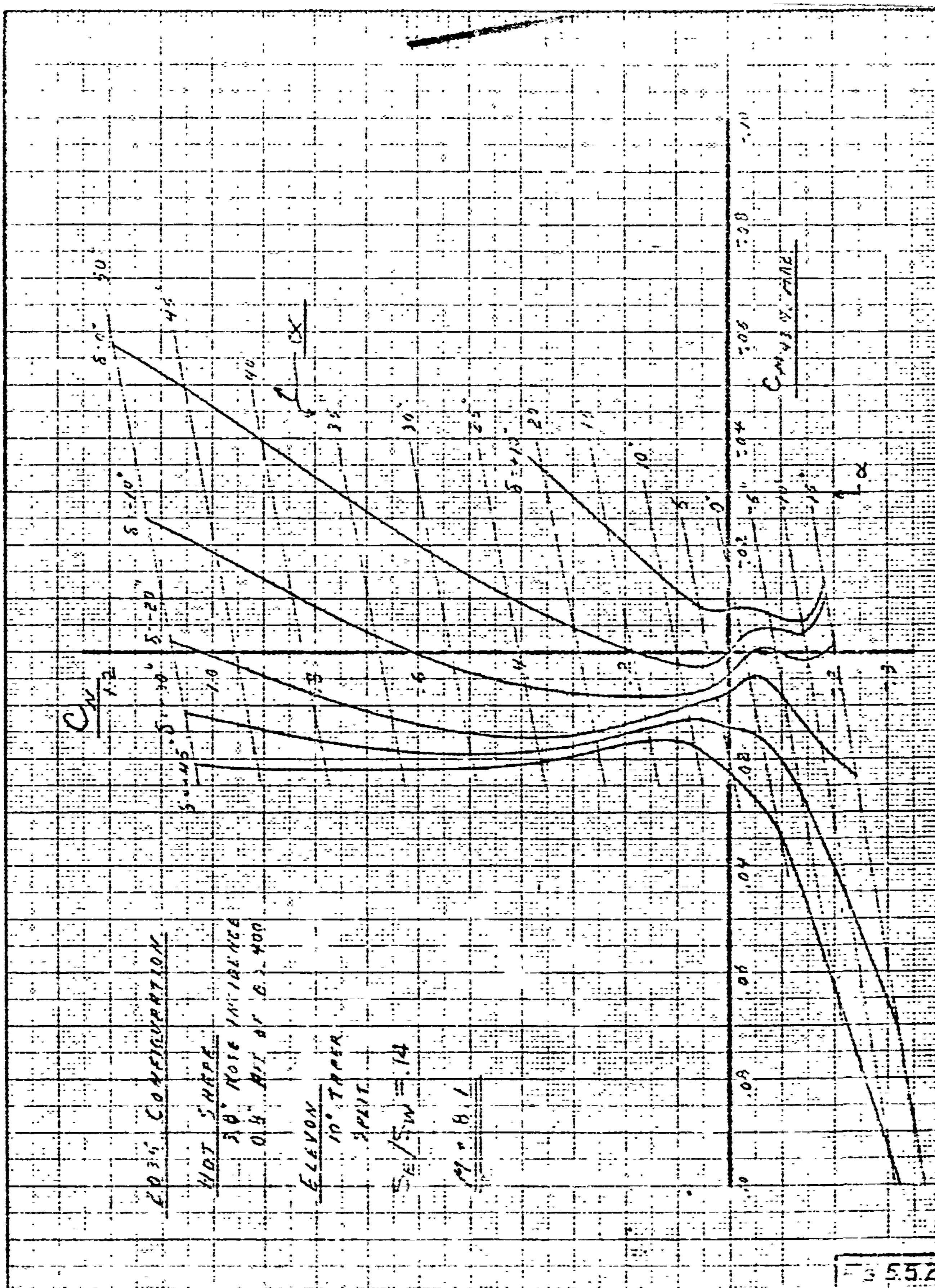


Fig 5.5.2

| CALC | P.W. 12-?-60 | REVISED | DATE |
|---|---|---|---|
| CHECK | | | |
| APR | | | |
| APR | | | |

LONGITUDINAL STABILITY
HOT SHAPE
M = 8.1

71

844-2035

D2-8174

BOEING AIRPLANE COMPANY
SEATTLE 24, WASHINGTON

PAGE 5.39

EAC 461 C-R4

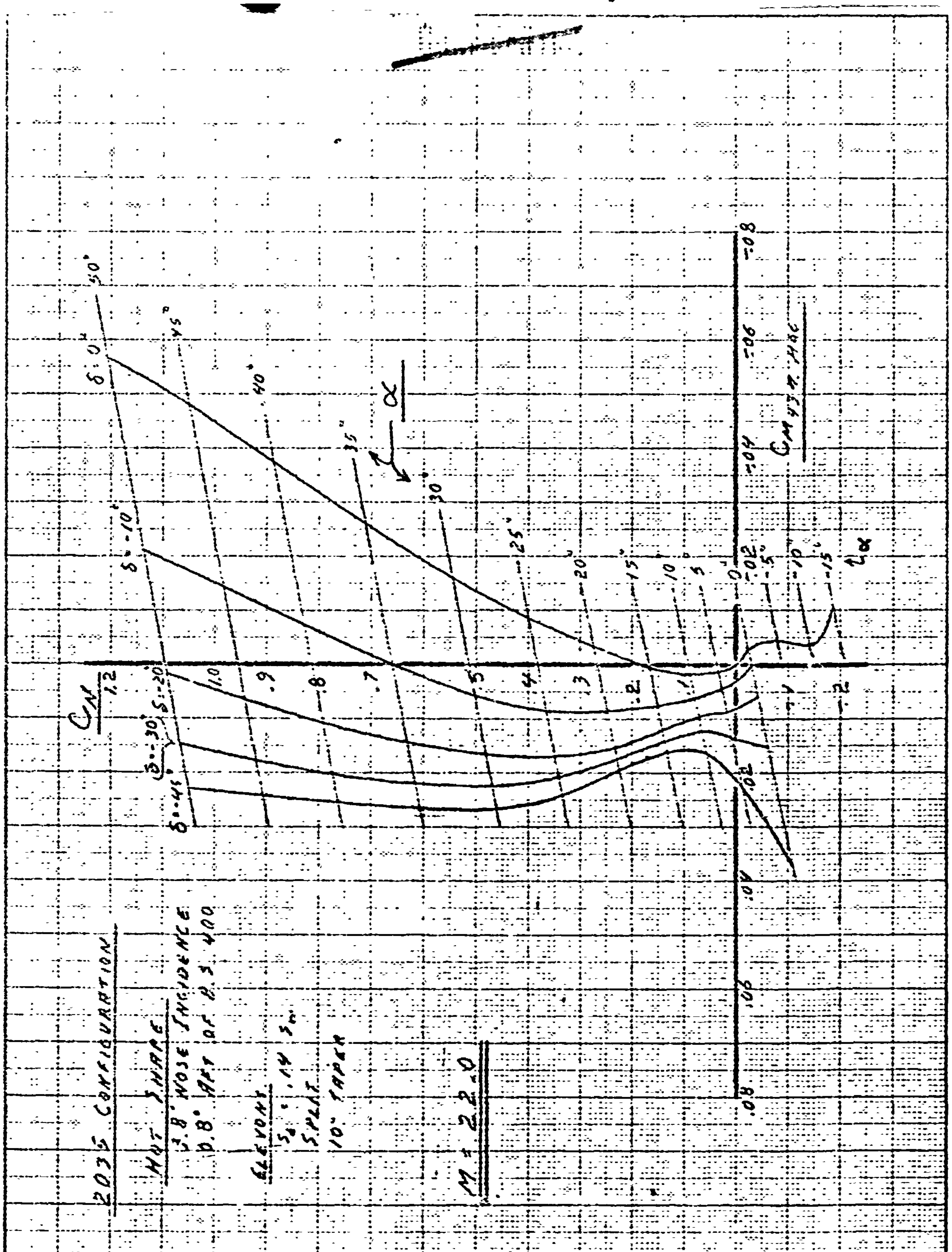


Fig. 5.53

| | | | |
|---|---|---|---|
| AW 12-9-60 | REVISED / DATE | LONGITUDINAL STABILITY<br>HOT SHAPE<br>M = 22.0 | 844-2035 |
| | | 72 | D2-8174 |
| | | BOEING AIRPLANE COMPANY | PAGE 540 |

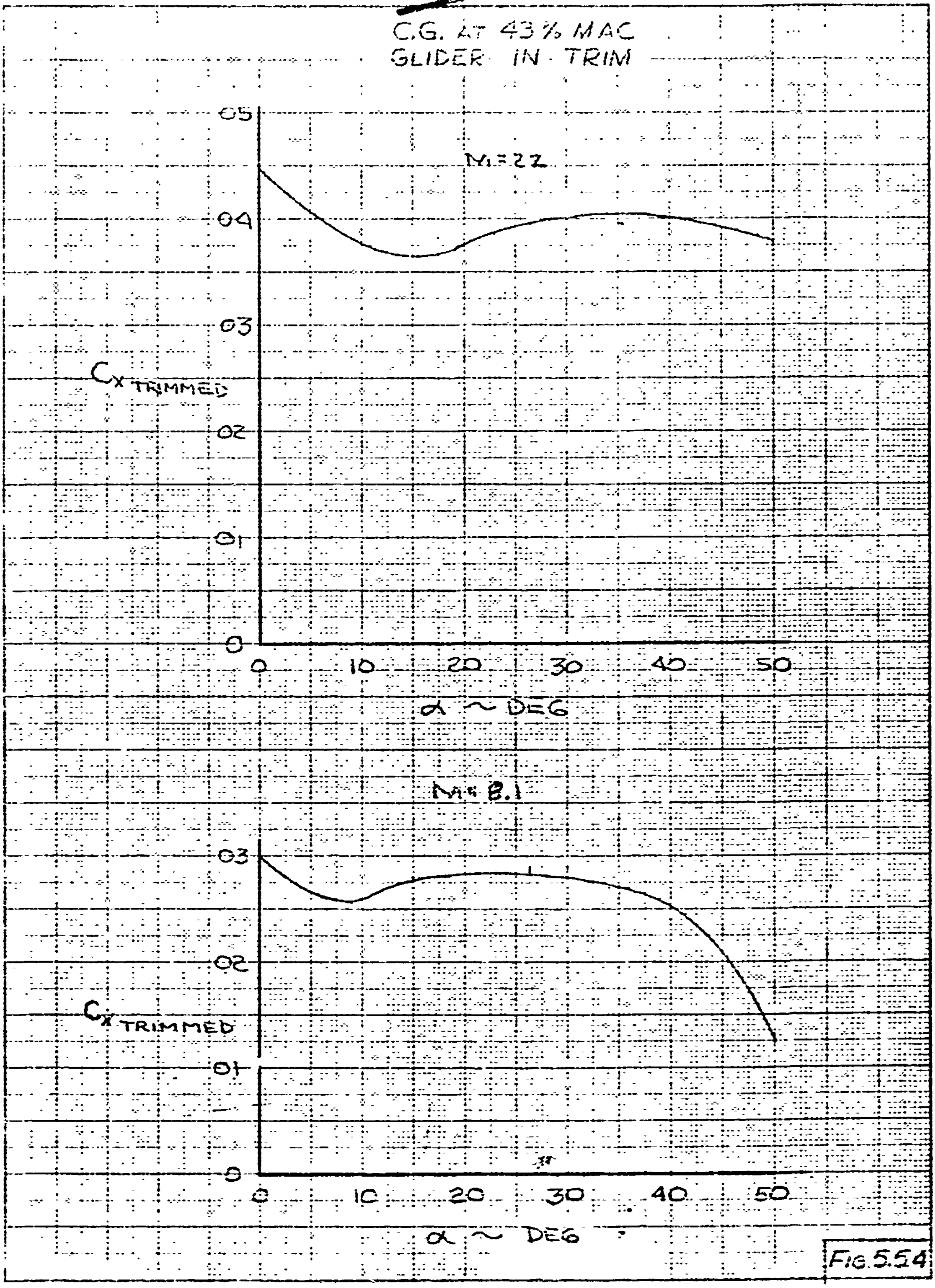


FIG. 5.54

W.E.J. 12-12-0

HYPERSONIC CHORD FORCE COEFFICIENT

844-2035

D2-8174

5.6 SPEED BRAKES (DRAG BRAKE)

The incremental effect of extending the speed brakes on longitudinal stability is shown on Figure 5.6.1. Data are shown at the three Mach numbers where test data have been obtained. The test data were obtained in the Boeing Transonic and Supersonic Wind Tunnels and have been modified to the present configuration. Further study of speed brake location, to minimize trim and stability changes, is being conducted.

The incremental effect of the speed brakes on axial force is shown on Figure 5.6.2 at supersonic and low speed.

DATA BASED ON BSWT 018.

$S_B/S_W = .0218$

BRAKE DEFLECTED 60°

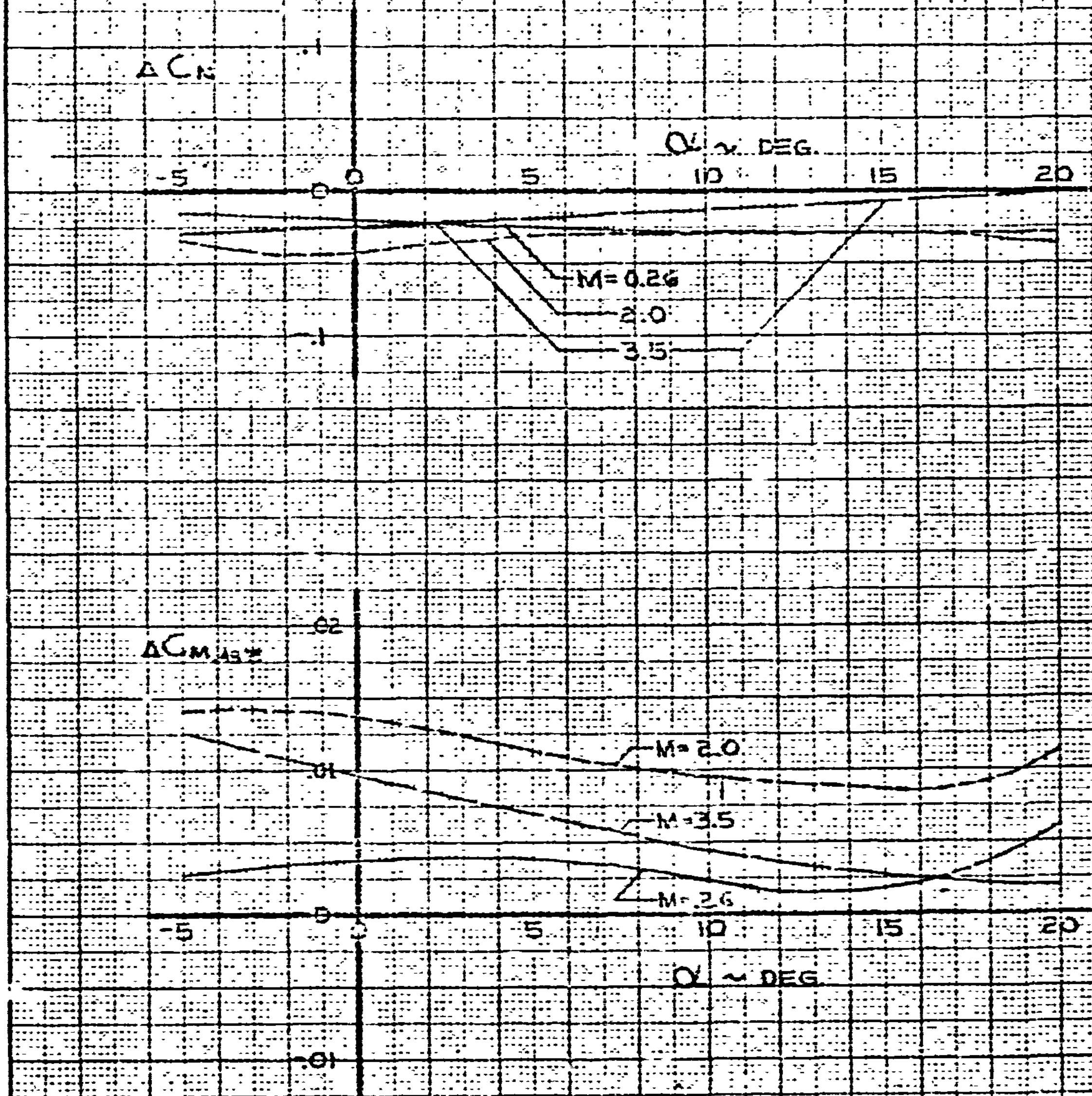


Fig. 5.8.7

| CALC | J. FRANCIS | 12-9-60 | REVISED | DATE |
|---|---|---|---|---|
| CHECK | | | | |
| APR | | | | |
| APR | | | | |
| TRAC | N.J. | 12-9-60 | | |

EFFECT OF DRAG BRAKE ON LONGITUDINAL STABILITY

75

BOEING AIRPLANE COMPANY

844-2035

D2-8174

PAGE 5.43

MODEL 2035

$S_E/S_W = .0218$

BRAKE DEFLECTED 60°

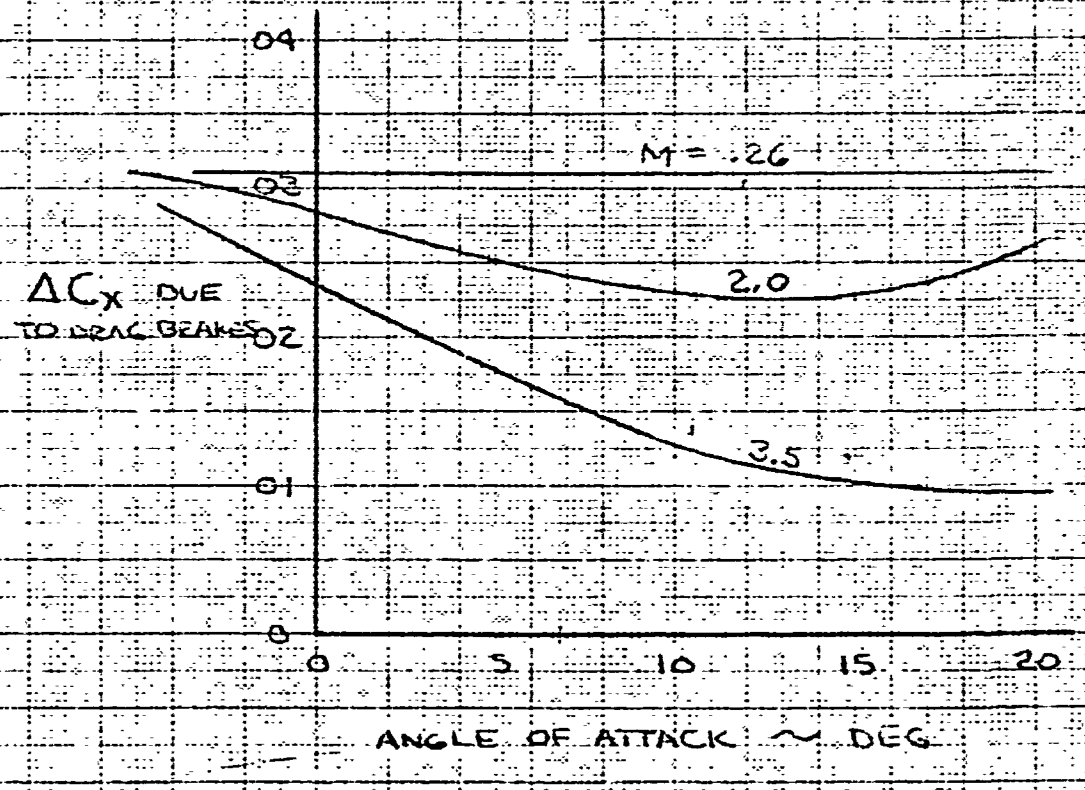


FIG 5.2.2

W.E.J. 12-22

EFFECT OF DRAG BRAKE ON CHORD FORCE COEFFICIENT

76

D2-3174

BOEING AIRPLANE COMPANY

5.7 ELEVON AS AILERON PITCH COUPLING

The effects of symmetrical elevon deflection for roll control on pitch stability and trim at subsonic through supersonic speeds are shown on Figures 5.7.1 and 5.7.2. The data were estimated from limited wind tunnel data and can be subject to major revision.

At hypersonic speeds, the changes in pitching moment and normal force are presented as functions of elevon deflection and angle of attack for one elevon deflected. Test data have shown that the deflection of one elevon has a negligible effect upon the flow about the other elevon at hypersonic speeds. Therefore, the effect of aileron deflection can be obtained by adding the individual effects of the two elevons. The increments in normal force and pitching moment due to deflection of one elevon are shown on Figures 5.7.3 through 5.7.8 for $M=8$ and 22. Elevon pitch trim requirements for various roll control deflection are shown on Figure 5.7.3 for $M=8$ and Figure 5.7.6 for $M=22$.

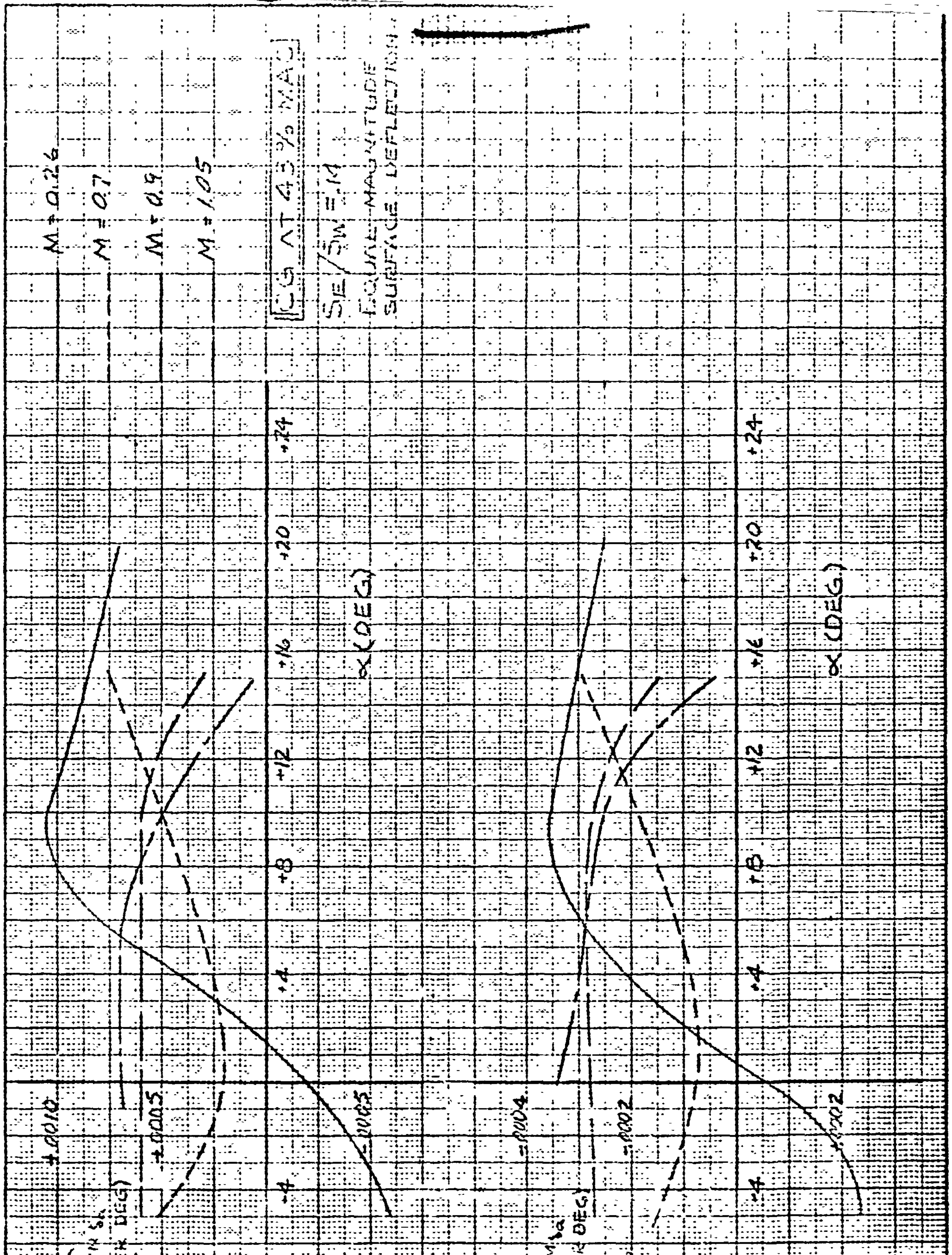


FIG. 5.7.8

| | | | | | | |
|---|---|---|---|---|---|---|
| CALC | G O M | 12-13-?? | REVISED | DATE | PITCH EFFECTS DUE TO AILERON DEFLECTION | 844-2035 |
| CHECK | | | | | SUBSONIC - TRANSONIC SPEED | D2-8174 |
| APR | | | | | BOEING AIRPLANE COMPANY | PAGE 5.46 |
| APR | | | | | | |

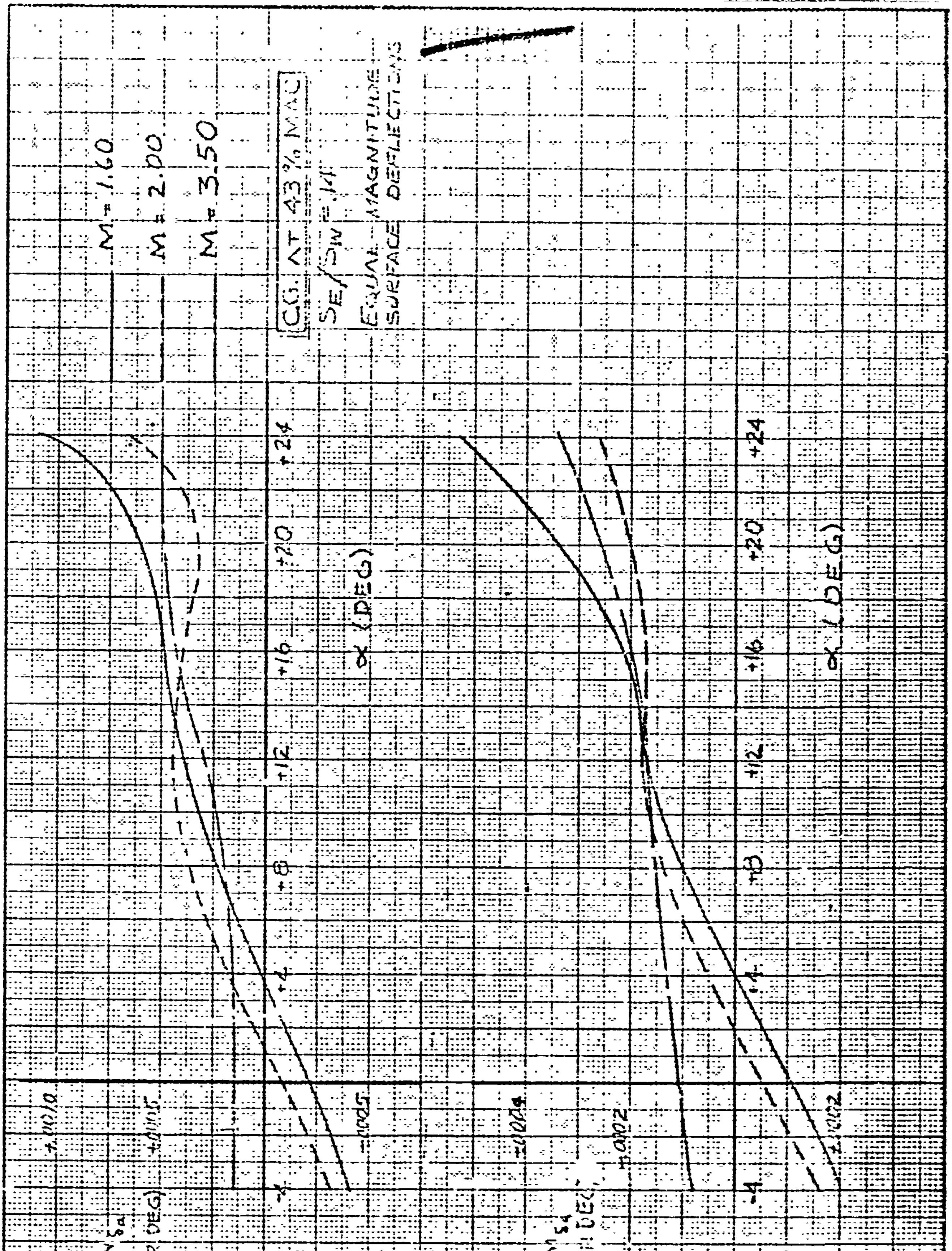


FIG 5.7.2

| CALC | GOM | 12/13/60 | REVISED | DATE |
|---|---|---|---|---|
| CHECK | | | | |
| APR | | | | |
| APR | | | | |

**PITCH EFFECTS DUE TO AILERON DEFLECTION**

SUPERSONIC SPEED

BOEING AIRPLANE COMPANY

344-2035

D2-8174

PAGE 5.47

2035 CONFIGURATION

M = 8.1

CG AT 43% MAC

HOT SHAPE
3.8° NOSE INCIDENCE
0.8° AFT OF B.S. 400

ELEVON
10° TAPER
SPLIT
$S_E/S_W = .14$

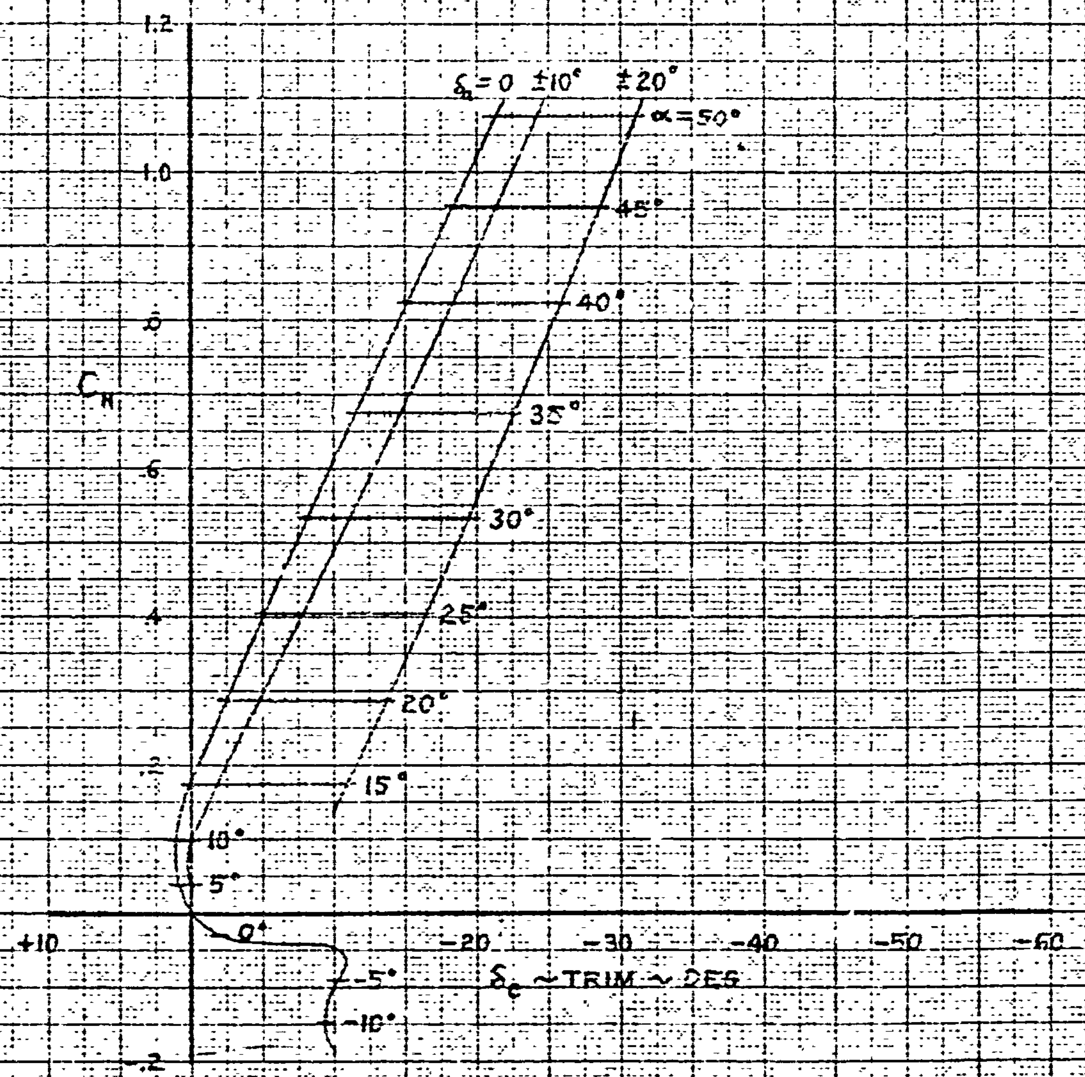


FIG. 5.7.3

| | | | | |
|---|---|---|---|---|
| CALC | Emp | 12/8/58 | REVISED | DATE |
| CHECK | | | | |
| APR | | | | |
| APR | | | | |

AILERON PITCH TRIM REQUIREMENTS
HOT SHAPE M = 8.1

80

BOEING AIRPLANE COMPANY
SEATTLE 14 WASHINGTON

844-2035

D2-3174

PAGE 545

BAC 461 C-R4

BASE CONFIGURATION

M = 3.1

C.G. AT 43 % MAC

HOT SHAPE

3.8° NOSE INCIDENCE

0.8° AFT OF B.S. 400

ELEVON

10° TAPER

SPLIT

$S_E/S_W = .14$

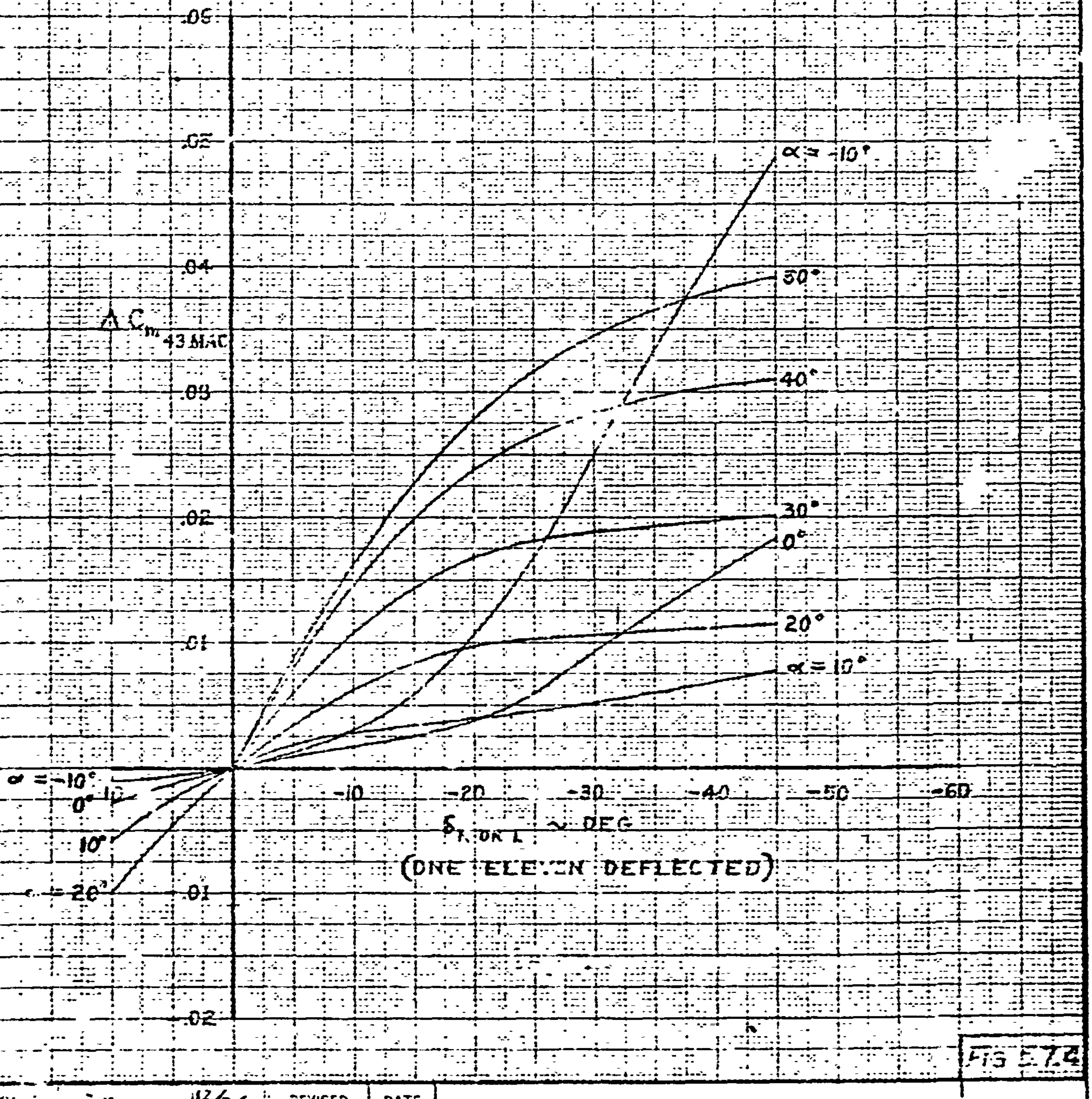


FIG 5.7.4

| CALC | 12/7/60 | REVISED | DATE |
|---|---|---|---|
| CHECK | | | |
| APR | | | |
| APR | | | |

EFFECT OF AILERONS ON PITCHING MOMENT

HOT SHAPE M = 3.1

D44-2035

D2-3174

BOEING AIRPLANE COMPANY

SEATTLE 24, WASHINGTON

81

PAGE 5.43

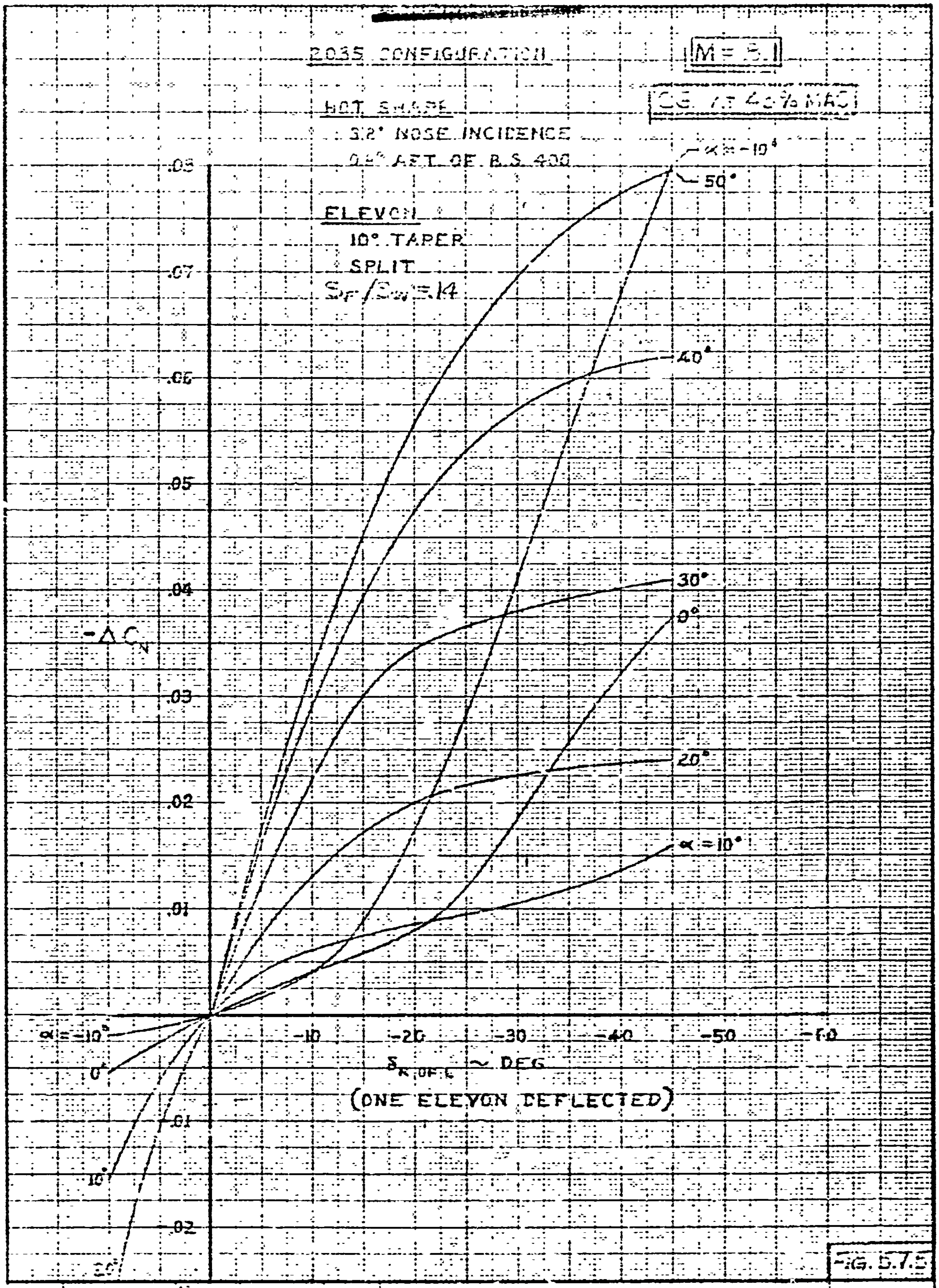


FIG. 5.7.5

| CALC | Emf | 12/7/60 | REVISED | DATE |
|---|---|---|---|---|
| CHECK | | | | |
| APR | | | | |
| APR | | | | |

EFFECT OF AILERONS ON NORMAL FORCE

HOT SHAPE M = 8.1

82

844-2035

D2-8174

BOEING AIRPLANE COMPANY
SEATTLE 24 WASHINGTON



BAC 451 C-R4

.035 CONFIGURATION

M = 22.0

C.G. = 43% MAC

HOT SHAPE
3.5° NOSE INCIDENCE
6.5° AFT OF B.S. 400

ELEVON
10° TAPER
SPLIT
$S_F/S_W = .14$

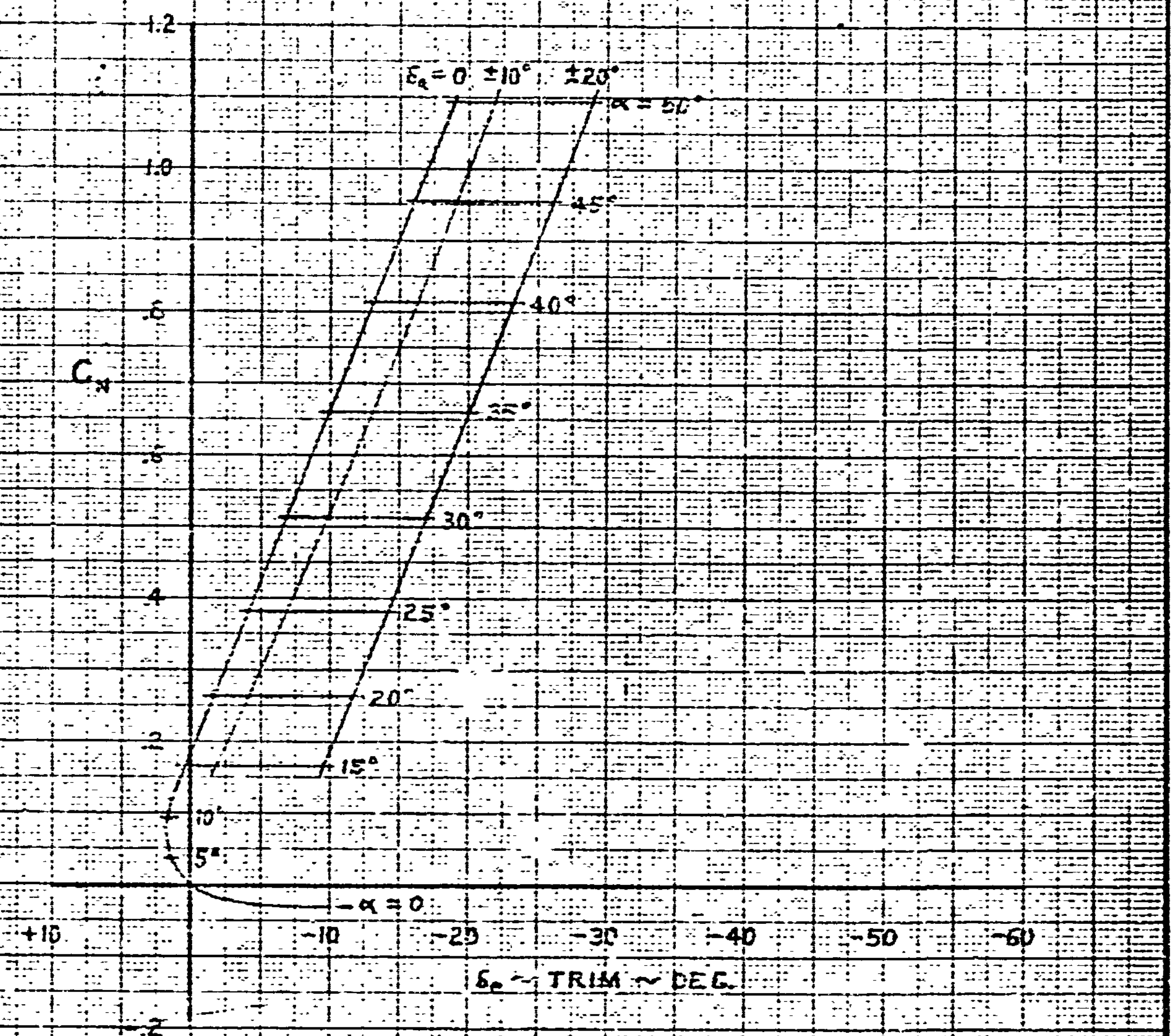


FIG 5.76

| CALC | EMT | 12/9/57 | REVISED | DATE | AILERON PITCH TRIM REQUIREMENTS HOT SHAPE M = 22.0 | 83 | E44-2035 |
|---|---|---|---|---|---|---|---|
| CHECK | | | | | | | D2-8174 |
| APR | | | | | | | |
| APR | | | | | BOEING AIRPLANE COMPANY SEATTLE 24, WASHINGTON | | PAGE 5.51 |

BAC 461 C-R4 K-E 60629

2035 CONFIGURATION

M = 22.0

C.G. AT 42% M.A.C.

HOT SHAPE
3.5° NOSE INCIDENCE
0.8% AFT OF B.S. 400

ELEVON
10° TAPER
SPLIT
$S_E/S_W = .14$

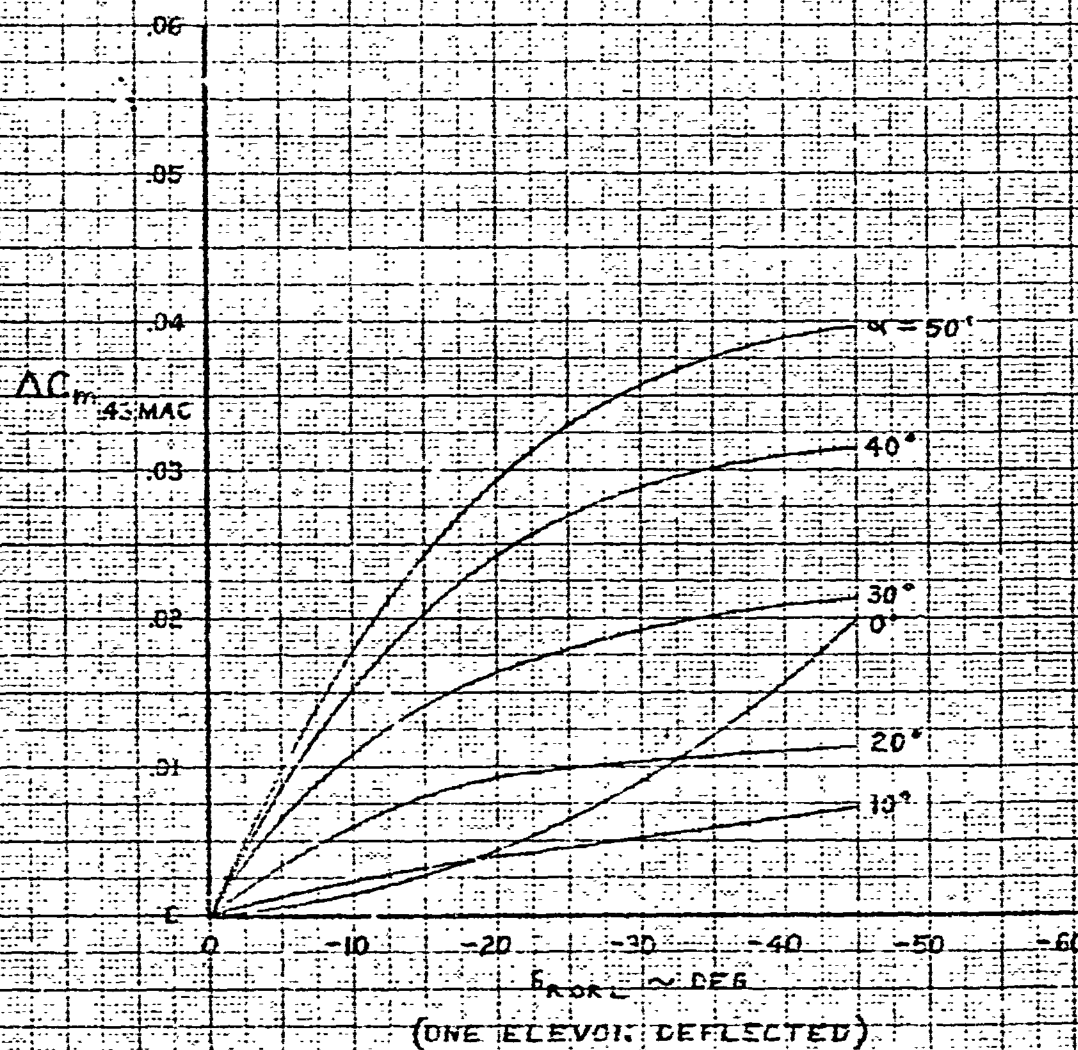


FIG. 5.77

| CALC | Em.M | 12/5/6 | REVISED | DATE |
|---|---|---|---|---|
| CHECK | | | | |
| APR | | | | |
| APR | | | | |

EFFECT OF AILERONS ON PITCHING MOMENT 84
HOT SHAPE M = 22.0

BOEING AIRPLANE COMPANY
SEATTLE 24 WASHINGTON

844-2035

D2-5174

PAGE 5.52

FAC 461 C-R4

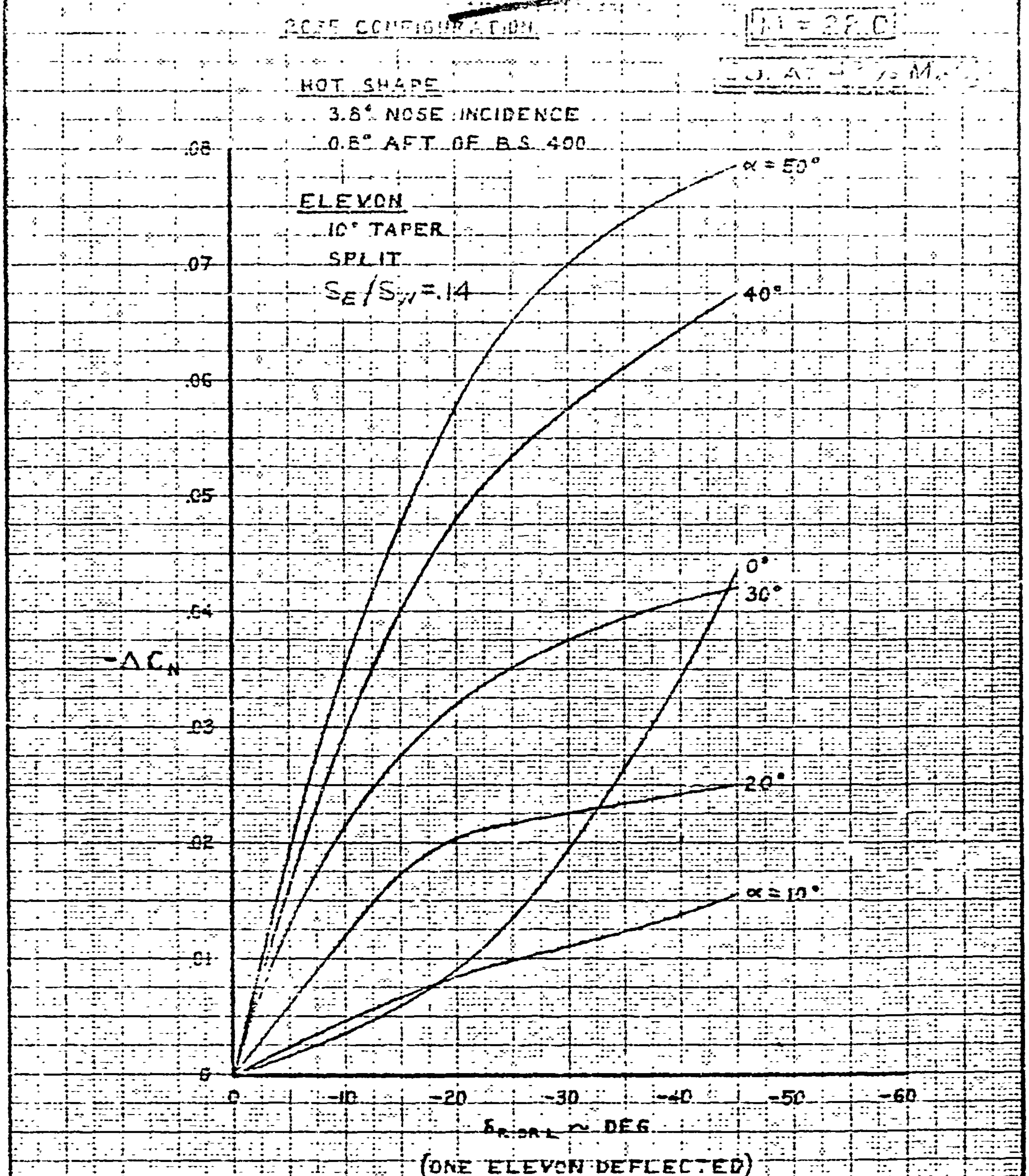


FIG. 5.73

| CALC | | 4/9/63 | REVISED | DATE |
|---|---|---|---|---|
| CHECK | | | | |
| APR | | | | |
| APR | | | | |

EFFECT OF AILERONS ON NORMAL FORCE

85

D44-2035

D2-8174

BOEING AIRPLANE COMPANY
SEATTLE 14 WASHINGTON

PAGE 5.53

BAC 801 C-R4

## 5.8 ROTARY DERIVATIVES

The pitch damping derivative, $C_{m_q}$ (shown on Figure 5.8.1), was obtained from NASA reports of similar configurations. These data were also compared with linear theory which was found to be in reasonable agreement at supersonic speeds but was nearly double the empirical value at subsonic speeds. Recent wind tunnel data were run showing the effects of angle of attack and oscillation frequency on $C_{m_q}$ and $C_{m_{\dot{\alpha}}}$ at low speed in the L.R.C. Free Flight Wind Tunnel. These data are currently being analyzed. Additional analytical and test work is being done and is planned, to define the necessary rotary derivatives further.

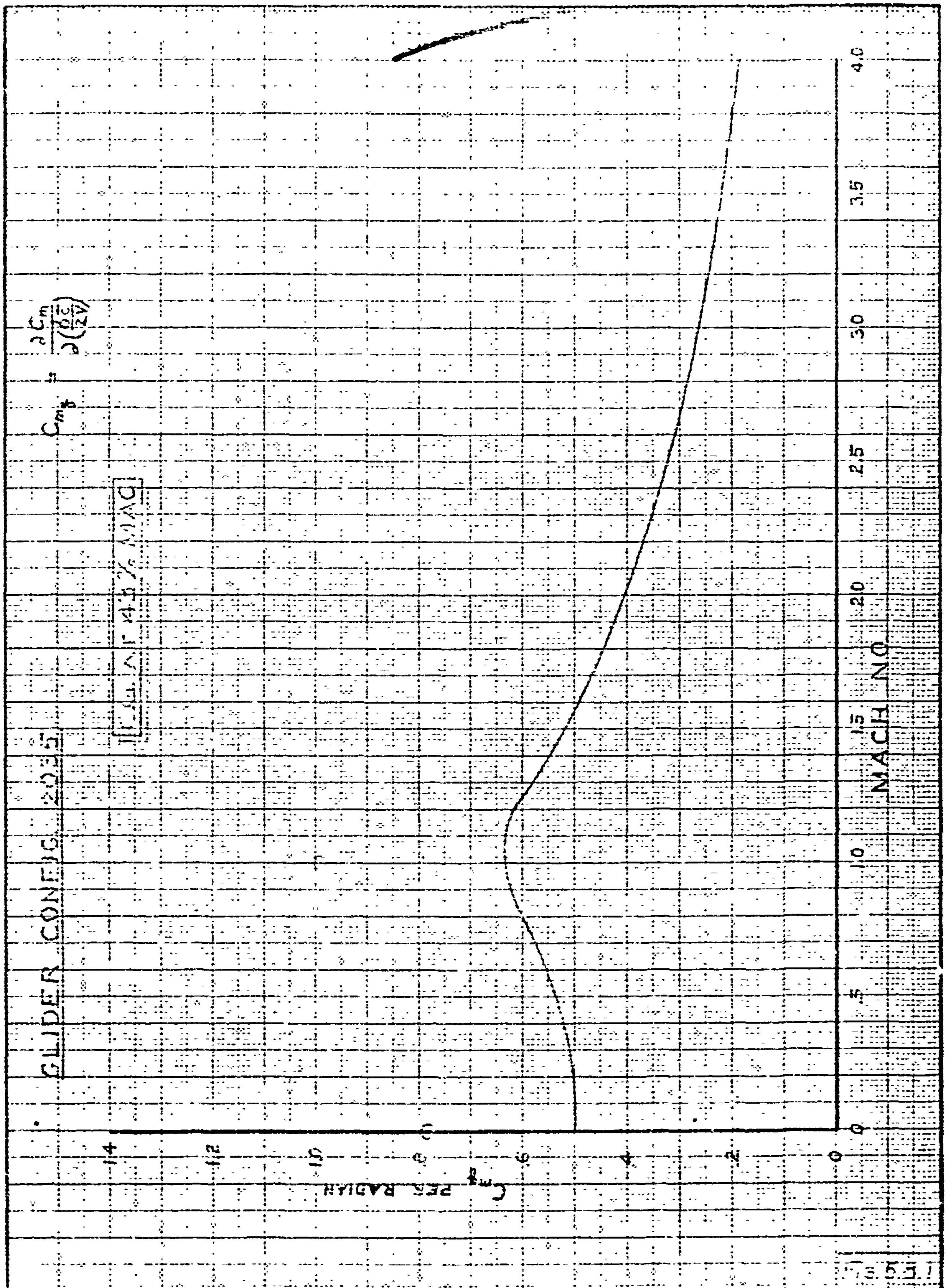


| CALC | Cmr | 12/5/60 | REVISED | DATE |
|---|---|---|---|---|
| CHECK | | | | |
| APR | | | | |
| APR | | | | |

PITCHING MOMENT DUE TO PITCHING VELOCITY

87

BOEING AIRPLANE COMPANY
SEATTLE 24 WASHINGTON

844-2035
D2-8174
PAGE 5.55

BAC 461 C-R4

## 5.9 ELEVON HINGE MOMENT CHARACTERISTICS

Variation of $C_{H_\alpha}$ and $C_{H_\delta}$ with Mach number is shown on Figure 5.9.1. These data were obtained from published N.A.S.A. reports on similar configurations.

Wind tunnel tests in the A.R.C. Unitary Wind Tunnel have been completed recently and further testing is planned to define these characteristics better as a function of Mach number, angle of attack and angle of elevon deflection.

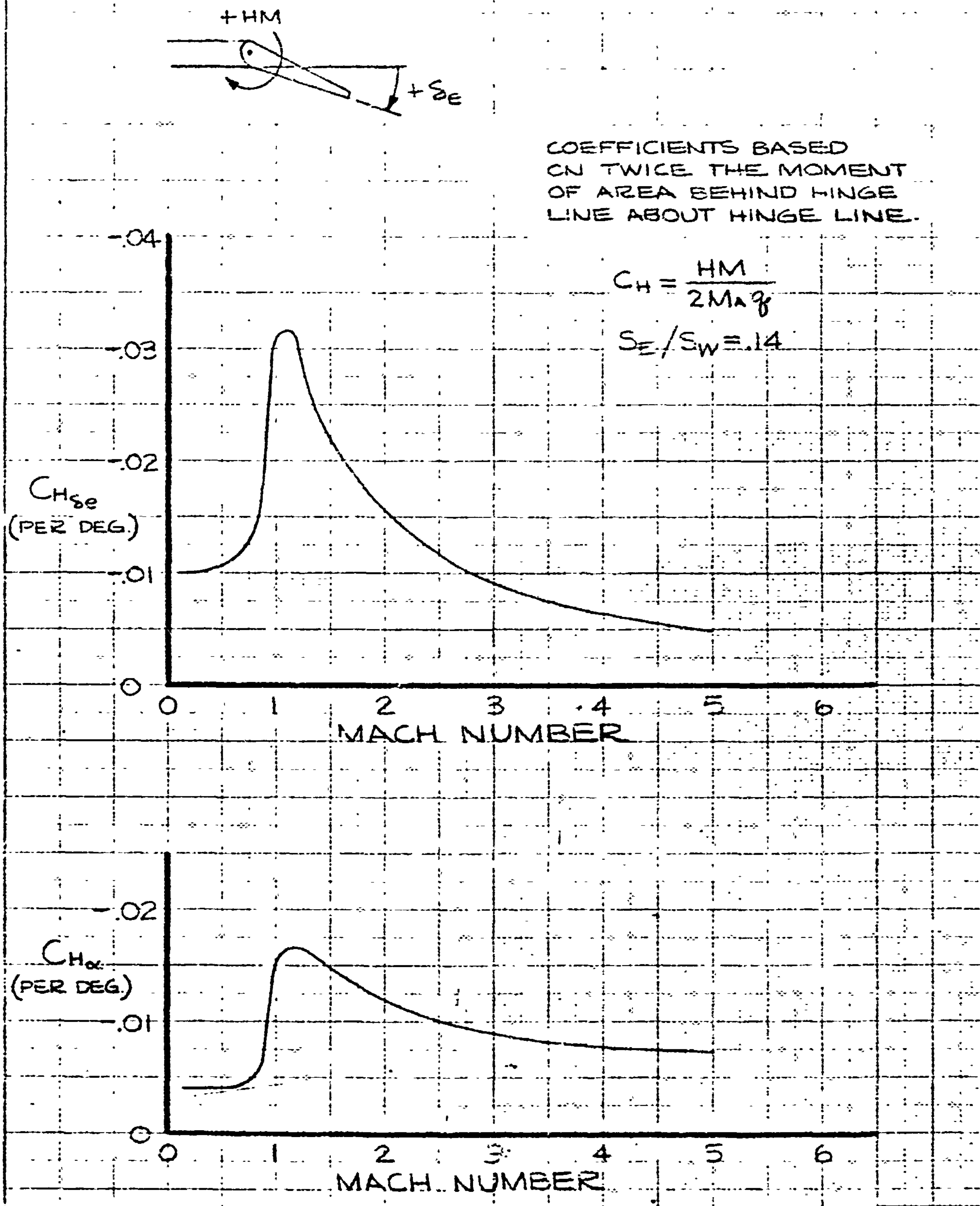


FIG. 5.9.1

PMJ 11/18/60

# ELEVON HINGE MOMENT COEFFICIENTS

844-2035

D2-8174

BOEING AIRPLANE COMPANY

PAGE 5.57

## 5.10 WING TIP EXTENSIONS

The incremental effect of wing tip extensions, located on the vertical tails, on pitching moment and normal force coefficients is shown on Figures 5.10.1 and 5.10.2. These data are based on tests performed in the A.R.C. 12-Foot Pressure Wind Tunnel and the Boeing Transonic and Supersonic Wind Tunnels. It was assumed that the tip extension would have only secondary effects on elevon effectiveness. The data obtained were not with the precise tip extension configuration for the [illegible]-2035 glider; consequently some variation in the increments shown may be anticipated.

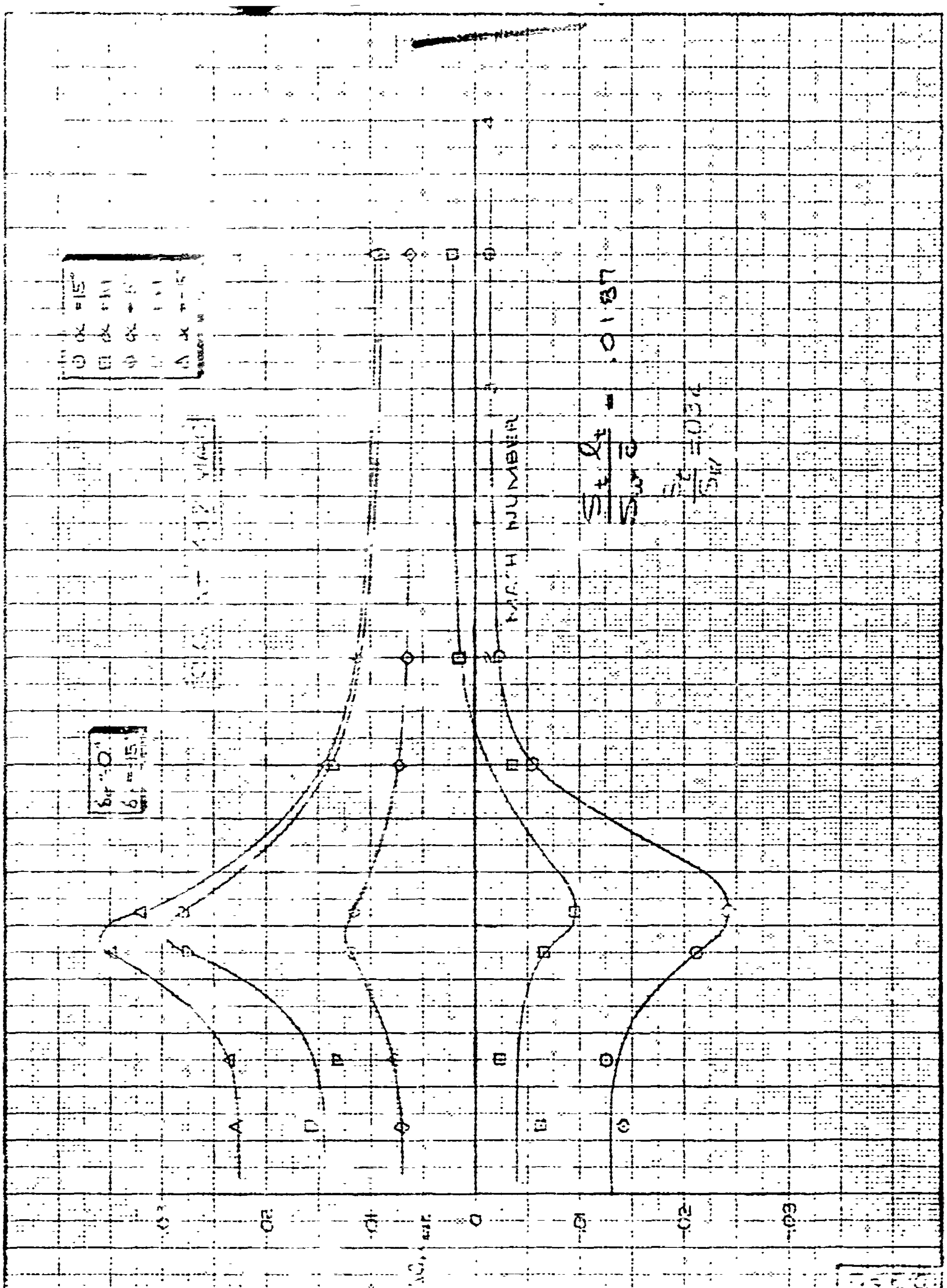


| | | | | | |
|---|---|---|---|---|---|
| CALC | W.L. FRANCIS | 12/6/60 | REVISED | DATE | |
| CHECK | E DJR | 12-7-0 | | | |
| APP | | | | | |
| APR | | | | | |

EFFECT OF WING TIP EXTENSIONS ON PITCHING MOMENT

91

BOEING AIRPLANE COMPANY

PAGE 59

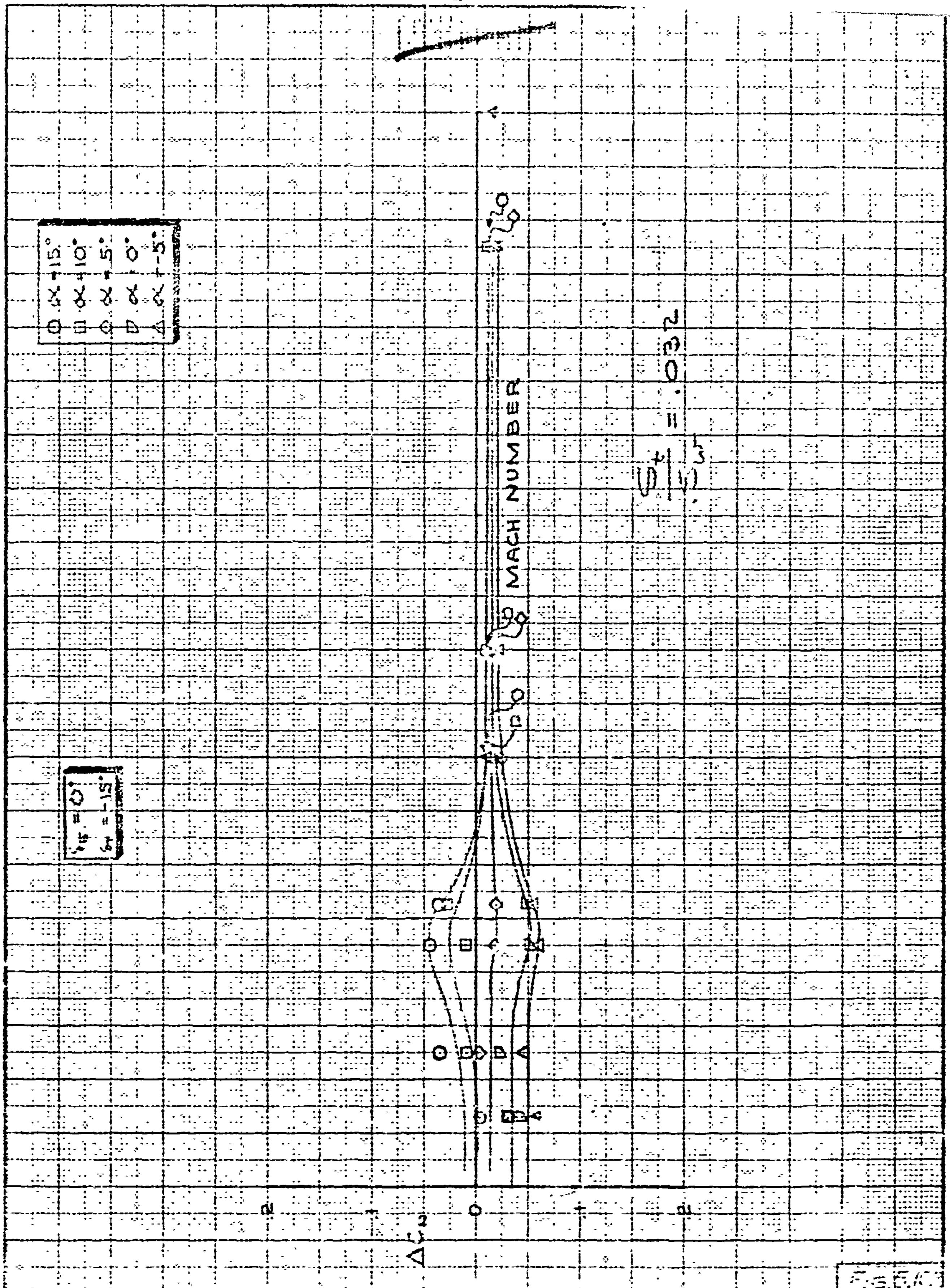


| CALC | J L FRANCIS | 4-6-57 | REVISED | DATE |
|---|---|---|---|---|
| CHECK | EDJR | 12-7-0 | | |
| APP | | | | |
| APR | | | | |

EFFECT OF WING TIP EXTENSIONS ON NORMAL FORCE

FIGURE 92

844-2037

D2-3174

PAGE 5.63

BOEING AIRPLANE COMPANY

## 6.0 LATERAL - DIRECTIONAL STABILITY AND CONTROL

The predicted force, moment, and directional control effectiveness characteristics are included in this section. The data are grouped in the following areas. A list of the data in each area is presented at the front of each group.

6.1 Lateral - Directional Stability Characteristics

6.2 Aileron Characteristics and Effectiveness

6.3 Rudder Characteristics and Effectiveness

6.4 Roll and Yaw Rotary Derivatives

The characteristics are presented for the 844-2035 configuration, Figure 3.1.1. The reference dimensions on which the characteristics are based are shown on Figure 3.3.3. All characteristics are presented for conventional body axes fixed in the vehicle.

6.1 LATERAL - DIRECTIONAL STABILITY CHARACTERISTICS

The lateral - directional stability is presented in Figures 6.1 through 6.24 for landing speed to high hypersonic speed. The yawing moment, rolling moment, and side force are presented versus sideslip angle and angle of attack at representative Mach numbers in order to show the non-linearity of the stability characteristics. The stability derivatives $C_{n_\beta}$, $C_{l_\beta}$, and $C_{Y_\beta}$ are also presented versus Mach number in order to indicate the interpolation between Mach numbers (Figures 6.1, 6.2, and 6.3). These derivatives are presented only for zero sideslip, and because of the non-linear nature of the stability characteristics, should not be used for large sideslip angles. Stability characteristics are presented for wing-tip extensions both retracted and extended from landing speed to M = 3.5.

The stability characteristics are presented at representative speeds corresponding approximately to wind tunnel test speeds, namely, M = 0.25, .70, .95, 1.05, 2.0, 3.5, 8.0 and 22.0. The landing speed data are based primarily on low speed tests on a similar configuration at the ARC 12-Foot Pressure Tunnel, test 122, and preliminary data from BTWT 619. Effects of Reynolds number (altitude) were shown to be small. The stability at $\alpha = 15°$ and $\beta$ greater than 12° was extrapolated. The incremental effect of extending the landing gear and extending the speed brakes is shown on Figures 6.7 and 6.8. No data on the influence of the ground is currently available; however, any effect of the ground on yawing moment and side force will probably be negligible, with the major effect a small reduction in aileron effectiveness and roll due to sideslip (dihedral effect).

The transonic characteristics were estimated from preliminary data from BTWT 623 on a similar glider configuration. The data have been extrapolated to the current configuration on the basis of body shape, vertical tail size, location, and planform, and fold-down wing tip size. The static stability is currently minimum in this speed range.

The supersonic stability characteristics were obtained from tests in the Boeing Supersonic Wind Tunnel at Mach numbers 2.0 and 3.5. Since $C_n$, $C_l$, and $C_Y$ are quite linear with $\beta$ in this Mach number region, data are presented for M = 3.5 only (wing tips extended and retracted) on Figures 6.22 and 6.21. These Figures are representative of the variation of these coefficients versus $\beta$ throughout the supersonic region. Figures 6.15 through 6.20 present $C_{n_\beta}$, $C_{l_\beta}$, and $C_{Y_\beta}$ versus $\alpha$ for M = 2.0 and 3.5, and for wing tips extended and retracted.

Lateral - directional stability at low hypersonic speeds were obtained from wind tunnel tests on the model 844-2005, a similar

configuration, at Mach numbers of 8.08 (AFDC-B, BAC 13) and 9.6 (LRC 11-Inch, Test 47 in air). The data have been adjusted for vertical tail size, planform and cant angle (Figure 3.1.1). The results are presented in Figure 6.23.

High hypersonic speed data were obtained at Mach 17.8 (LRC 11-Inch, Test 47 in helium) and Mach 16 and 22 (HHST 006). The helium data were obtained on a model identical to the low hypersonic speed model. The hot shot data, however, were on a cone-cylinder body configuration, and additional corrections had to be made for the body shape. This was performed by comparing the cone-cylinder and SA4-2005 body effects at Mach 9.6 and adjust the Mach 22.0 data accordingly. Figure 6.24 shows the lateral - directional stability characteristics at high hypersonic speeds. Characteristics at angles of attack above 20° were extrapolated from lower Mach number data.

No information is currently available on the influence of altitude (i.e., Reynolds number) variation at high hypersonic speeds on the lateral - directional force-moment characteristics. Until data become available, it is assumed that the effect of altitude will be negligible on $C_n$, $C_l$ and $C_Y$. The primary effect of altitude will be to increase boundary layer thickness. However, the areas of the glider that are most important in establishing directional stability are the glider fore-body and vertical tail; regions which are not expected to have significant boundary layer growth because of short boundary layer runs.

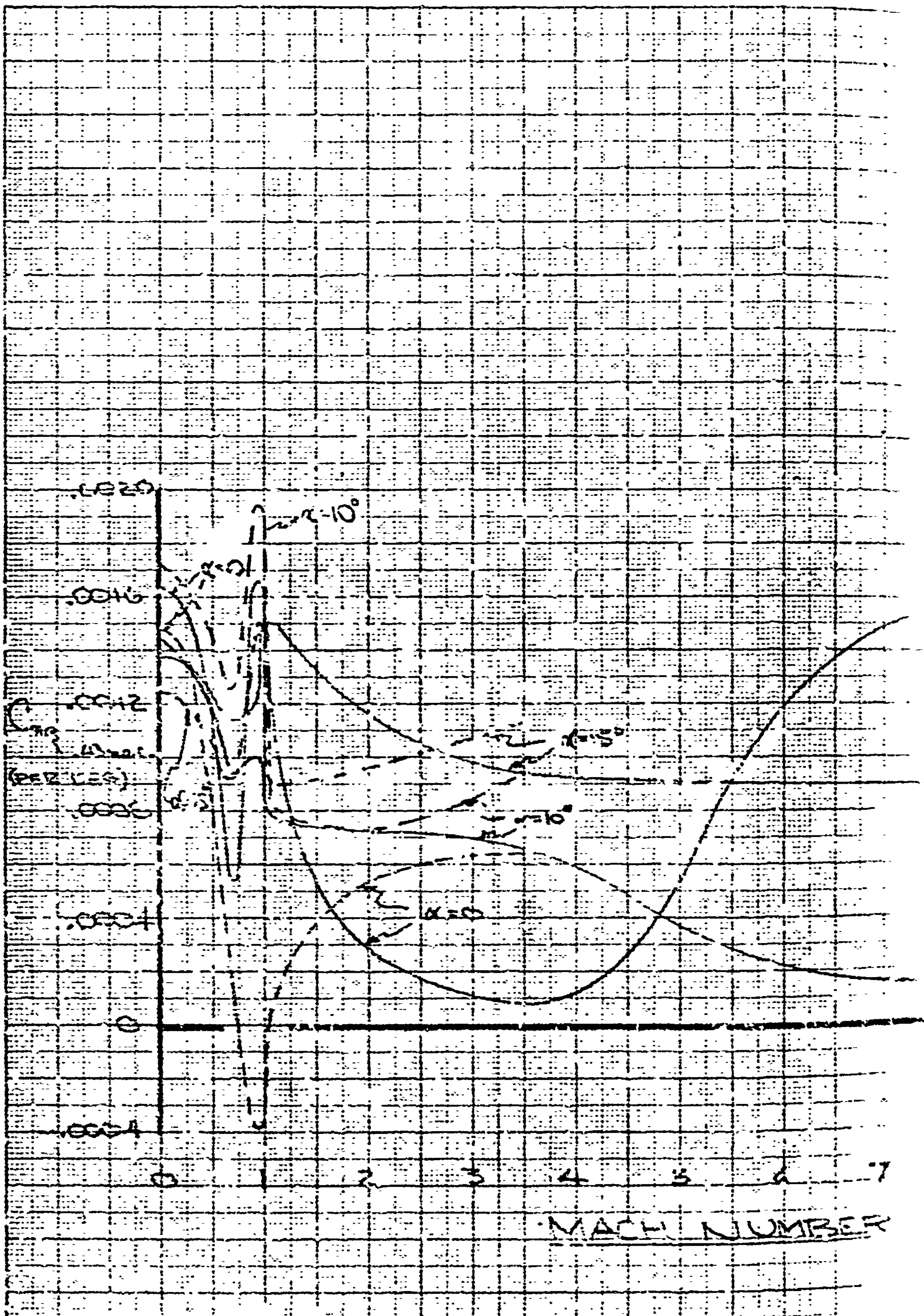

.0020
.0016
.0012
.0008
.0004
0
.0004
0
1
2
3
4
5
6
7
MACH NUMBER
α=10°
α=5°
α=10°
α=0

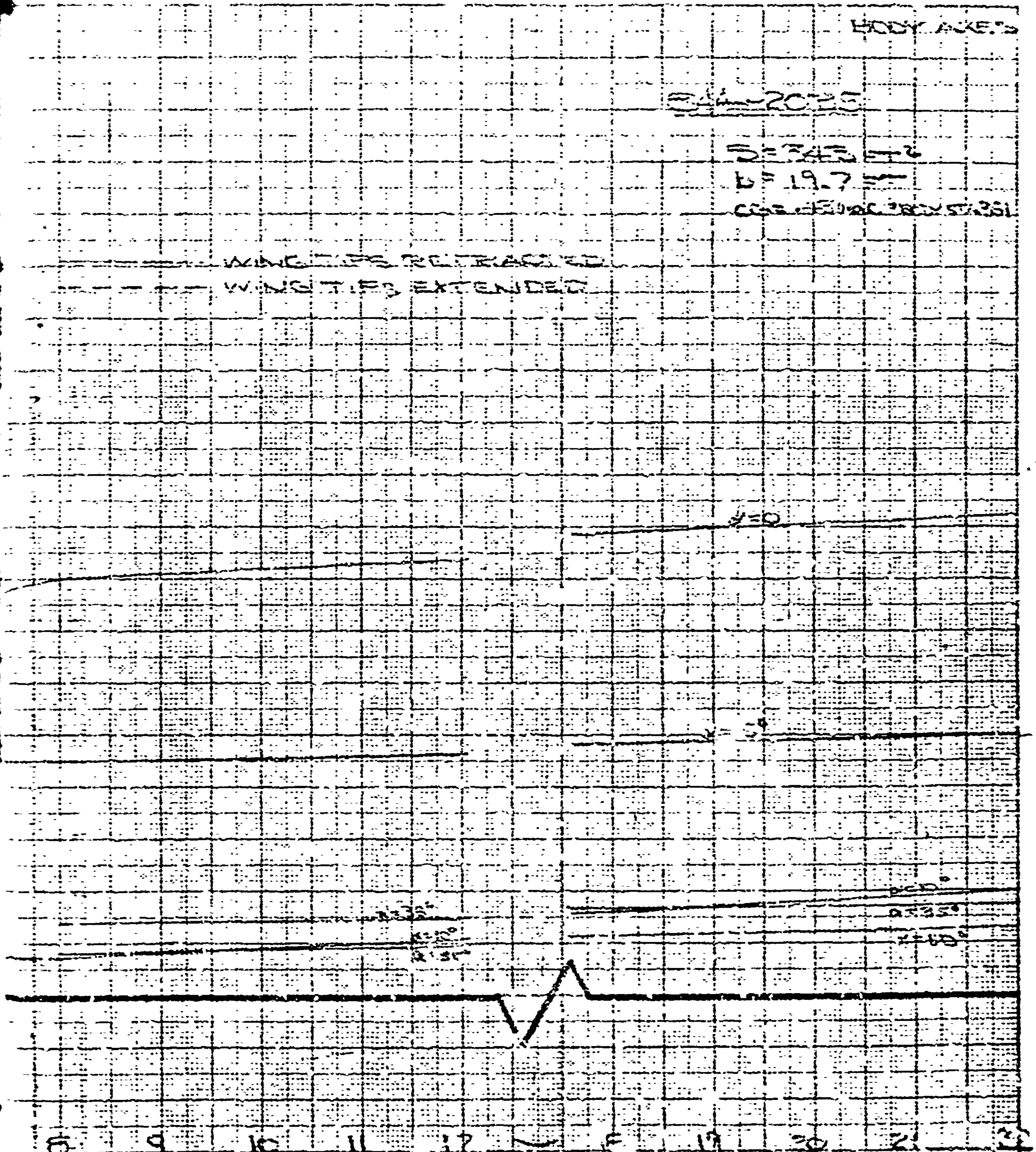


FIG 6.1

DIRECTIONAL STABILITY

D7-8174

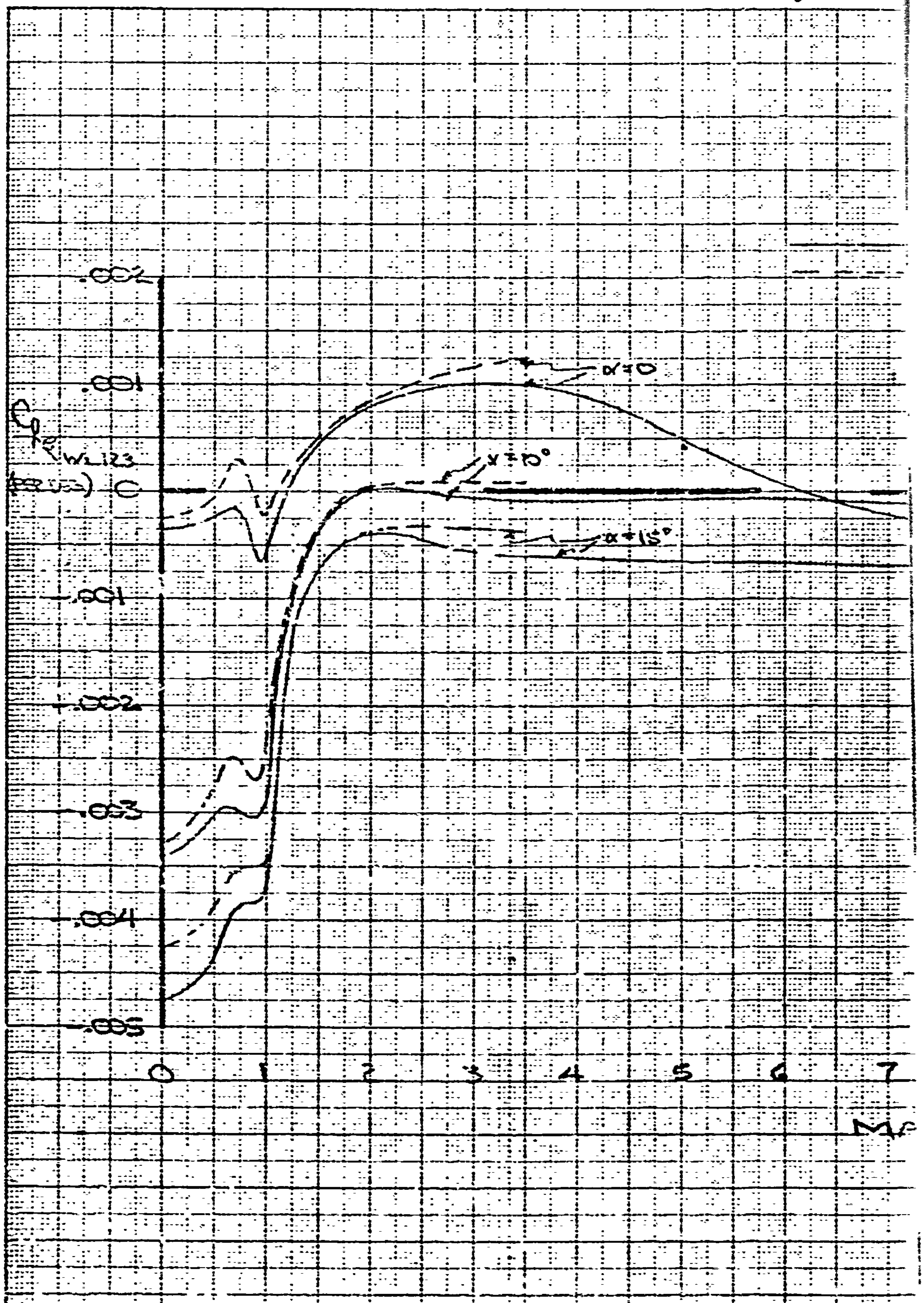

.002
.001
0
-.001
-.002
-.003
-.004
-.005
$C_{\ell_\beta}$
WL 123
α = 0
α = 10°
α = 15°
0
1
2
3
4
5
6
7

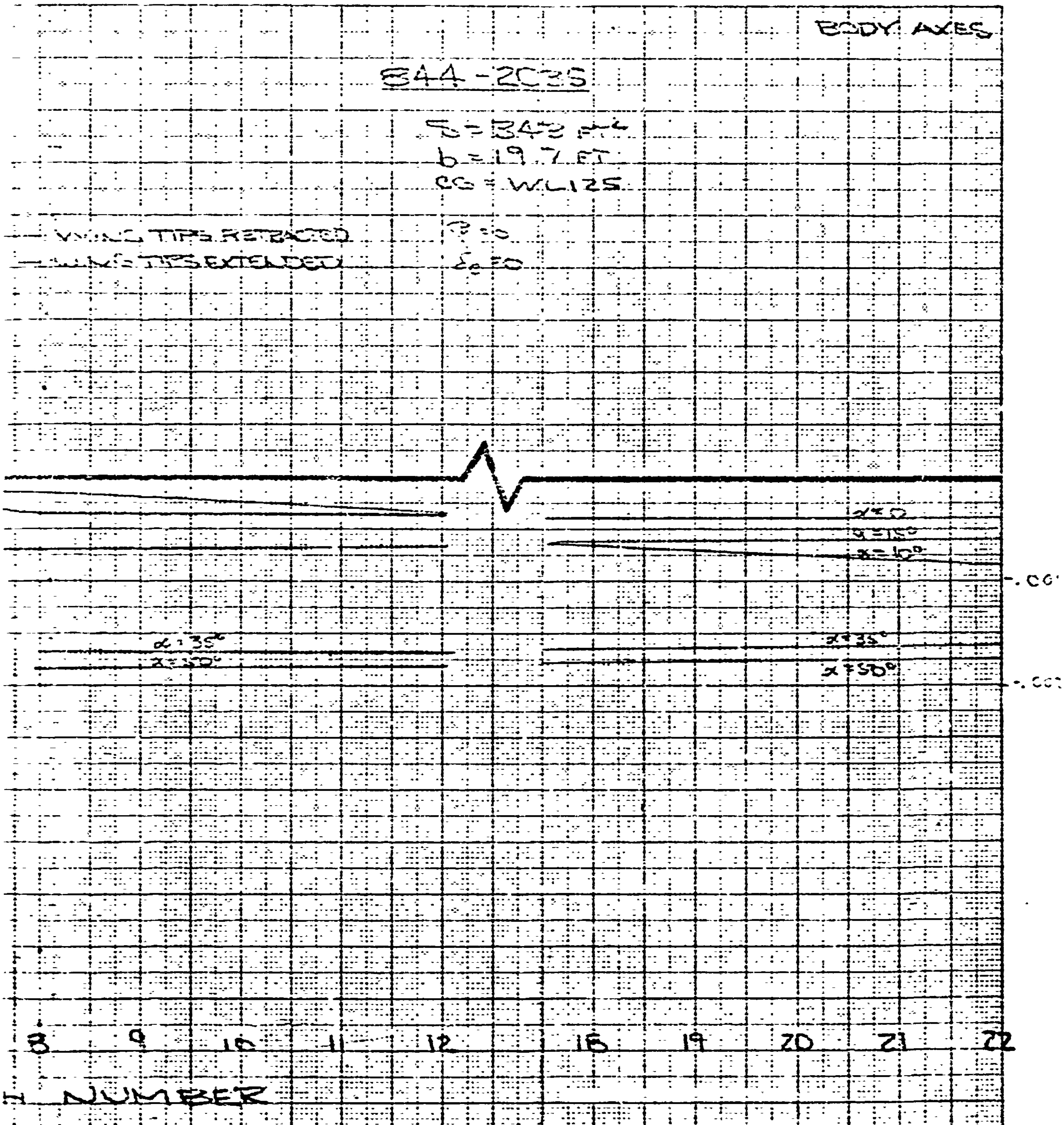


FIG. 6.2
844-2035

LATERAL STABILITY

CALC RER 12-2-20 | REVISED | DATE
CHECK
APPD
APPD

D2-8174
PAGE 6.5

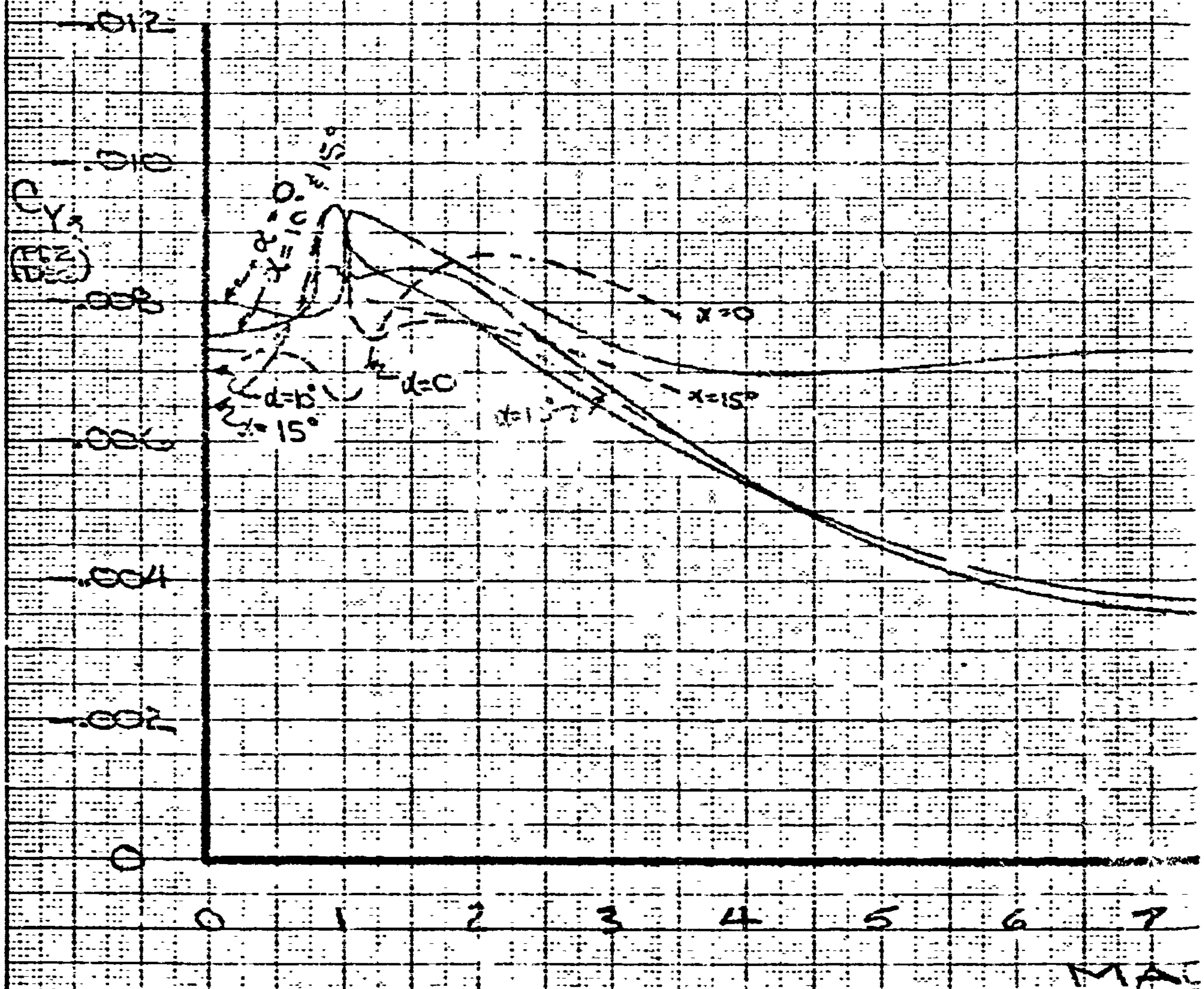
.012
.010
$C_{Y_\beta}$
.008
.006
.004
.002
0
0
1
2
3
4
5
6
7
MACH
α=0
α=15°
α=0
α=15°

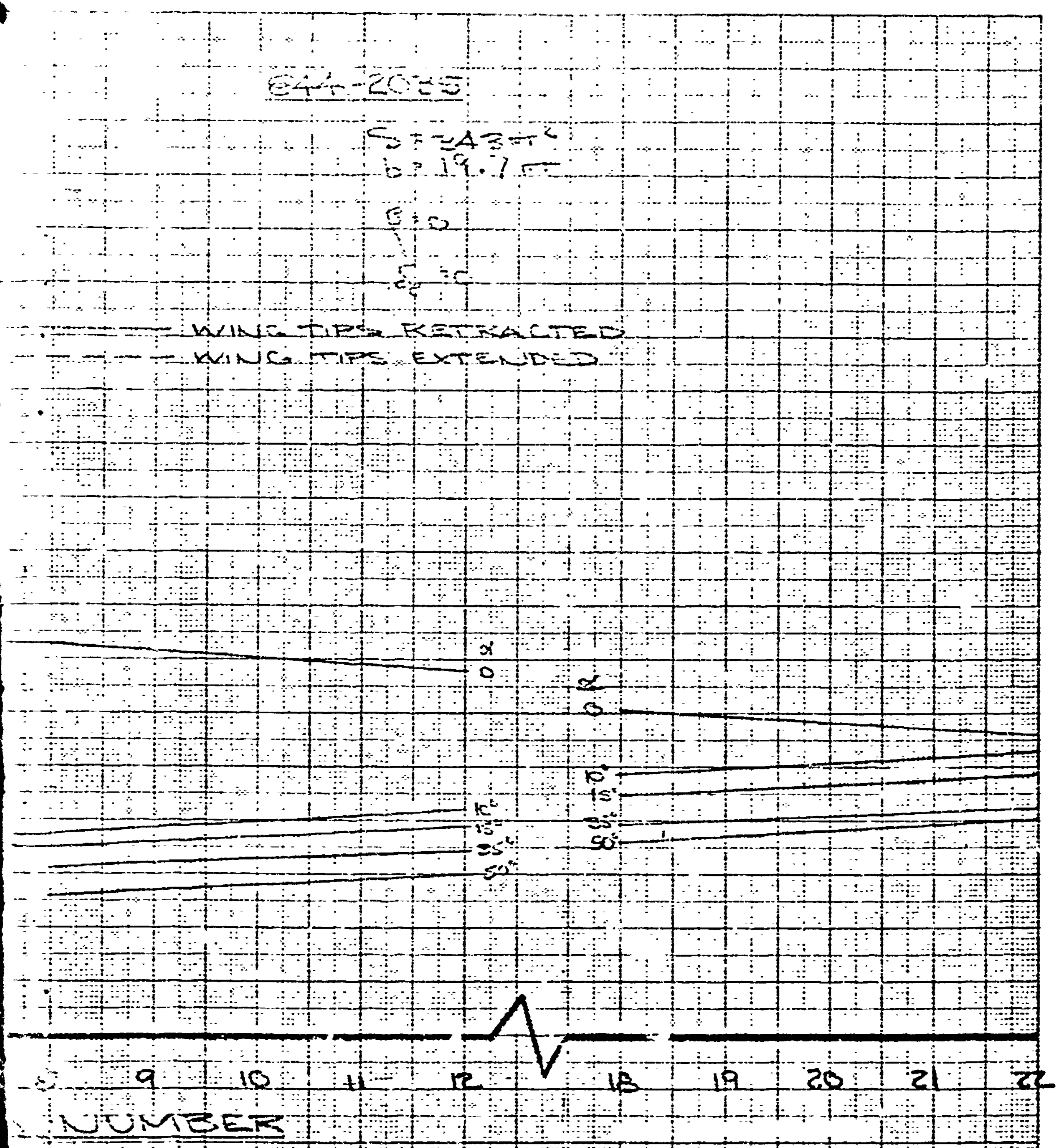


| | | | | |
|---|---|---|---|---|
| CALC EER | 12-22-C | REVISED | DATE | |
| CHECK | | | | SIDE FORCE |
| APD | | | | |
| APD | | | | |

FIG 6.9
644-2055
D2-8174
6.6

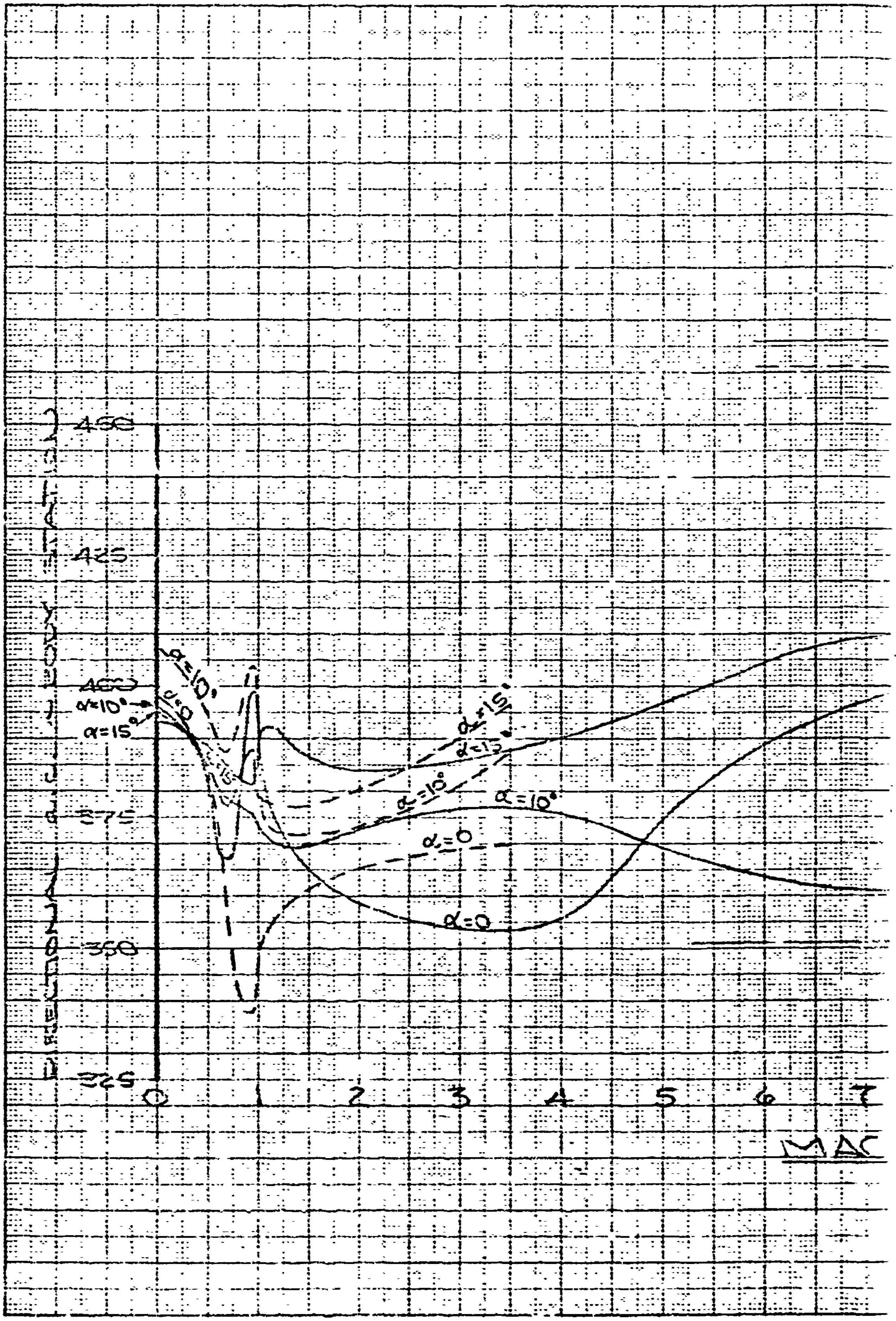
450
425
400
375
350
325
α=10°
α=15°
α=10°
α=0
α=15°
α=15°
α=15°
α=10°
α=10°
α=0
α=0
0
2
3
4
5
6
7
MACH

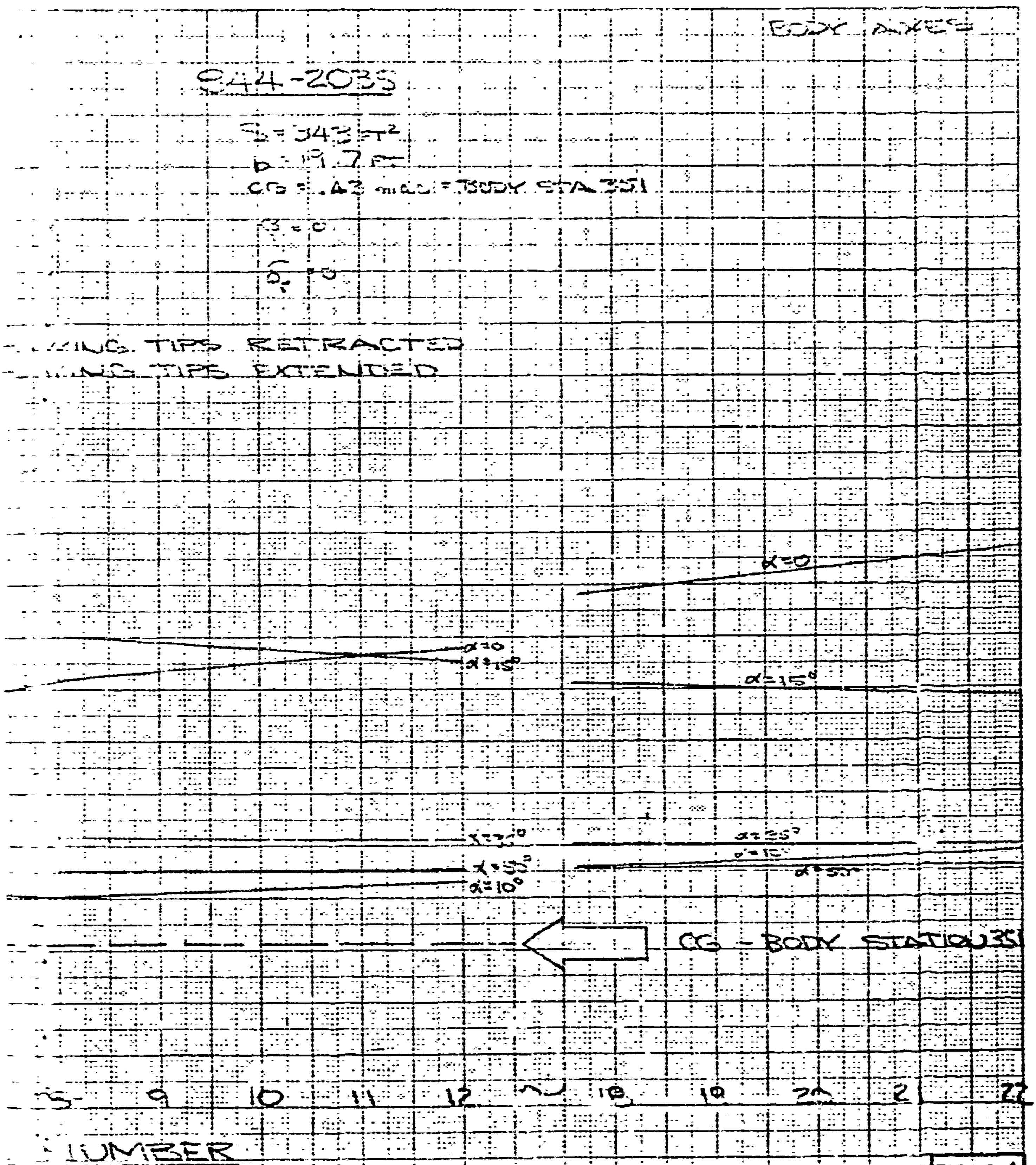


| | | | | |
|---|---|---|---|---|
| CALC BFR | 12-2-0 | REVISED | DATE | FIG 6.4 844-2035 |
| CHECK | | DIRECTIONAL a.c. | | D2-8174 |
| APPD | | | | PAGE 6.7 |
| APPD | | | | |

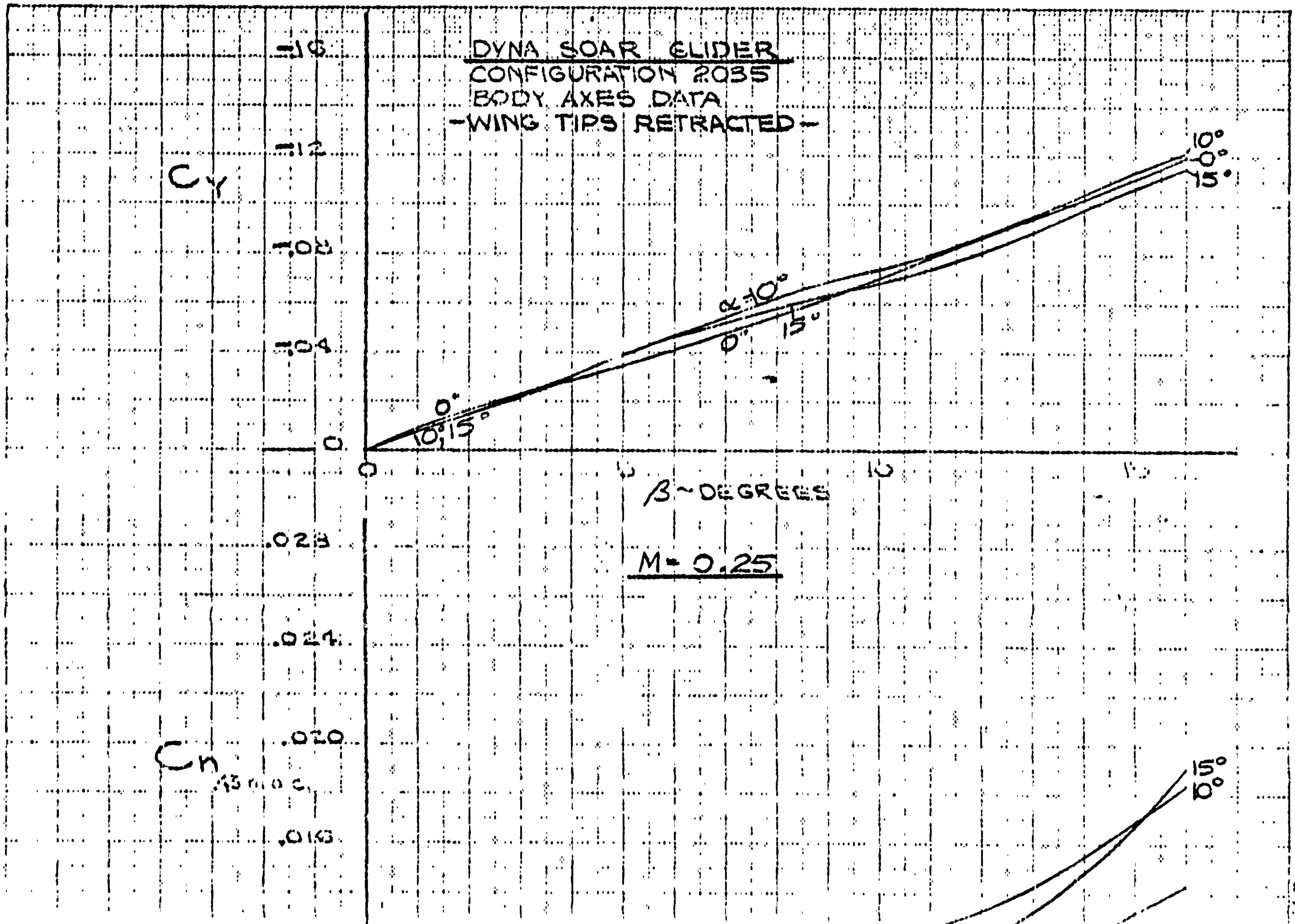
DYNA SOAR GLIDER
CONFIGURATION 2035
BODY AXES DATA
-WING TIPS RETRACTED-
$C_Y$
-.16
-.12
-.08
-.04
0
.028
.024
.020
.016
$C_{n_{.35\ m.a.c.}}$
0
10
$\beta$ ~ DEGREES
M = 0.25
$\alpha$ = 10°
0°
15°
10°, 15°
10°
0°
15°
15°
10°

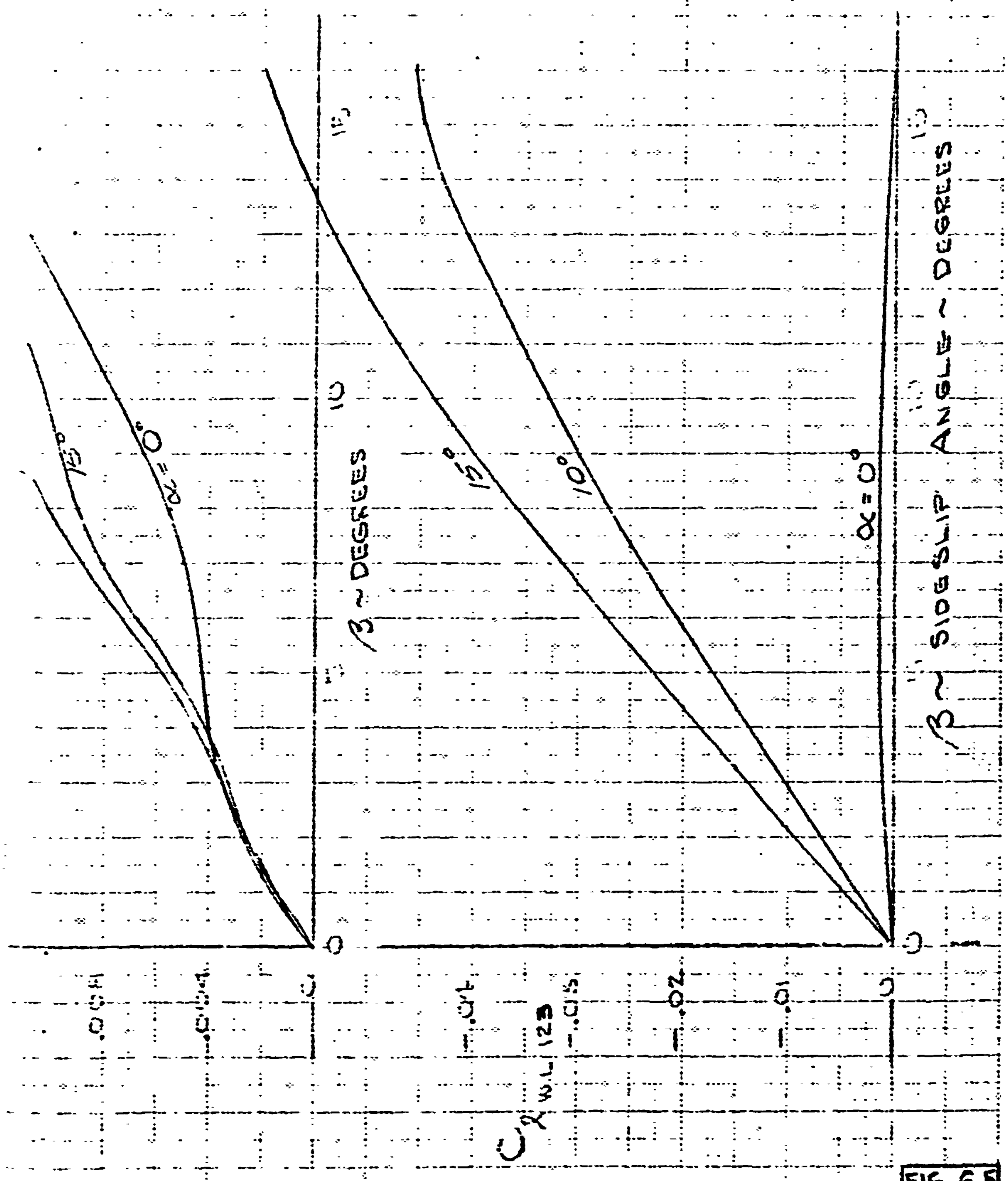


| | | |
|---|---|---|
| RKR/PTV 12-7 | LATERAL - DIRECTIONAL STABILITY CHARACTERISTICS —WING TIPS RETRACTED— —LANDING SPEED— | FIG 6.5 844-2035 D2-8174 6.8 |

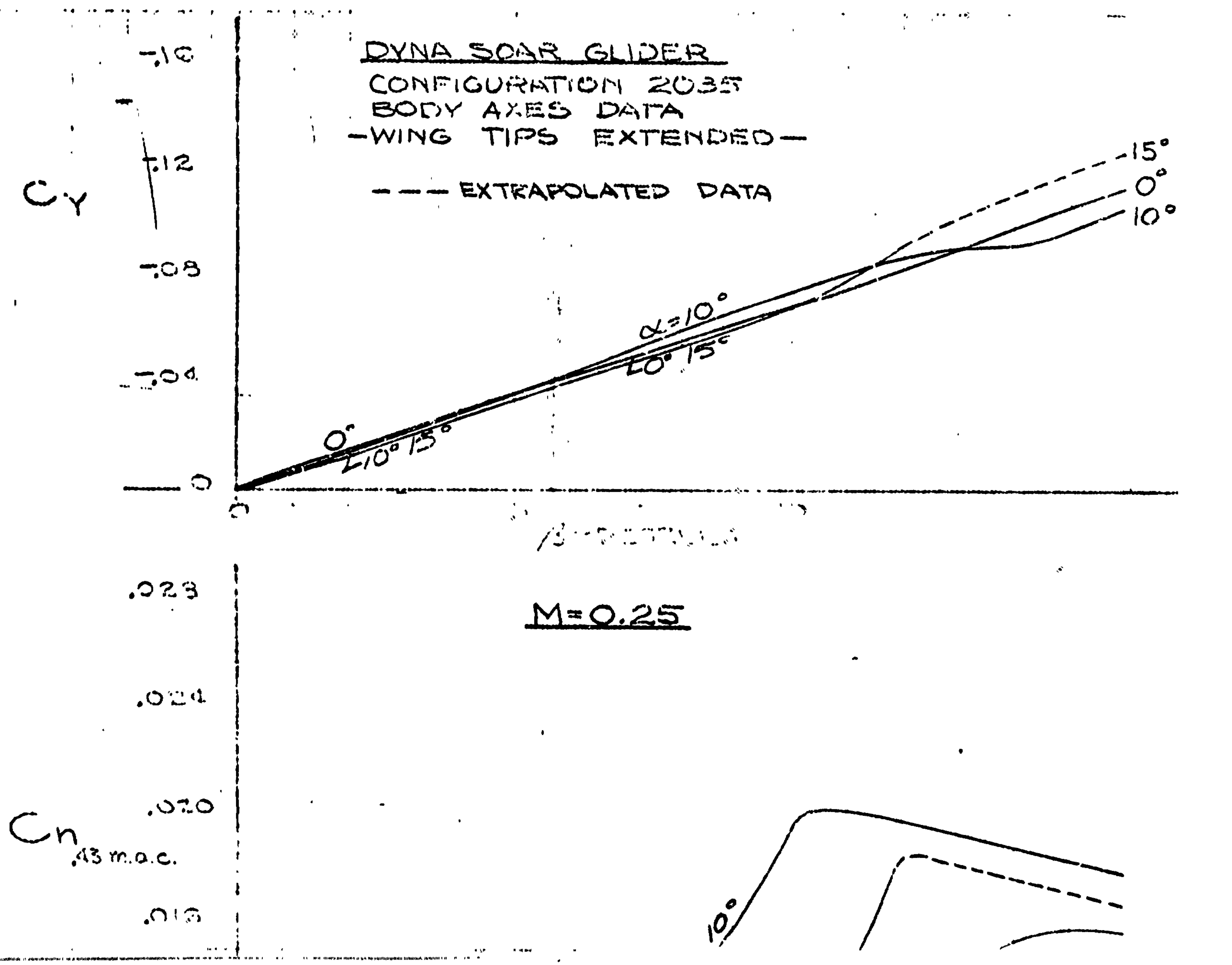

DYNA SOAR GLIDER
CONFIGURATION 2035
BODY AXES DATA
-WING TIPS EXTENDED-
--- EXTRAPOLATED DATA
$C_Y$
-.16
-.12
-.08
-.04
0
15°
0°
10°
α=10°
0°
15°
M=0.25
$C_{n_{.43\,m.a.c.}}$
.028
.024
.020
.016

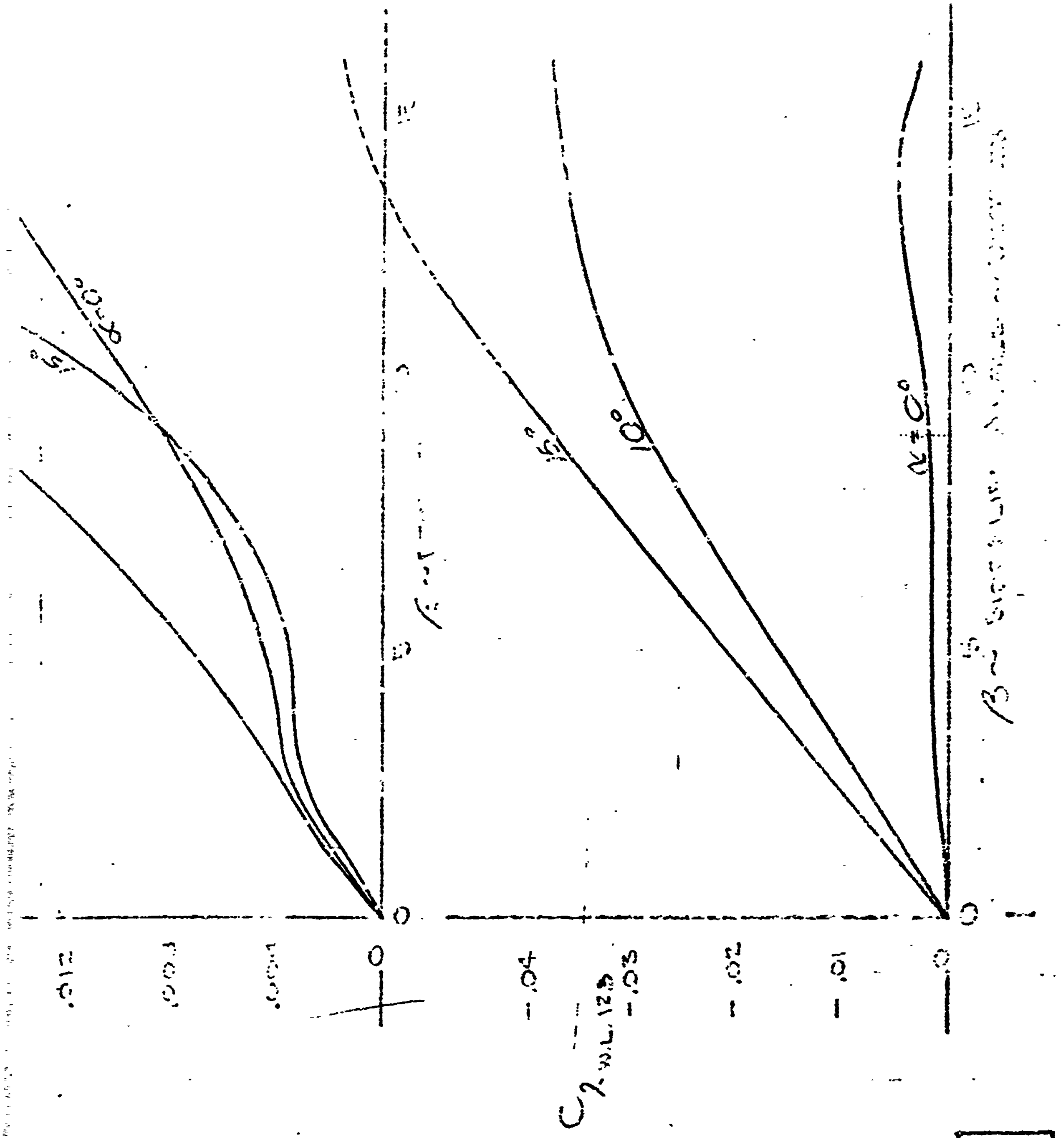


| | | | | | | |
|---|---|---|---|---|---|---|
| CALC | RWSVEY | 12 ... | REVISED | DATE | LATERAL - DIRECTIONAL STABILITY CHARACTERISTICS — WING TIPS EXTENDED — | FIG 6.3 |
| CHECK | | | | | | 844-2035 |
| APPD | | | | | | D2-8174 |
| APPD | | | | | — LANDING SPEED — | PAGE 6.9 |

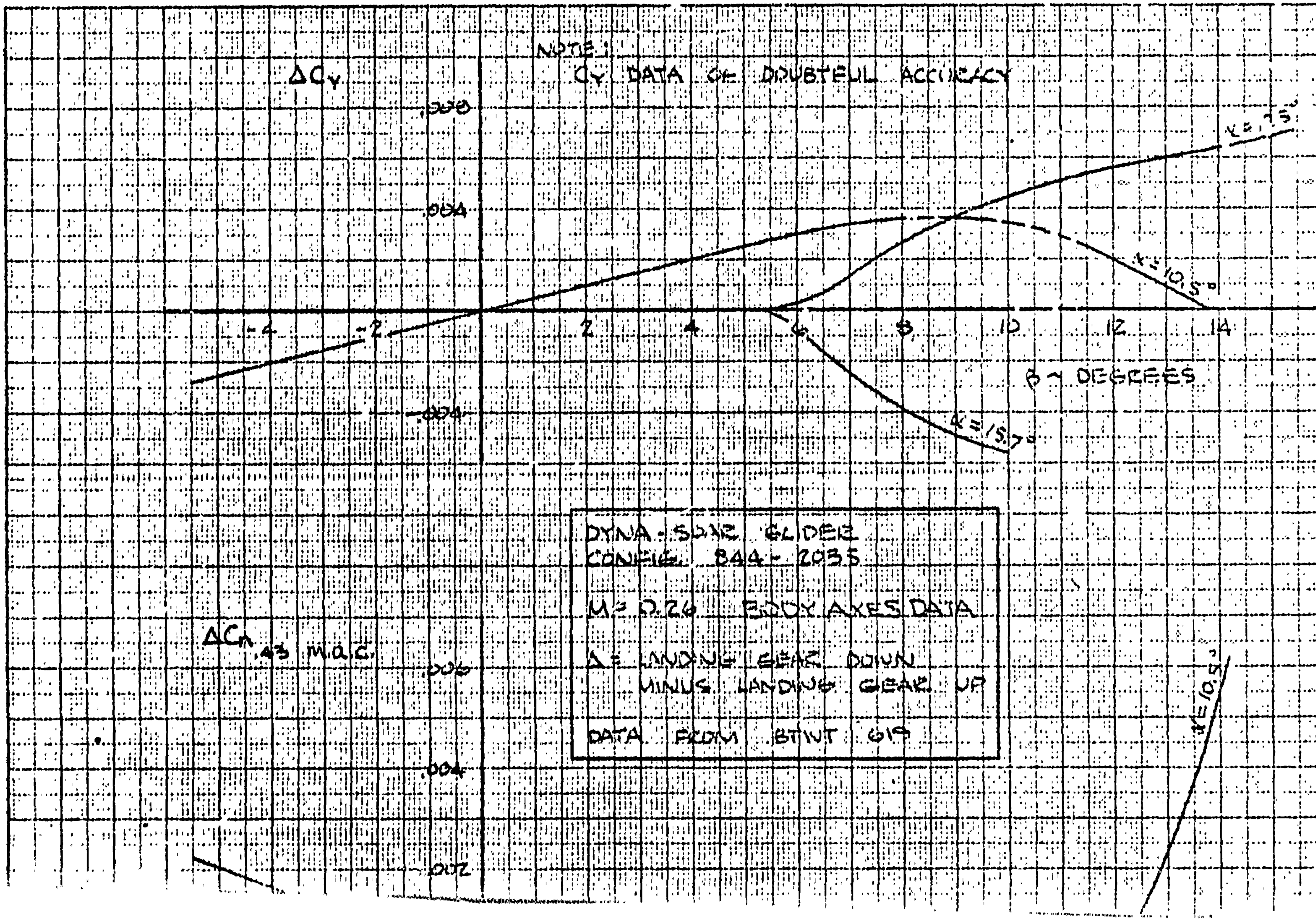

NOTE:
CY DATA OF DOUBTFUL ACCURACY
ΔCy
.008
.004
-.004
α=7.5°
α=10.5°
α=15.7°
-4
-2
2
4
6
8
10
12
14
β ~ DEGREES
DYNA-SOAR GLIDER
CONFIG. 844-2035
M=0.26 BODY AXES DATA
Δ= LANDING GEAR DOWN
MINUS LANDING GEAR UP
DATA FROM BTWT 619
ΔCn .43 M.a.c.
.006
.004
.002
α=10.5°

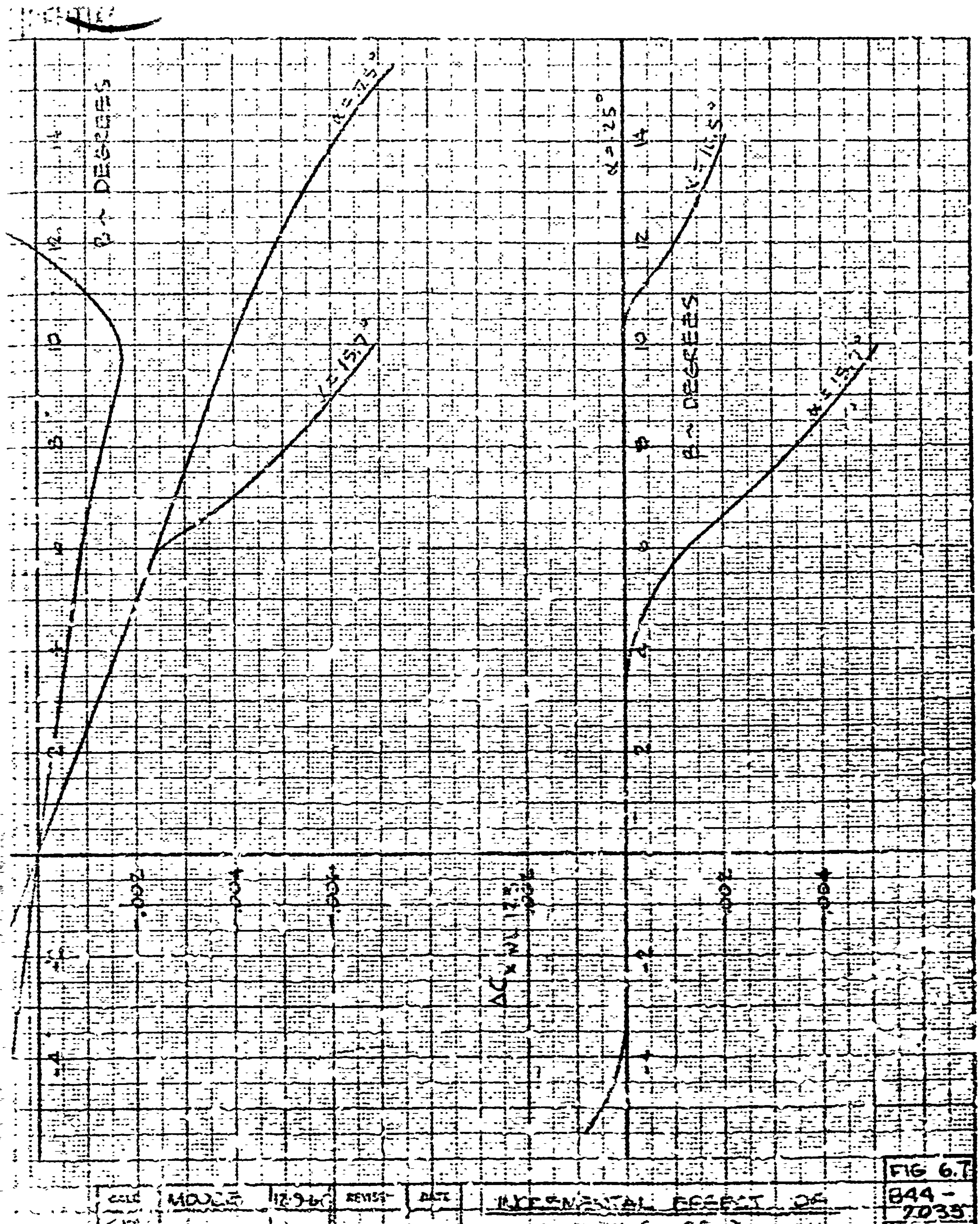


| | | | | | |
|---|---|---|---|---|---|
| CALC | MOORE | 12-9-60 | REVISED | DATE | INCREMENTAL EFFECT OF LANDING GEAR |
| CHECK | | | | | |
| APPD | | | | | |
| APPD | | | | | BOEING AIRPLANE COMPANY<br>SEATTLE 14, WASHINGTON |

FIG 6.7

844-7035

D2-8174

PAGE 6.10



BAC 1033-R-4

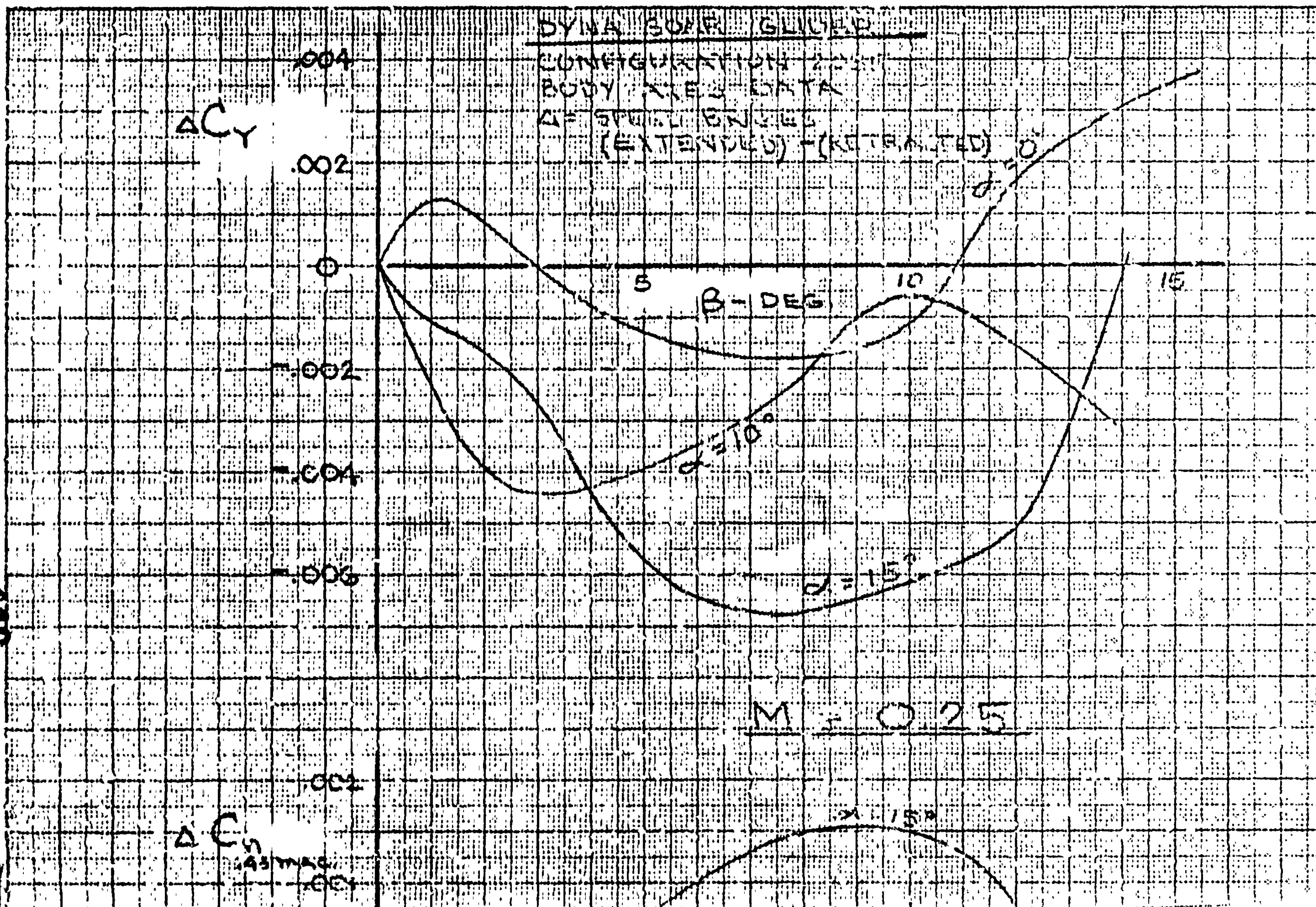
DYNA SOAR GLIDER
CONFIGURATION 2-2
BODY AXES DATA
Δ = STALL ENGINES (EXTENDED) - (RETRACTED)
ΔC_Y
.004
.002
0
-.002
-.004
-.006
5
10
15
β - DEG
α = 0°
α = 10°
α = 15°
M = 0.25
ΔC_n .45 mac
.002
.001
α = 15°

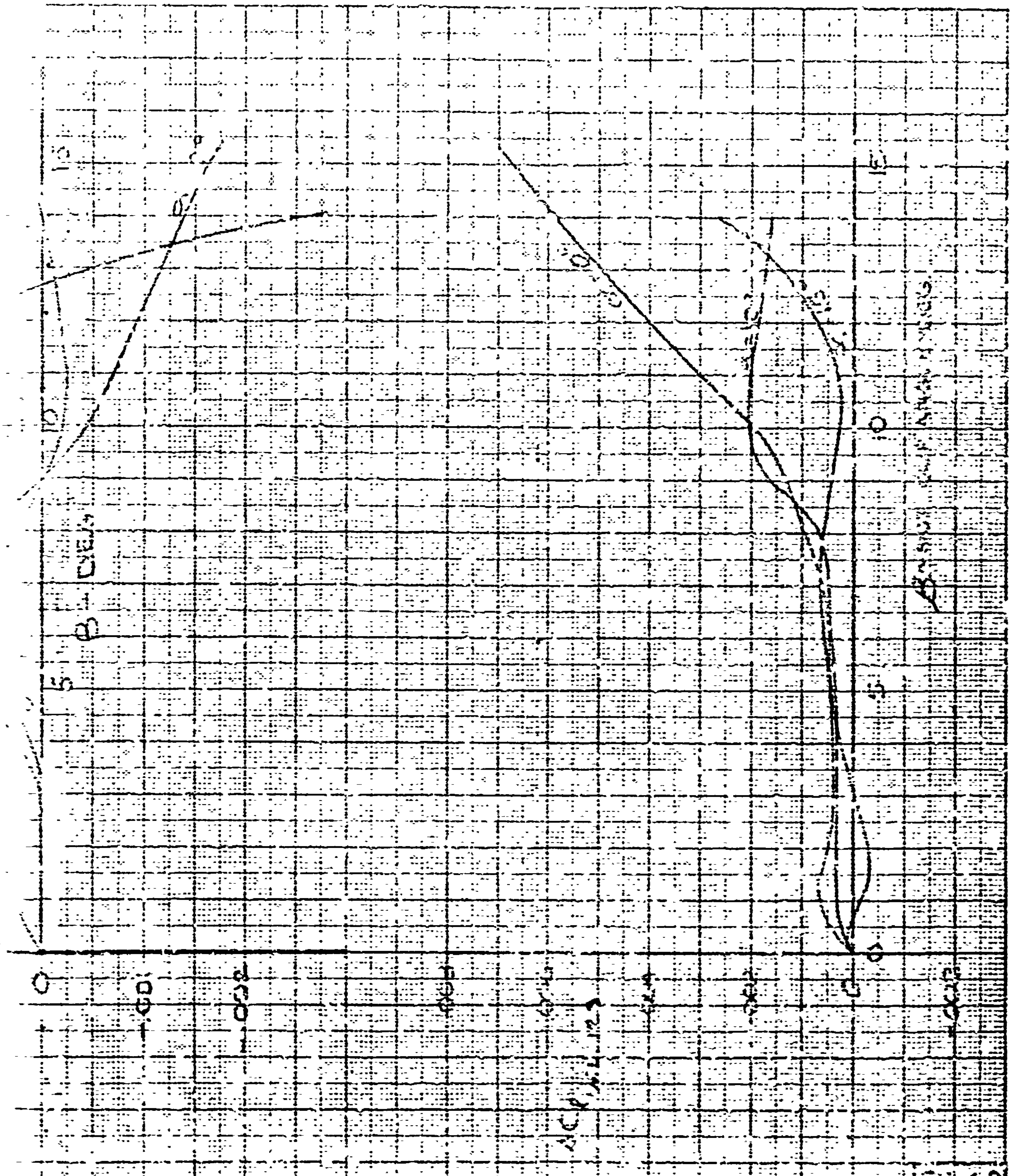

INCREMENTAL EFFECT OF SPEED BRAKES

LANDING SPEED

FTV

D2-6174

6.11

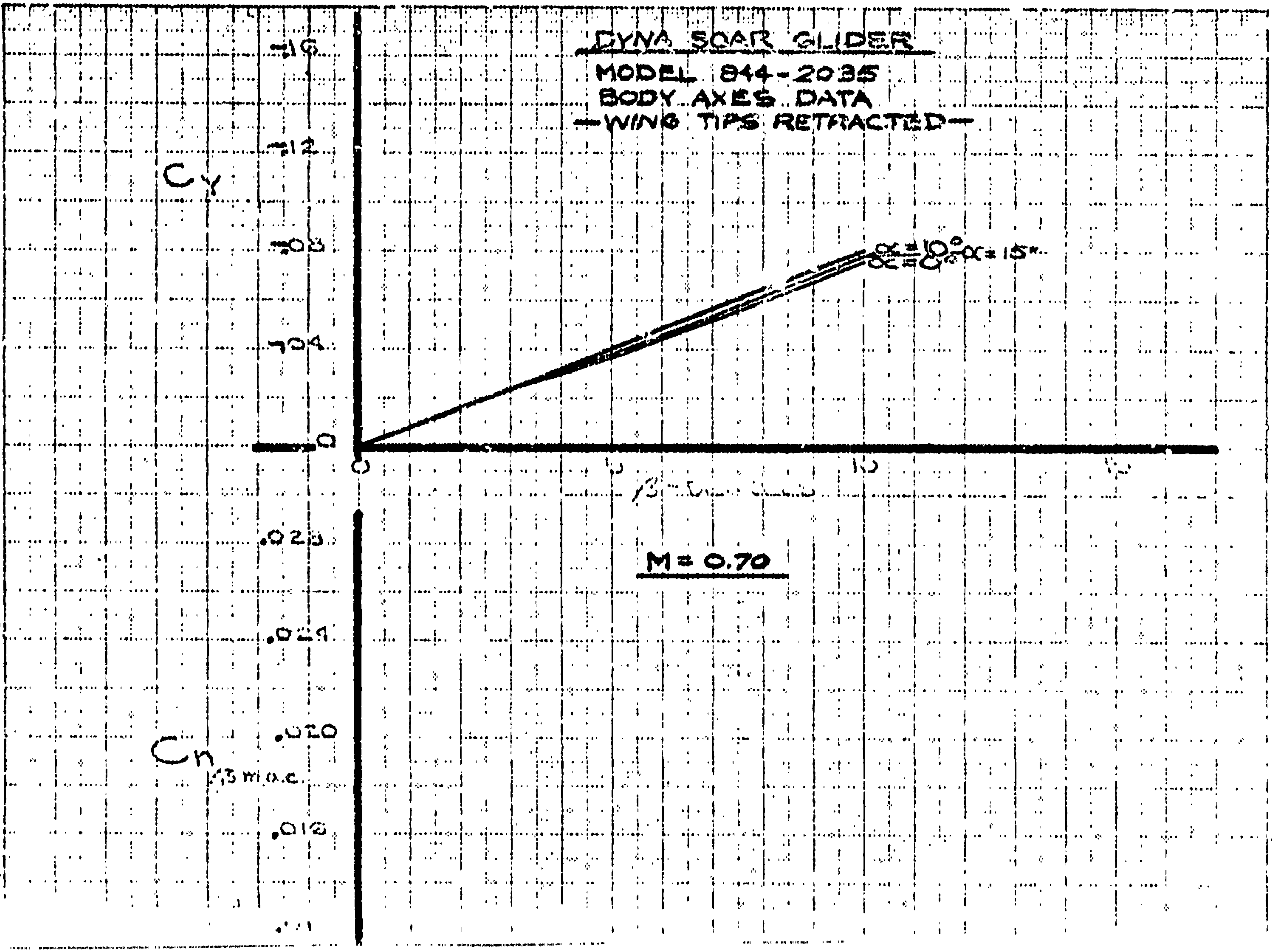
DYNA SOAR GLIDER
MODEL 844-2035
BODY AXES DATA
—WING TIPS RETRACTED—
M = 0.70
Cy
Cn
.016
.020
.024
.028
-.16
-.12
-.08
-.04
0
0
α = 10°
α = 15°

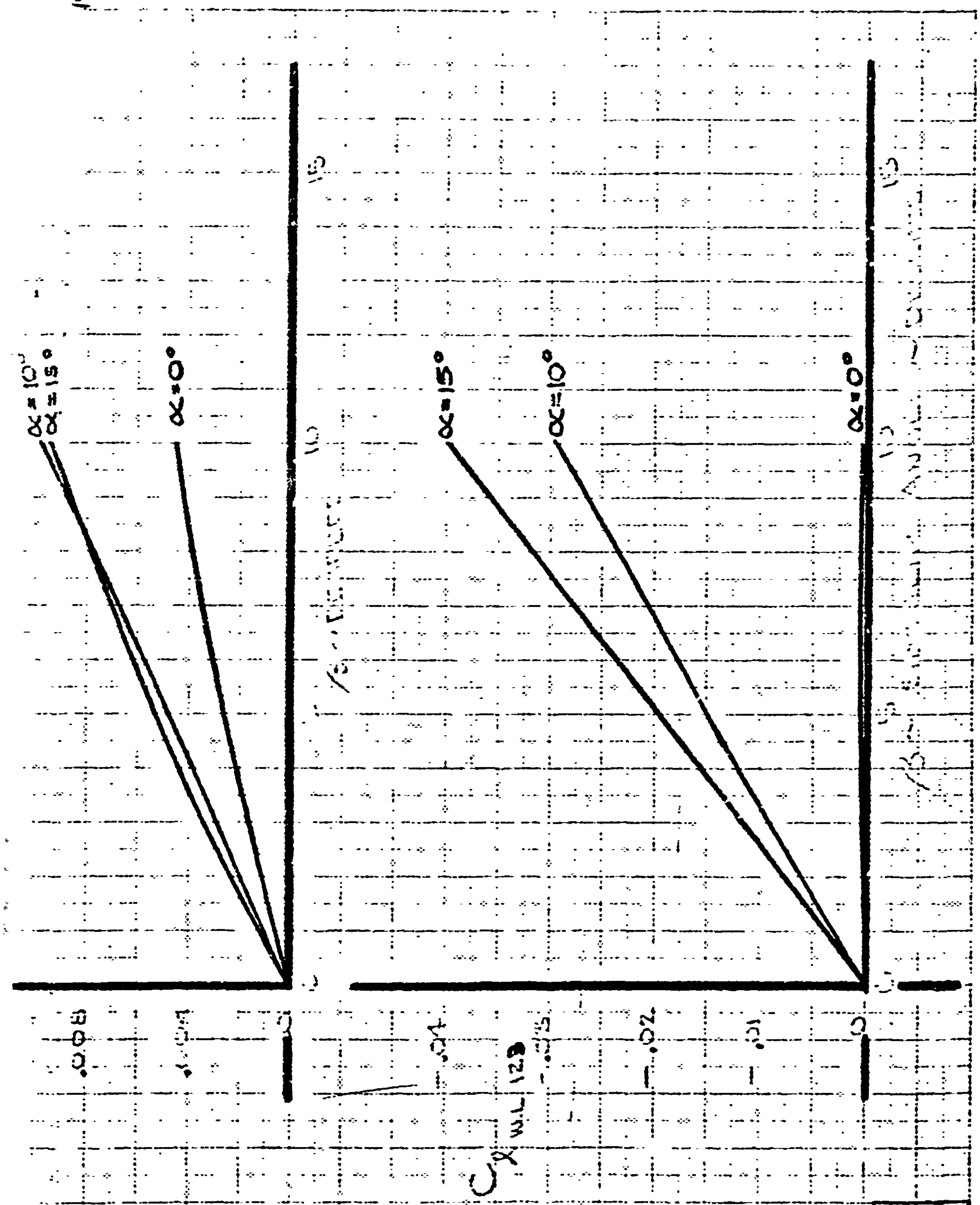


| | | |
|---|---|---|
| RKR 12-2060 | LATERAL-DIRECTIONAL STABILITY CHARACTERISTICS- WING TIPS RETRACTED | FIG 6.9 |
| | | 844-2055 |
| | | D2-8174 |
| | M= 0.70 | 6.12 |

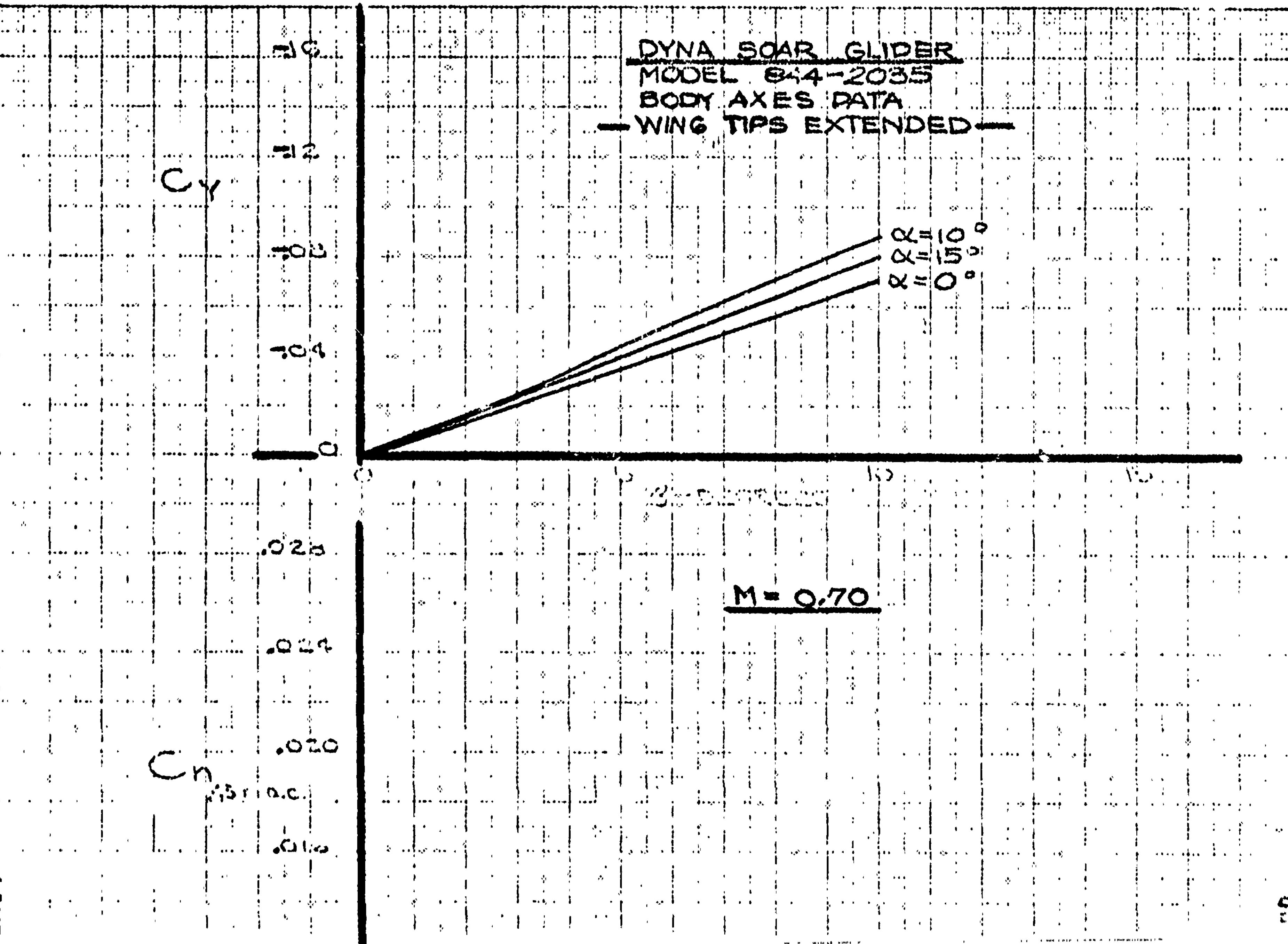
DYNA SOAR GLIDER
MODEL 844-2035
BODY AXES DATA
—WING TIPS EXTENDED—
α=10°
α=15°
α=0°
M= 0.70
$C_Y$
$C_{n_{.15\bar{c}\ a.c.}}$
0
.020

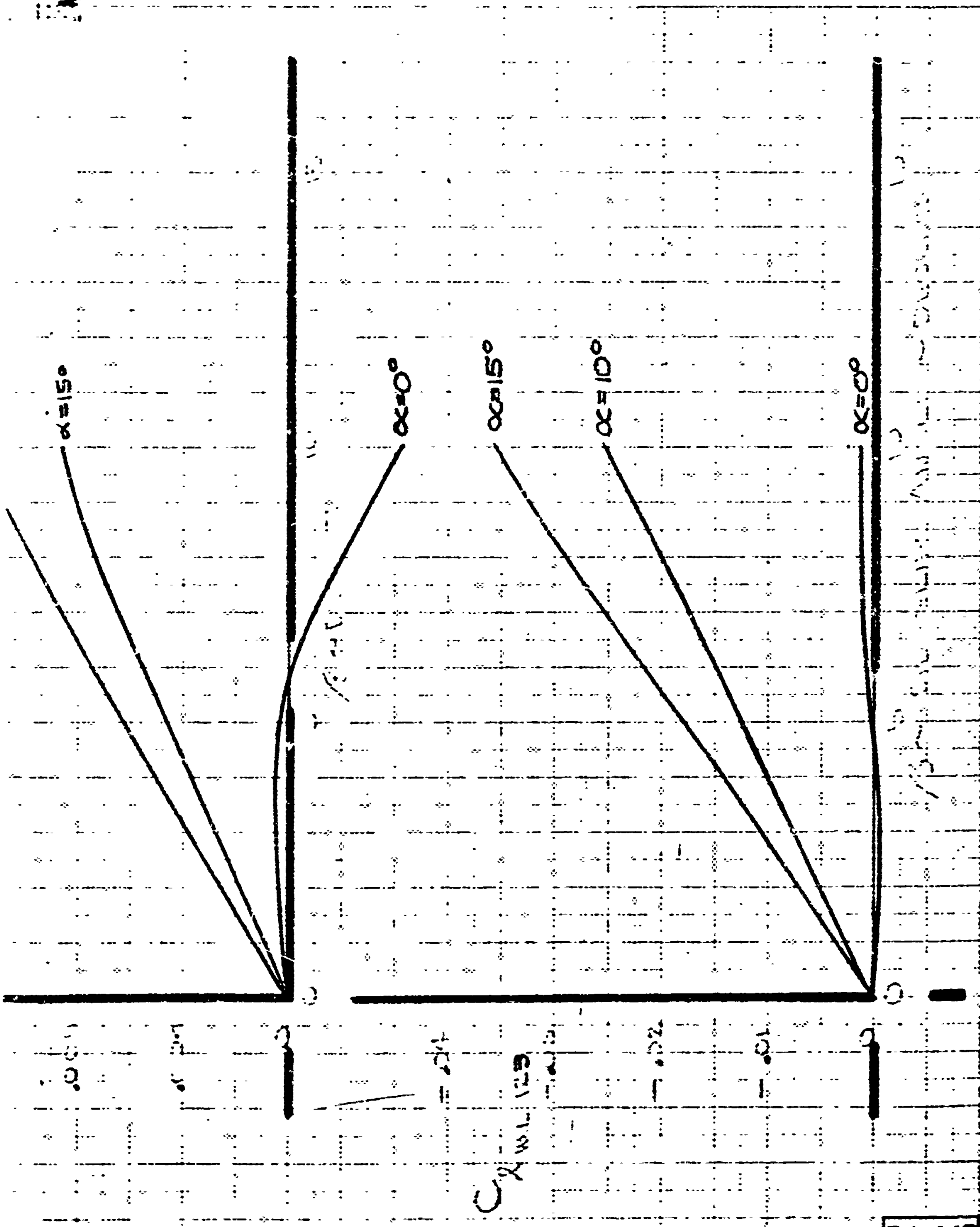


FIG 6.10

RKR 12-20-61

LATERAL - DIRECTIONAL
STABILITY CHARACTERISTICS
—WING TIPS EXTENDED—

M = 0.70

244-2095

D2-8174

6.13

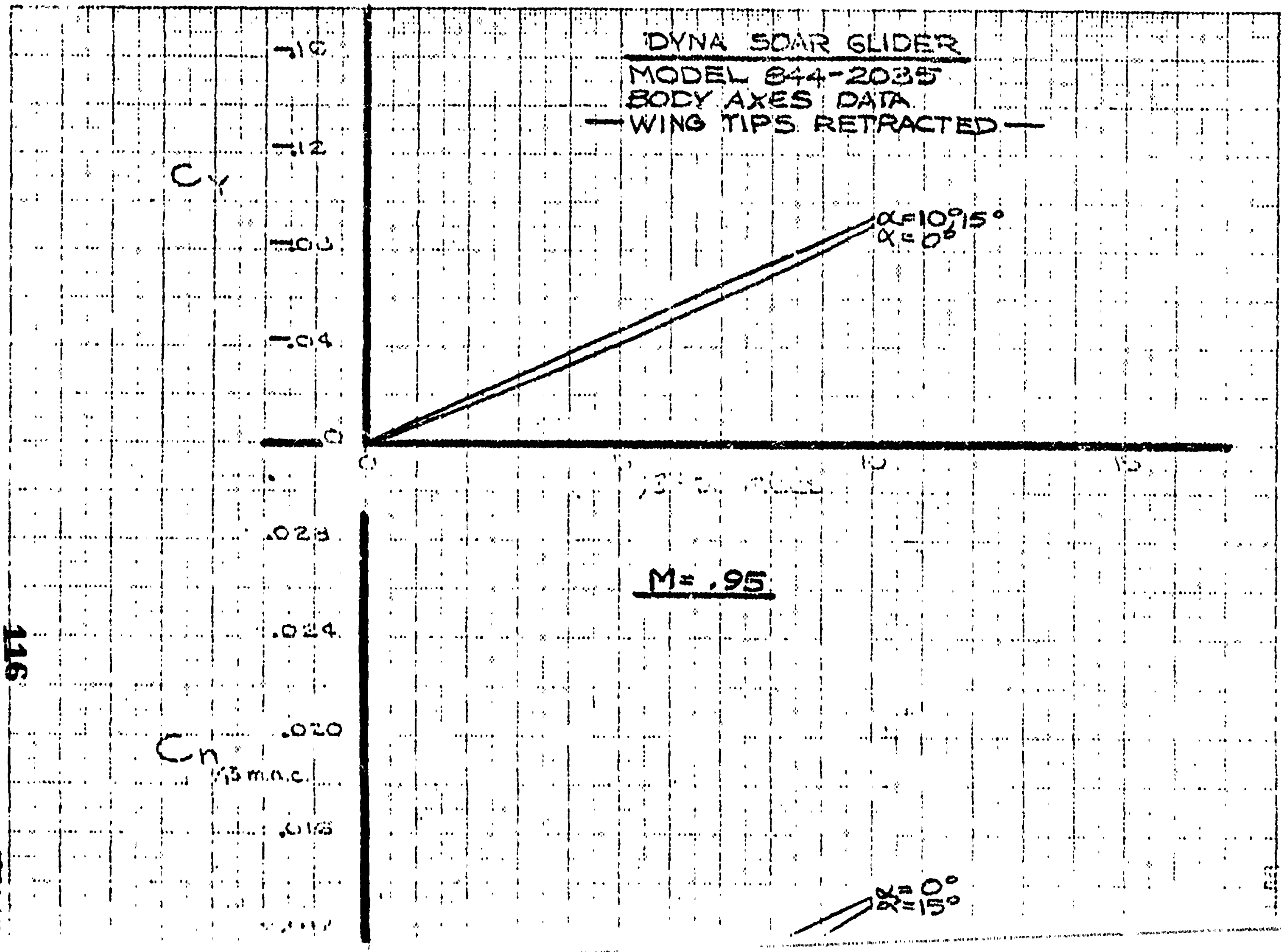
DYNA SOAR GLIDER
MODEL 844-2035
BODY AXES DATA
WING TIPS RETRACTED
α=10°,15°
α=0°
M= .95
α=0°
α=15°
Cy
Cn .25 m.a.c.
-.16
-.12
-.08
-.04
0
.028
.024
.020
.016
0
10

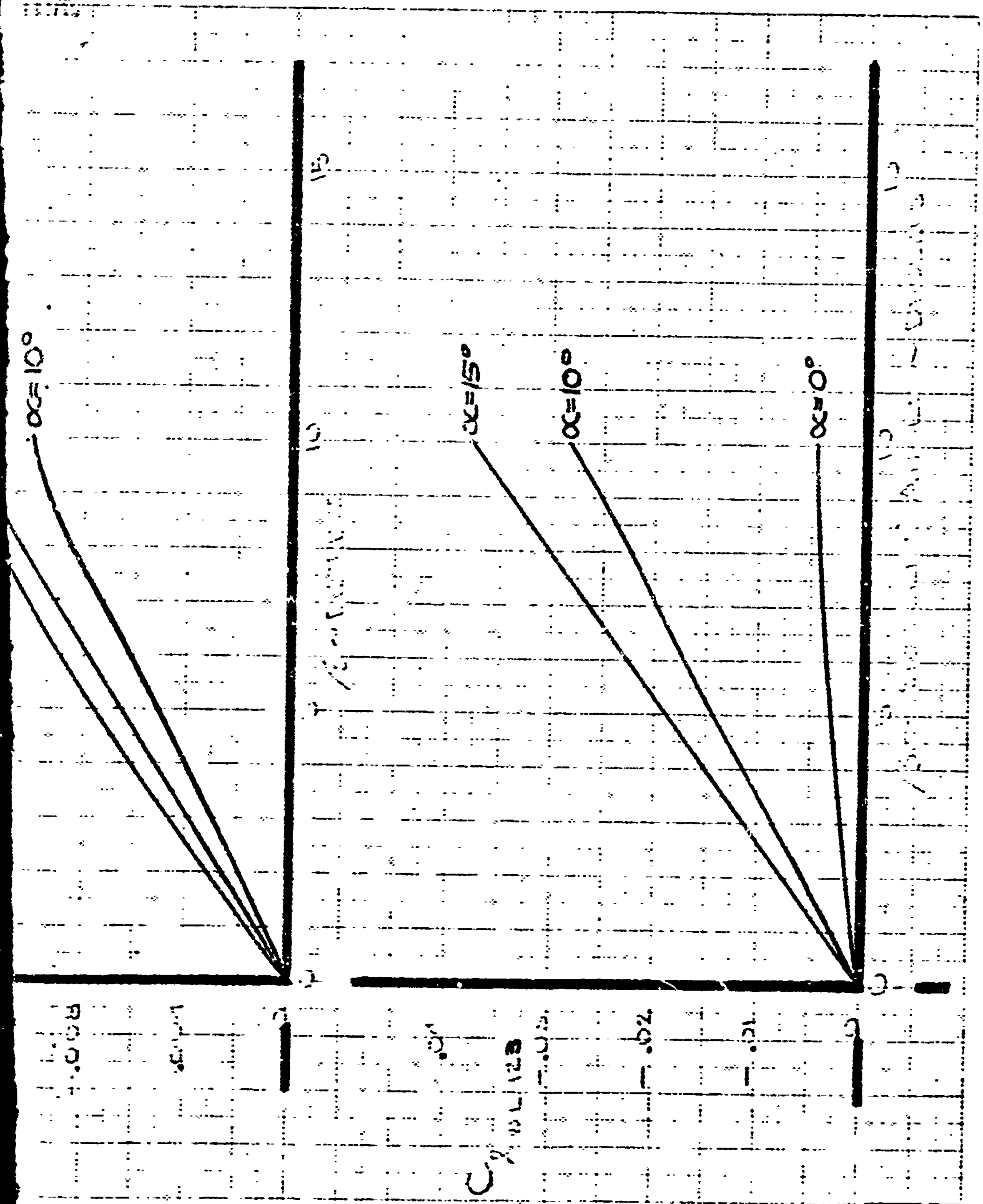


| | | | |
|---|---|---|---|
| RKR | 12-22-60 | LATERAL-DIRECTIONAL STABILITY CHARACTERISTICS WING TIPS RETRACTED | FIG 6.11 844-2055 D2-8174 |
| | | M=.95    117 | 6.14 |

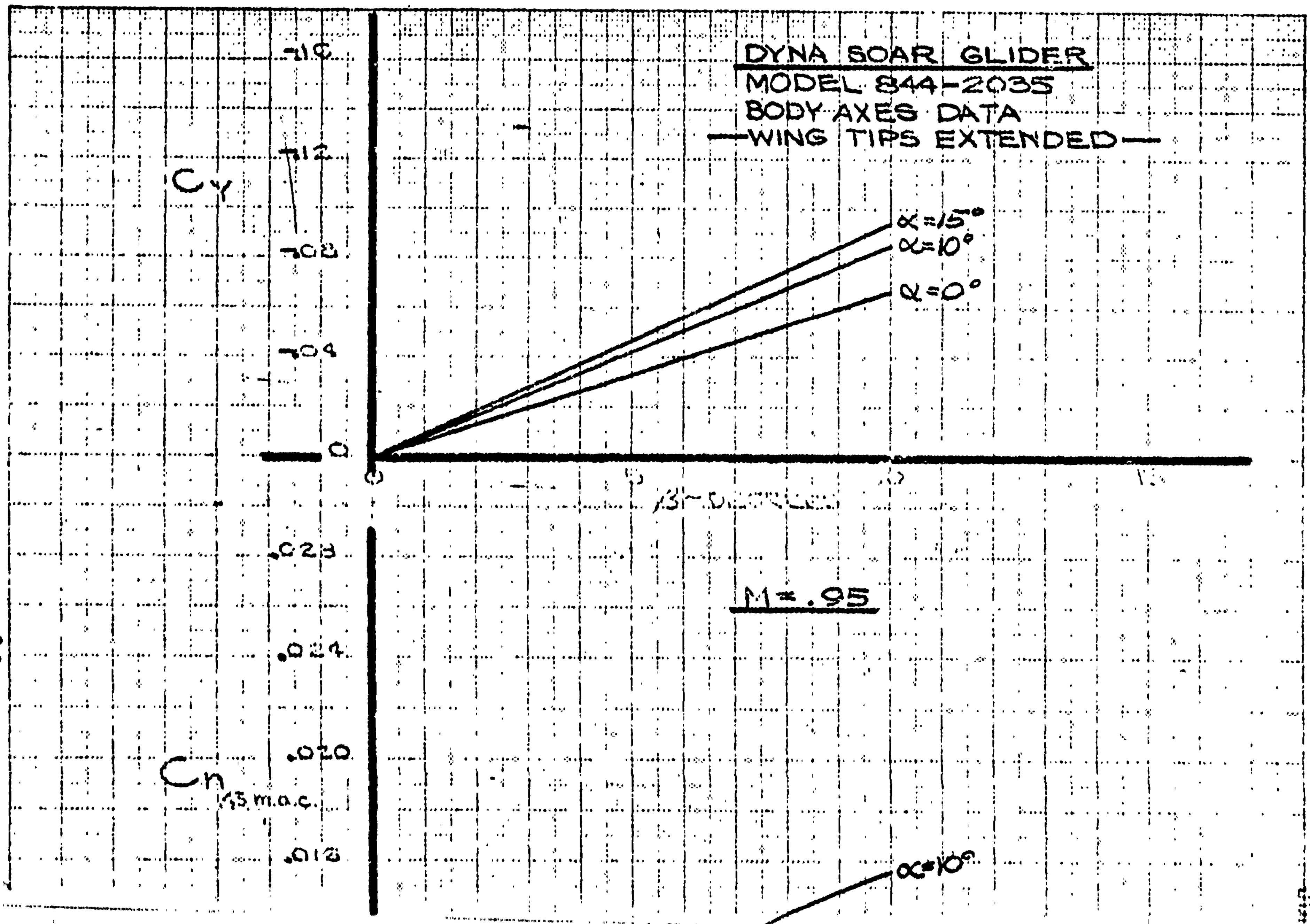
DYNA SOAR GLIDER
MODEL 844-2035
BODY AXES DATA
—WING TIPS EXTENDED—
$C_Y$
-.16
-.12
-.08
-.04
0
$\alpha=15°$
$\alpha=10°$
$\alpha=0°$
$M=.95$
.028
.024
.020
.016
$C_{n_{.35\,m.a.c.}}$
$\alpha=10°$

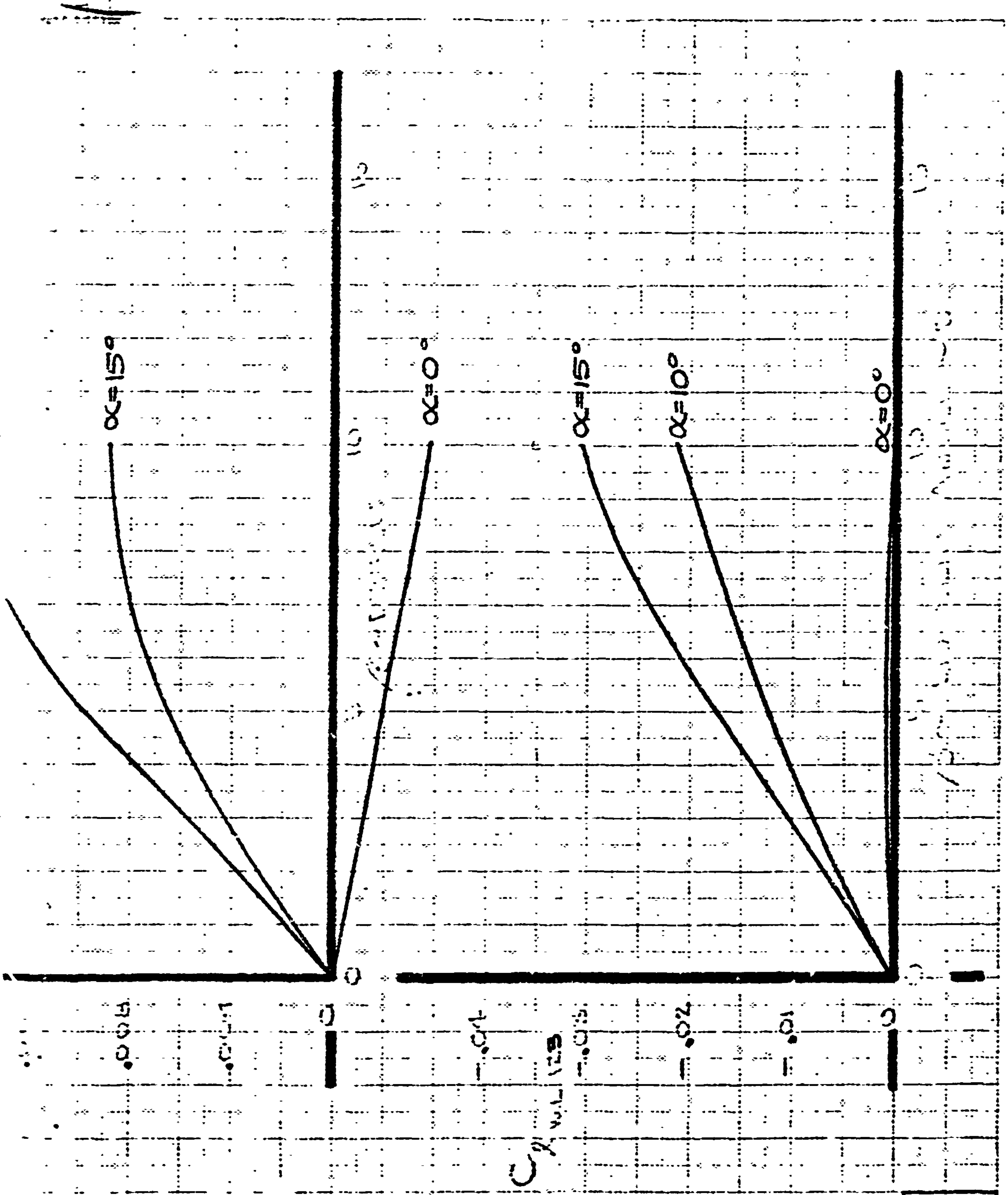


RKR/NTU 12-22-60

LATERAL- DIRECTIONAL
STABILITY CHARACTERISTICS
—WING TIPS EXTENDED—
M=.95

FIG 6.12
644-2955
D2-8174
6.15

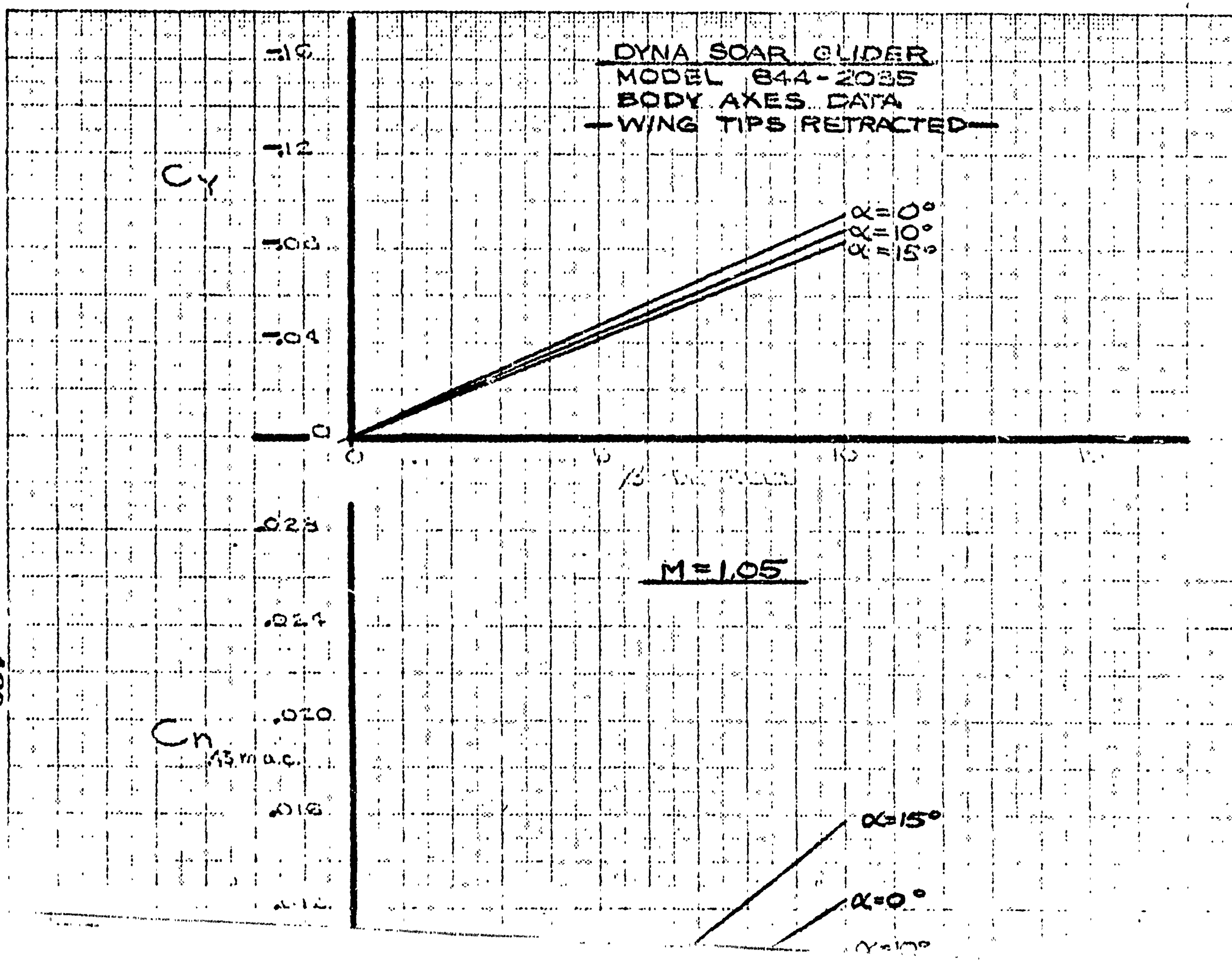
DYNA SOAR GLIDER
MODEL 844-2035
BODY AXES DATA
—WING TIPS RETRACTED—
M=1.05
$C_Y$
-.16
-.12
-.08
-.04
0
$C_{n_{.43\,m.a.c.}}$
.028
.024
.020
.016
α=0°
α=10°
α=15°

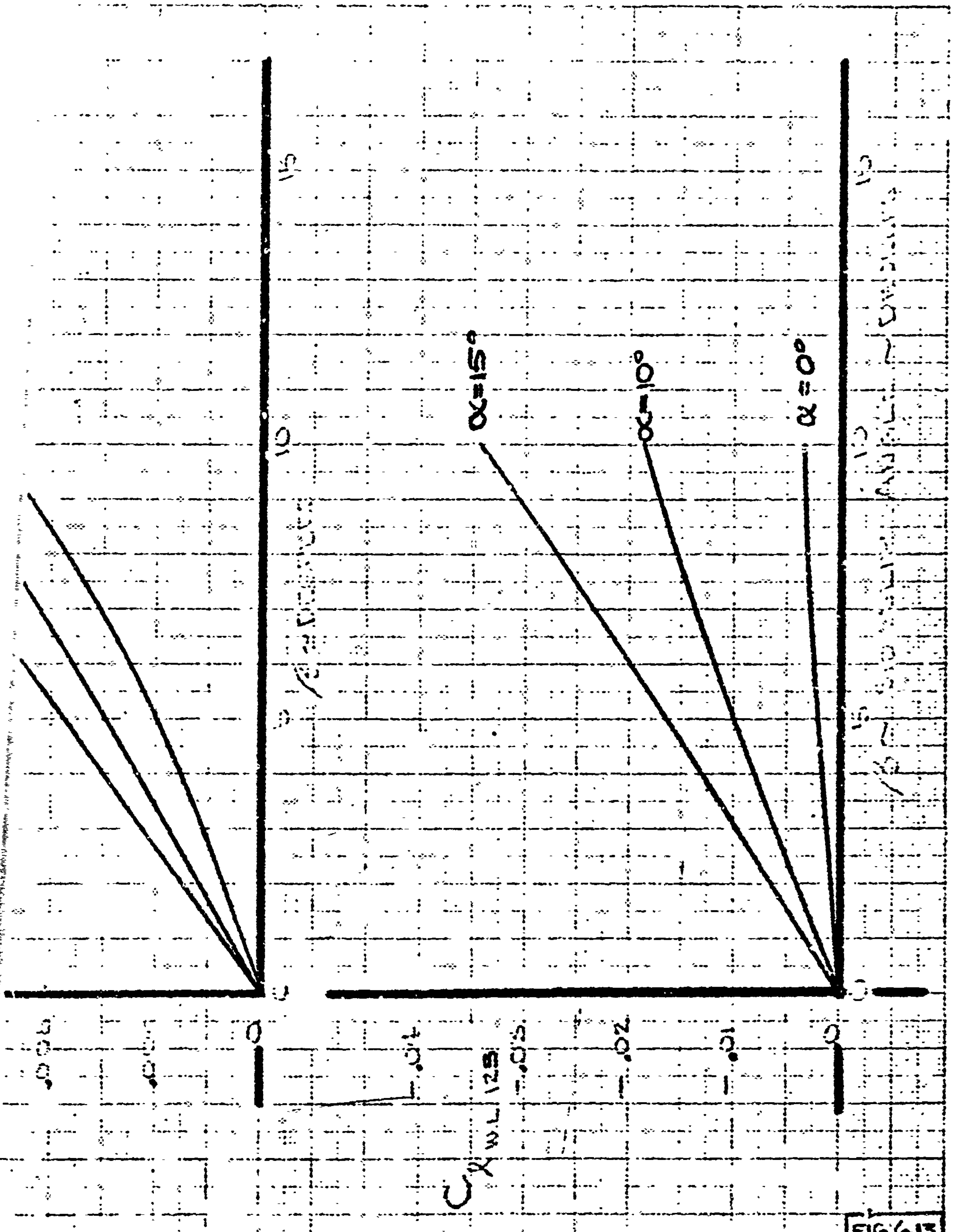


FIG. 6.13

RKR 12-20-60

LATERAL - DIRECTIONAL STABILITY CHARACTERISTICS

WING TIPS RETRACTED

M= 1.05

D2-8174

6.16

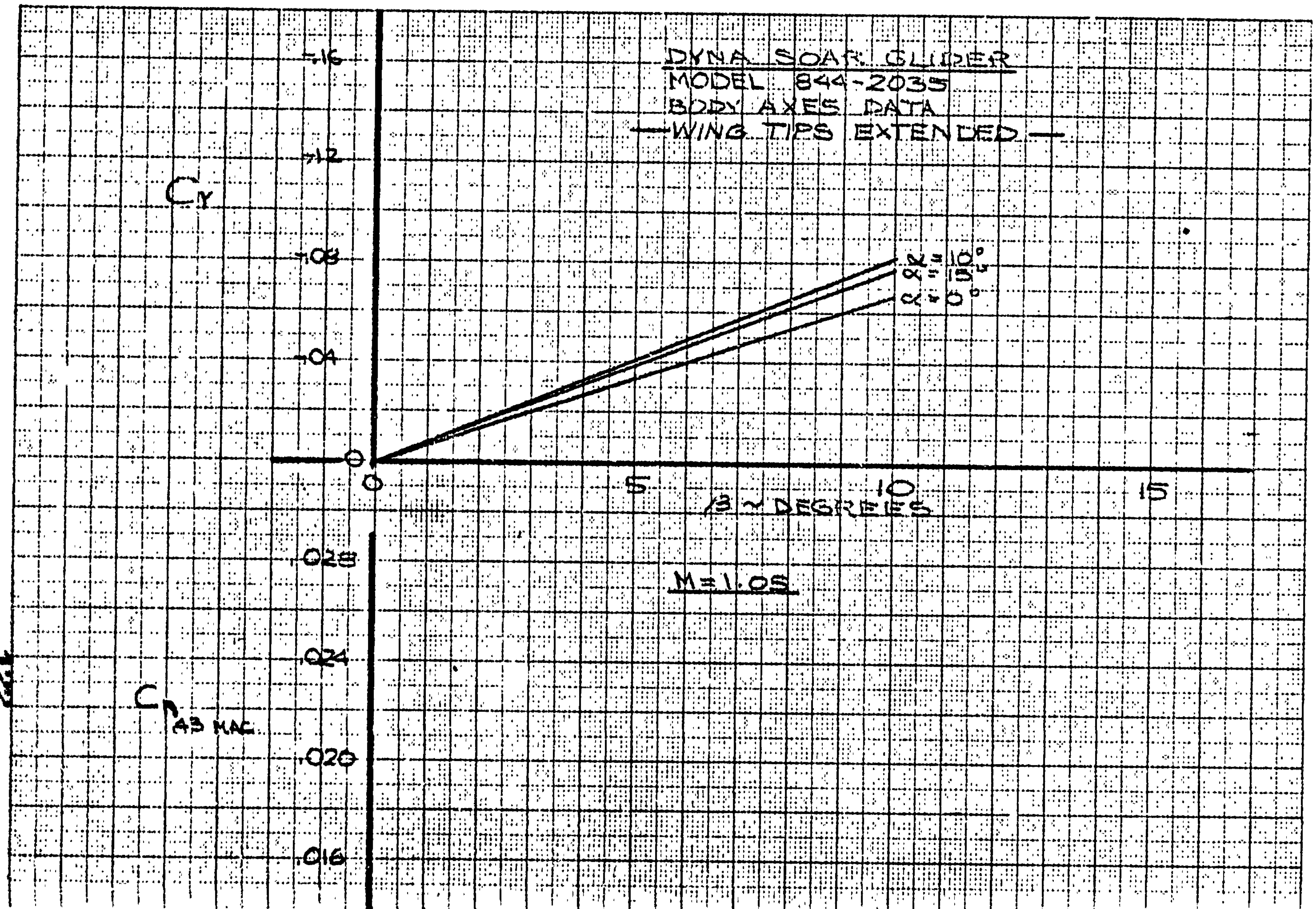
DYNA SOAR GLIDER
MODEL 844-2035
BODY AXES DATA
—WING TIPS EXTENDED—
α = 10°
α = 15°
α = 0°
$C_Y$
.16
.12
.08
.04
0
0
5
10
15
β ~ DEGREES
M = 1.05
.028
.024
.020
.016
$C_{n_{.43\,MAC}}$

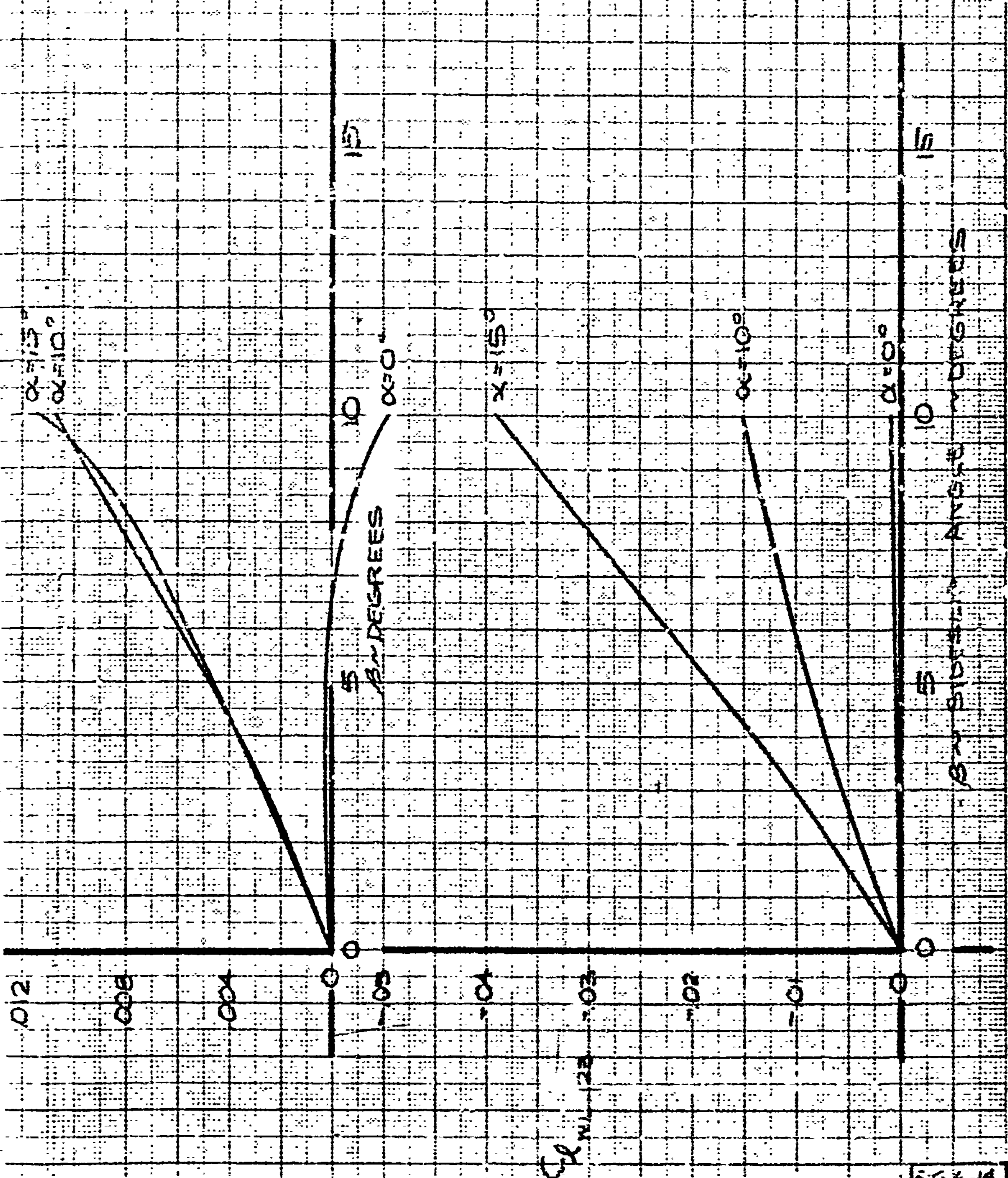


CONFIDENTIAL

| CALC | RKR | | REVISED | DATE | LATERAL - DIRECTIONAL STABILITY CHARACTERISTICS | FIG. 6.14 |
|---|---|---|---|---|---|---|
| CHECK | | | | | | |
| APPD | | | | | | D2-8174 |
| APPD | | | | | WING TIPS EXTENDED — M=1.05 | PAGE 6.17 |

844-2035

S = 845 ft²
b = 19.7 ft
CG = FUS STA 251 [illegible]

—— WINGTIPS EXTENDED
— — — " " RETRACTED

M = 2.0

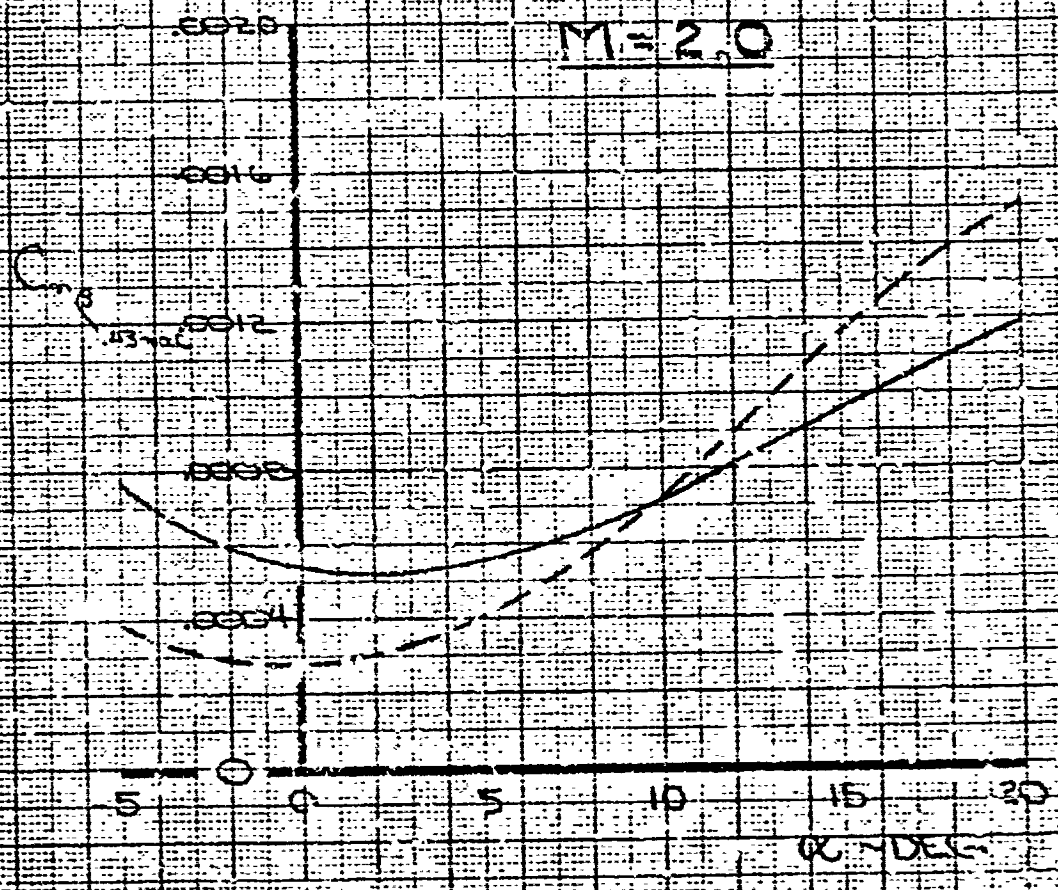


FIG. 6.18

| CALC | EK | 12-2-60 | REVISED | DATE | DIRECTIONAL STABILITY<br>M = 2.0<br>124 | 844-2035 |
|---|---|---|---|---|---|---|
| CHECK | | | | | | D2-8174 |
| APR | | | | | BOEING AIRPLANE COMPANY | PAGE 6.18 |
| APR | | | | | | |

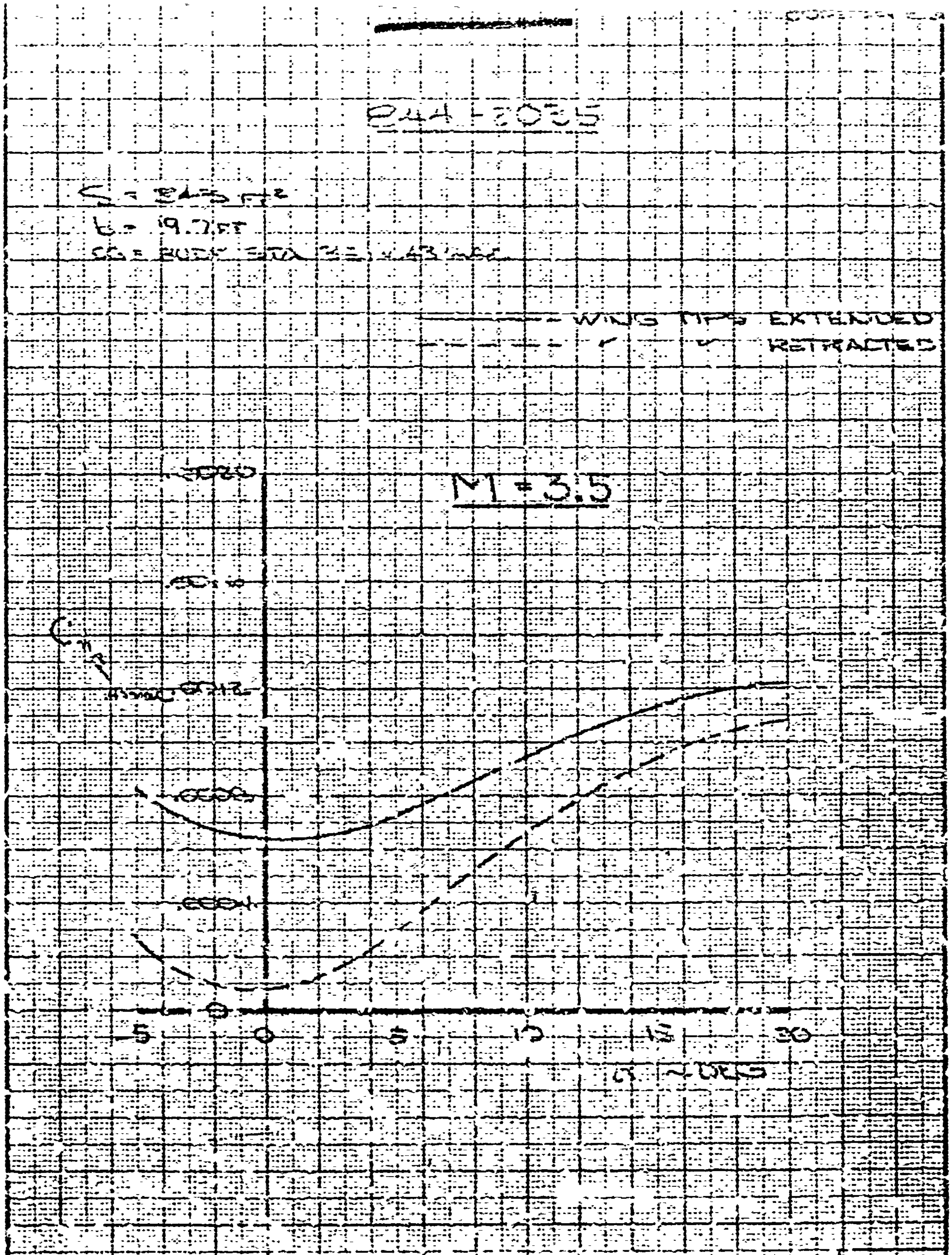


FIG. 6.16

| CALC | | | REVISED | DATE | DIRECTIONAL STABILITY | 844-2035 |
|---|---|---|---|---|---|---|
| CHECK | | | | | M = 3.5 125 | D2-6174 |
| APD | | | | | | |
| APR | | | | | BOEING AIRPLANE COMPANY | PAGE 6.19 |

BODY AXES

E44-2035

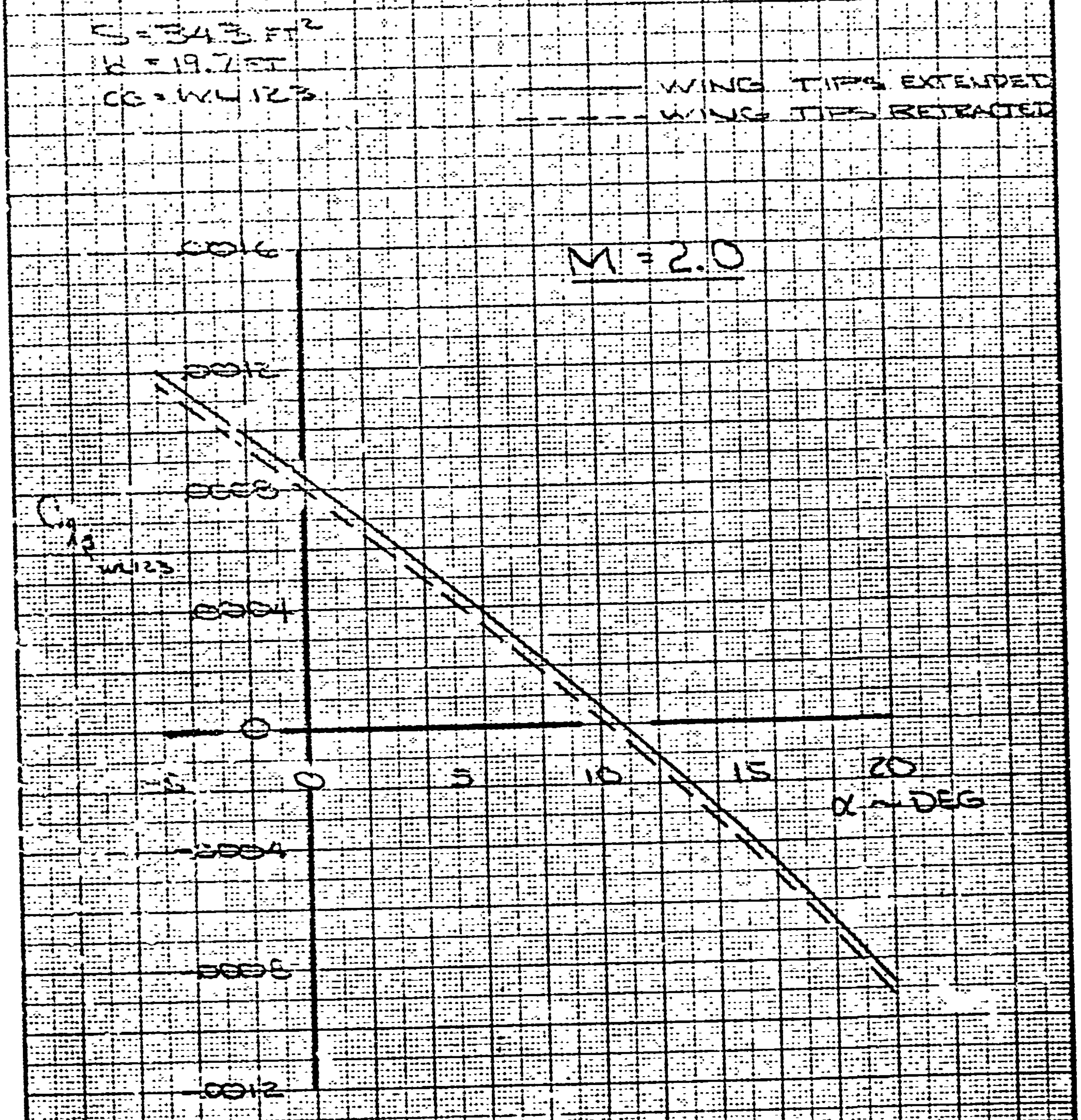


FIG. 6.17

| CALC | E.J.R. | 12-2-6 | REVISED | DATE | LATERAL STABILITY M = 2.0 | E44-2035 |
|---|---|---|---|---|---|---|
| CHECK | | | | | 126 | D2-8174 |
| APR | | | | | BOEING AIRPLANE COMPANY | PAGE 6.20 |
| APR | | | | | | |

K-E

BODY AXES

844-2035

S = 343 FT²
b = 19.7 FT
CG = W.L. 123

——— WING TIPS EXTENDED
— — — — WING TIPS RETRACTED

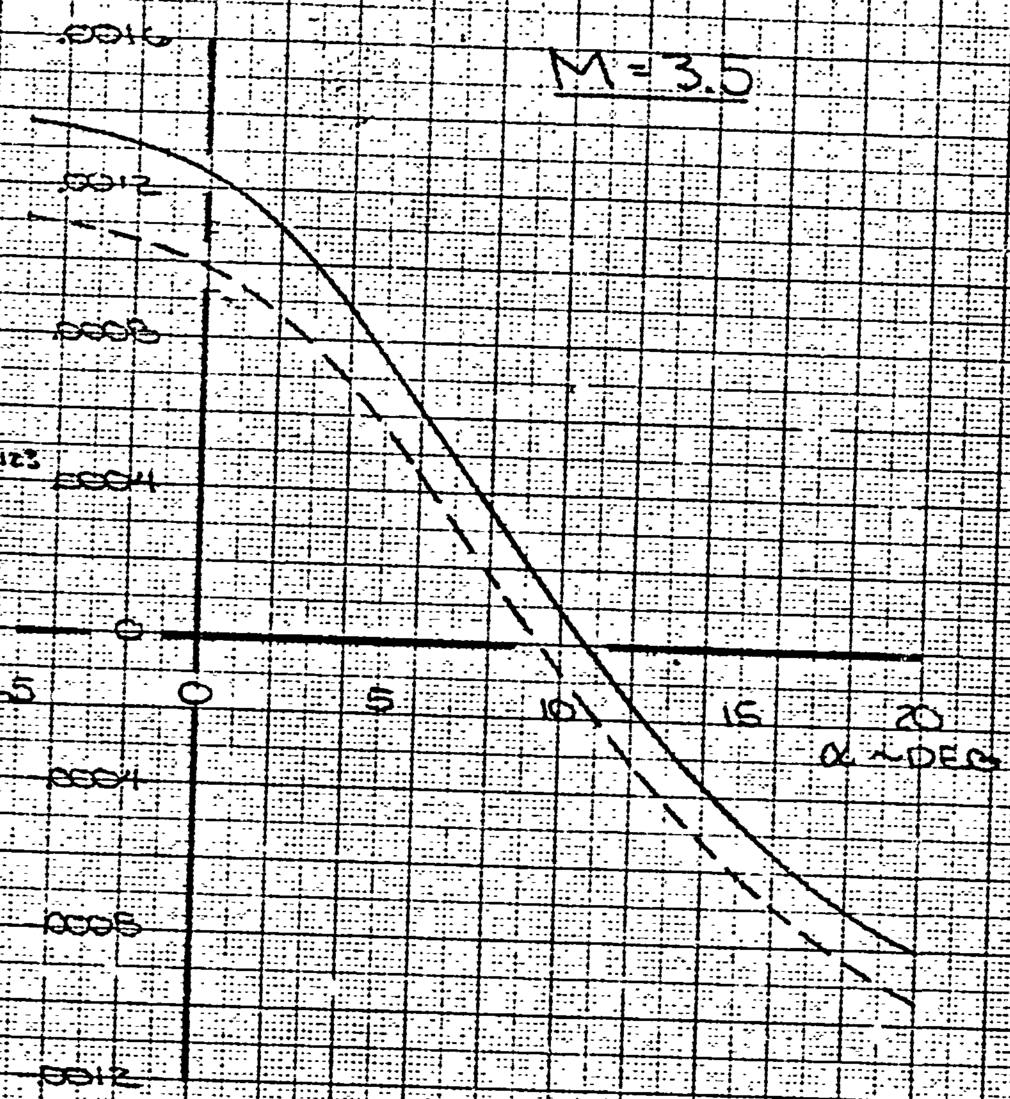


| | | | | | |
|---|---|---|---|---|---|
| CALC | EJR | 12-2-0 | REVISED | DATE | LATERAL STABILITY M = 3.5 |
| CHECK | | | | | |
| APR | | | | | |
| AFR | | | | | |

127

BOEING AIRPLANE COMPANY

FIG. 6.18

844-2035

D2-8174

[redacted]

844-2035

S = 3443 FT²

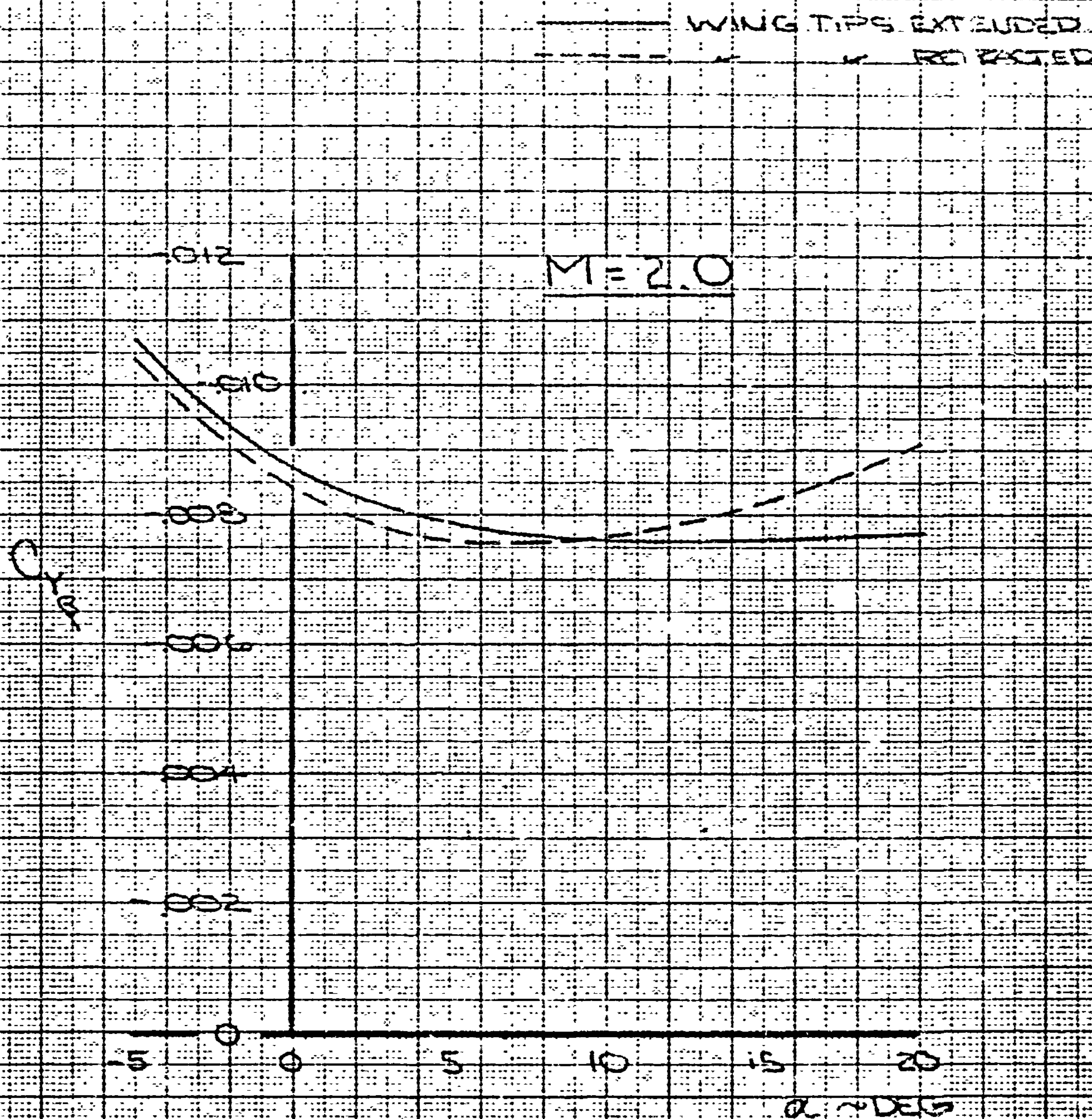


FIG. 6.19

| CALC | KFK | 12-2-0 | REVISED | DATE | SIDE FORCE | 844-2035 |
|---|---|---|---|---|---|---|
| CHECK | | | | | M = 2.0 **128** | D2-8174 |
| APR | | | | | BOEING AIRPLANE COMPANY | PAGE 6.22 |
| APR | | | | | | |

[redacted]

K·E 60629

[redacted]

844-2035

S = 343 FT²

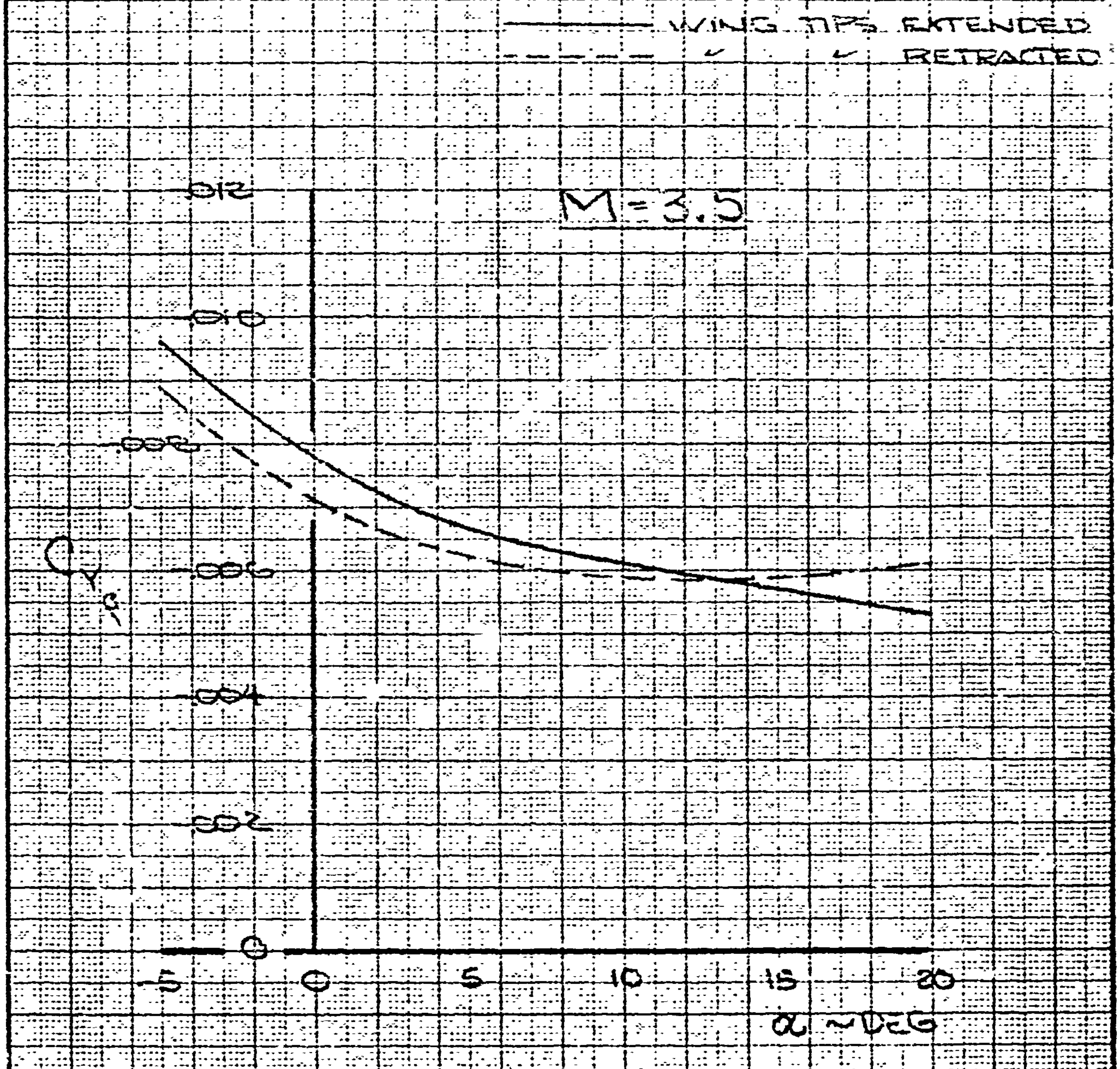


FIG.6.20

| CALC | BTR | 2-2-0 | REVISED | DATE |
|---|---|---|---|---|
| CHECK | | | | |
| APR | | | | |
| APR | | | | |

SIDE FORCE

M = 3.5 **129**

BOEING AIRPLANE COMPANY

844-2035

D2-8174

PAGE 6.23

[redacted]

109

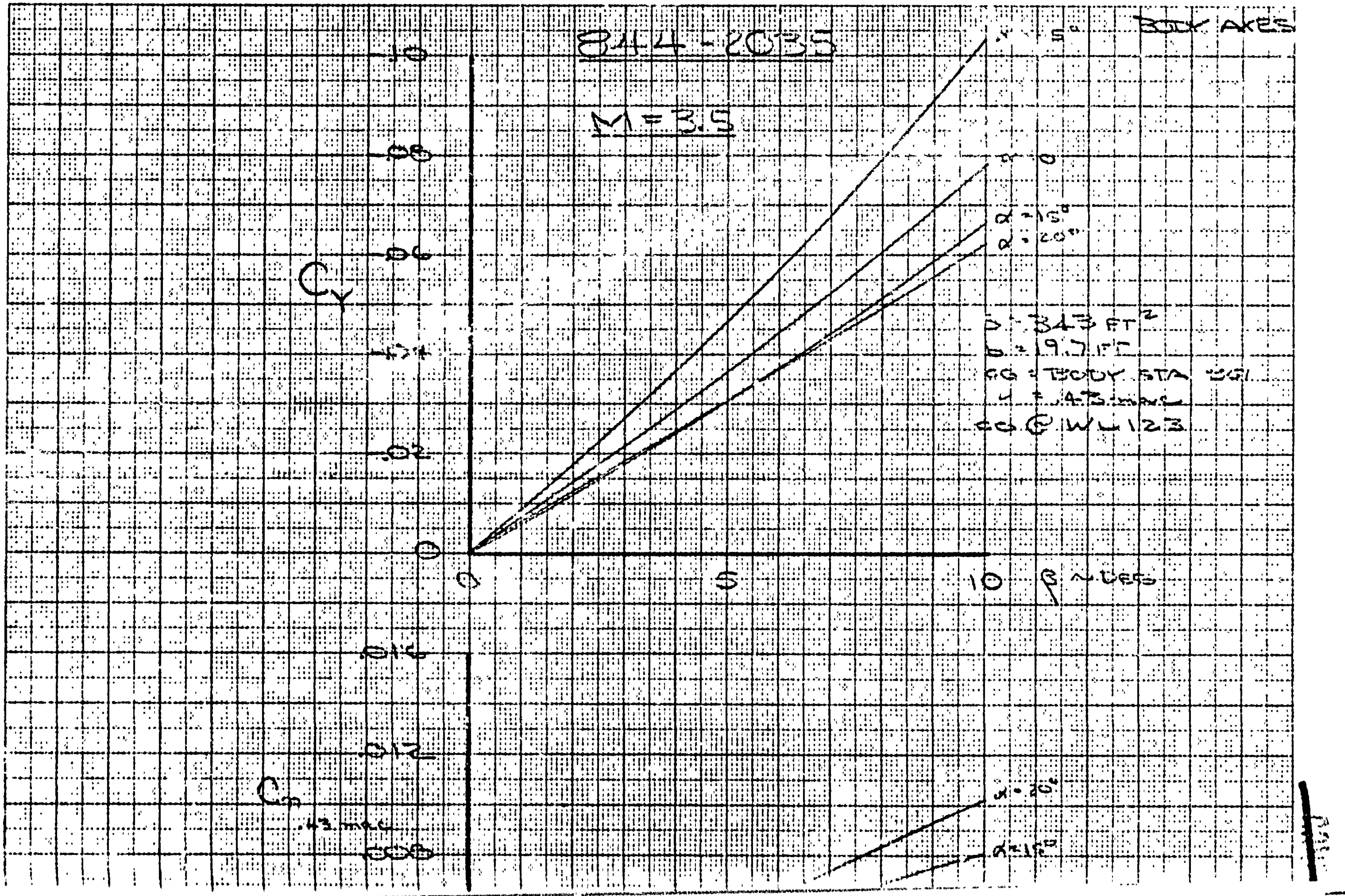

844-2035
BODY AXES
M = 3.5
$\alpha = 5°$
$\alpha = 0$
$\alpha = 15°$
$\alpha = 20°$
S = 343 FT²
b = 19.7 FT
CG = BODY STA 351
= .43 mac
CG @ WL 123
$C_Y$
.10
.08
.06
.04
.02
0
0
5
10
$\beta$ ~ DEG
.016
.012
.008
$C_n$
.43 mac
$\alpha = 20°$
$\alpha = 15°$

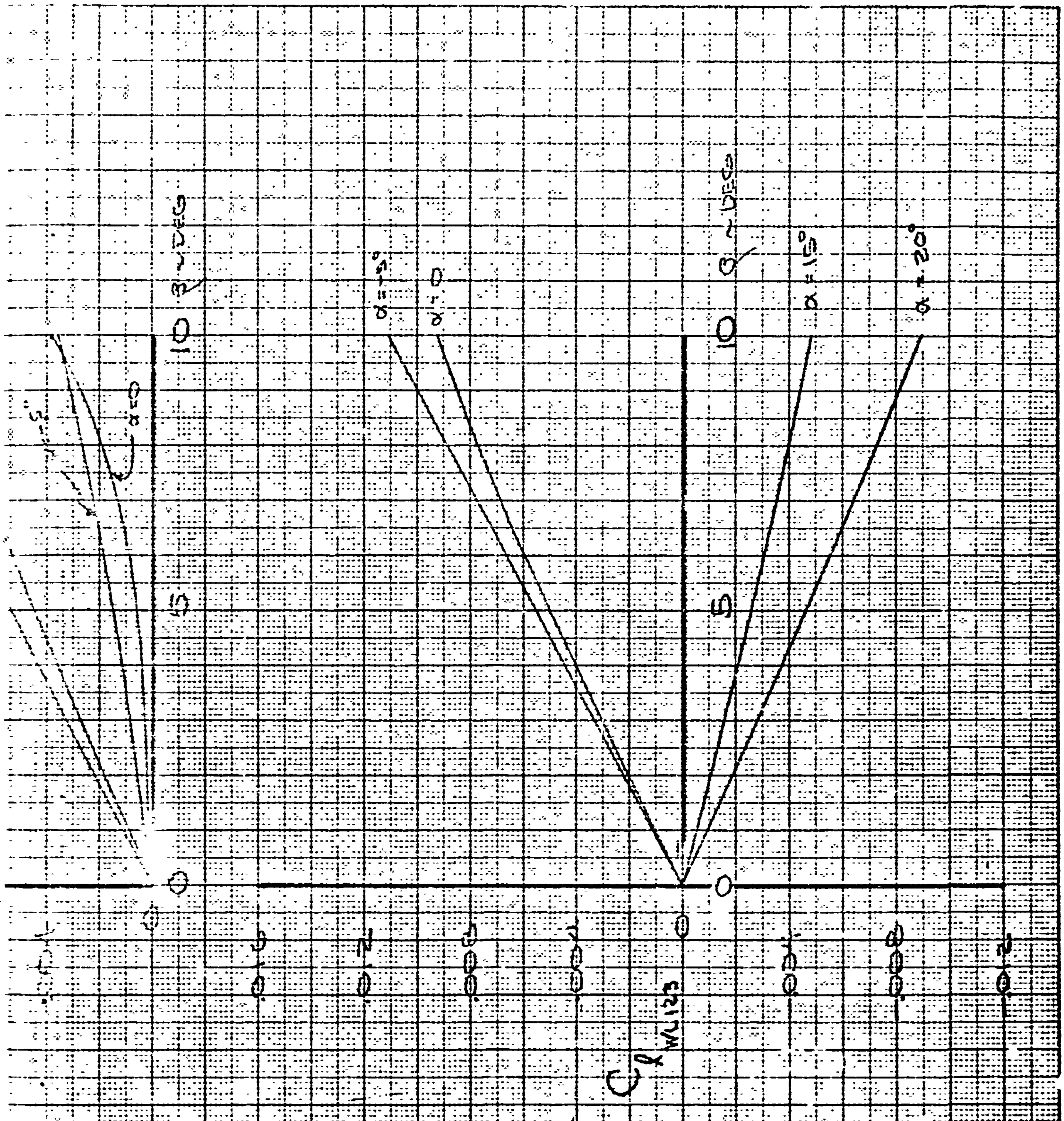


FIG. 6.21

244-2035

LATERAL-DIRECTIONAL STABILITY ~ M=0.5 ~ WING TIPS RETRACTED

D2-8174

PAGE 6.24

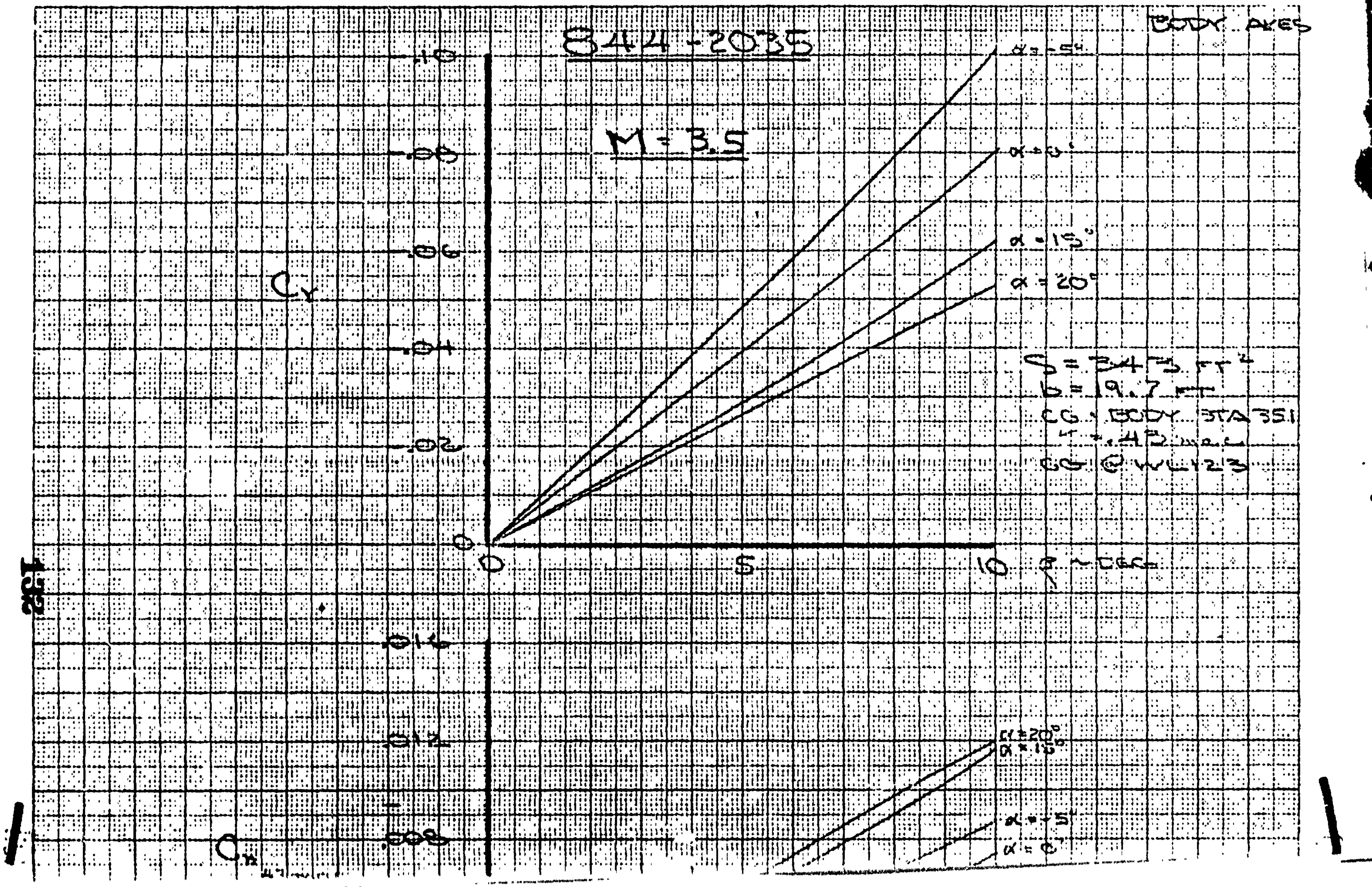
BODY AXES
844-2035
M = 3.5
.10
.08
.06
.04
.02
0
$C_Y$
α = -5°
α = 0°
α = 15°
α = 20°
S = 343 FT²
b = 19.7 FT
CG: BODY STA 351
.43 m.a.c.
CG @ WL123
0
5
10
β ~ DEG
.016
.012
.008
α = 20°
α = 15°
α = -5°
α = 0°

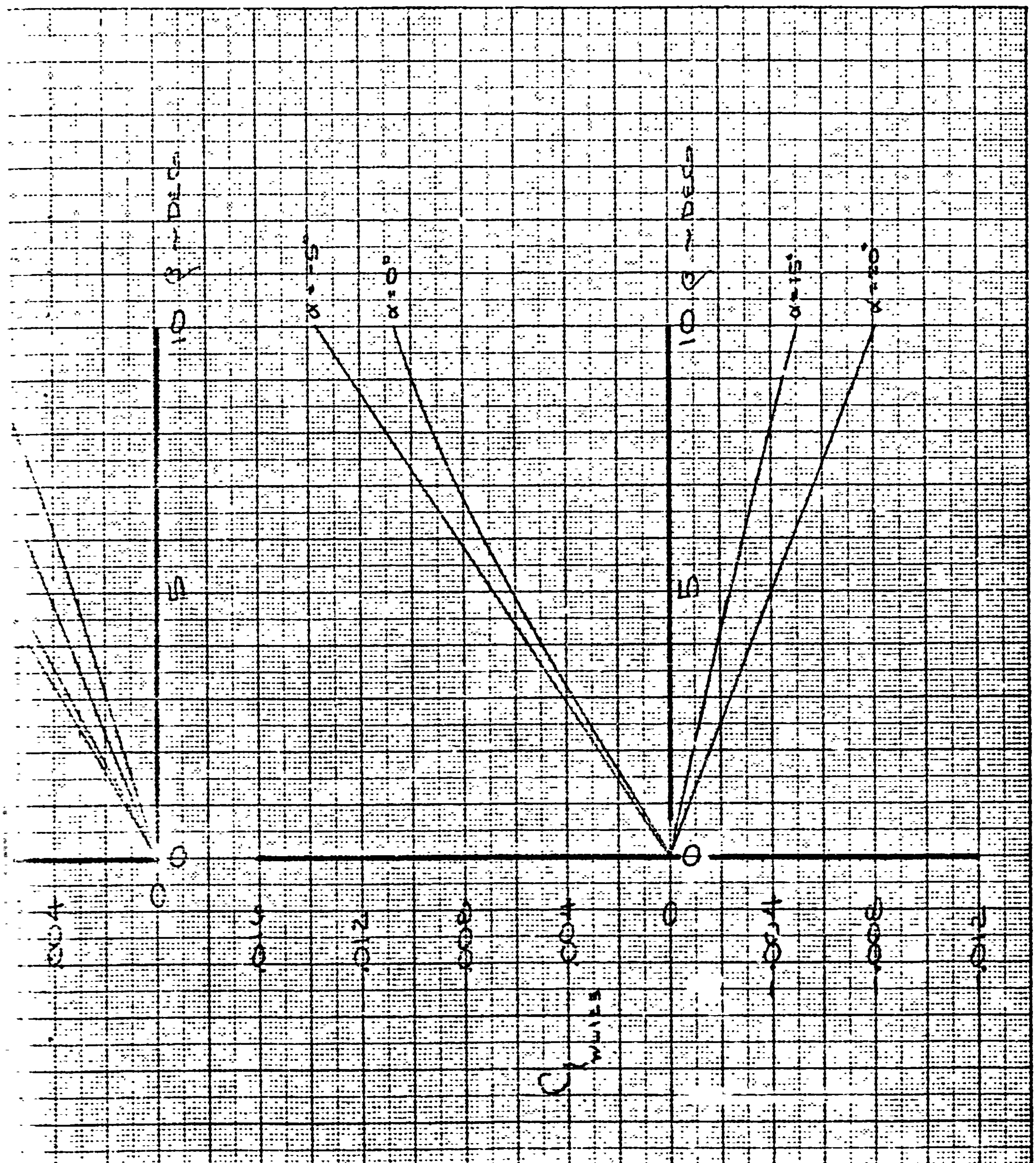


| | | | |
|---|---|---|---|
| CALC TYR 2-5-C | REVISED DATE | LATERAL-DIRECTIONAL | FIG. 6.22 |
| CHECK | | STABILITY ~ M = 3.5 ~ | 644-2055 |
| APR | | WING TIPS EXTENDED | D2-3174 |
| | | | PAGE 6.45 |

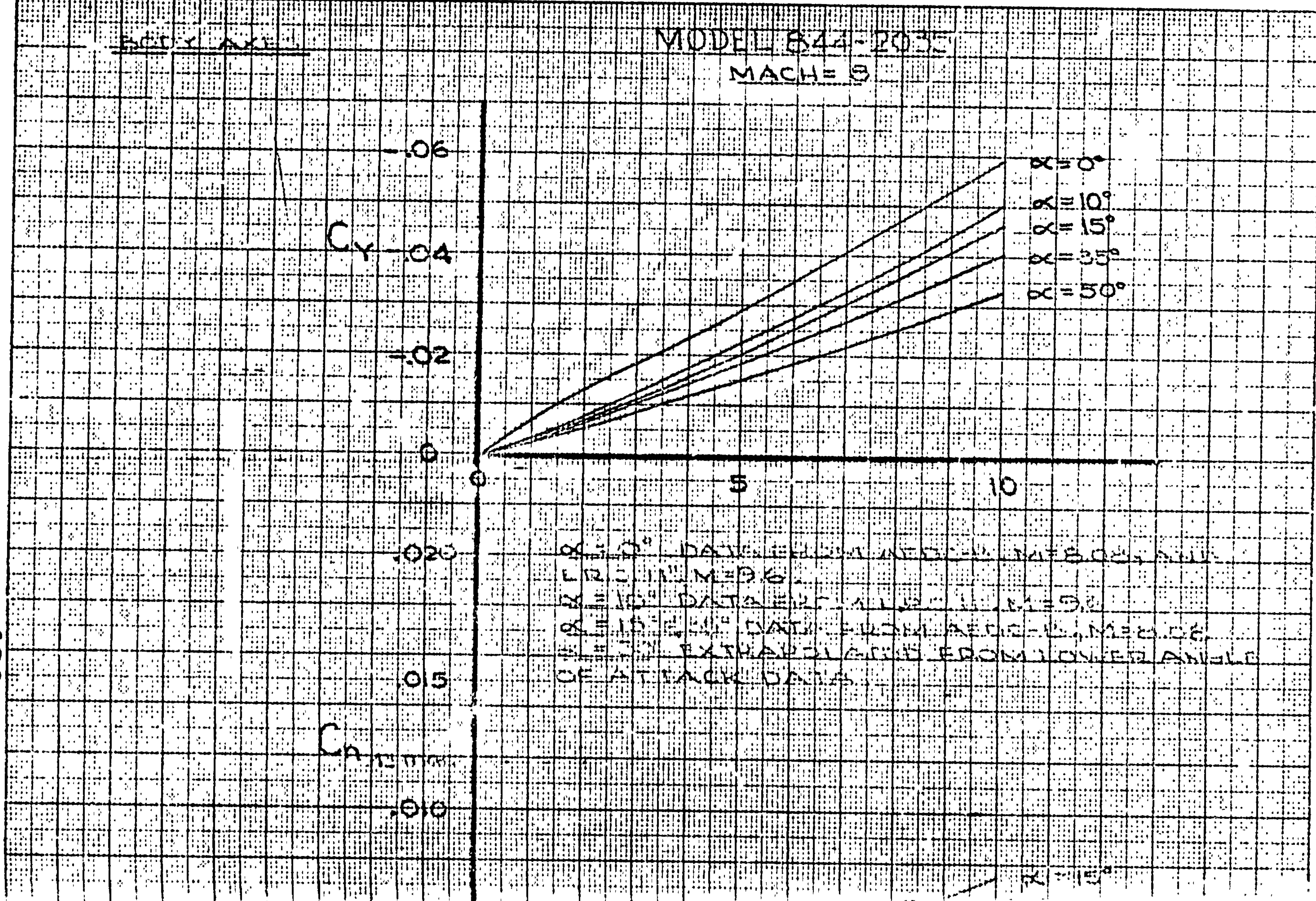
MODEL 844-2035
MACH= 8
α = 0°
α = 10°
α = 15°
α = 35°
α = 50°
Cy
-.06
-.04
-.02
0
5
10
.020
.015
.010
Cn
OF ATTACK DATA

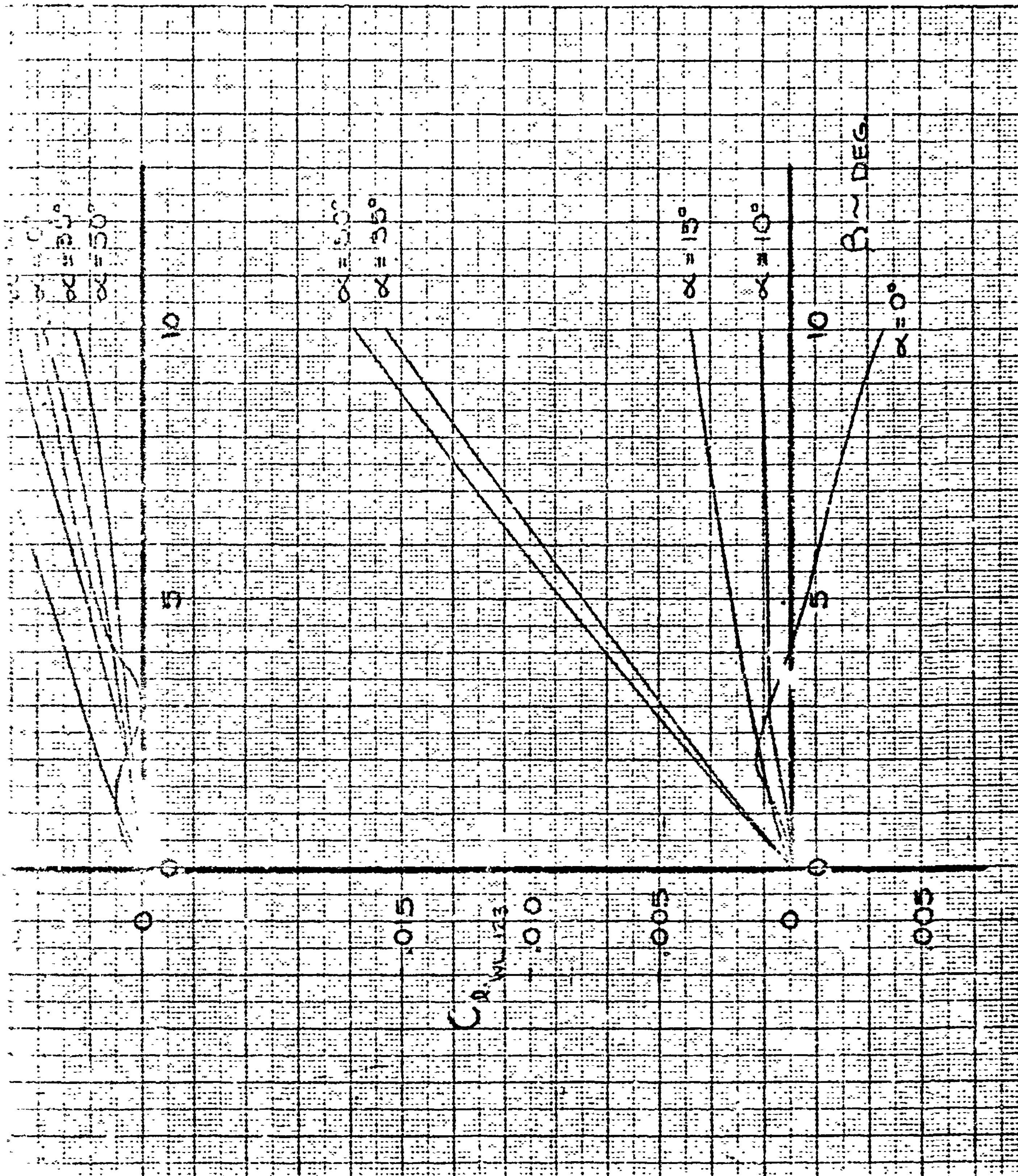


| | | | | | |
|---|---|---|---|---|---|
| CALC | JEB | 7/26/66 | REVISED | DATE | FIG. 6.23 |
| CHECK | | | | | 844-2035 |
| APPD | | | | | D2-8974 |
| APPD | | | | | PAGE 6.26 |

LATERAL DIRECTIONAL STABILITY
LOW HYPERSONIC SPEEDS

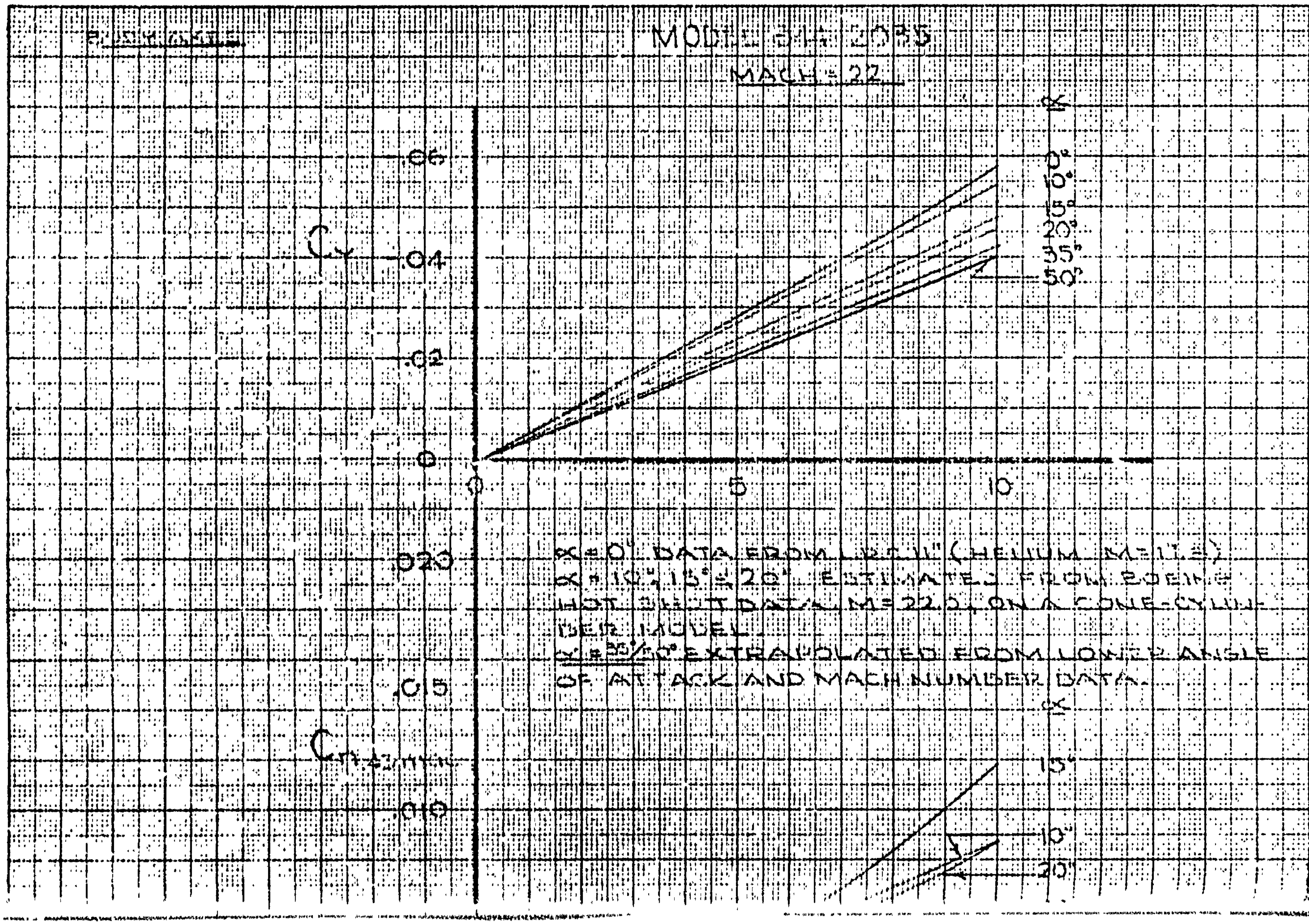

MACH = 22
$C_Y$
.06
.04
.02
0
0
5
10
.020
.015
.010
α
0°
10°
15°
20°
35°
50°
OF ATTACK AND MACH NUMBER DATA.
α
15°
10°
20°

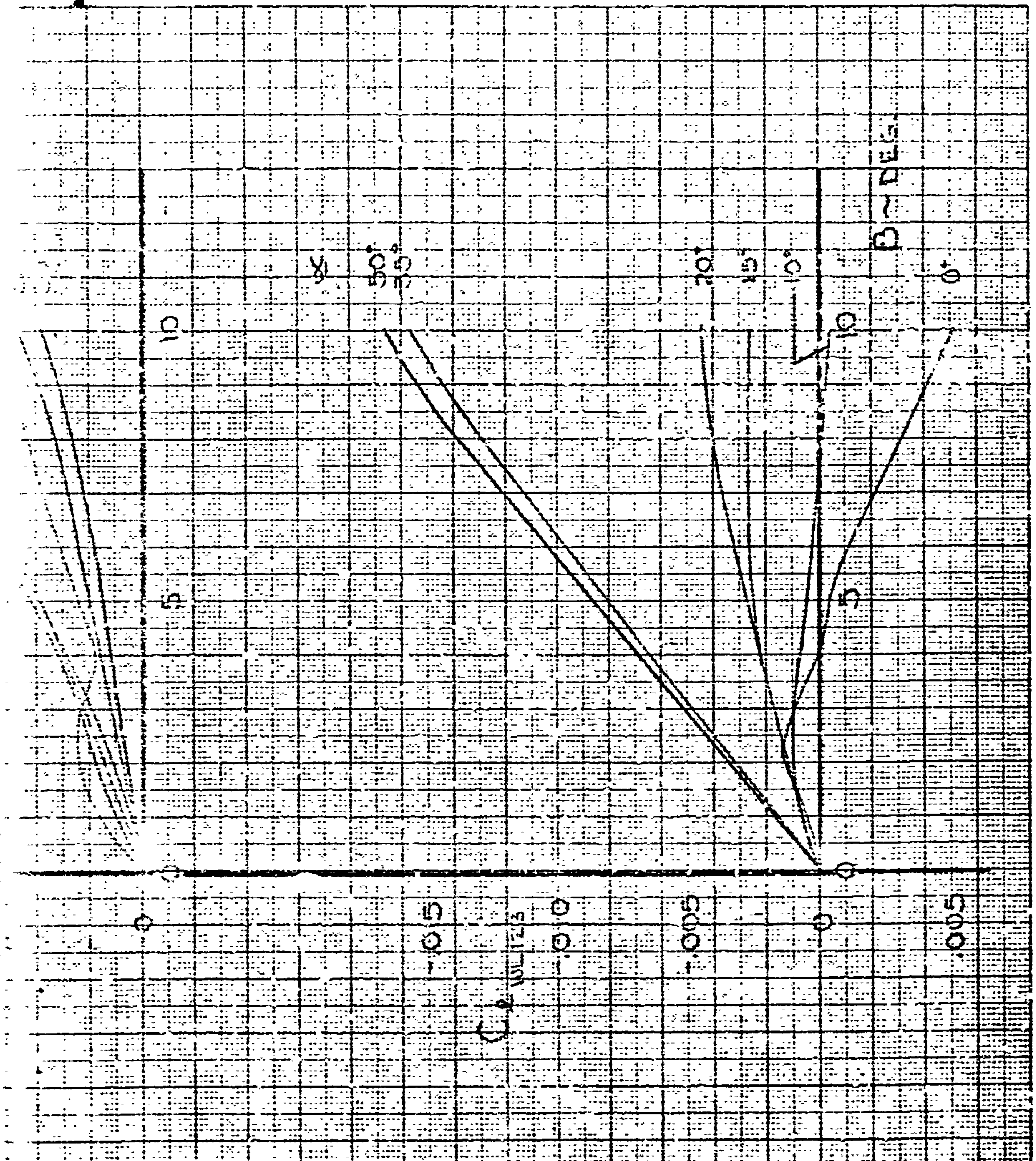


| | | | | | |
|---|---|---|---|---|---|
| CALC JEB | 12/6/66 | REVISED | DATE | LATERAL-DIRECTIONAL STABILITY | FIG 6.28 |
| CHECK | | | | HIGH HYPERSONIC CRUISE | B44 - 2035 |
| APRD | | | | | D2-874 |
| APRD | | | | | PAGE 6.37 |

6.2 AILERON CHARACTERISTICS AND EFFECTIVENESS

Aileron effectiveness data for the 844-2035 configuration are presented in Figures 6.25 through 6.42. Summary curves of $C_{\ell_{\delta_a}}$, $C_{n_{\delta_a}}$ and $C_{Y_{\delta_a}}$ versus Mach number are presented on Figures 6.25, 6.26 and 6.27 to show the variation between the Mach numbers; more detailed data are presented on Figures 6.28 through 6.42.

The data presented are based on wind tunnel data on similar configurations adjusted to the dimensions of the 844-2035 configuration. All data are based on configurations with 10° swept elevon hinge lines, with the exception of the transonic region where the hinge line was unswept. The effects of hinge line sweep have not been established precisely; consequently $C_n$ and $C_Y$ may be changed when wind tunnel data on the 844-2035 configuration become available.

The hypersonic aileron characteristics are presented for both surfaces deflected symmetrically about $\delta_e$ of 0 and -30° and also for one elevon deflected through a range of 10° to -45° while the other is at 0° deflection. The "one-surface-deflected" data are presented in order to facilitate estimation of the effects of deflecting the ailerons unequally.

The effect of altitude (i.e., Reynolds number) on aileron effectiveness is similar to the effect on elevon effectiveness in pitch. Aileron effectiveness is influenced by a thickening boundary layer with increasing altitude which decreases the effectiveness. High hypersonic speed hot-shot data show little change in effectiveness however, and at this time it is assumed that aileron characteristics should not be changed significantly with altitude.

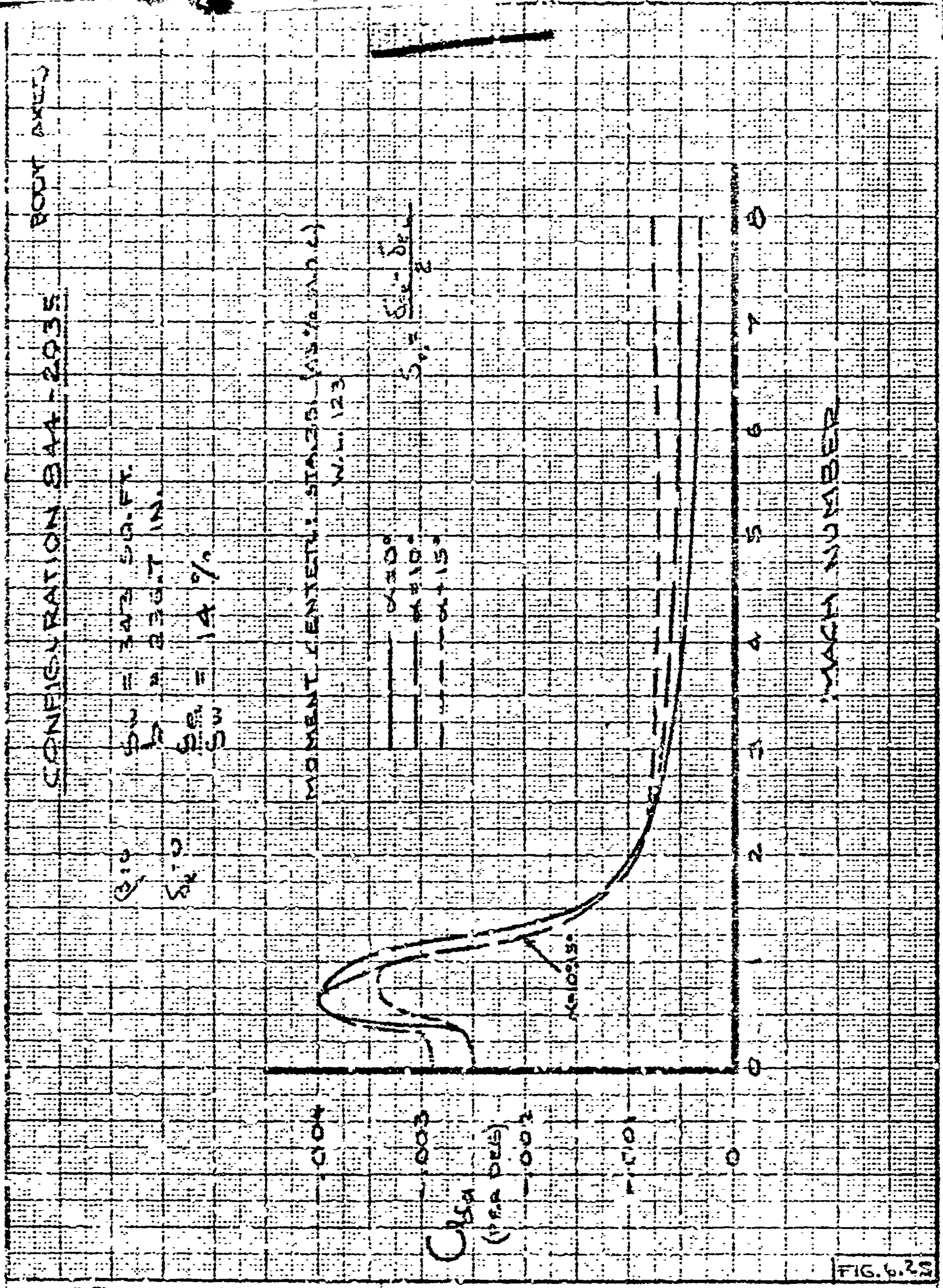


FIG. 6.25

| | | | | |
|---|---|---|---|---|
| CALC EB | | REVISE | DATE | ROLLING MOMENT DUE TO AILERON |
| CHECK | | | | |
| APR | | | | |
| APR | | | | BOEING AIRPLANE COMPANY |

844-2035

D2-8174

PAGE 6.29

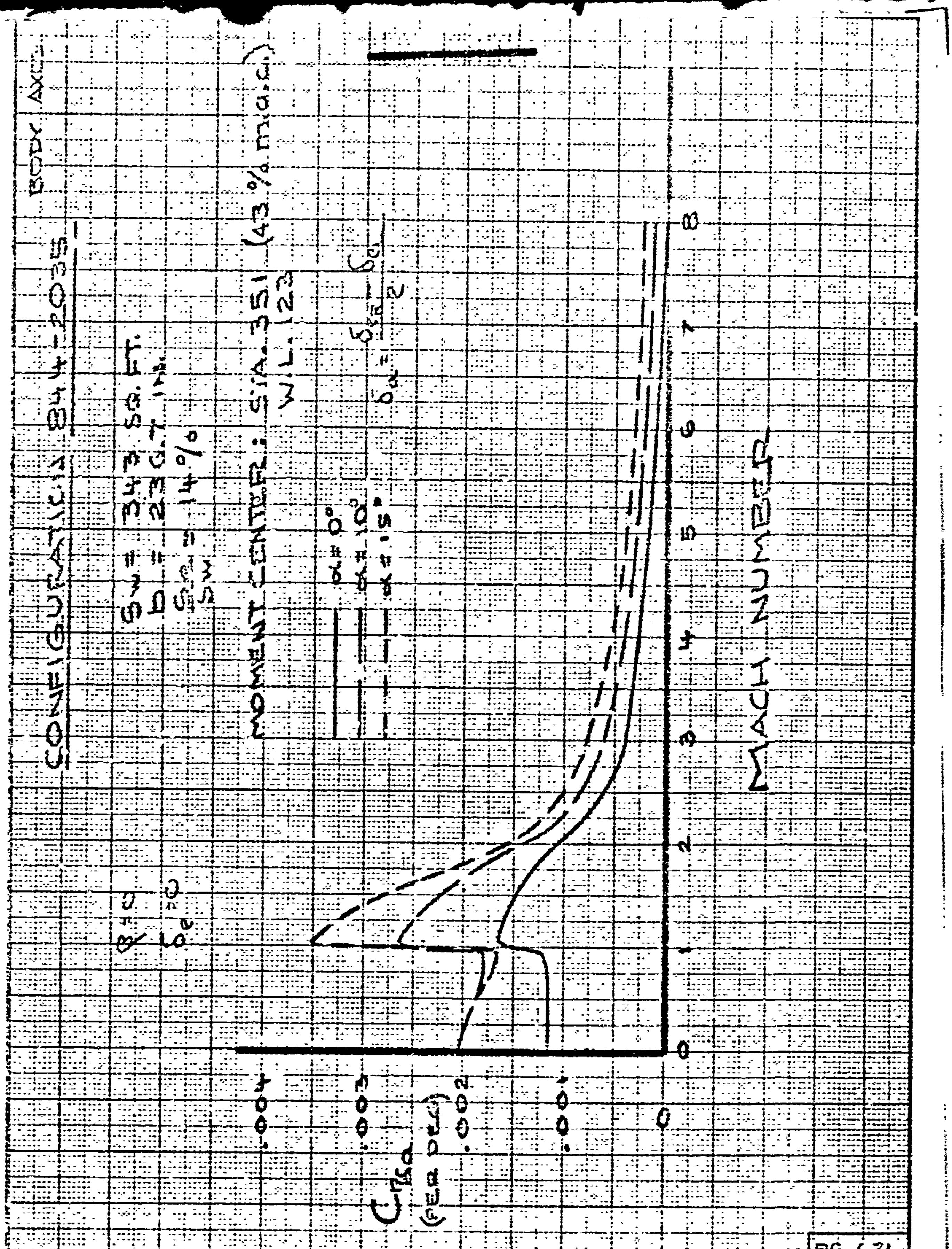


FIG. 6.26

| | | | | | |
|---|---|---|---|---|---|
| CALC | DB | 12/14/0 | REVISED | DATE | YAWING MOMENT DUE TO AILERON |
| CHECK | | | | | |
| APR | | | | | |
| APR | | | | | BOEING AIRPLANE COMPANY |

844-2035

D2-8174

PAGE 6.30

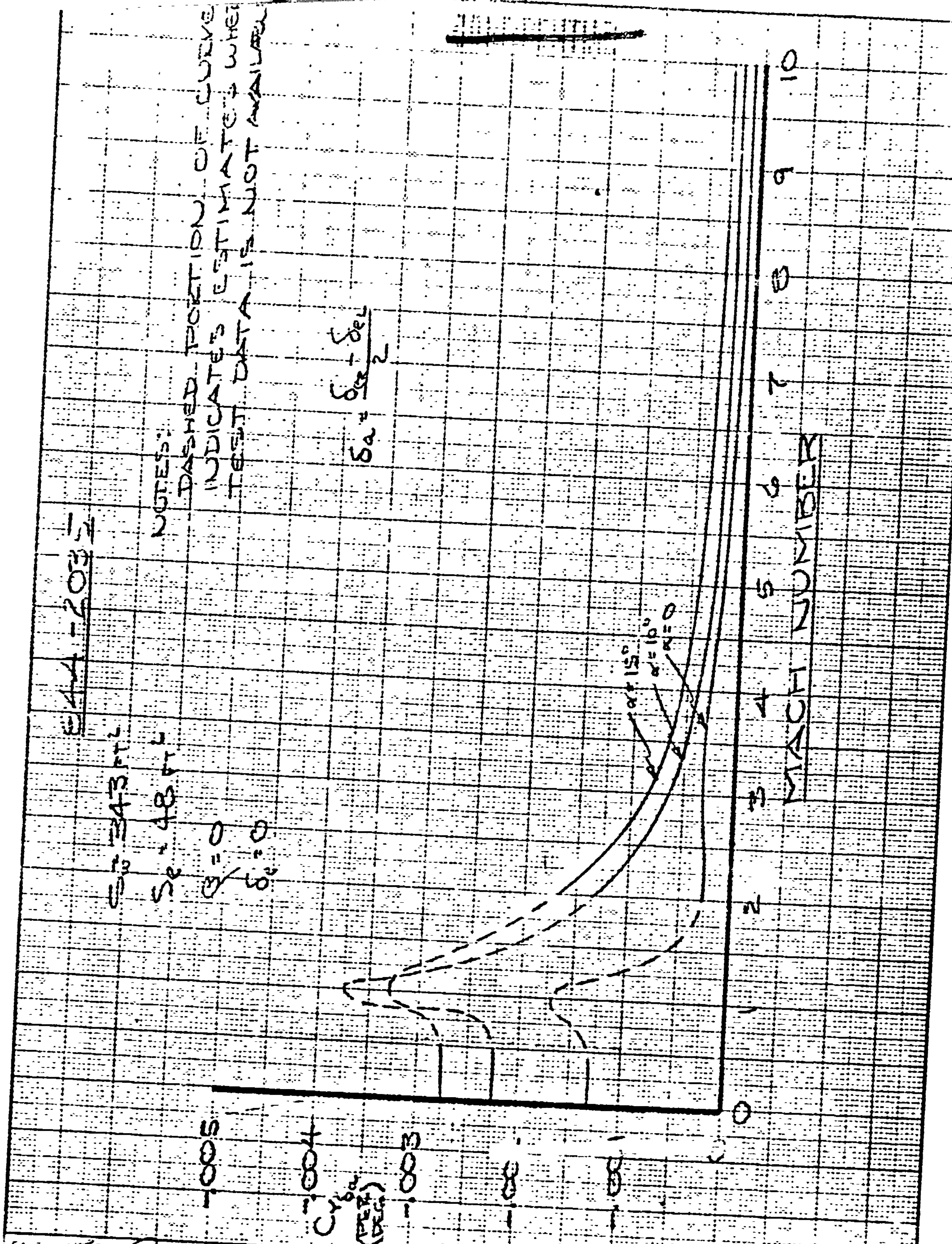


| CALC | DJR | 12-2-57 | REVISED | DATE | | FIG. 6.27 |
|---|---|---|---|---|---|---|
| CHECK | | | | | SIDE FORCE DUE | 844-2035 |
| APR | | | | | TO AILERON **141** | D2-8174 |
| APR | | | | | BOEING AIRPLANE COMPANY | PAGE 6.31 |

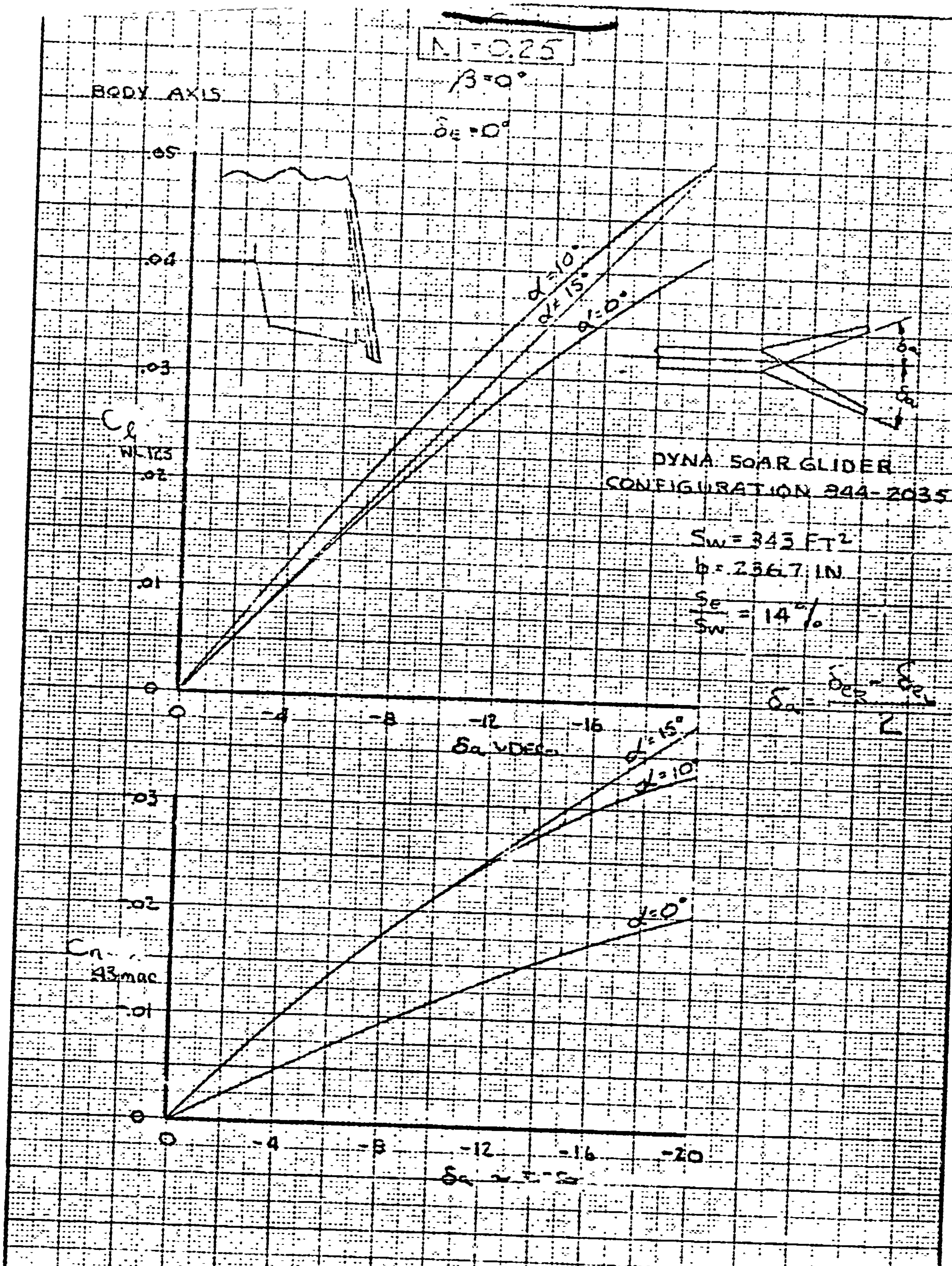


| CAL | EJH | 12/14/60 | REVISED | DATE |
|---|---|---|---|---|
| CHECK | [illegible] | ✓ | | |
| APR | | | | |
| APR | | | | |

AILERON EFFECTIVENESS
LANDING SPEED
$\delta_E = 0$

FIG. 6.28
844-2035

BOEING AIRPLANE COMPANY

142

D2-8174

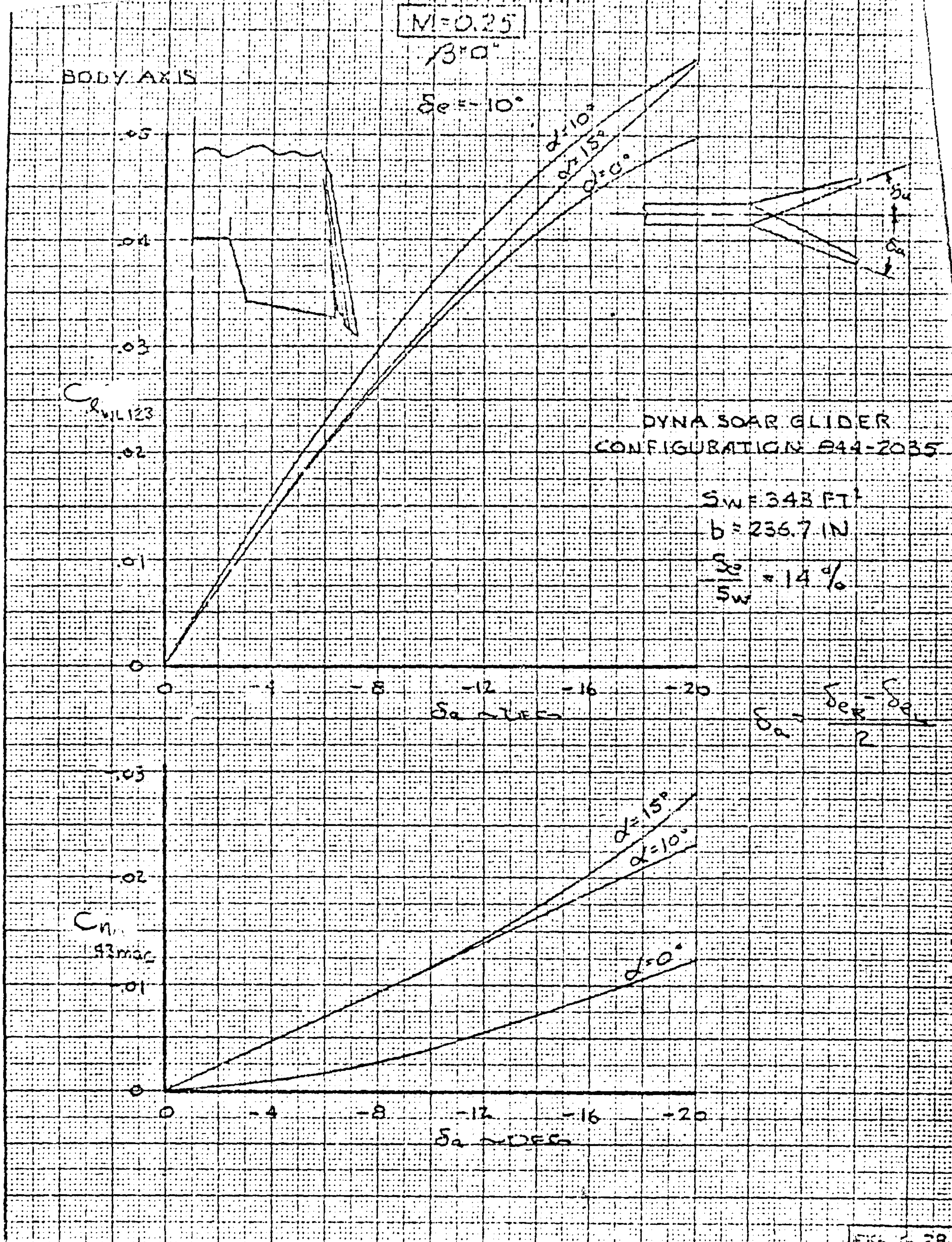


| CALC | EJH | 14/14/0 | REVISED | DATE |
|---|---|---|---|---|
| CHECK | G.L. Wagoner | – | | |
| APR | | | | |
| APR | | | | |

AILERON EFFECTIVENESS
LANDING SPEED
$\delta_e = -10°$

**143**

BOEING AIRPLANE COMPANY

FIG. 6.29
E44-2035
D2-3174
PAGE 6.33

M = 0.25

B44-2035

$\beta = 0°$

$S_W = 343$ FT.²

$S_e/S_W = 14\%$

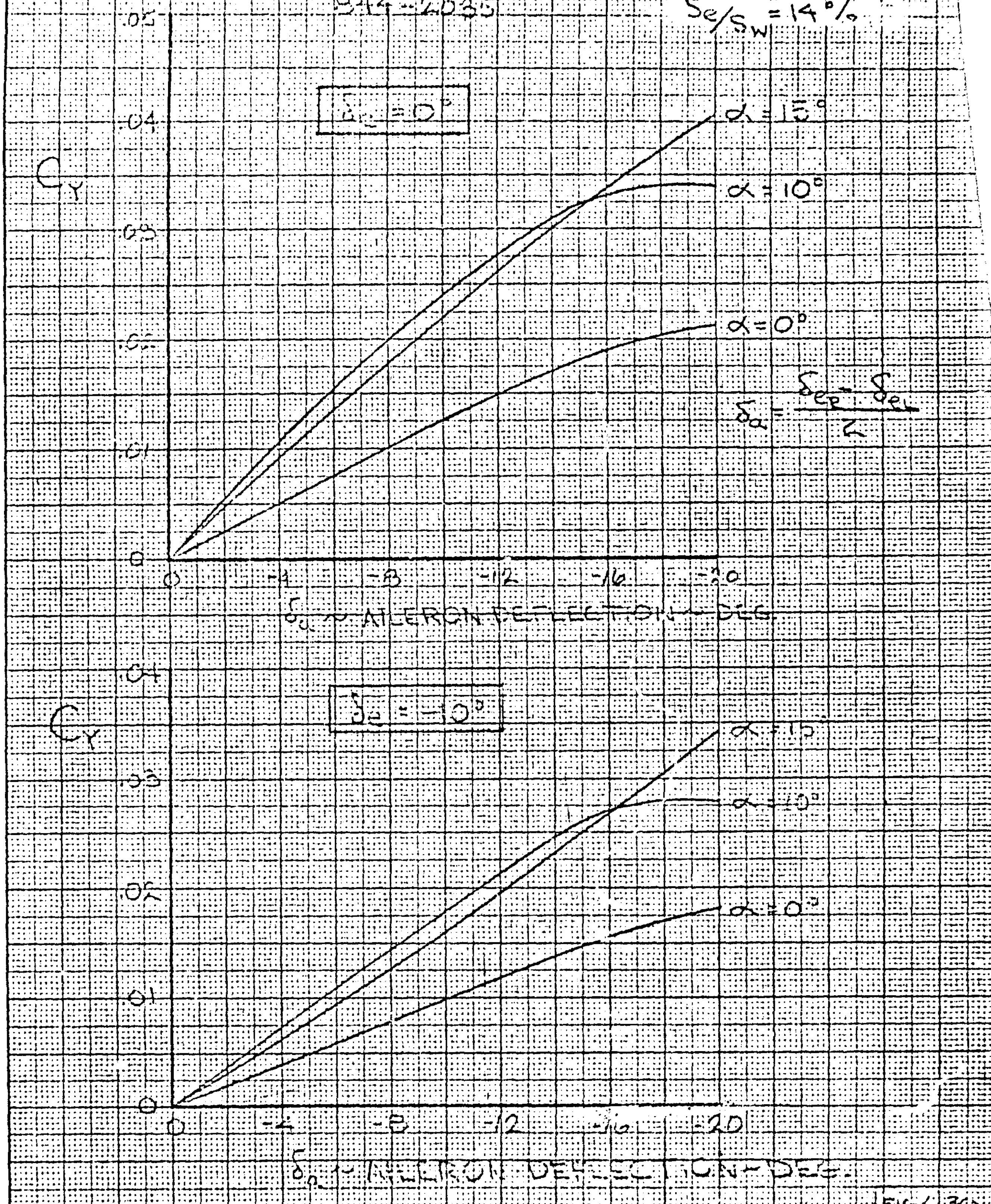


FIG. 6.30

| CALC | EH | | REVISED | DATE | SIDE FORCE DUE TO AILERON-LANDING SPEED | 644-2035 |
|---|---|---|---|---|---|---|
| CHECK | | | | | | D2-8174 |
| APR | | | | | | |
| APR | | | | | BOEING AIRPLANE COMPANY | PAGE |
| COPIED | PTV | 12-21 | | | 144 | 6.34 |

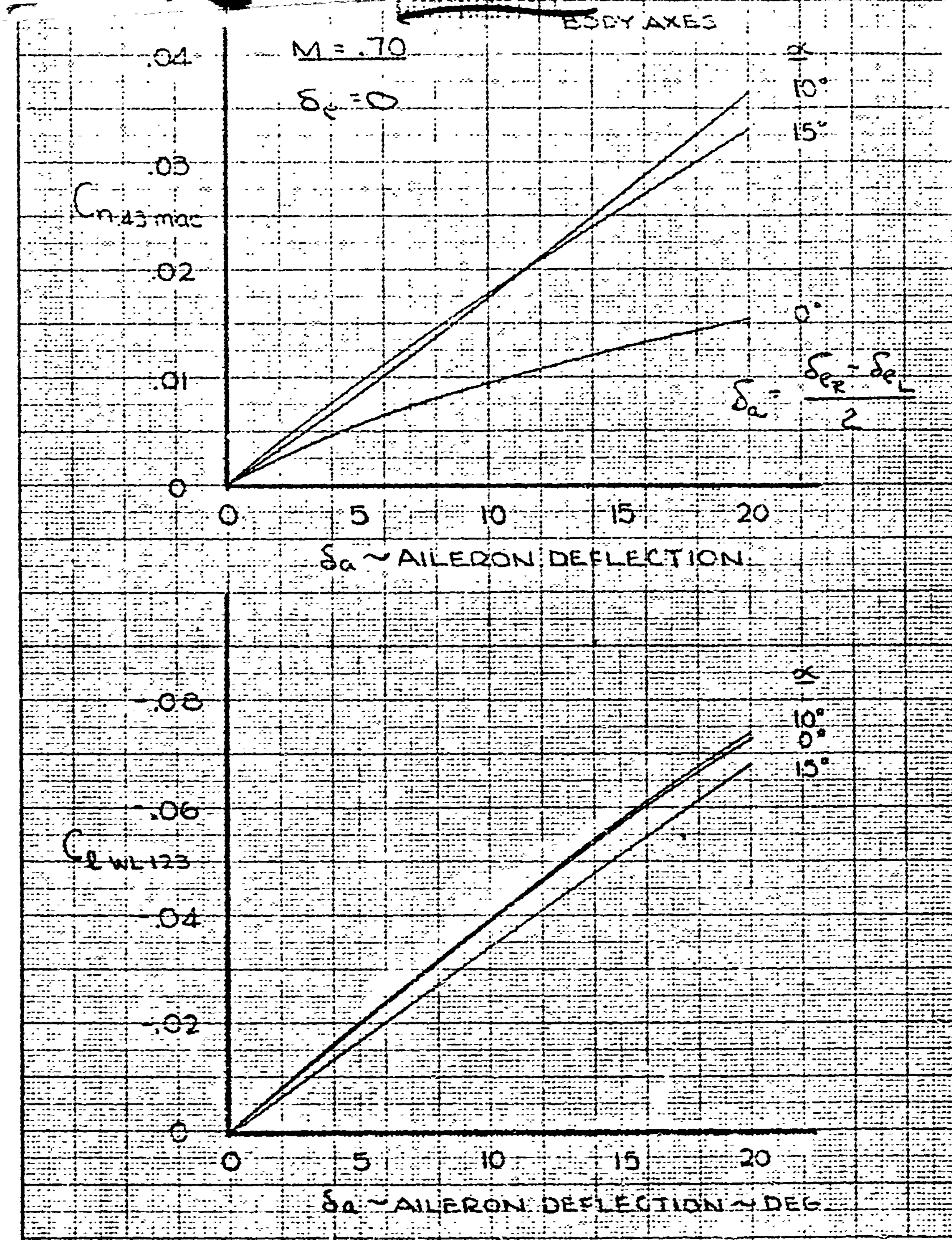


FIG 6.31

| | | | | | |
|---|---|---|---|---|---|
| CALC JES/RTE | 12/5/60 | REVISED | DATE | AILERON CHARACTERISTICS<br>M = .70 | 644-2035 |
| CHECK | | | | **145** | D2-8174 |
| APR | | | | | |
| APR | | | | BOEING AIRPLANE COMPANY | PAGE 6.35 |

BAC 461 C R4

CONFIDENTIAL

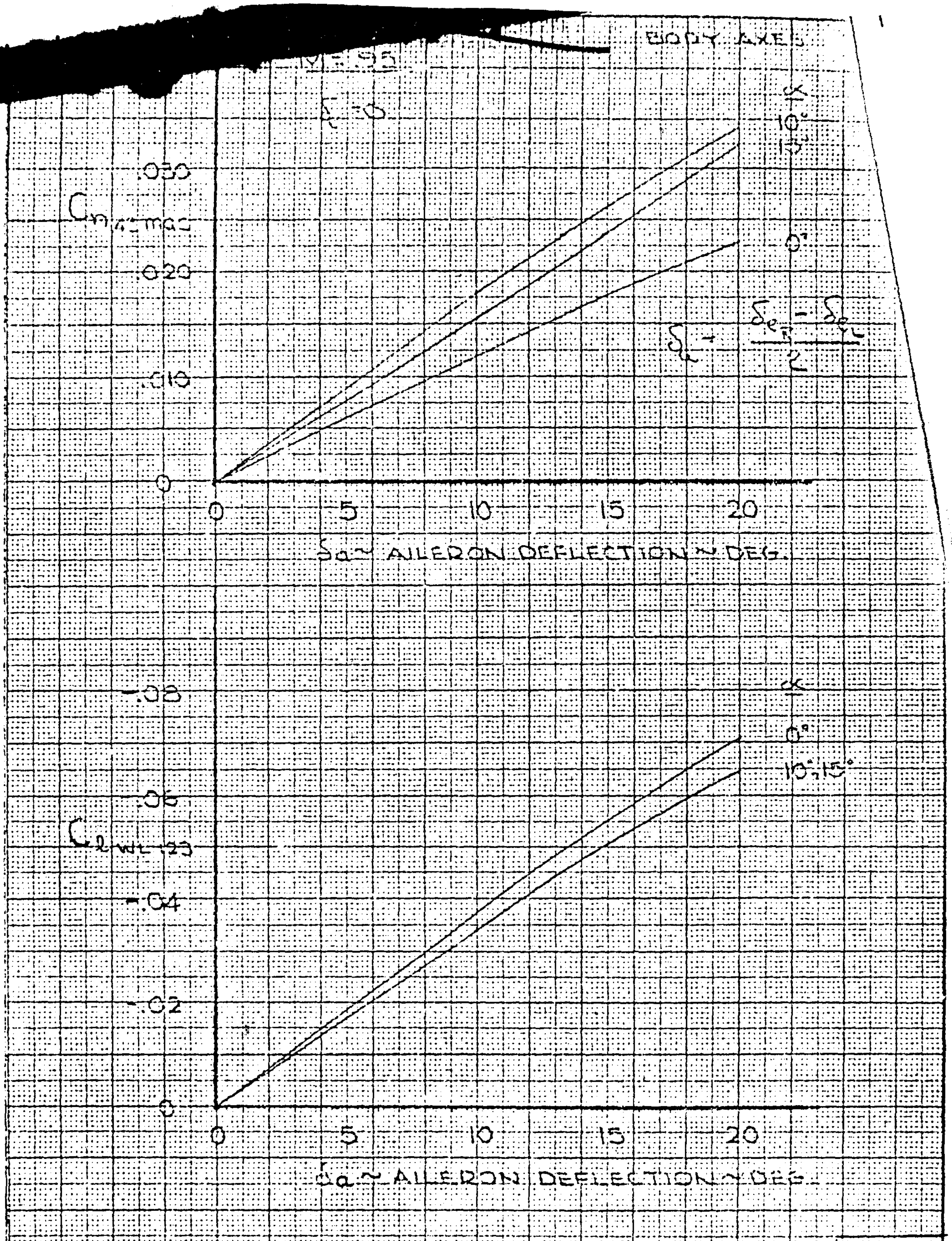


FIG. 6.32

| | | | | | | |
|---|---|---|---|---|---|---|
| CALC | WED/RTB | 12/9/60 | REVISED | DATE | AILERON CHARACTERISTICS | 844-2035 |
| CHECK | | | | | M = .95 | |
| APR | | | | | | D2-8174 |
| APR | | | | | BOEING AIRPLANE COMPANY | PAGE |

**146**

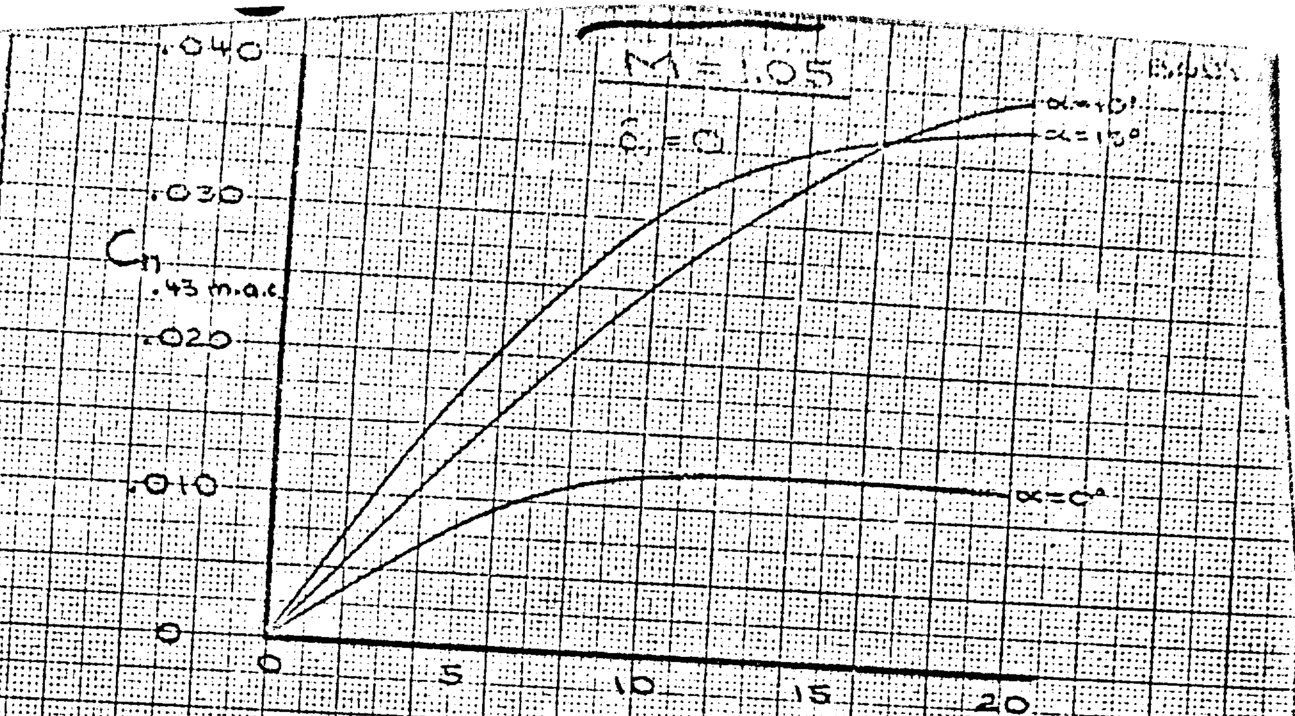


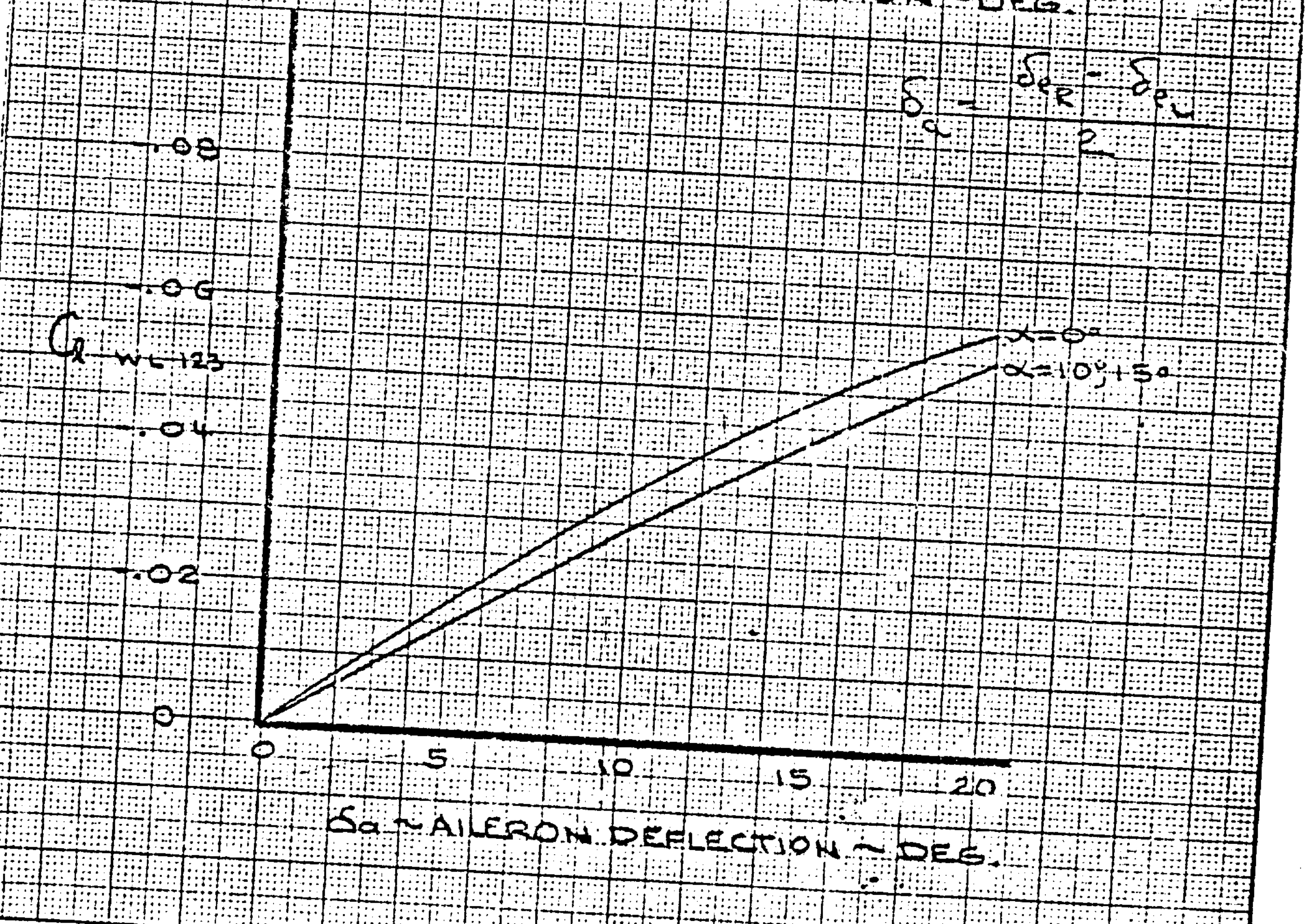


| | | | | | | |
|---|---|---|---|---|---|---|
| CALC | JEB/RTB | 12/9/60 | REVISED | DATE | AILERON CHARACTERISTICS | FIG. 6.33 |
| CHECK | | | | | M = 1.05 | 844-2035 |
| APR | | | | | BOEING AIRPLANE COMPANY | D2-8174 |
| APR | | | | | | PAGE 6.37 |

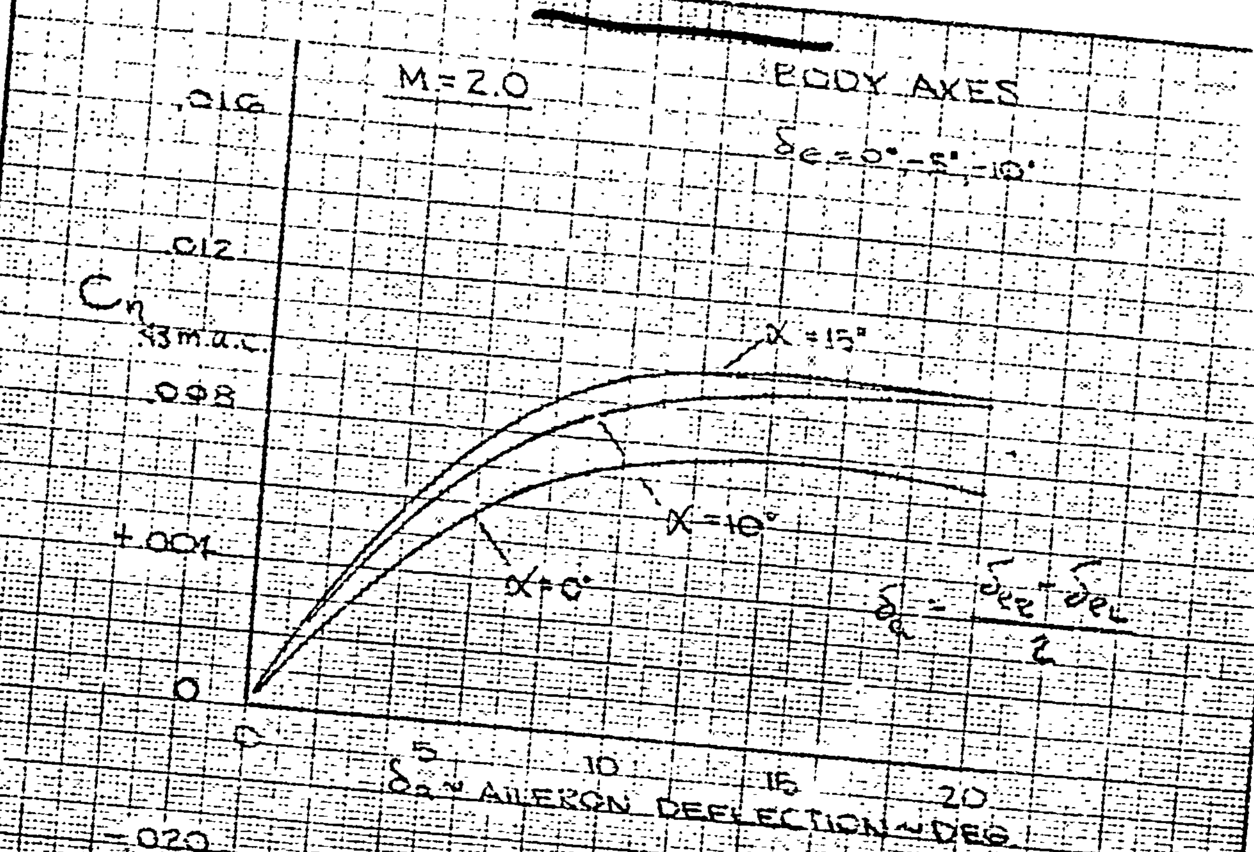


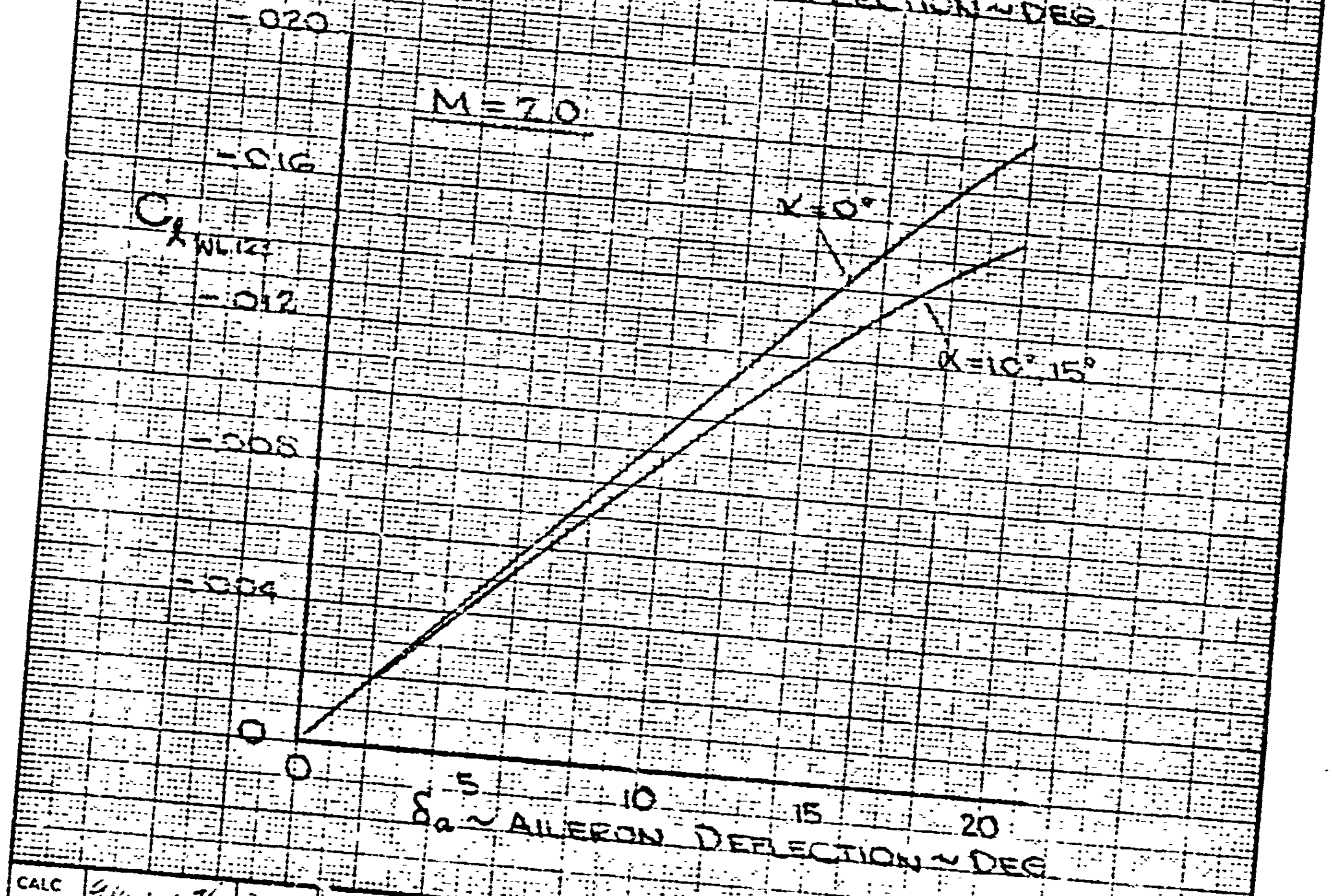


| | | | | | |
|---|---|---|---|---|---|
| CALC | [illegible] | 12-1-60 | REVISED | DATE | |
| CHECK | | | | | AILERON CHARACTERISTICS M = 2.0 |
| APR | | | | | |
| APR | | | | | |

148

FIG. 6.34
844-2035

**BOEING AIRPLANE COMPANY**
SEATTLE 24 WASHINGTON

D2-8174
PAGE 6.38

BAC 461 C-R4

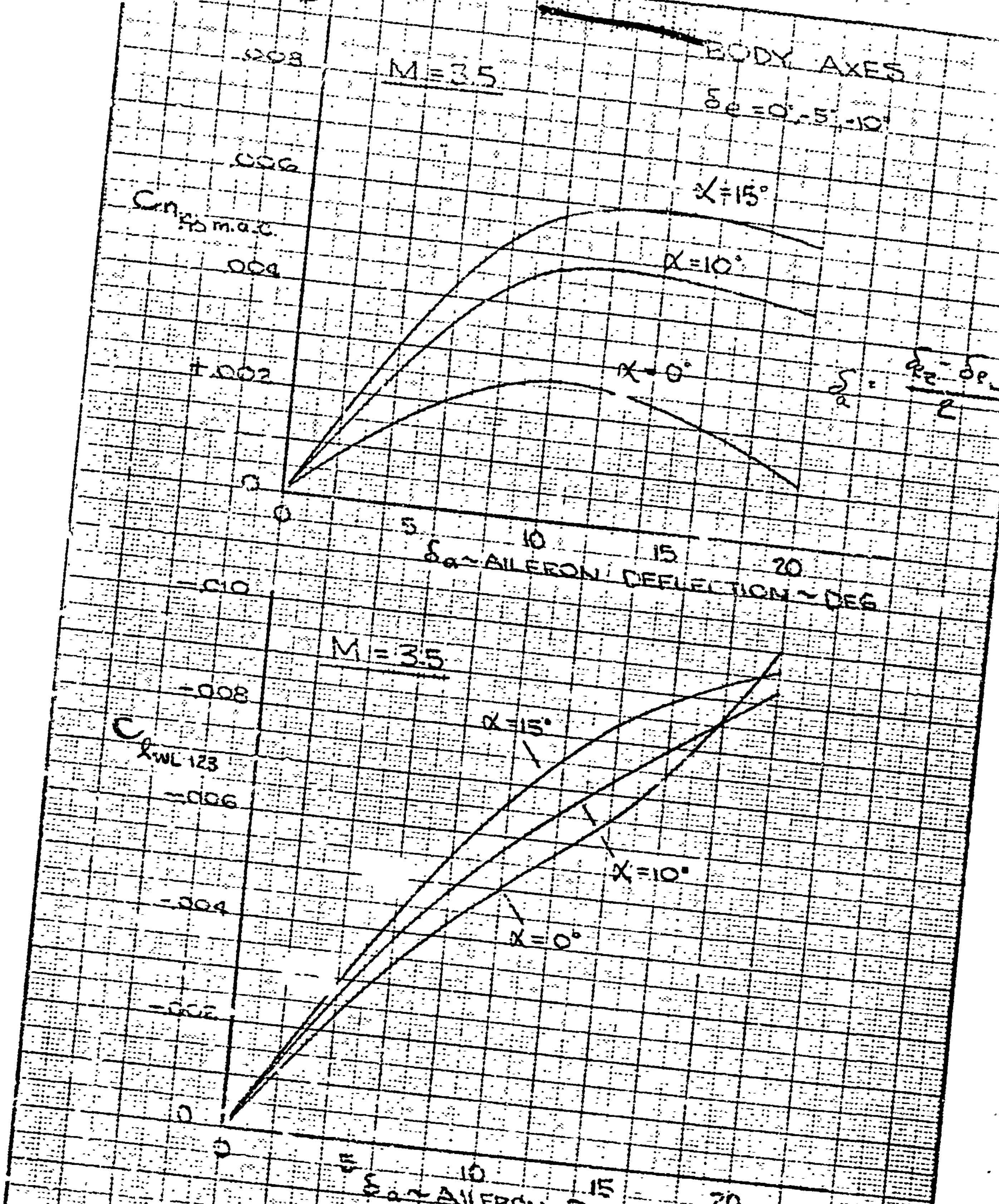


| CALC | 9 W.E. with 12/5/61 | REVISED | DATE |
|---|---|---|---|
| CHECK | | | |
| APR | | | |
| APR | | | |

AILERON CHARACTERISTICS

M = 3.5

149

BOEING AIRPLANE COMPANY

FIG. 6.35

244-2035

D2-8174

PAGE 6.39

BAC 461 C-R4

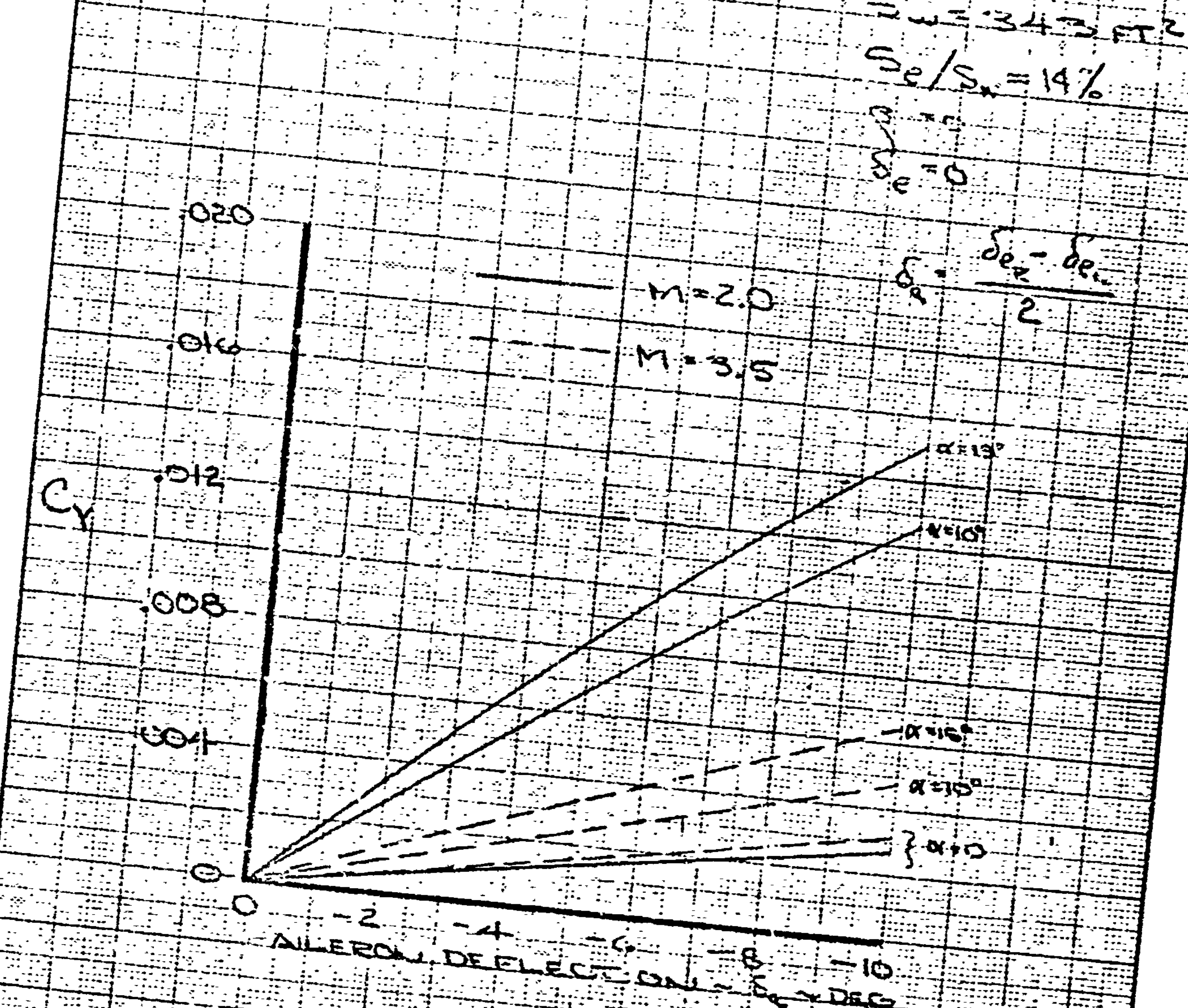


| CALC | EH/EFR | 12-21-? | REVISED | DATE | SIDE FORCE DUE TO AILERON DEFLECTION M = 2.0 AND 3.5 | FIG. 36 E44-2035 |
|---|---|---|---|---|---|---|
| CHECK | | | | | | D2-8124 |
| APR | | | | | BOEING AIRPLANE COMPANY | PAGE 6.40 |

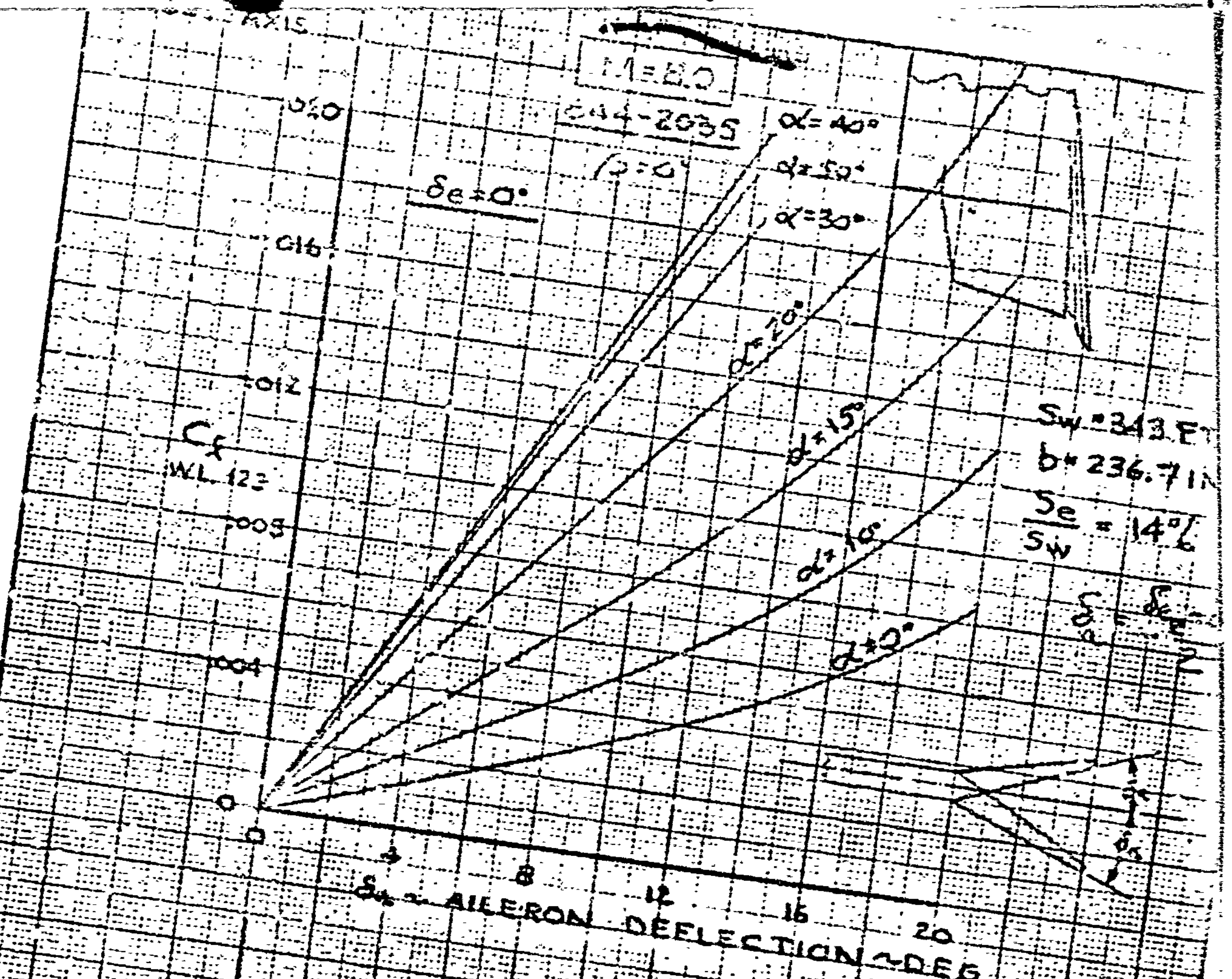


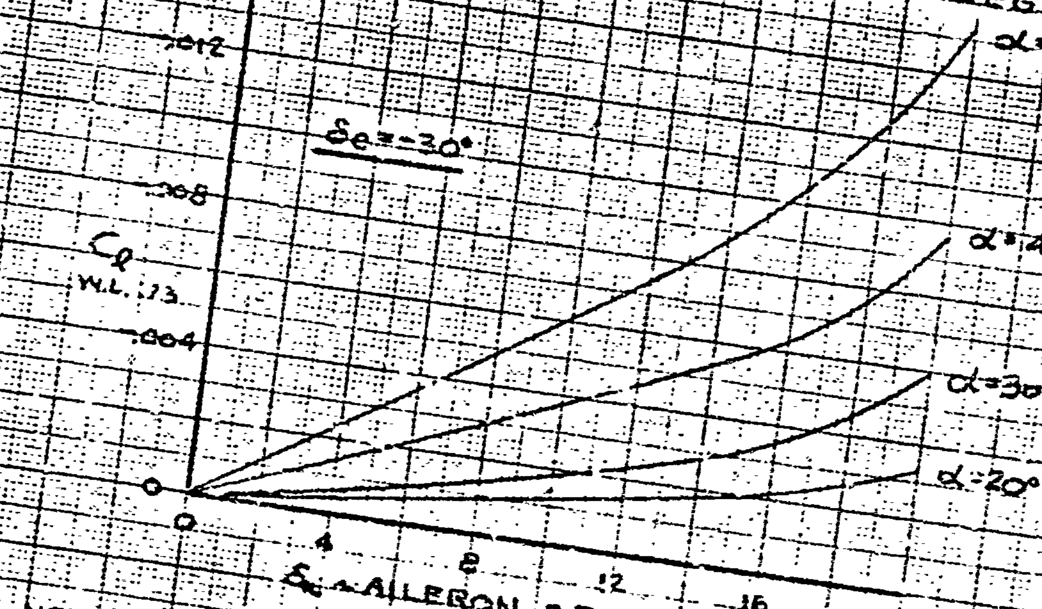


NOTE: THESE CURVES ARE BASED ON M=8.1 TEST DATA AND PARTIALLY SUBSTANTIATED BY M=9.5 TEST DATA

| CALC | EJH | 11/8/61 | REVISED | DATE |
|---|---|---|---|---|
| CHECK | | | | |
| APR | | | | |
| APR | | | | |

ROLLING MOMENT DUE TO AILERON HYPERSONIC SPEED

BOEING AIRPLANE COMPANY

151

FIG 6.37

844-2035

D2-8174

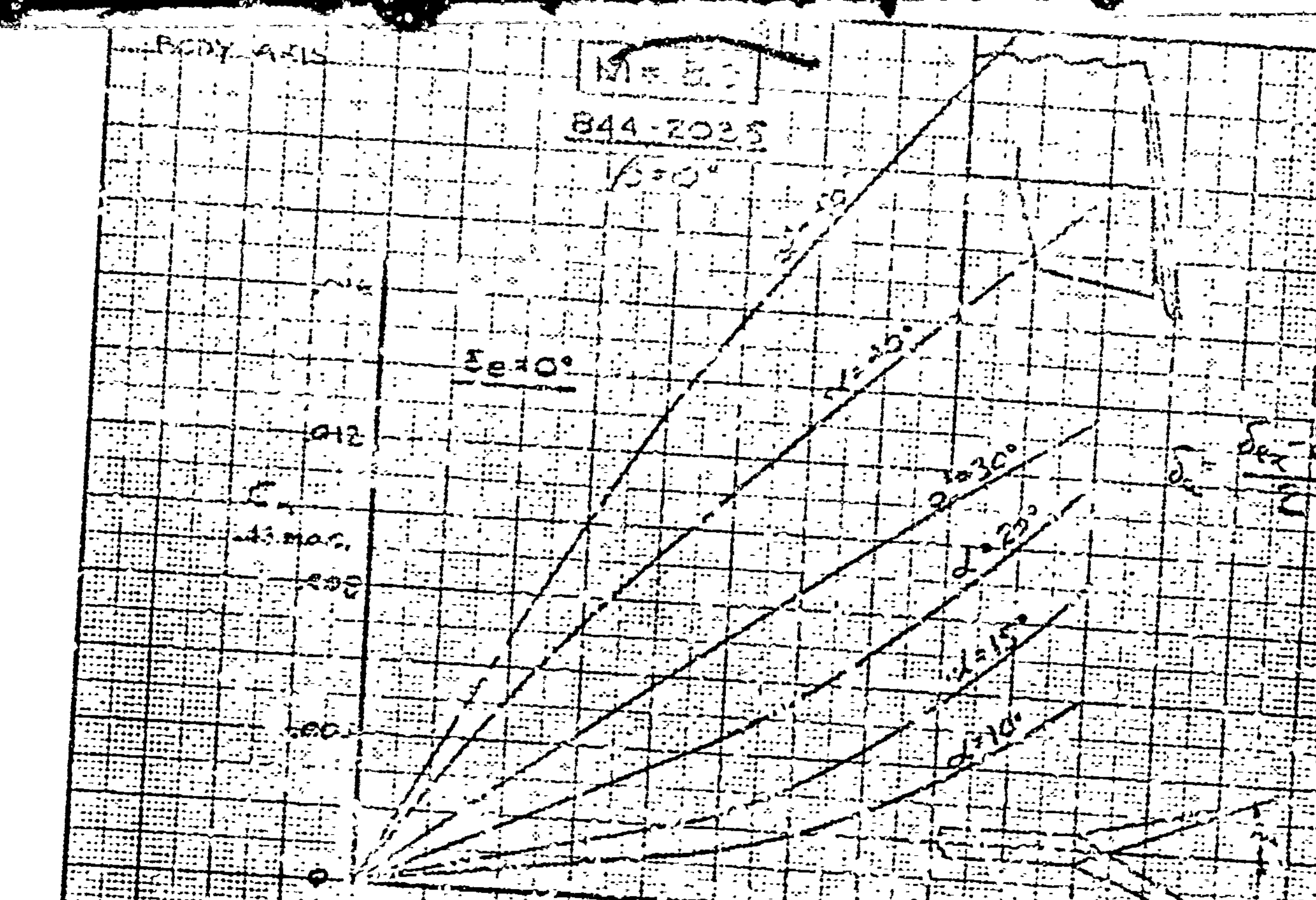


$S_W$ = 343 FT²
b = 236.7 IN
$\frac{S_a}{S_W}$ = 14%

NOTE: THESE CURVES ARE BASED ON M=6.1 TEST DATA AND PARTIALLY SUBSTANTIATED BY M=9.5 TEST DATA.

| | | | |
|---|---|---|---|
| CALC | ECH | 12/8/60 | REVISED / DATE |
| CHECK | | | |
| APR | | | |
| APR | | | |

YAWING MOMENT DUE TO AILERON HYPERSONIC SPEED

**152**

BOEING AIRPLANE COMPANY

844-2008

T2-8174

PAGE 6.42

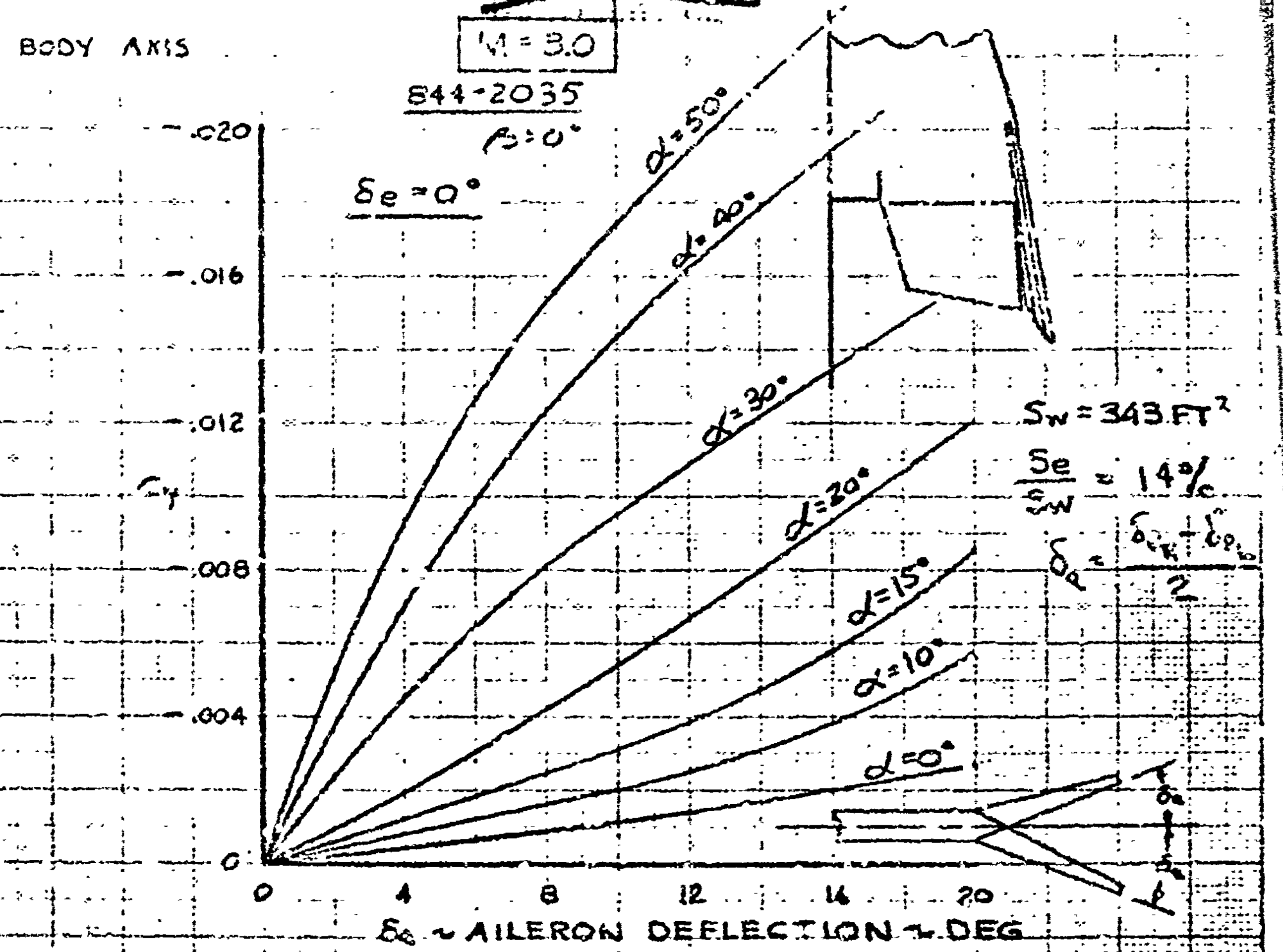


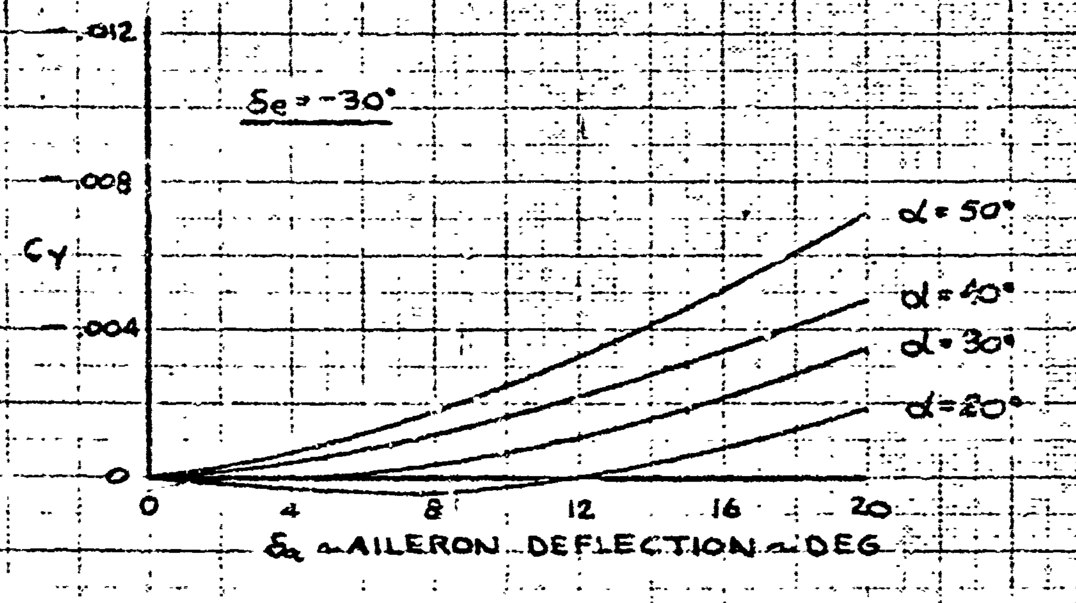


NOTE: THESE CURVES ARE BASED ON M=8.1 TEST DATA AND PARTIALLY SUBSTANTIATED BY M=9.5 TEST DATA.

FIG. 6.39

| CALC EJH 14/8/61 | REVISED | DATE | SIDE FORCE DUE TO AILERON HYPERSONIC SPEED | 844-2035 |
|---|---|---|---|---|
| CHECK | | | | D2-8174 |
| APR | | | BOEING AIRPLANE COMPANY | PAGE 6.43 |
| APR | | | | |

153

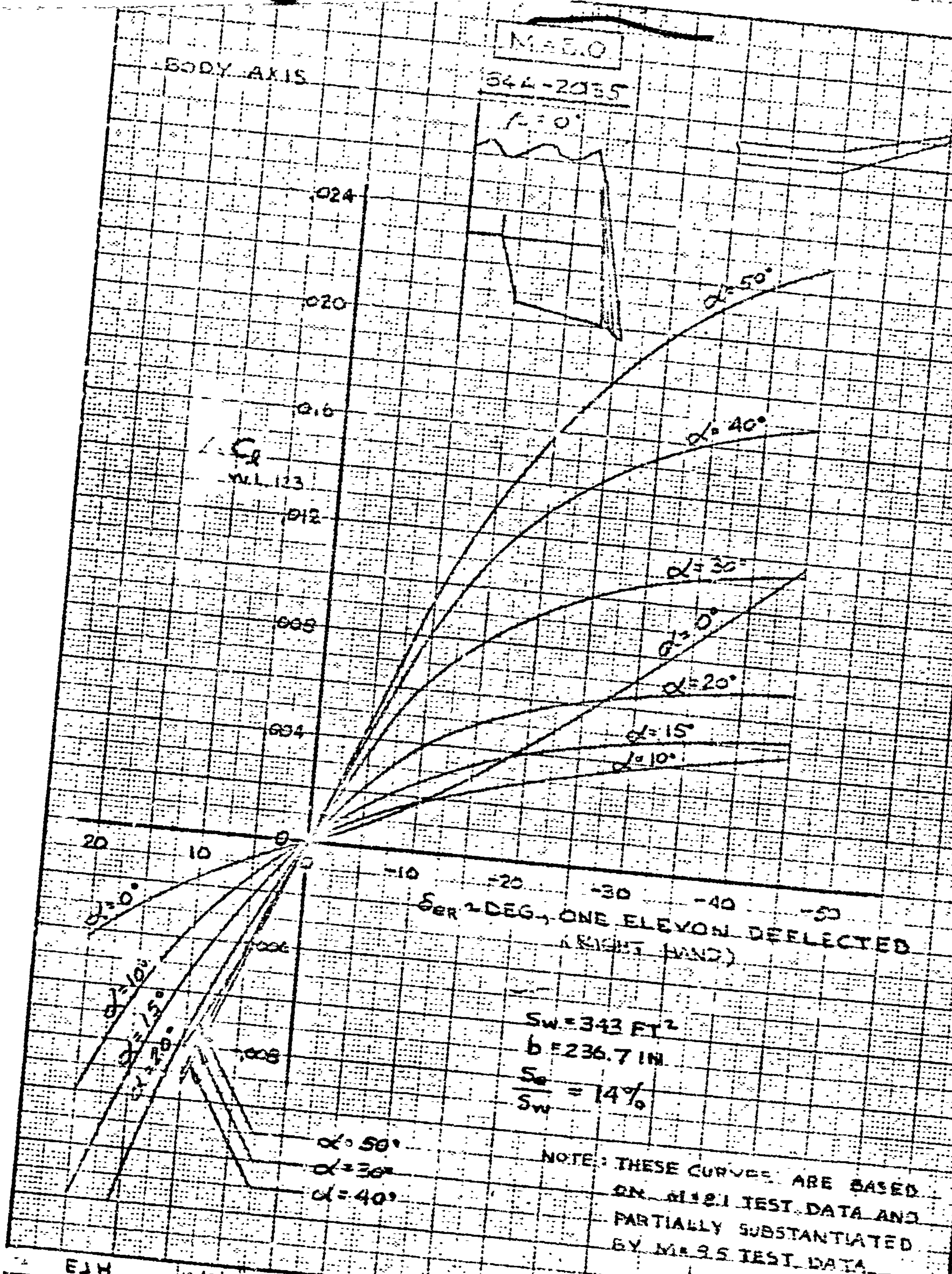


EJH 12/8/5 REVISED DATE
CHECK
APR
APR

FIG. 6.40

ROLLING MOMENT DUE TO ONE ELEVON HYPERSONIC SPEED

844-2035

D2-8174

BOEING AIRPLANE COMPANY

154

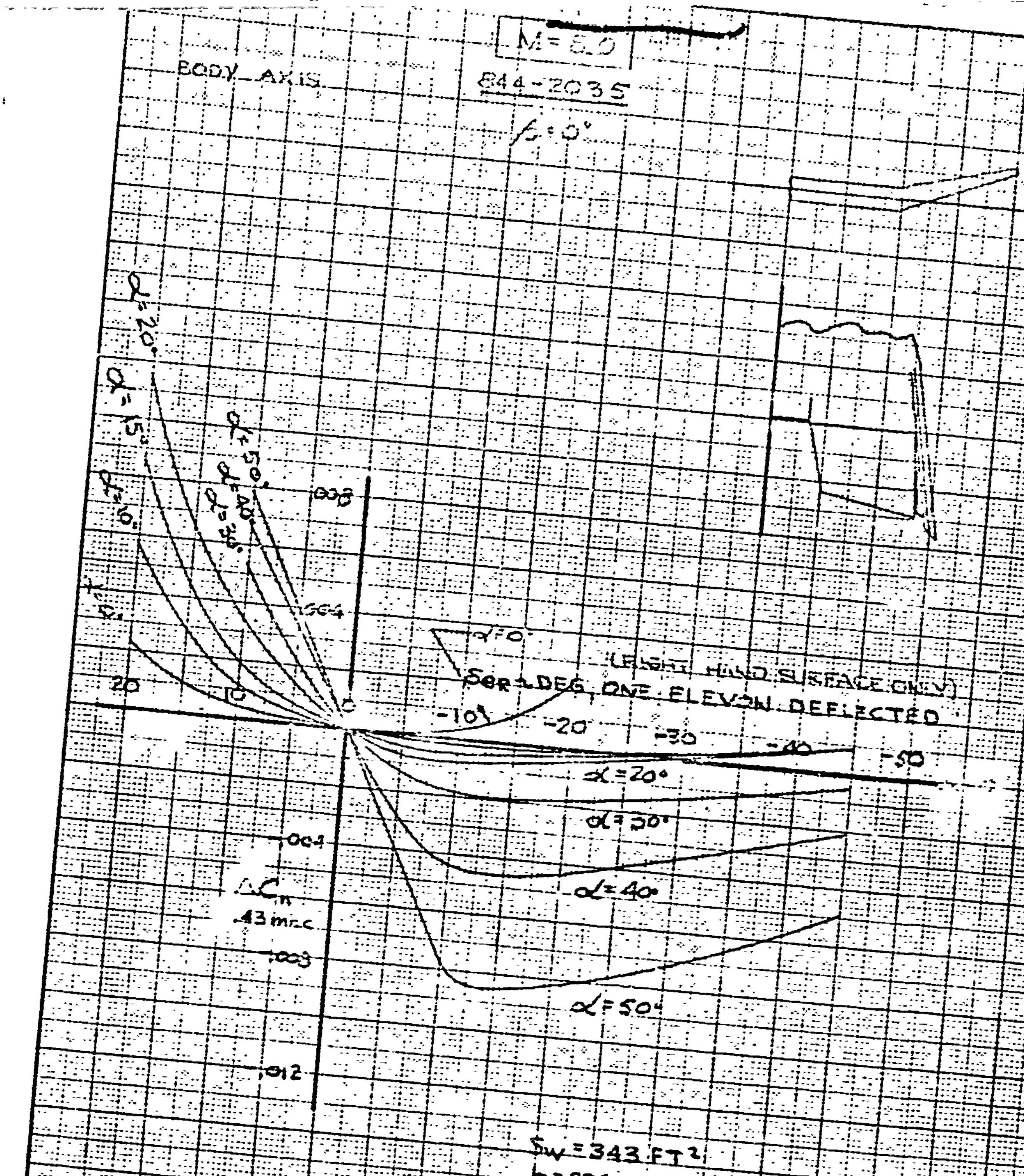


$S_W = 343\ FT^2$

$b = 236.7\ IN$

$\frac{S_e}{S_w} = 14\%$

NOTE: THESE CURVES ARE BASED ON M = 8.1 TEST DATA AND PARTIALLY SUBSTANTIATED BY M = 5.5 TEST DATA

| | | | | |
|---|---|---|---|---|
| CALC EJH | 11/8/0 | REVISED | DATE | |
| CHECK | | | | |
| APR | | | | |
| APR | | | | |

YAWING MOMENT DUE TO ONE ELEVON HYPERSONIC SPEED

155

BOEING AIRPLANE COMPANY

FIG. 6.41

844-2035

D2-8174

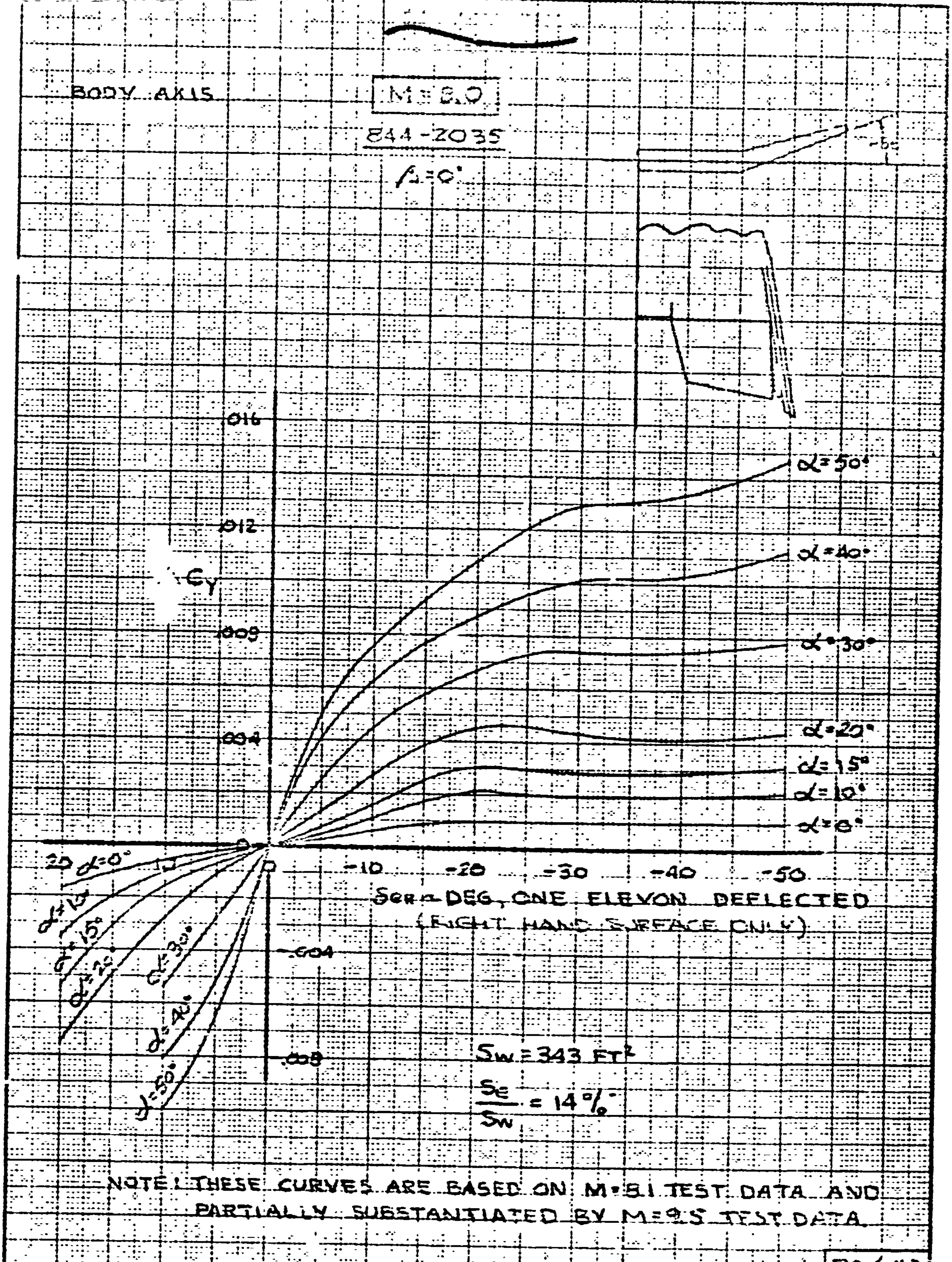


FIG. 6.42

| CALC EJH | 1-18/0 | REVISED | DATE |
|---|---|---|---|
| CHECK | | | |
| APR | | | |
| APR | | | |

SIDE FORCE DUE TO
ONE ELEVON
HYPERSONIC SPEED **156**

BOEING AIRPLANE COMPANY

844-2035

D2-8174

PAGE 6.46

## 6.3 RUDDER CHARACTERISTICS AND EFFECTIVENESS

Rudder effectiveness data for the 844-2035 configuration are presented in Figures 6.43 through 6.51. Summary curves of $C_{n_{\delta_r}}$, $C_{Y_{\delta_r}}$, and $C_{\ell_{\delta_r}}$ versus Mach number are presented on Figures 6.43, 6.44, and 6.45; more detailed data are presented on Figures 6.46 through 6.51. The data presented are based on wind tunnel data on similar configurations adjusted to the dimensions of the 844-2035.

Landing speed rudder effectiveness is based on preliminary data from BTWT 619. Transonic and supersonic effectiveness were obtained from wind tunnel tests of a model 814-1047 at M = .905, 2.0 and 3.5. The hypersonic characteristics are presented for M = 8, based on a model similar to 814-1050 at AEDC-B (test BAC 8). These characteristics are currently considered to apply for higher hypersonic speeds. The effect of altitude (i.e., Reynolds number) is assumed to be negligible.

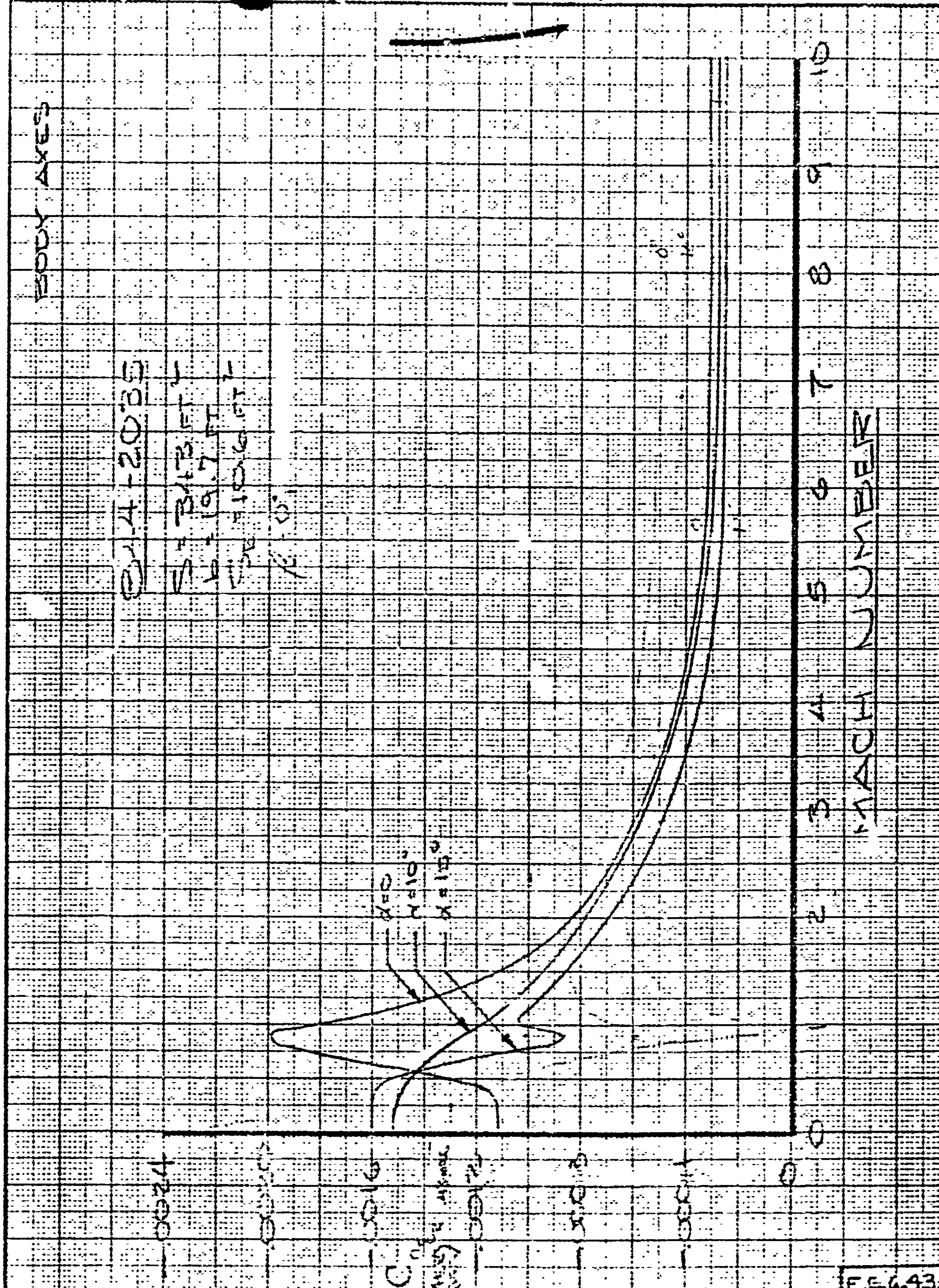


FIG 6.43

| CALC | BJK | 12-8-? | REVISED | DATE | YAWING MOMENT DUE TO RUDDER | E44-2035 |
|---|---|---|---|---|---|---|
| CHECK | | | BJK | 12-15-? | | D2-6174 |
| APR | | | | | BOEING AIRPLANE COMPANY | PAGE 6.48 |
| APR | | | | | | |

158

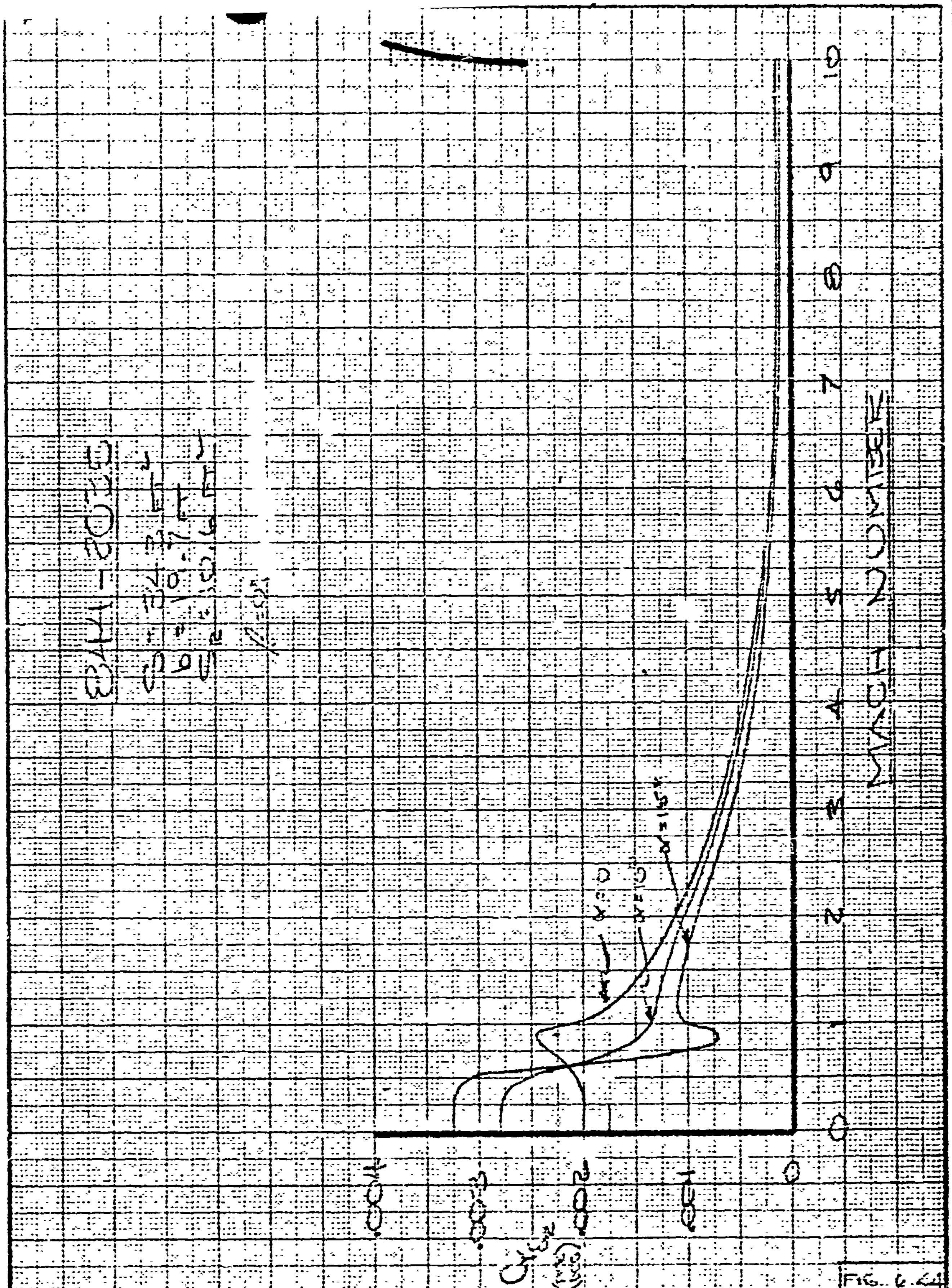


FIG. 6.44

| | | | REVISED | DATE | | |
|---|---|---|---|---|---|---|
| CALC | BJR | 12-8-60 | | | SIDE FORCE DUE TO RUDDER | 844-2035 |
| CHECK | | | BJR | 12-15-60 | | D2-8174 |
| APR | | | | | BOEING AIRPLANE COMPANY | PAGE 6.49 |
| APR | | | | | | |

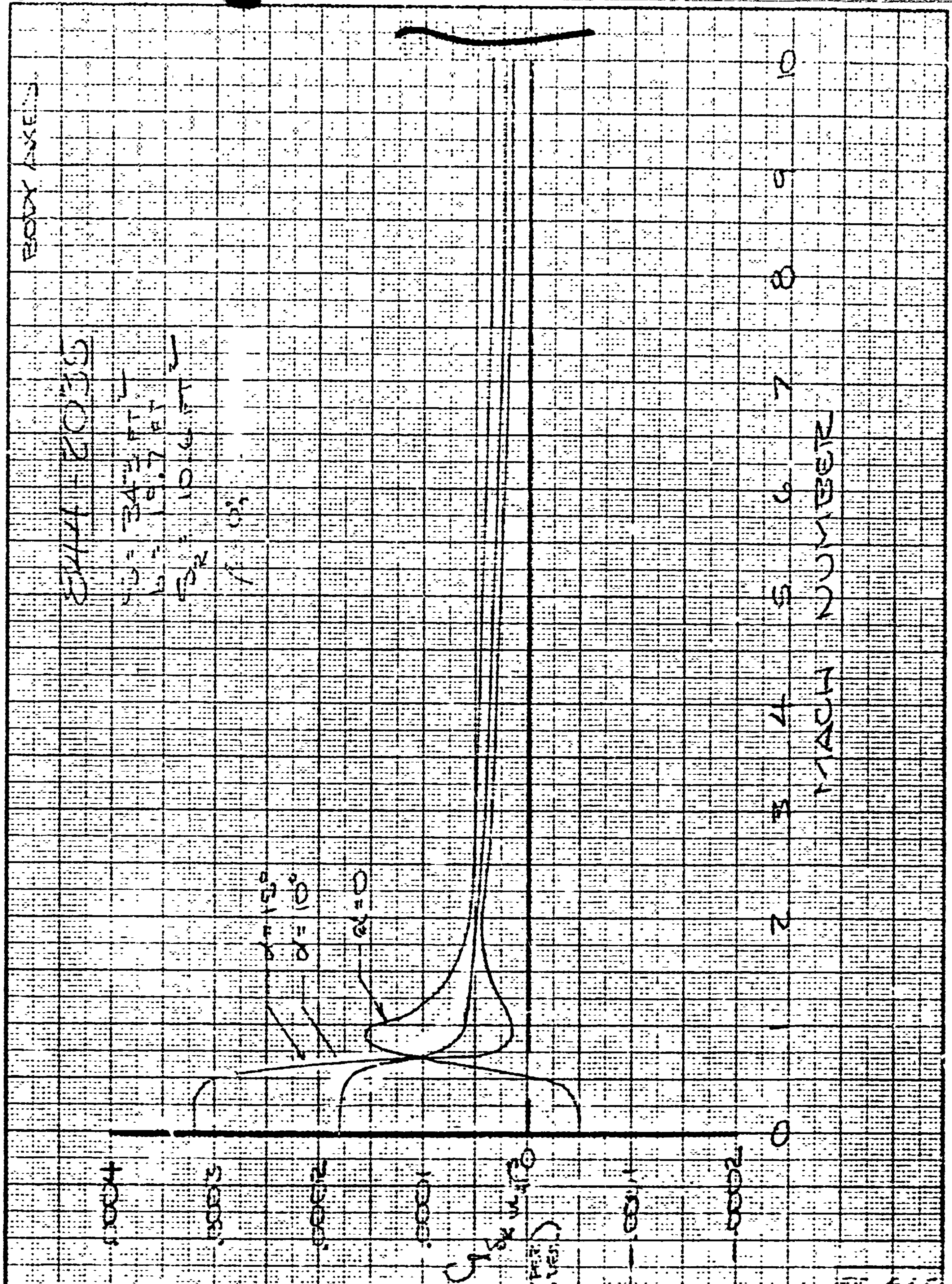


| CALC | | | REVISED | DATE | ROLLING MOMENT DUE TO RUDDER | E44-2035 |
|---|---|---|---|---|---|---|
| CHECK | | | KFR | 12-1-50 | | D2-6174 |
| APR | | | | | BOEING AIRPLANE COMPANY | PAGE 6.50 |
| APR | | | | | | |



K-E

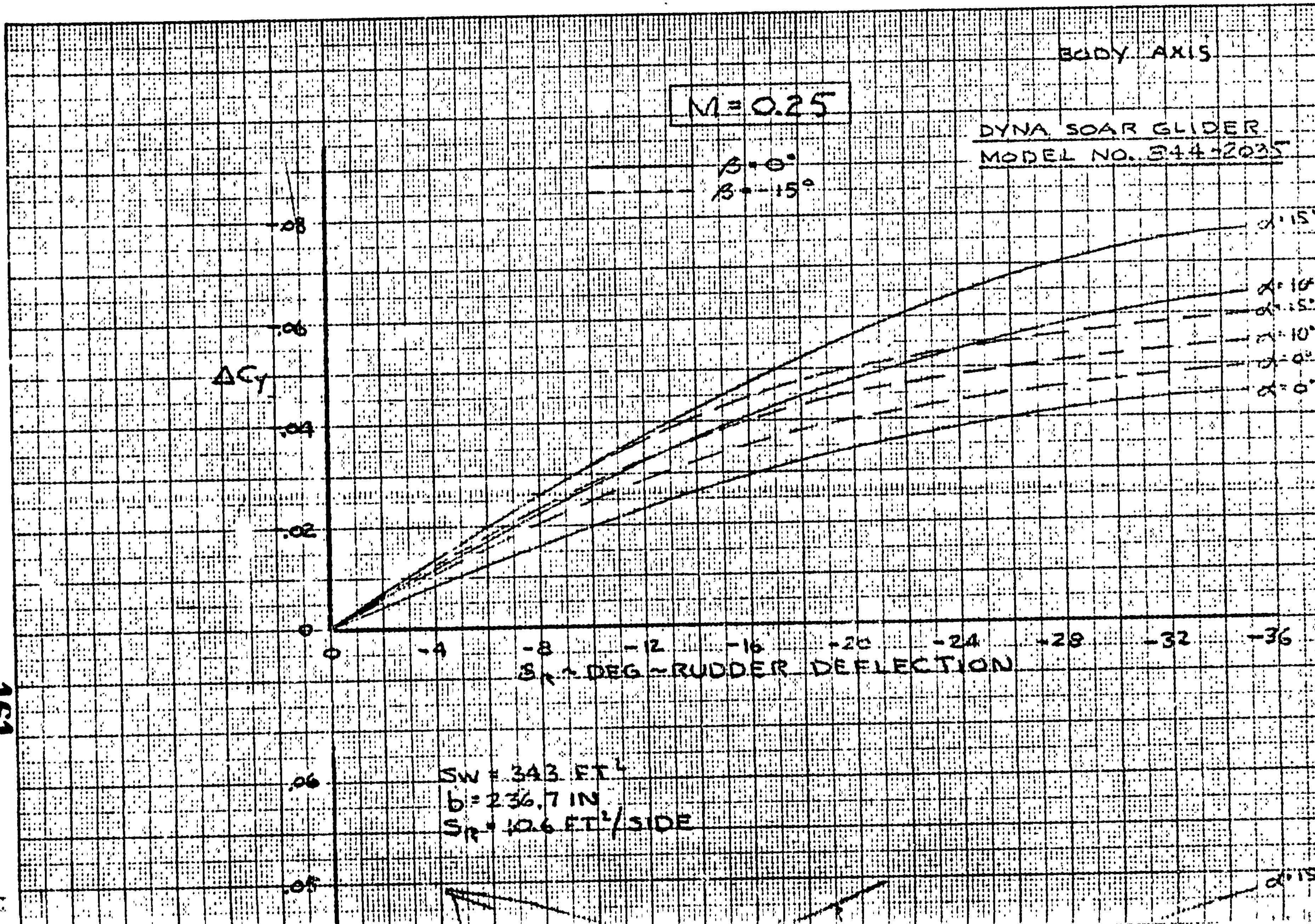
BODY AXIS
M = 0.25
DYNA SOAR GLIDER
MODEL NO. 314-2035
$\beta = 0°$
$\beta = -15°$
$\alpha = 15°$
$\alpha = 10°$
$\alpha = 15°$
$\alpha = 10°$
$\alpha = 0°$
$\alpha = 0°$
$\Delta C_Y$
.08
.06
.04
.02
0
.06
.08
0
-4
-8
-12
-16
-20
-24
-28
-32
-36
$\delta_R$ ~ DEG ~ RUDDER DEFLECTION
$S_W$ = 343 FT$^2$
b = 236.7 IN
$S_R$ = 10.6 FT$^2$/SIDE
$\alpha = 15°$

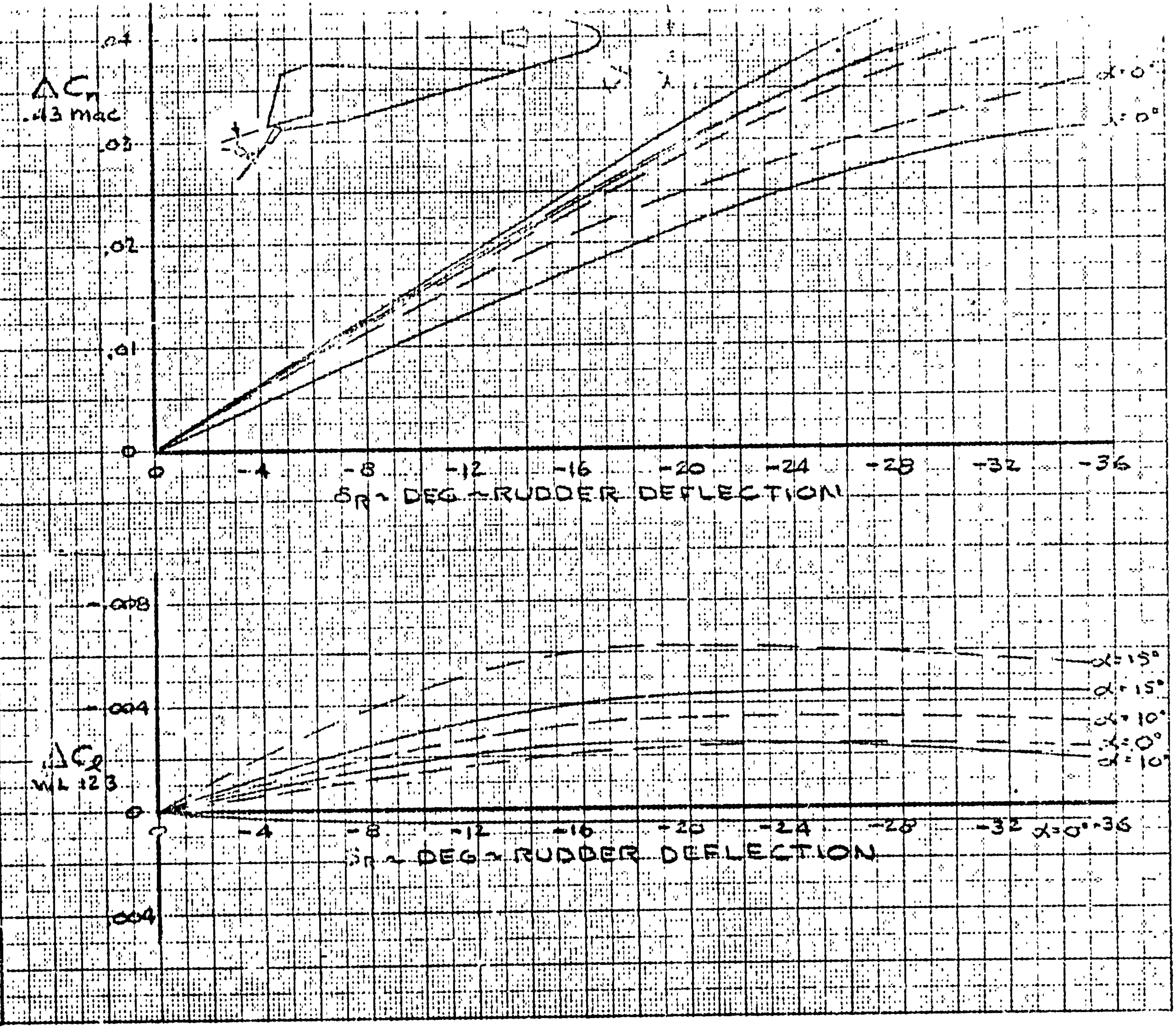


| | | | |
|---|---|---|---|
| CALC | EJH | 11/9/60 | REVISED / DATE |
| CHECK | | | |
| APPD | | | |
| APPD | | | |

RUDDER EFFECTIVENESS
LANDING SPEED

FIG. 6.46
844-2035
D2-8174
PAGE 6.51

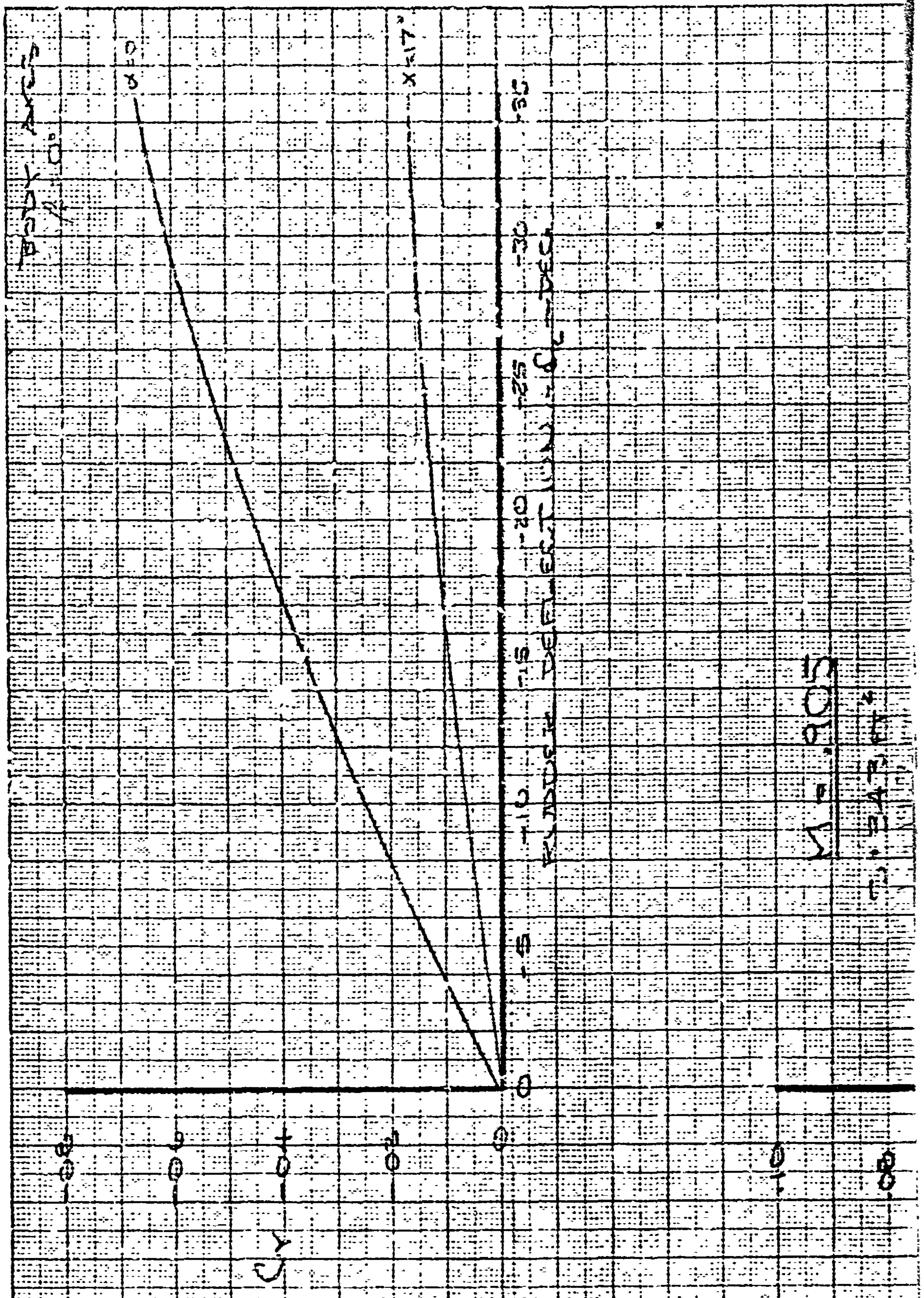

M = .905
α = 0
α = 17°
0
-5
-10
-15
-20
-25
-30
$C_y$

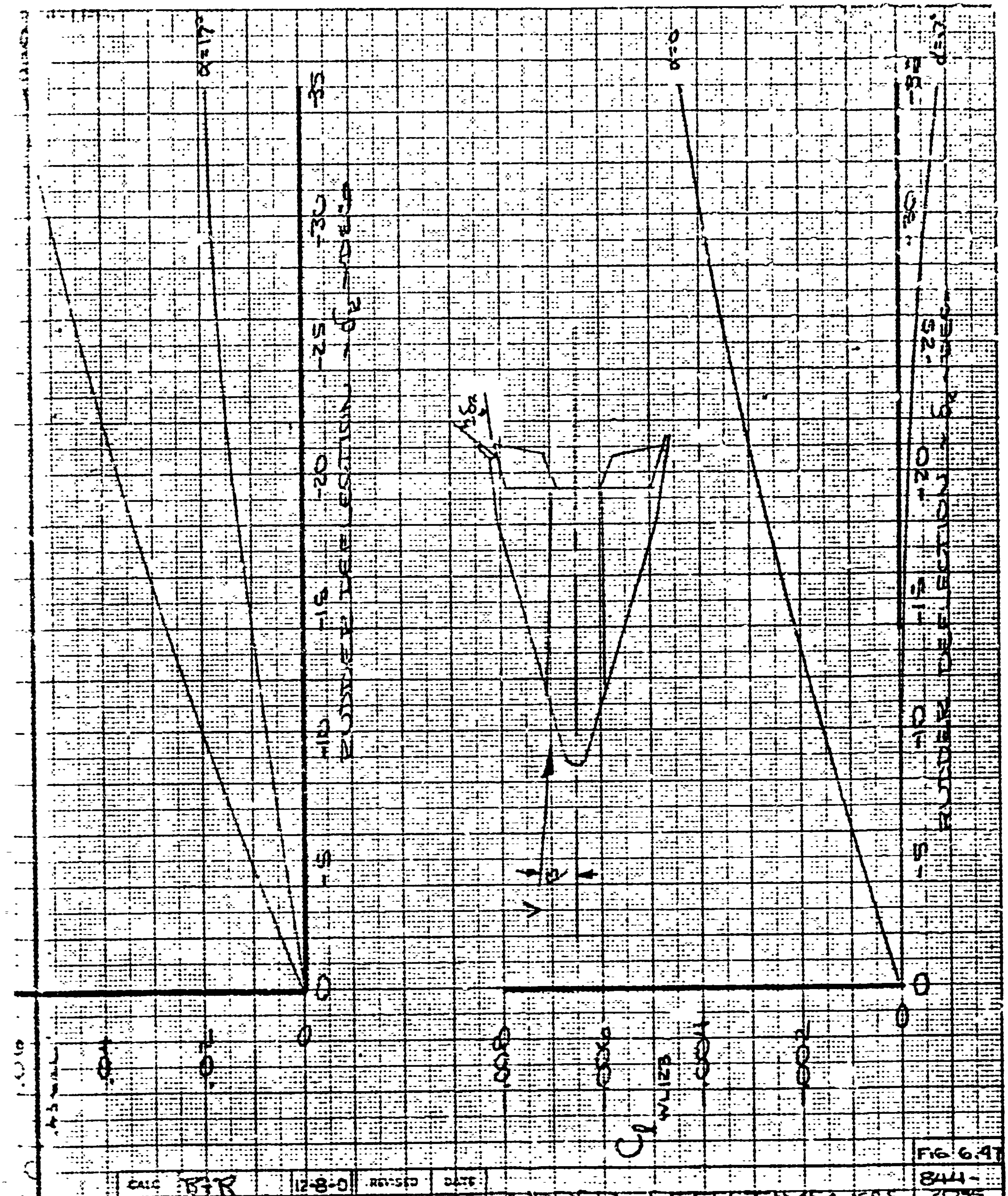


| CALC | BJR | 12-8-0 | REVISED | DATE | | FIG. 6.47 |
|---|---|---|---|---|---|---|
| CHECK | | | | | RUDDER EFFECTIVENESS | 844-2095 |
| APPD | | | | | M=.905 | D2-8174 |
| APPD | | | | | | PAGE 6.52 |

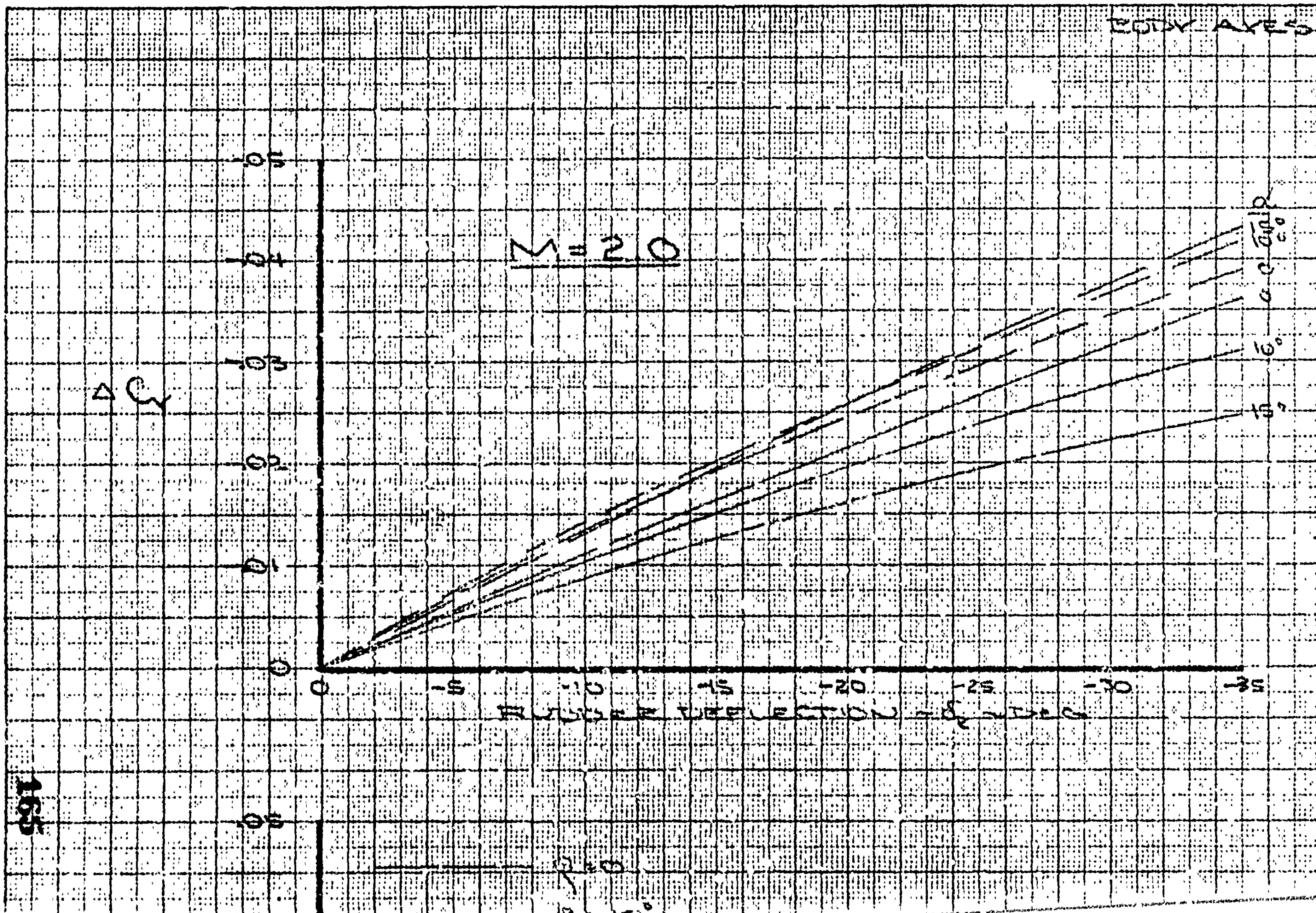
BODY AXES
M=2.0
ΔCy
RUDDER DEFLECTION ~ δr ~ DEG
.05
.04
.03
.02
.01
0
-5
-10
-15
-20
-25
-30
-35
10°
15°

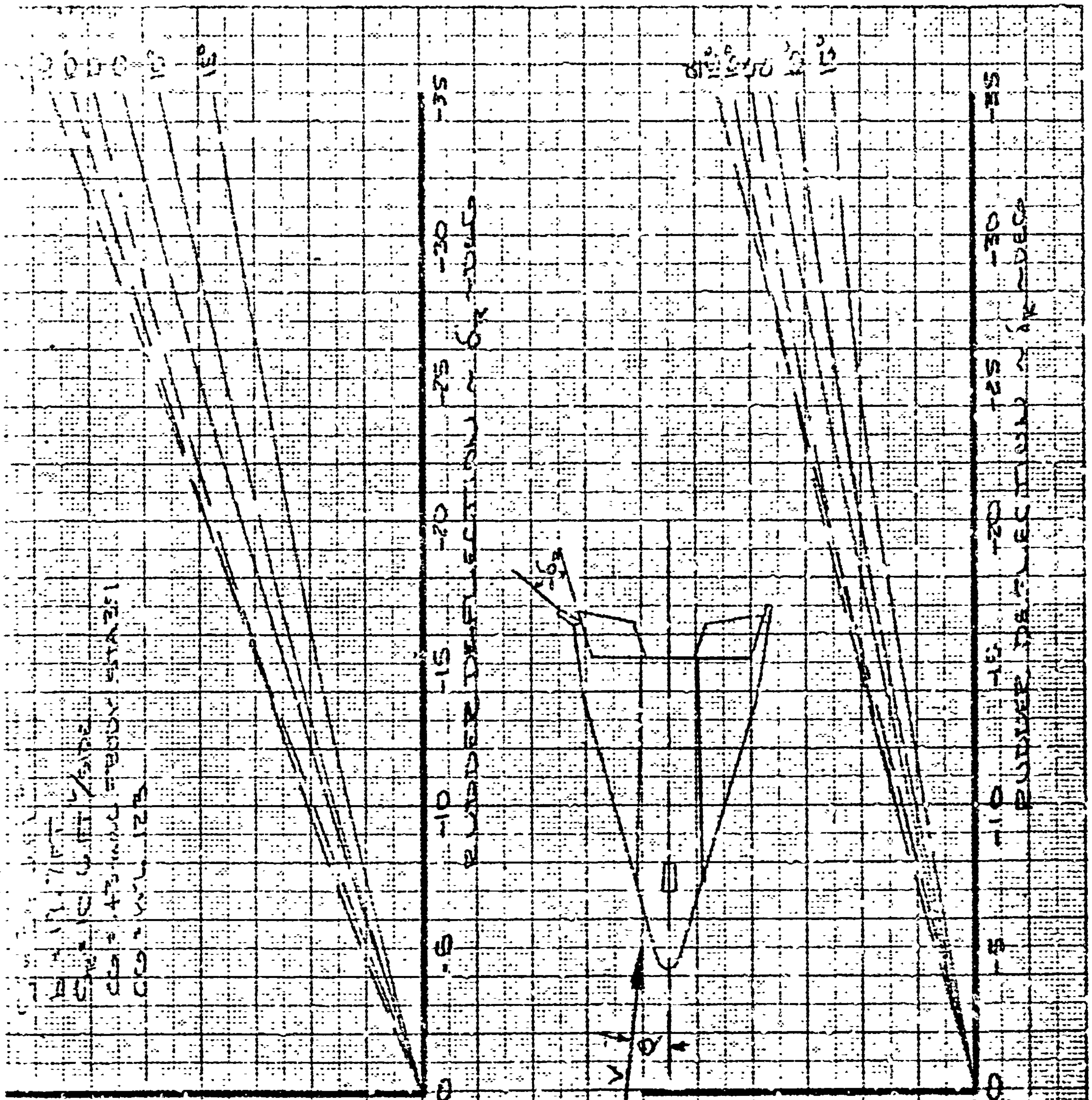


RUDDER EFFECTIVENESS

M = 2.0

FIG. 6.43

PAGE 6.53

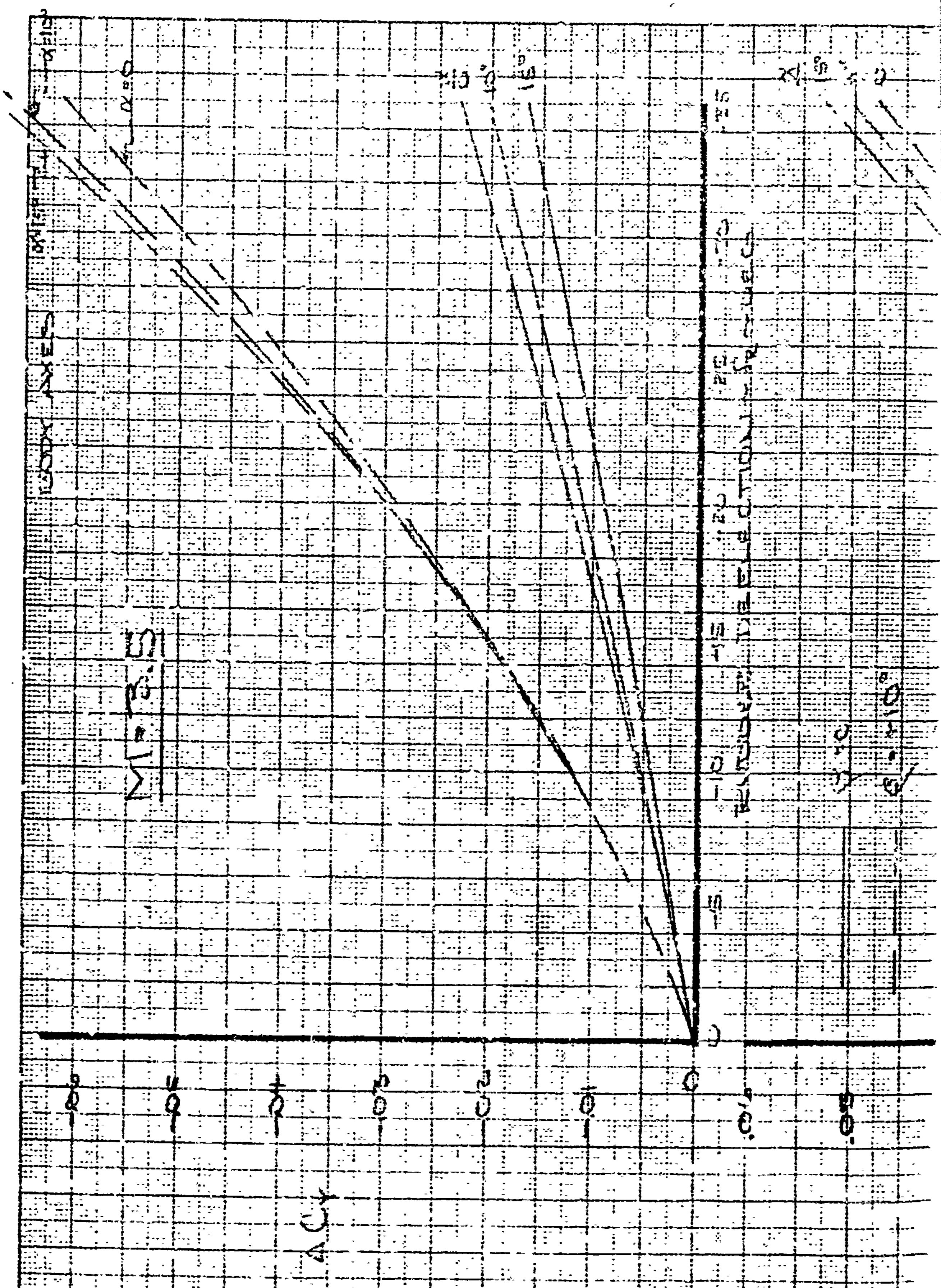

BODY AXES
M = 2.5
ΔCY
RUDDER DEFLECTION - δr - DEG

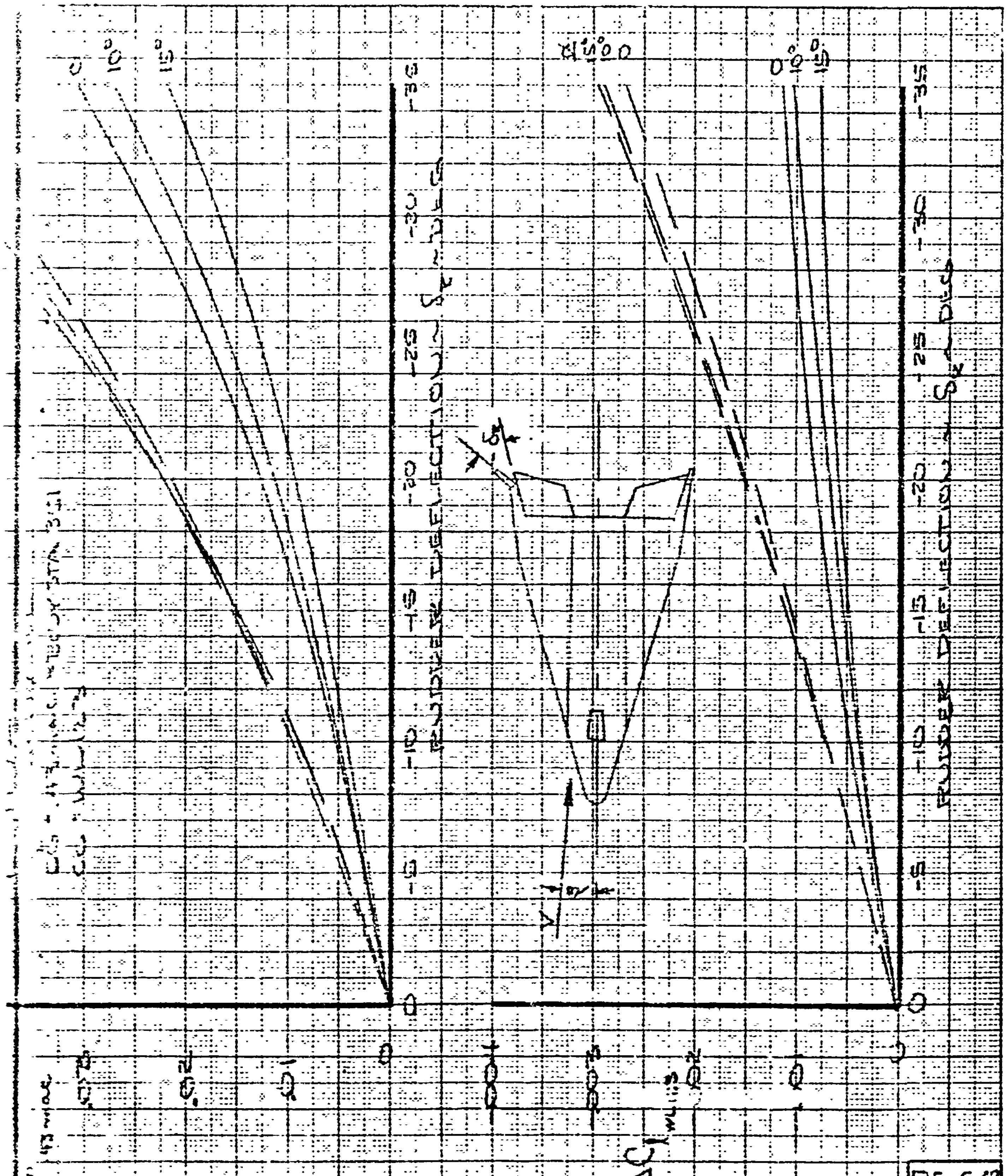


| CALC | | | REVISED | DATE | RUDDER EFFECTIVENESS<br>M = 3.5 | FIG. 6.49<br>244-1035 |
|---|---|---|---|---|---|---|
| CHECK | | | | | | D2-8174 |
| APPD | | | | | | PAGE 6.54a |
| APPD | | | | | | |

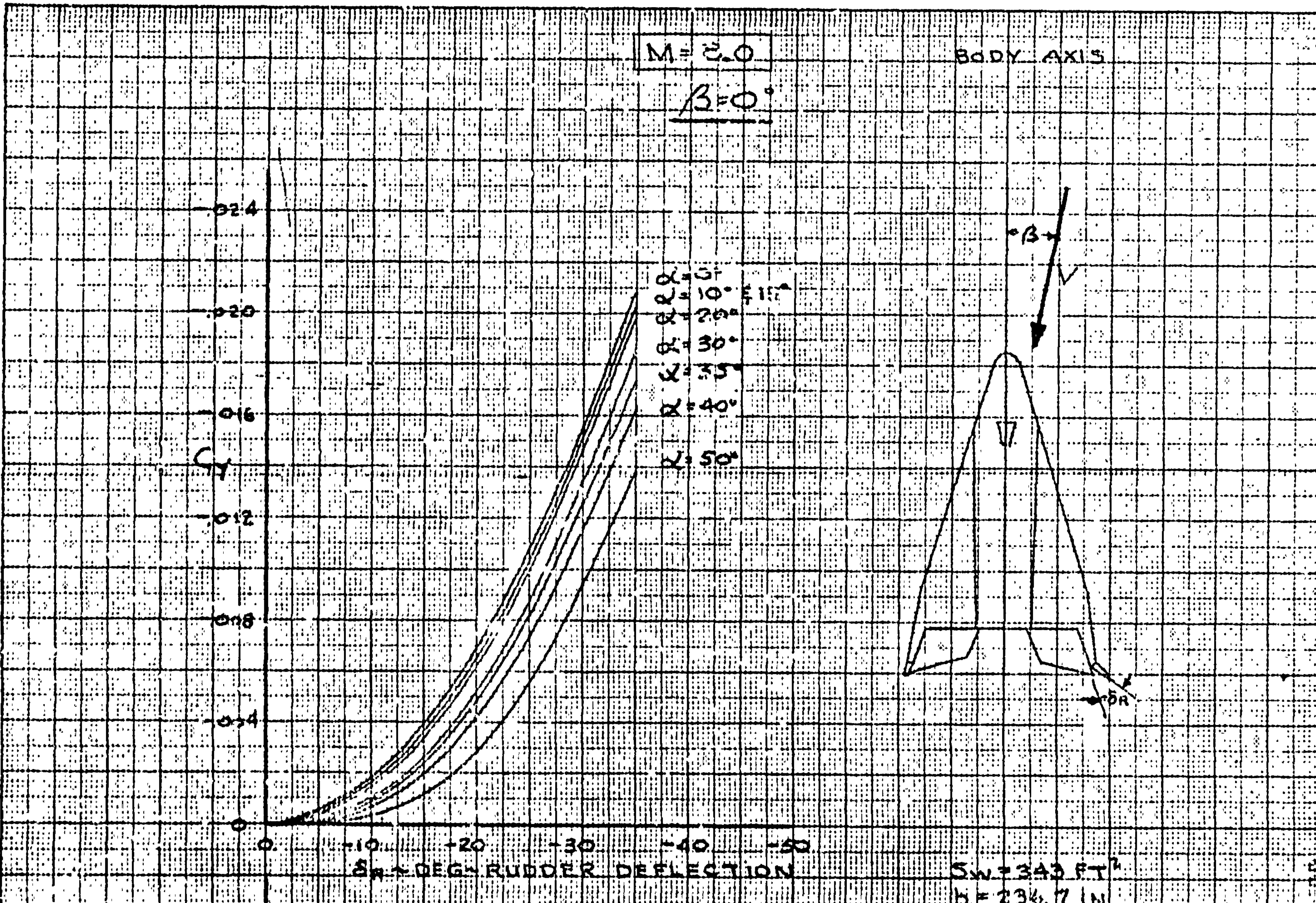
M = 2.0
β = 0°
BODY AXIS
.024
.020
.016
.012
.008
.004
0
$C_Y$
0
-10
-20
-30
-40
-50
δR ~ DEG ~ RUDDER DEFLECTION
α = 5°
α = 10° & 15°
α = 20°
α = 30°
α = 35°
α = 40°
α = 50°
β
V
δR
Sw = 343 FT²
b = 234.7 IN

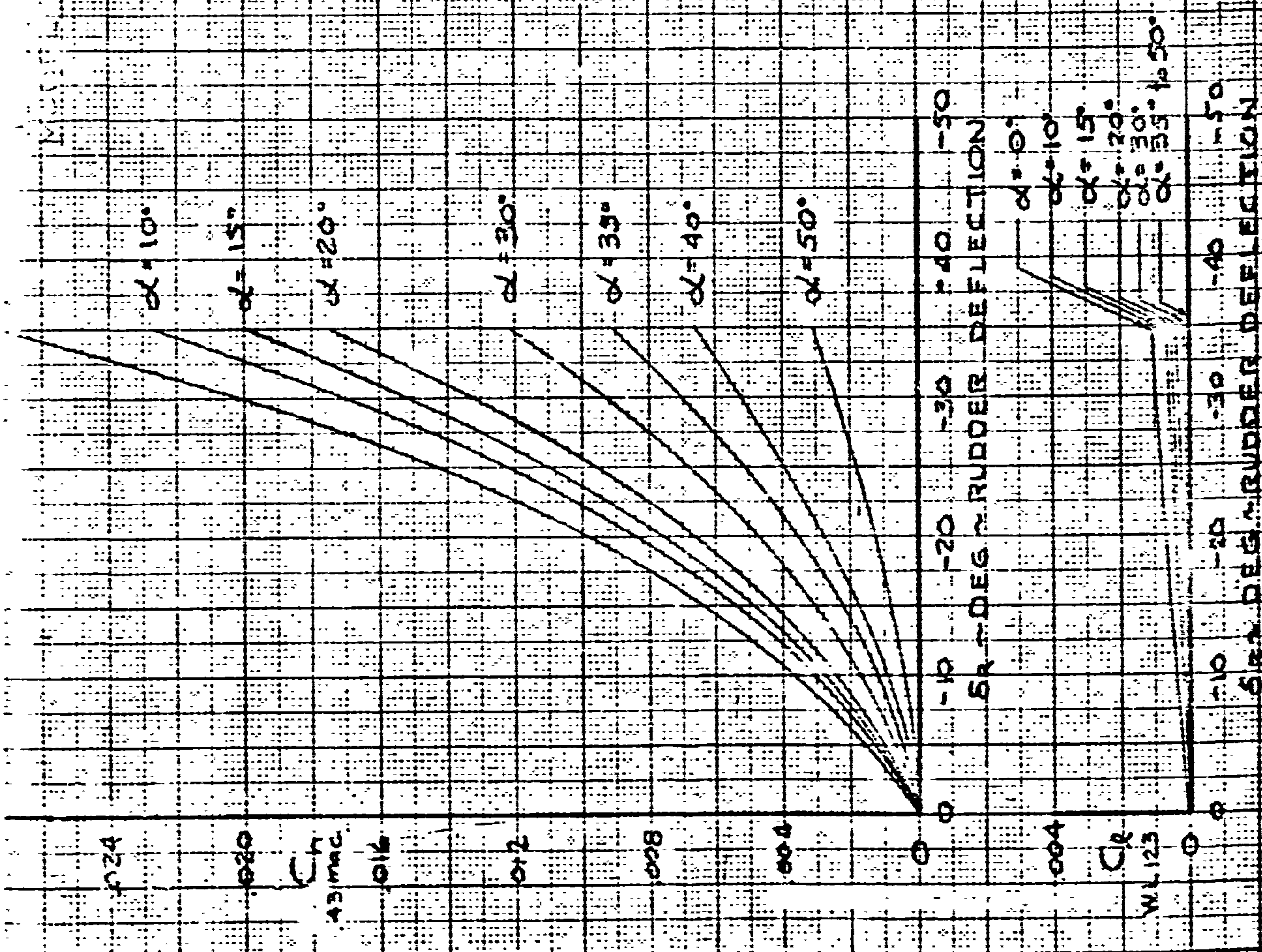


| | | | |
|---|---|---|---|
| CALC | E.J.H. | 12/8/10 | REVISED | DATE |
| CHECK | | | | |
| APPD | | | | |
| APPD | | | | |

**RUDDER EFFECTIVENESS**

HYPERSONIC SPEED ~ θ...

FIG. 6.50

344-2035

D2-8174

PAGE 6.55-a

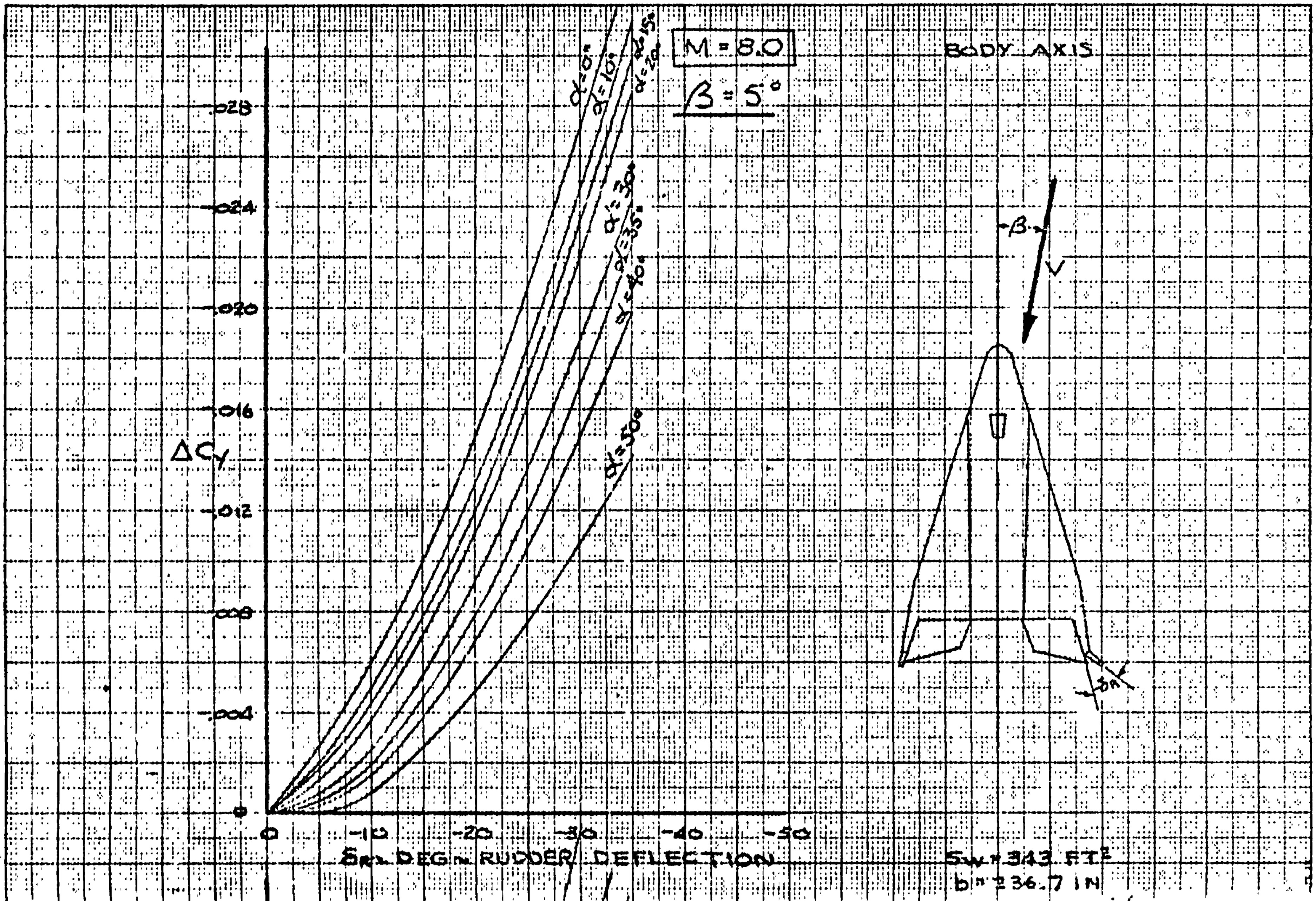
M = 8.0
β = 5°
BODY AXIS
α = 0°
α = 10°
α = 15°
α = 20°
α = 30°
α = 35°
α = 40°
α = 50°
ΔCy
.028
.024
.020
.016
.012
.008
.004
0
0
-10
-20
-30
-40
-50
δR ~ DEG ~ RUDDER DEFLECTION
β
V
δR
Sw = 343 FT²
b = 236.7 IN



6-55-41

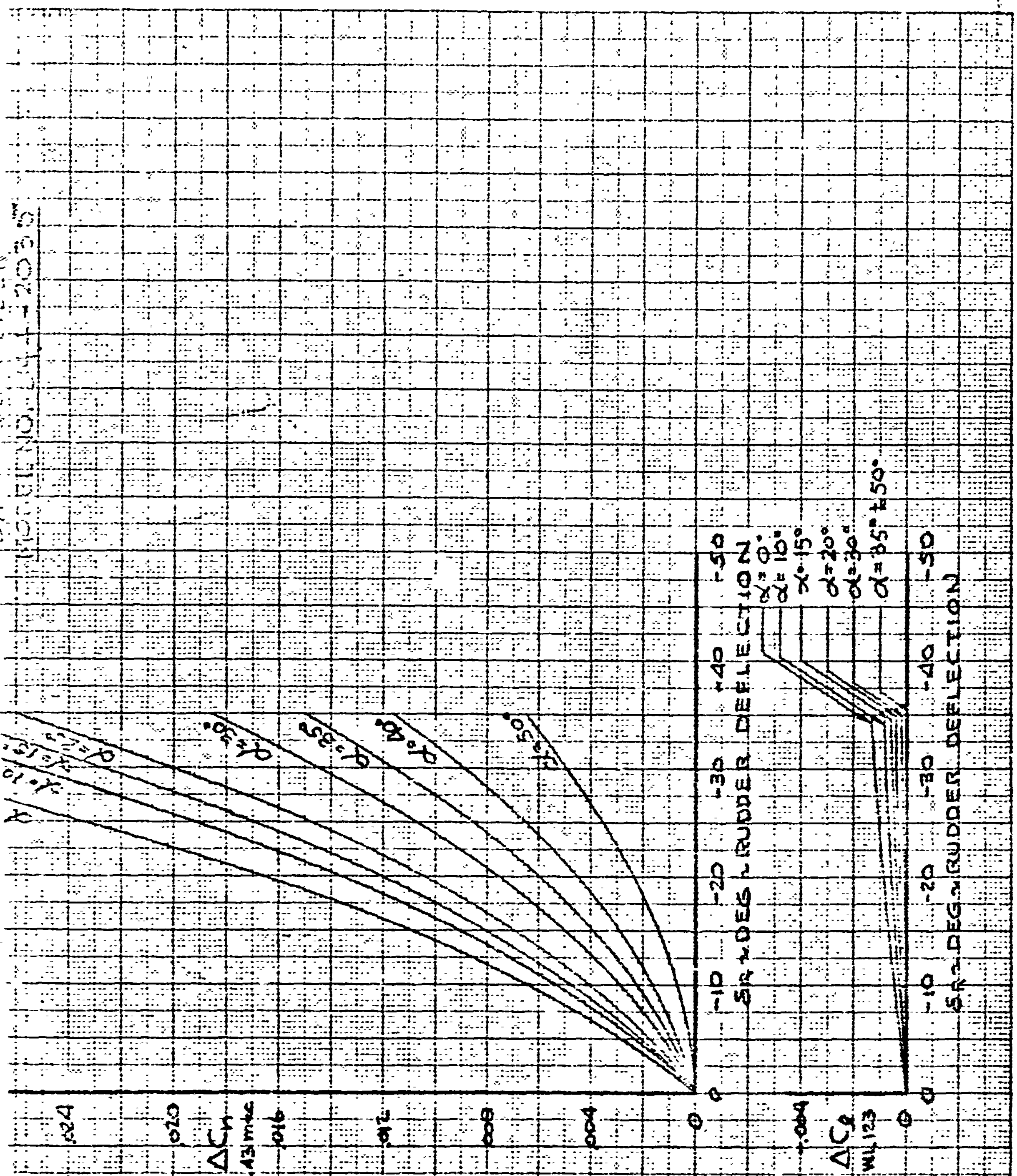


| | | | | | |
|---|---|---|---|---|---|
| CALC | EJH | 12/8/60 | REVISED | DATE | |
| CHECK | | | | | |
| APPD | | | | | |
| APPD | | | | | |

FIG. 6.51

644-2035

# RUDDER EFFECTIVENESS
## HYPERSONIC SPEED

D2-8174

PG. 6.56

## 6.4 ROLL AND YAW ROTARY DERIVATIVES

The roll and yaw rate damping derivatives are presented on Figures 6.52 and 6.53 for various angles of attack at landing speed, and on Figures 6.54 and 6.55 for various Mach numbers. The landing speed derivatives are presented in the form that they would be obtained from rotary-derivative wind tunnel tests. The derivatives presented versus Mach number include a theoretical estimate of the contribution due to rate-of-change-of-sideslip. This estimate is included in order to permit use of these rotary derivatives for root-solutions and simulator studies where rate-of-change-of-sideslip may not be desired. Further study may alter this estimate significantly.

The landing speed rotary derivatives are based upon preliminary Langley Research Center rotary derivative test data on a model of configuration 814-2002, a model of the NASA Space Ferry (similar to the Dyna Soar glider), and the Bell-Martin Phase I Dyna Soar glider (Reference b ). The data have been correlated by theoretical computations which are based on steady rolling or steady yawing (Reference c ).

The rotary derivatives versus Mach number, Figures 6.54 and 6.55, were obtained from Figures 6.52 and 6.53 for landing speed, and the variation with Mach number was obtained from theoretical formulae and rotary derivative tests of the X-15 airplane (Reference d ).

DATA SOURCE:

THEORETICAL PREDICTIONS FROM NACA TN 2409 CORRELATED WITH FREE TO DAMP OSCILLATION TESTS OF THE

① BELL-MARTIN VEHICLE (C119-ER-1044)

② NASA SPACE FERRY (PRELIMINARY DATA)

③ BAC MODEL 2007 ( " " )

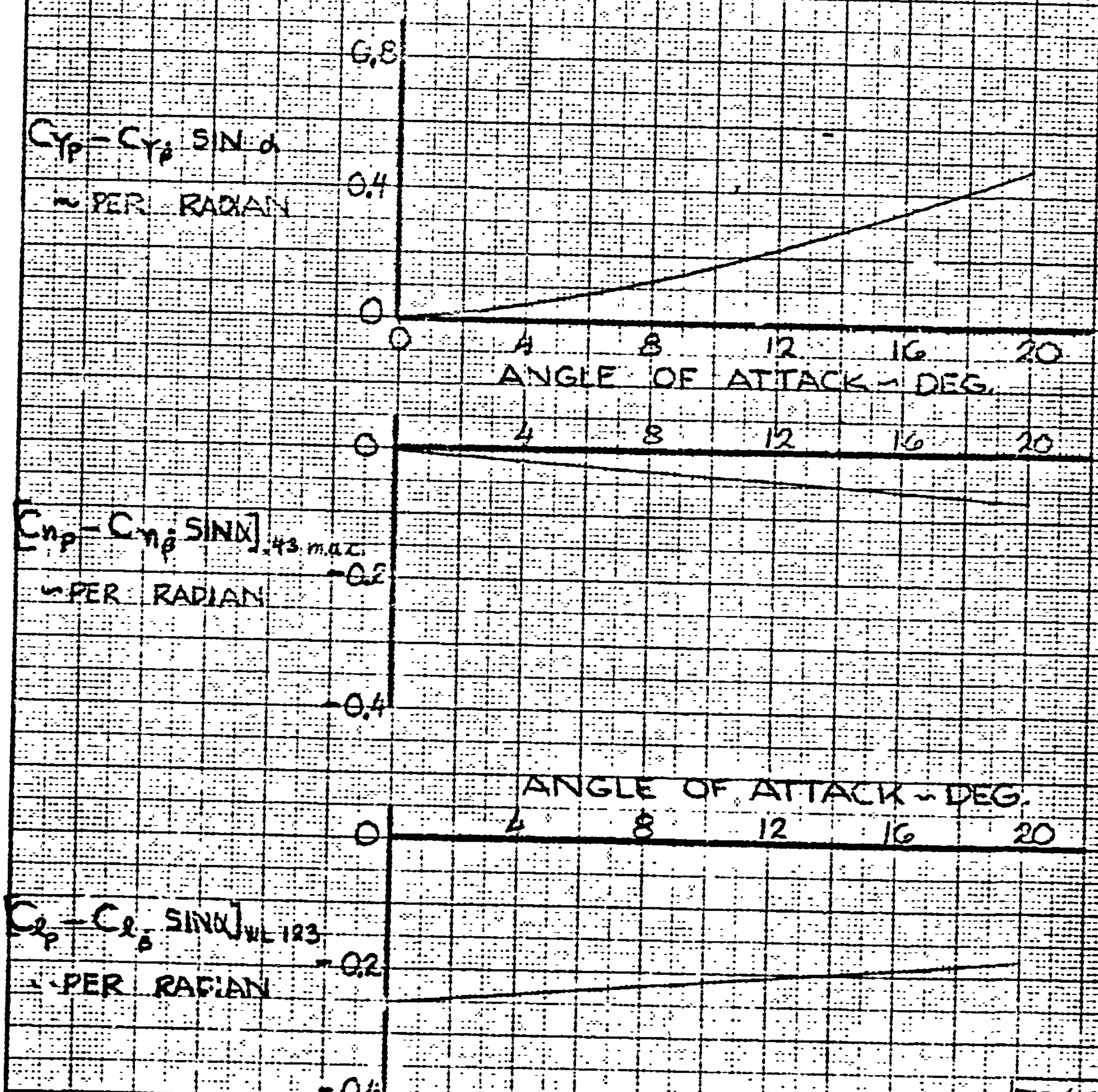


| CALC | | 12-3-64 | REVISED | DATE | EFFECT OF ANGLE OF ATTACK ON ROLLING DERIVATIVES ~ LANDING SPEED | FIG 6.52 |
|---|---|---|---|---|---|---|
| CHECK | | | | | | 844-2035 |
| APR | | | | | | D2-8174 |
| APR | | | | | BOEING AIRPLANE COMPANY | PAGE 6.58 |



K-E

DATA SOURCES:
THEORETICAL PREDICTIONS FROM NACA TN 2409 CORRELATED WITH FREE TO DAMP "OSCILLATION TESTS OF THE
① BELL - MARTIN VEHICLE (C119-ER-10440)
② NASA SPACE FERRY (PRELIMINARY DATA)
③ BAC MODEL 2002 ( " " )

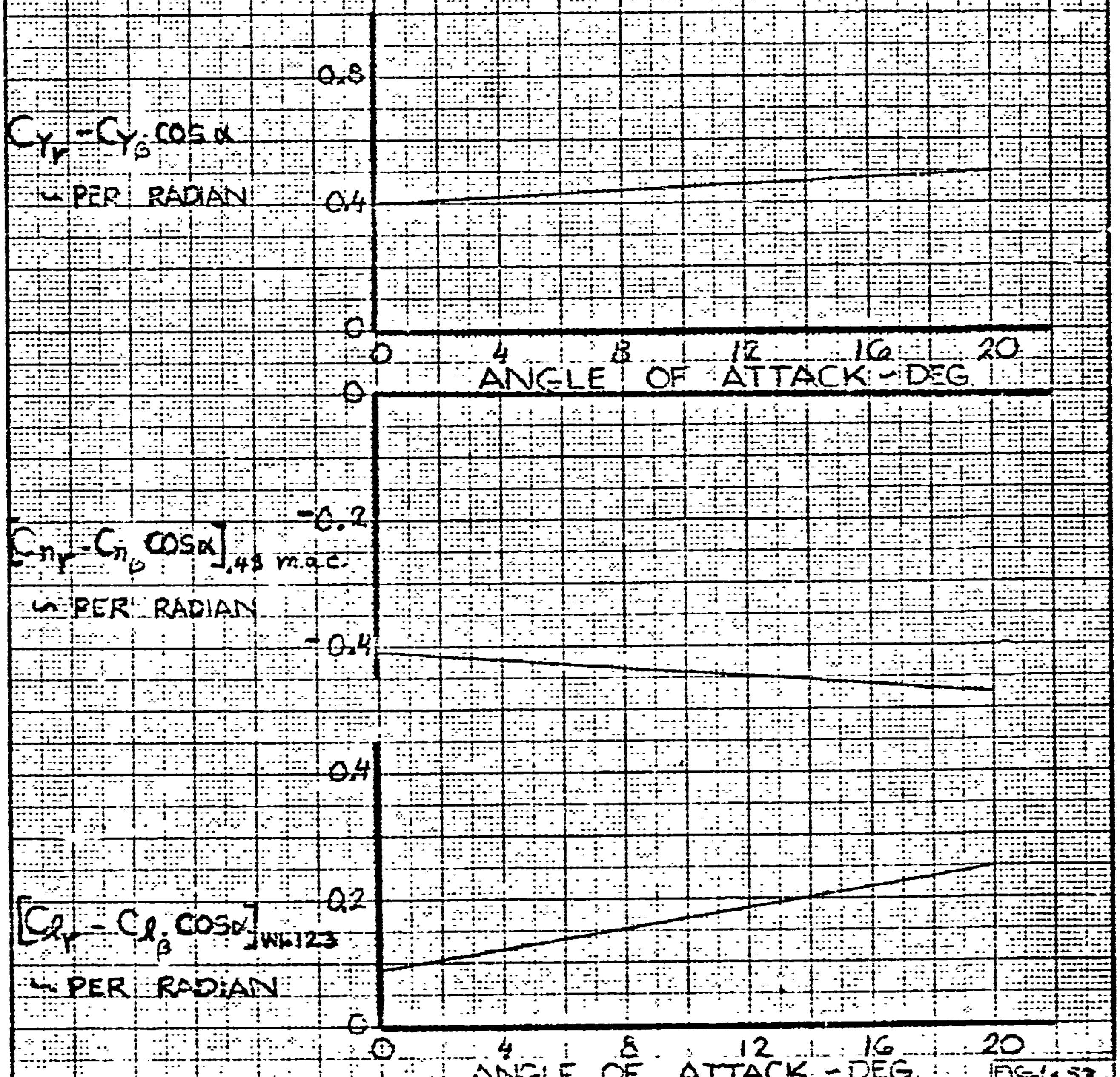


FIG. 6.53

| | | | |
|---|---|---|---|
| CALC | BMS | 12-9-60 | REVISED / DATE |
| CHECK | | | |
| APR | | | |
| APR | | | |

EFFECT OF ANGLE OF ATTACK ON YAWING DERIVATIVES ~ LANDING SPEED

844-2035

D2-8174

BOEING AIRPLANE COMPANY

175

PAGE 6.59

BODY AXES

DATA SOURCE:

SUBSONIC DATA FROM FIGS. 6.58 & 6.59
SUPERSONIC PREDICTIONS AND TEST DATA FROM NASA TM X-287 (X-15 AIRPLANE)

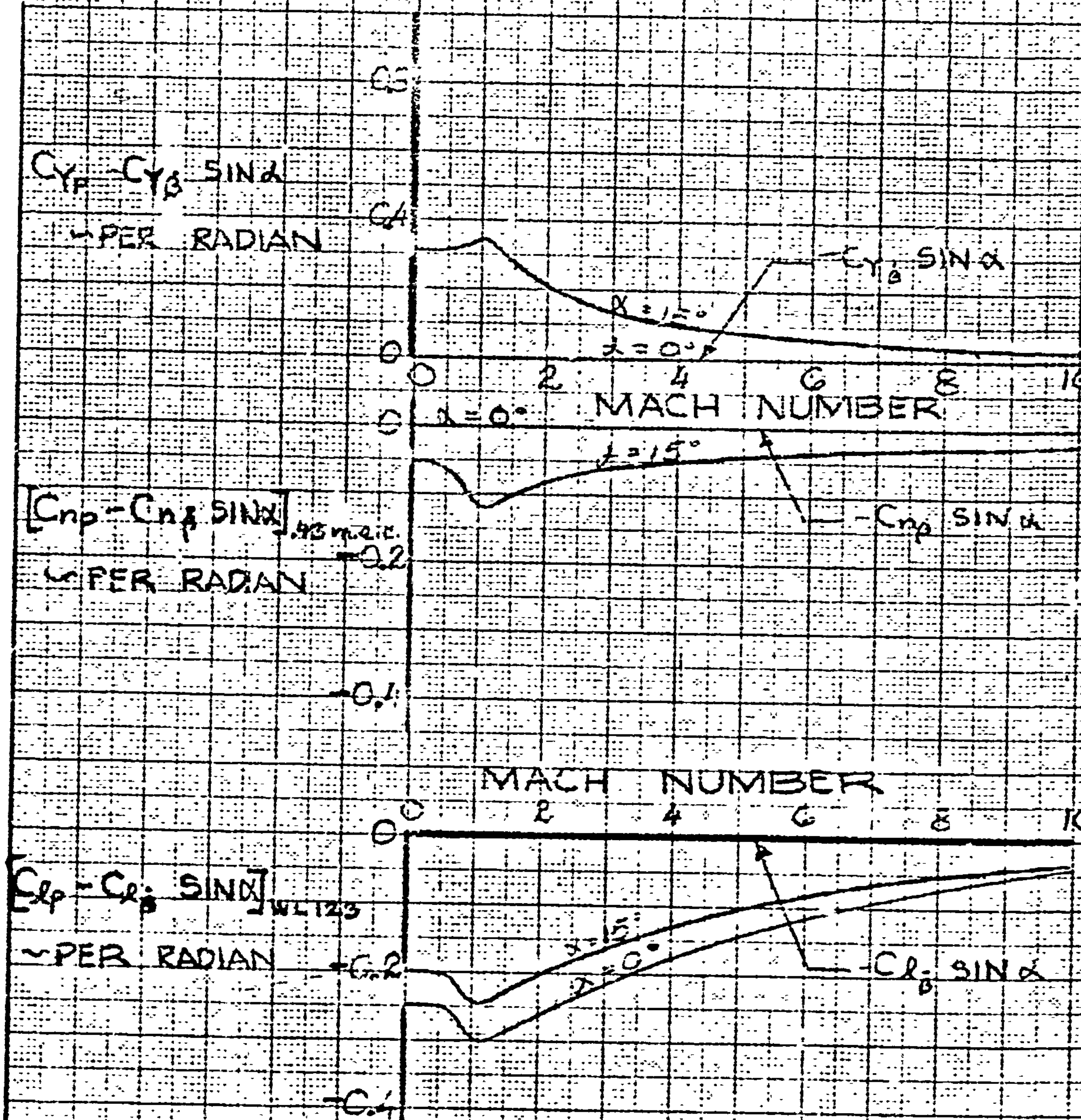


| | | | | | |
|---|---|---|---|---|---|
| CALC | RMS | 12-8-60 | REVISED | DATE | FIG. 6.54 |
| CHECK | | | | | EFFECT OF MACH NUMBER ON ROLLING DERIVATIVES |
| APR | | | | | 544-2055 |
| APR | | | | | D2-8174 |
| | | | | | BOEING AIRPLANE COMPANY |

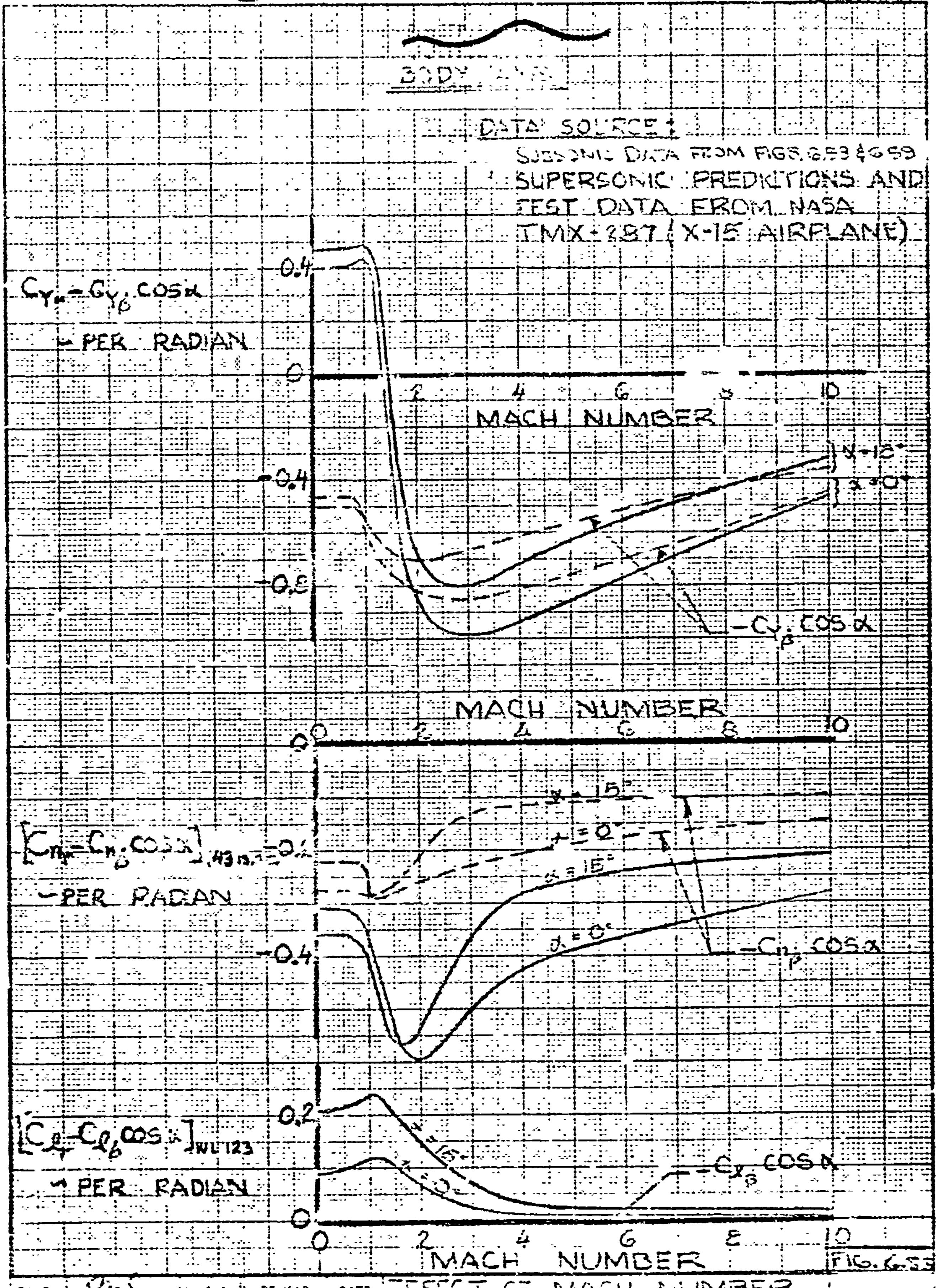


| CALC | | 12-8-60 | REVISED | DATE | EFFECT OF MACH NUMBER ON YAWING DERIVATIVES | 844-2035 |
|---|---|---|---|---|---|---|
| CHECK | | | | | **177** | D2-8174 |
| APR | | | | | BOEING AIRPLANE COMPANY | PAGE 6.61 |
| APR | | | | | | |

## 7.0 GLIDER WITH TRANSITION SECTION

The addition of the third stage rocket and transition section to the glider moves the center of gravity rearward and changes the glider pitch and yaw characteristics. These effects are reflected in the longitudinal and lateral-directional stability data shown in Figures 7.1 through 7.13 . Wind Tunnel data available for pitch characteristics were used from M = .7 to M=3.5; at lower and higher speeds, theoretical estimations were necessary. The lateral directional data were estimated. The reference centers of gravity for the moments were those for the instant of ignition of the third stage rocket and at burn out after 19 seconds of rocket burning. The c.g. moves forward 8.8% m.a.c. during third stage powered flight. Present plans include modifying the transition shape and length from that shown to reduce the zero lift pitching moment and to increase the glider static stability at transonic speeds. The effect of change of shape to reduce the zero lift pitching moment has been estimated and included in the data shown. The effect of length to increase stability has not been included.

## 7.1 LONGITUDINAL STABILITY AND CONTROL

The addition of the transition section to the glider creates positive zero-lift pitching moment and reduces the vehicle normal force. This effect is most prevalent at subsonic and transonic speeds, diminishing at supersonic speeds. The increments of normal force and pitching moment for various angles of attack and Mach numbers with no elevon deflection were determined from wind tunnel tests of an early configuration and modified to reflect the current configuration. Data were available for a range of speeds from M = .7 to M = 3.5. These increments were added to the glider-alone data.

The data reflect the 66 inch transition length tested rather than the 55 inch length shown in Reference a. The transition length will be established from aerodynamic and performance requirements. The 55 inch length represents a logical separation plane from structural design considerations since the pressure bulkhead for the heat blast diagram is located in that region. However, sufficient static stability may not be available from the 55 inch transition section.

Two center of gravity locations are shown on the plots in Figures 7.1 through 7.8. These are: (1) the initial center of gravity at the instant of separation from the second stage and (2) the center of gravity at rocket burnout.

Lines of constant elevon deflection and constant angle of attack are shown only for the initial center of gravity location at .562 m.a.c. Other fore and aft center of gravity locations can be represented on these plots by a rotation of the vertical ($C_N$) axis. This rotation is shown for the center of gravity at rocket burnout of .474 m.a.c. The vertical center of gravity location is assumed fixed when the $C_N$ axis is rotated to represent a different fore and aft center of gravity location.

The following method can be used to determine the amount of rotation of the $C_N$ axis required to represent other center of gravity locations. (1) Assume center of gravity travel linear with burn time (t).

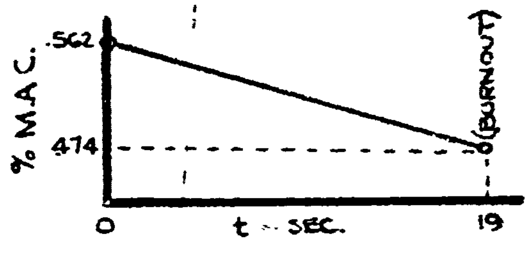


Then determine the center of gravity location in present m.a.c. for the time (t) desired as shown in the sketch above.

(2) Shift the $C_N$ axis to reflect the center of gravity location for the time (t).

Example: Shift the center of gravity 2 percent m.a.c. forward.
(1) locate on the $C_N$ vs $C_m$ plot the point at $C_N$=1.0 and $C_m$ = .02.
(2) Draw a line through the point and the origin as shown in the sketch below.

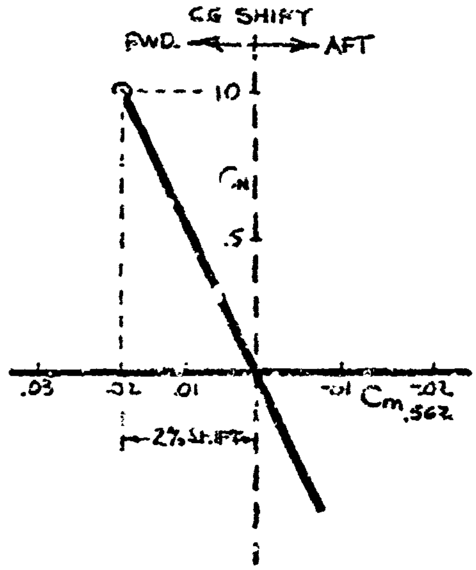

7.2 LATERAL AND DIRECTIONAL STABILITY AND CONTROL

Static directional stability characteristics are presented in Figures 7.9 and 7.10 for the effects of angle of attack, folding wing tip extensions, and center of gravity location. Theoretical estimations for the effects of the transition section were added to the glider-alone stability derivatives. The data represent the glider plus transition section aerodynamic characteristics reasonably well for ±5° sideslip. The data shows the fold down tip in the down, or extended, position to M = 3.5. The precise speed to which the folding tips will be extended is to be determined.

The effects of rudder deflection on the glider plus transition directional characteristics are shown in Figures 7.11 through 7.13 for two angles of attack. The effectiveness differs from the glider-alone characteristics because of the center of gravity location.

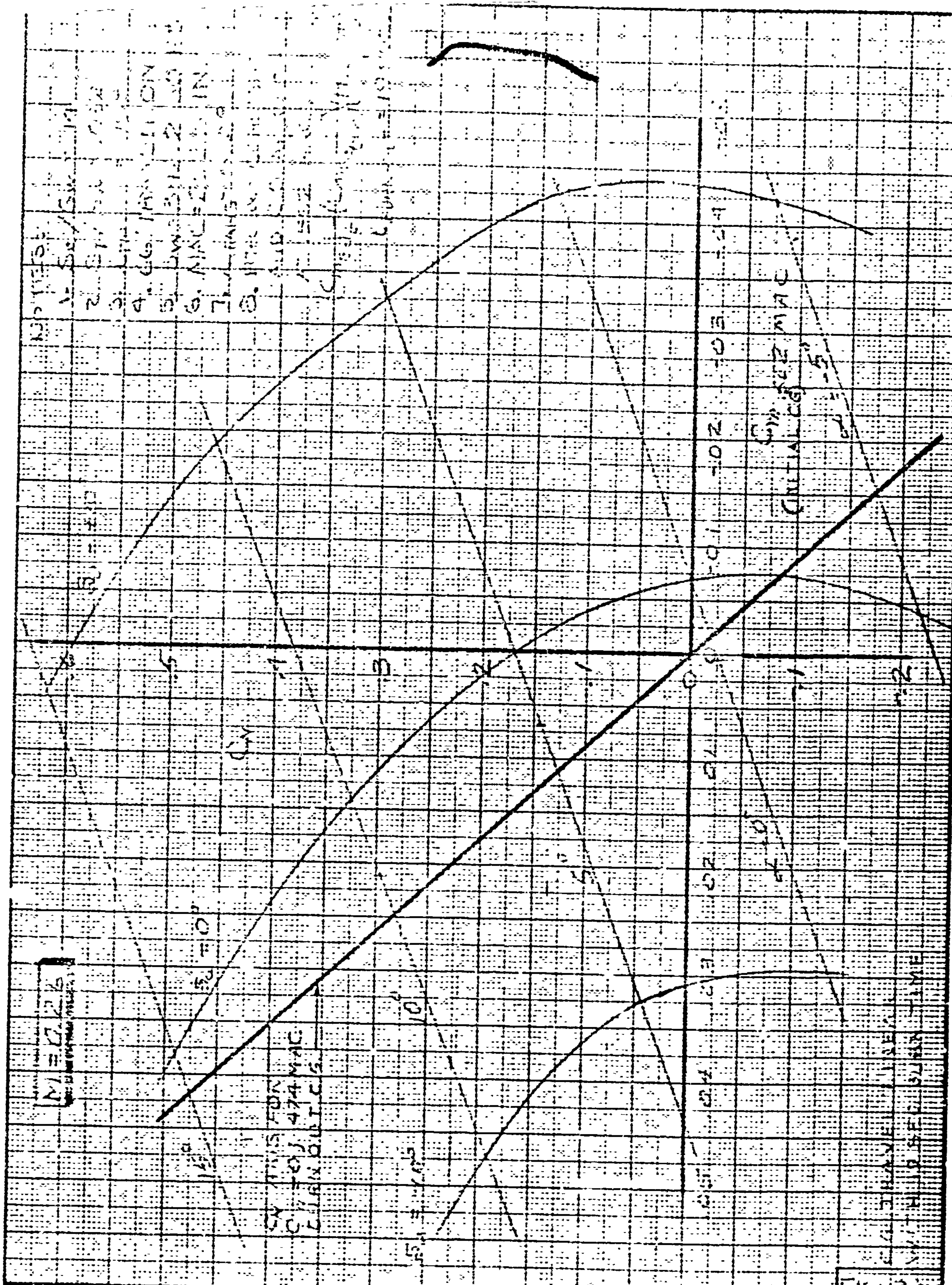

Fig. 7-1

| CALC | K | | REVISED | DATE |
|---|---|---|---|---|
| CHECK | | | | |
| APR | | | | |
| APR | | | | |

LONGITUDINAL STABILITY 1844-2035

TIPS EXTENDED - C6' TRANSITION

D2-6174

BOEING AIRPLANE COMPANY M=.26

PAGE 7.5

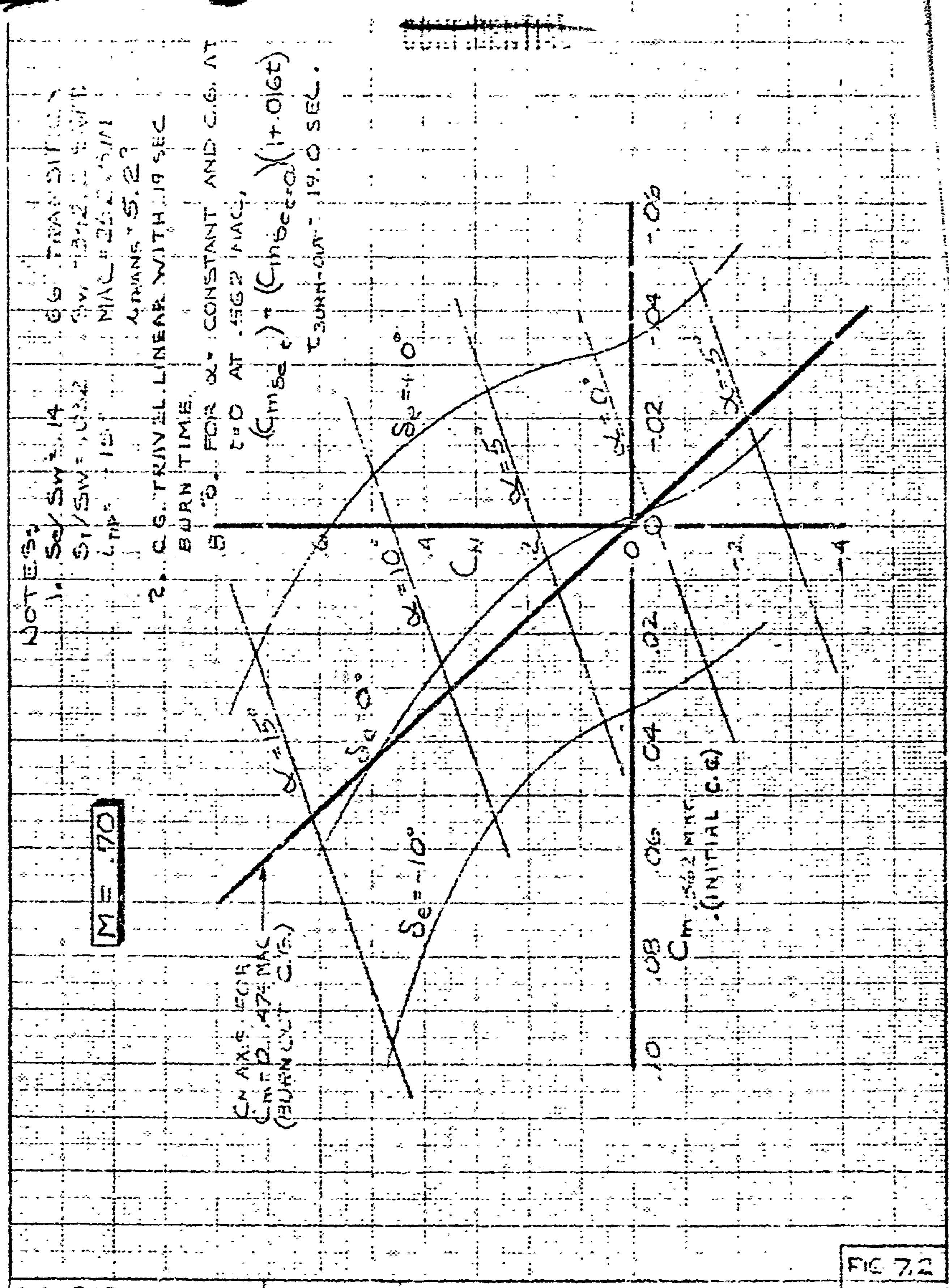


FIG 7.2

| | | | |
|---|---|---|---|
| CALC DEP | REVISED | DATE | LONGITUDINAL STABILITY 6H-2035 |
| CHECK | | | TIPS EXTENDED - 66" TRANSITION D2-8174 |
| APP | | | 183 |
| APP | | | BOEING AIRPLANE COMPANY M=.70 7.6 |

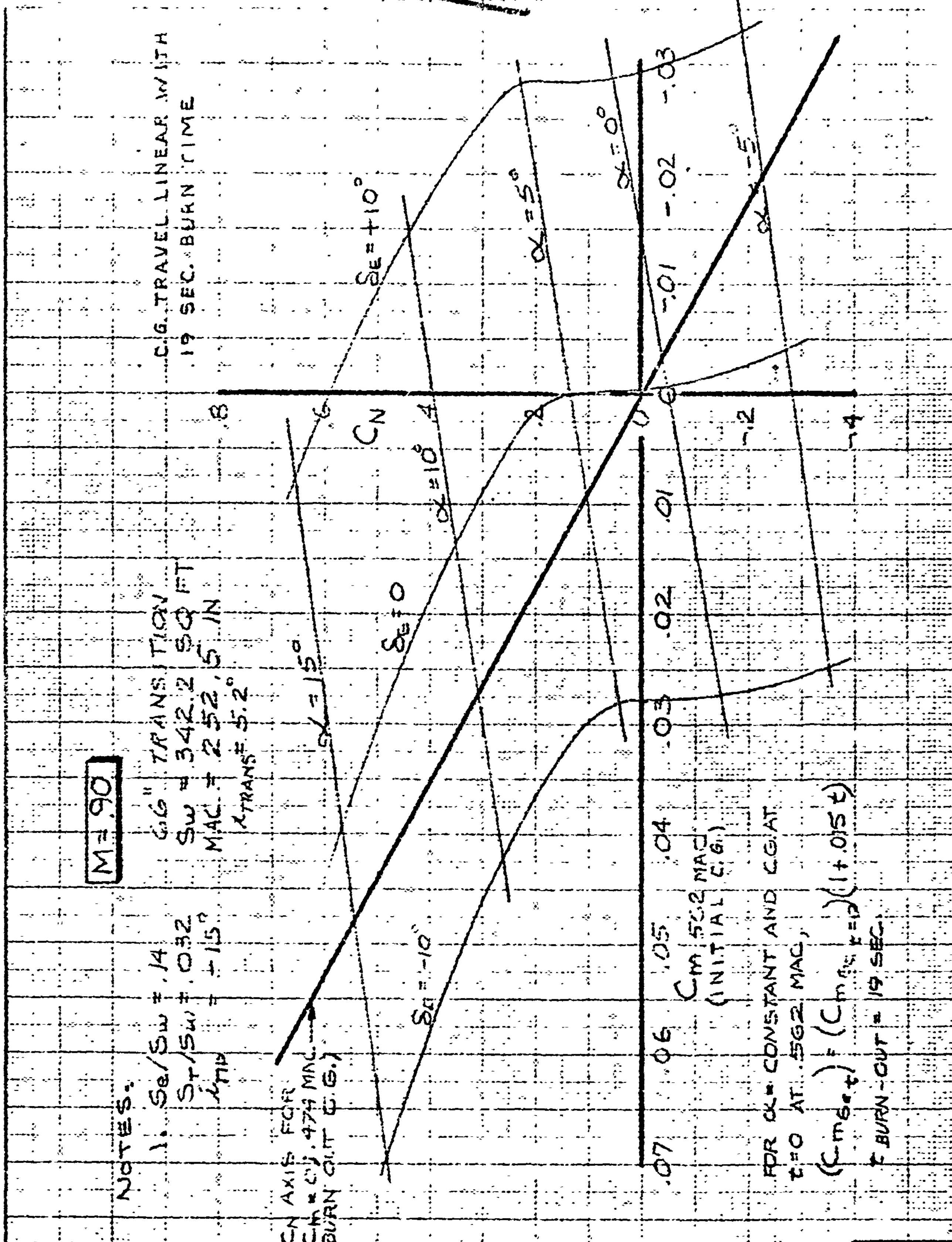


FIG. 7.3

| | | |
|---|---|---|
| CALC DEP 12-2-... | REVISED DATE | LONGITUDINAL STABILITY 844-2035 |
| CHECK | | TIPS EXTENDED - 66" TRANSITION D2-6174 |
| APR | | |
| APR | | BOEING AIRPLANE COMPANY M=.90 PAGE 7.7 |

BAC 4... C R4

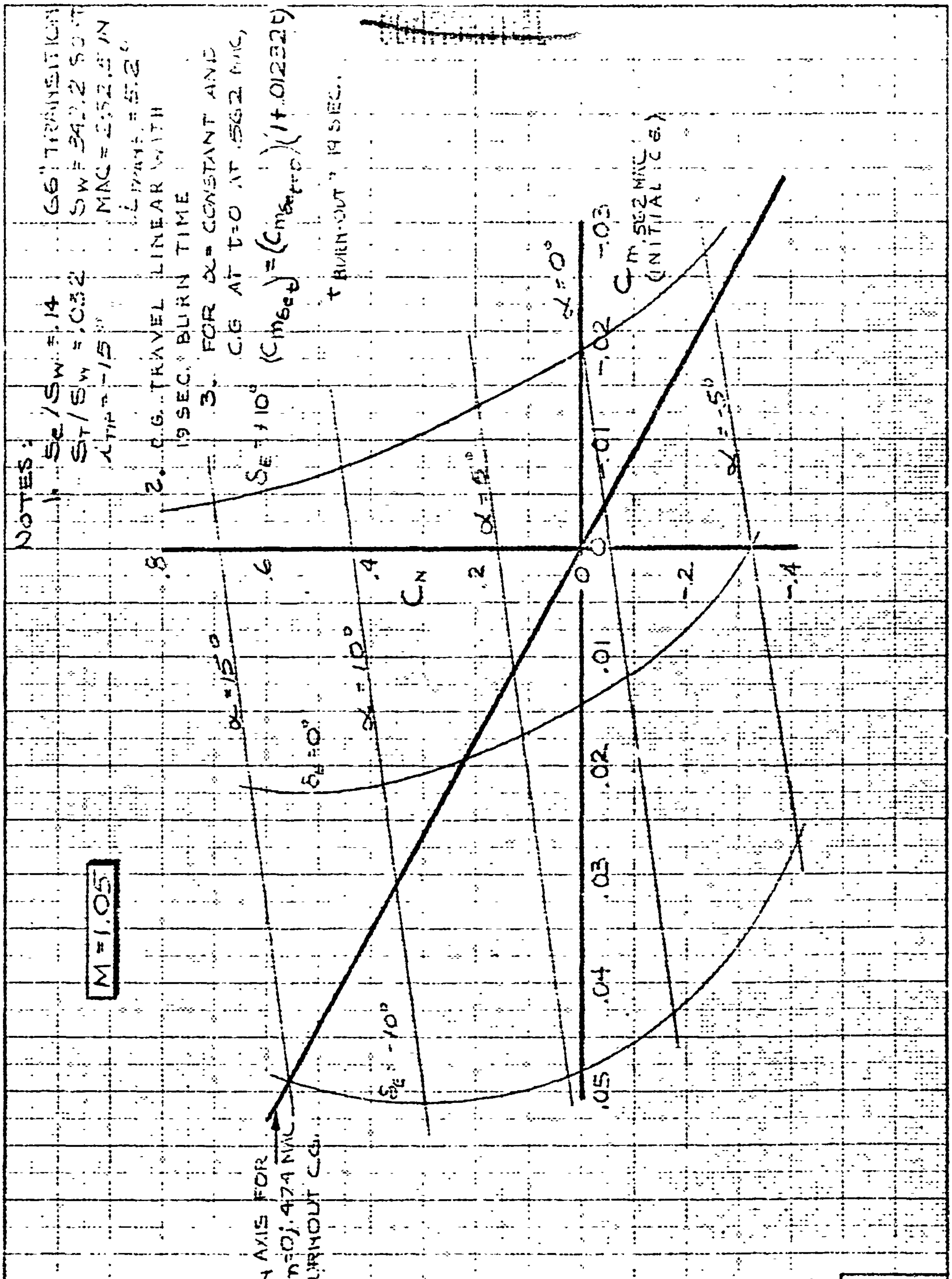


FIG 7.4

| | | | | |
|---|---|---|---|---|
| CALC DEP | | REVISED | DATE | LONGITUDINAL STABILITY — 844-2035 |
| CHECK | | | | TIPS EXTENDED - 66' TRANSITION — D2-3174 |
| APR | | | | |
| APR | | | | BOEING AIRPLANE COMPANY M=1.05 — PAGE 7.8 |

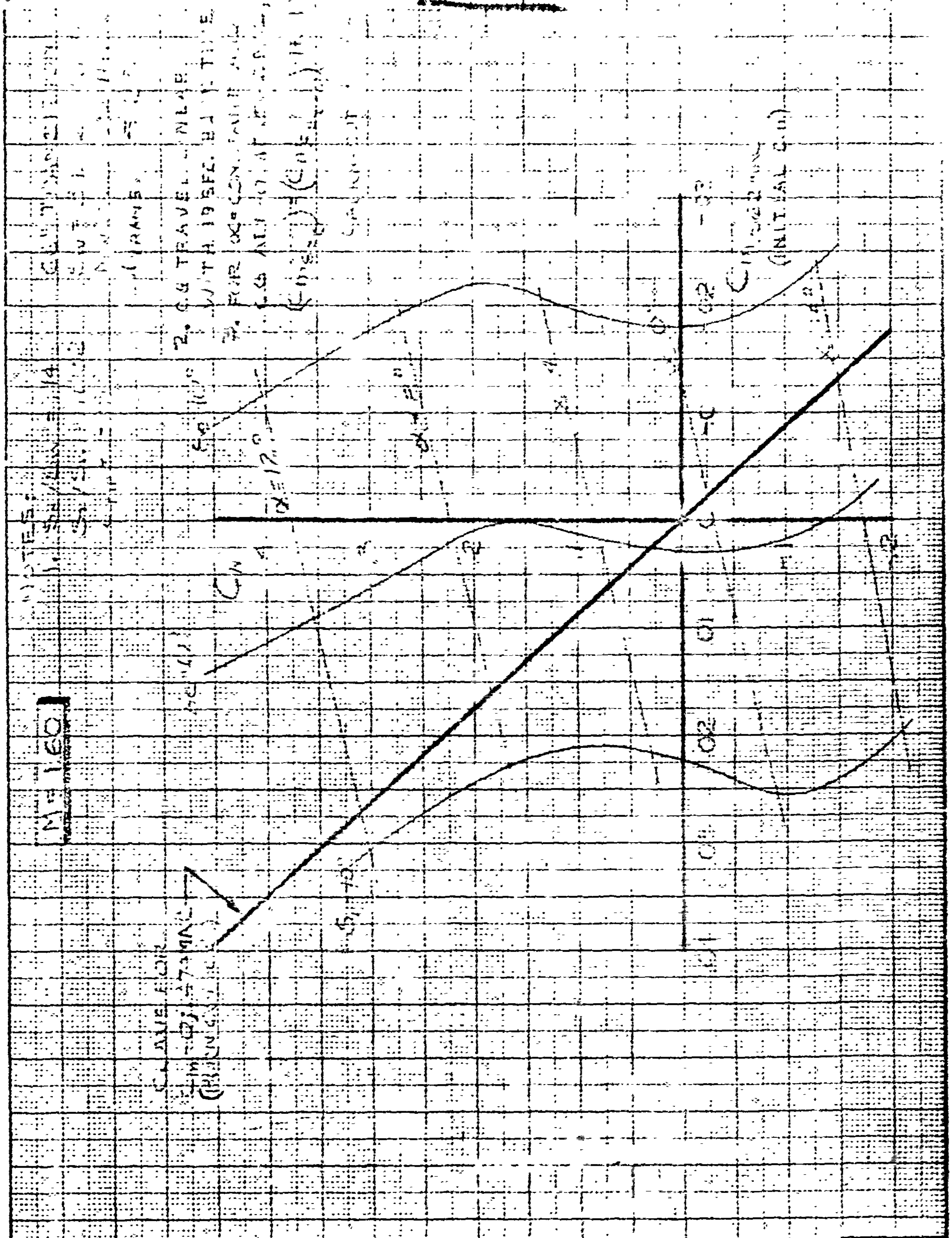


FIG 7.5

| CALC | | | REVISED | DATE |
|---|---|---|---|---|
| CHECK | | | | |
| APR | | | | |
| APR | | | | |

LONGITUDINAL STABILITY

TIP EXTENDED

BOEING AIRPLANE COMPANY

M=1.60

D2-8174

PAGE 7.9

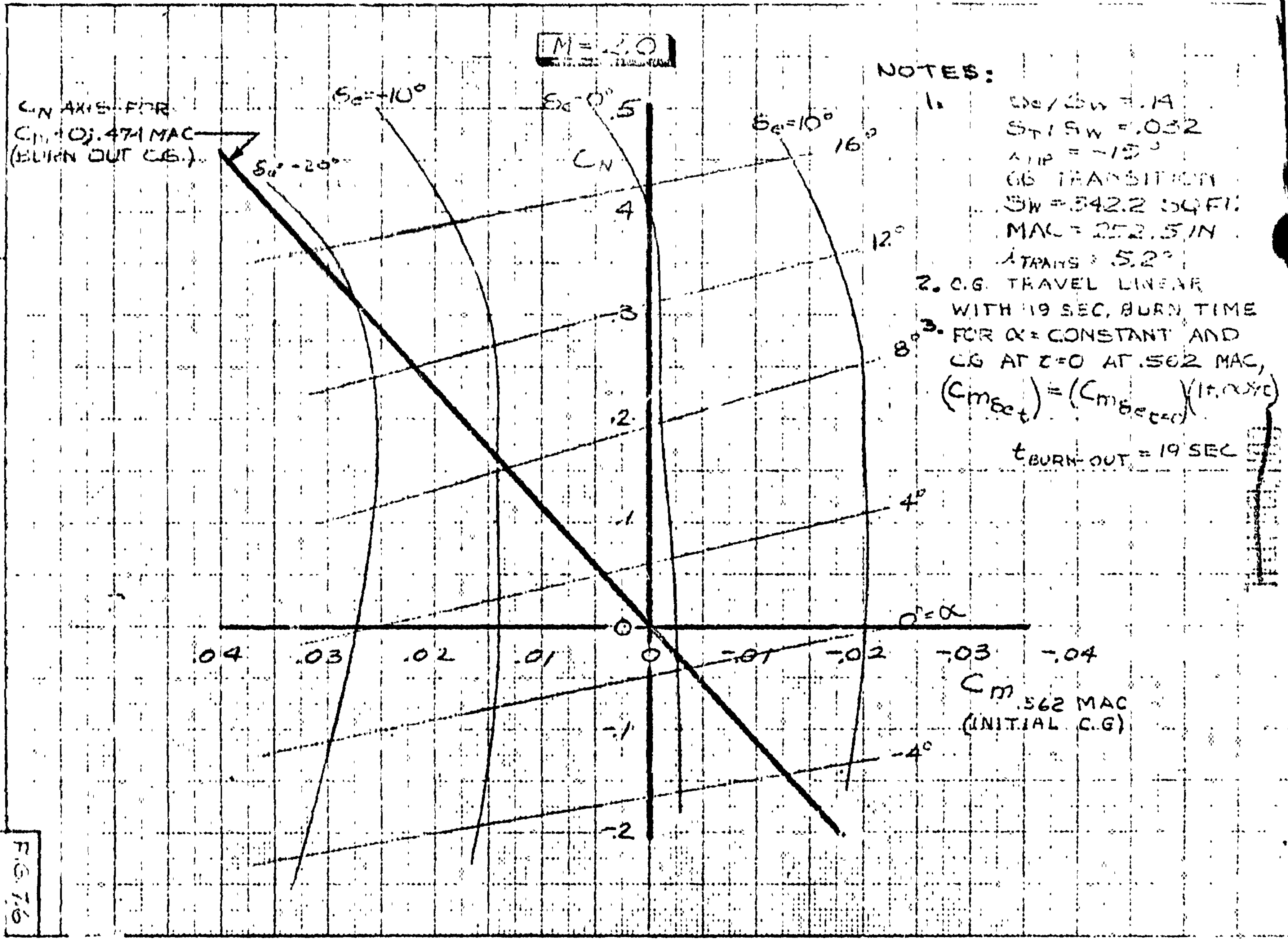


FIG. 7.6

LONGITUDINAL STABILITY

TIPS EXTENDED · 66 TRANSIT...

BOEING AIRPLANE COMPANY M=2.20

344-2035

D2-3174

7.6

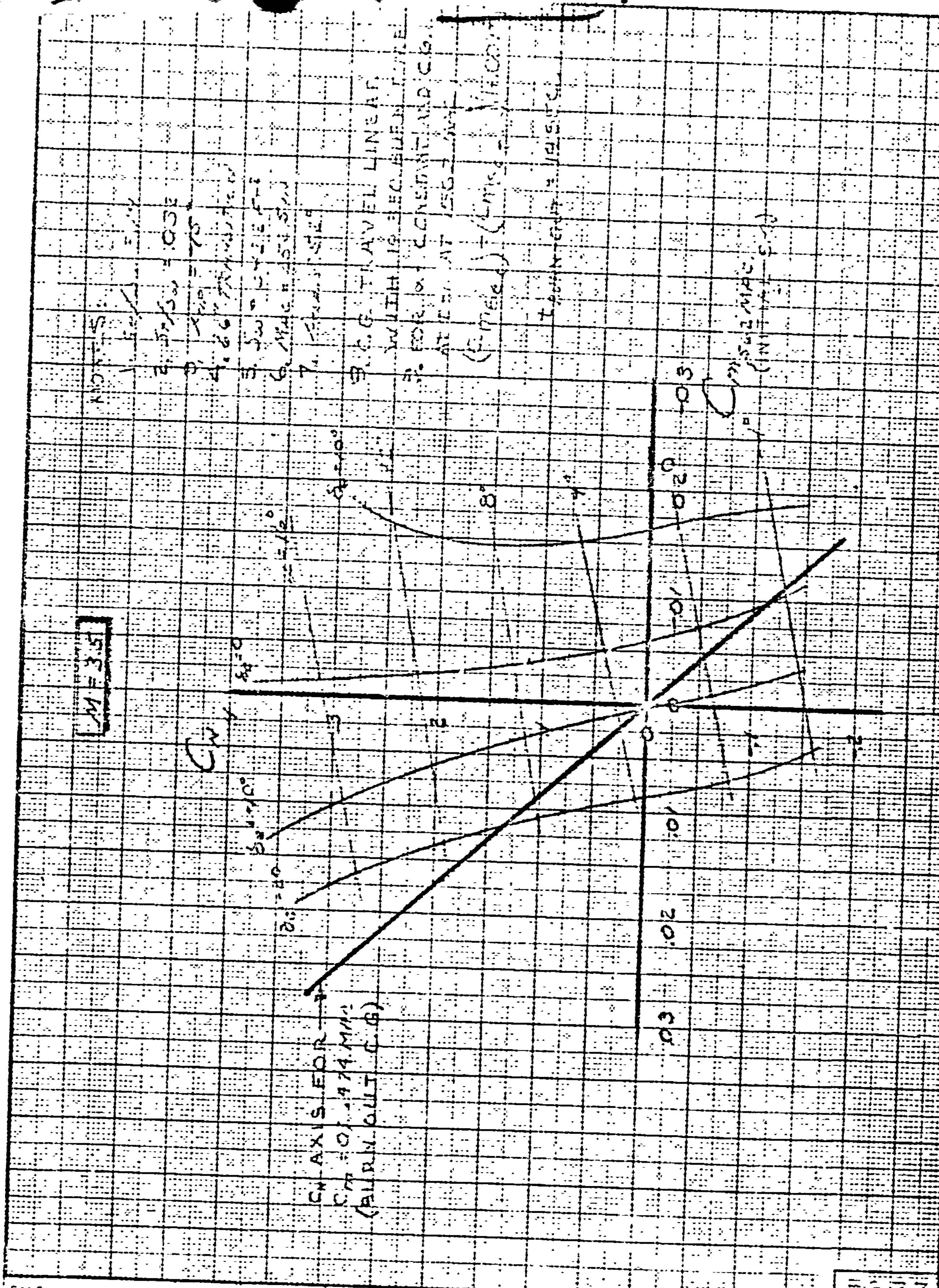


FIG 7.7

| | | | |
|---|---|---|---|
| CALC W.S.C. 10-22-60 | REVISED | DATE | |
| CHECK | | | |
| APR | | | |
| APR | | | |

LONGITUDINAL STABILITY

TIPS EXTENDED – 66" TRANSITION

BOEING AIRPLANE COMPANY M = 3.5

844-2035

D2-8174

PAGE 7.11

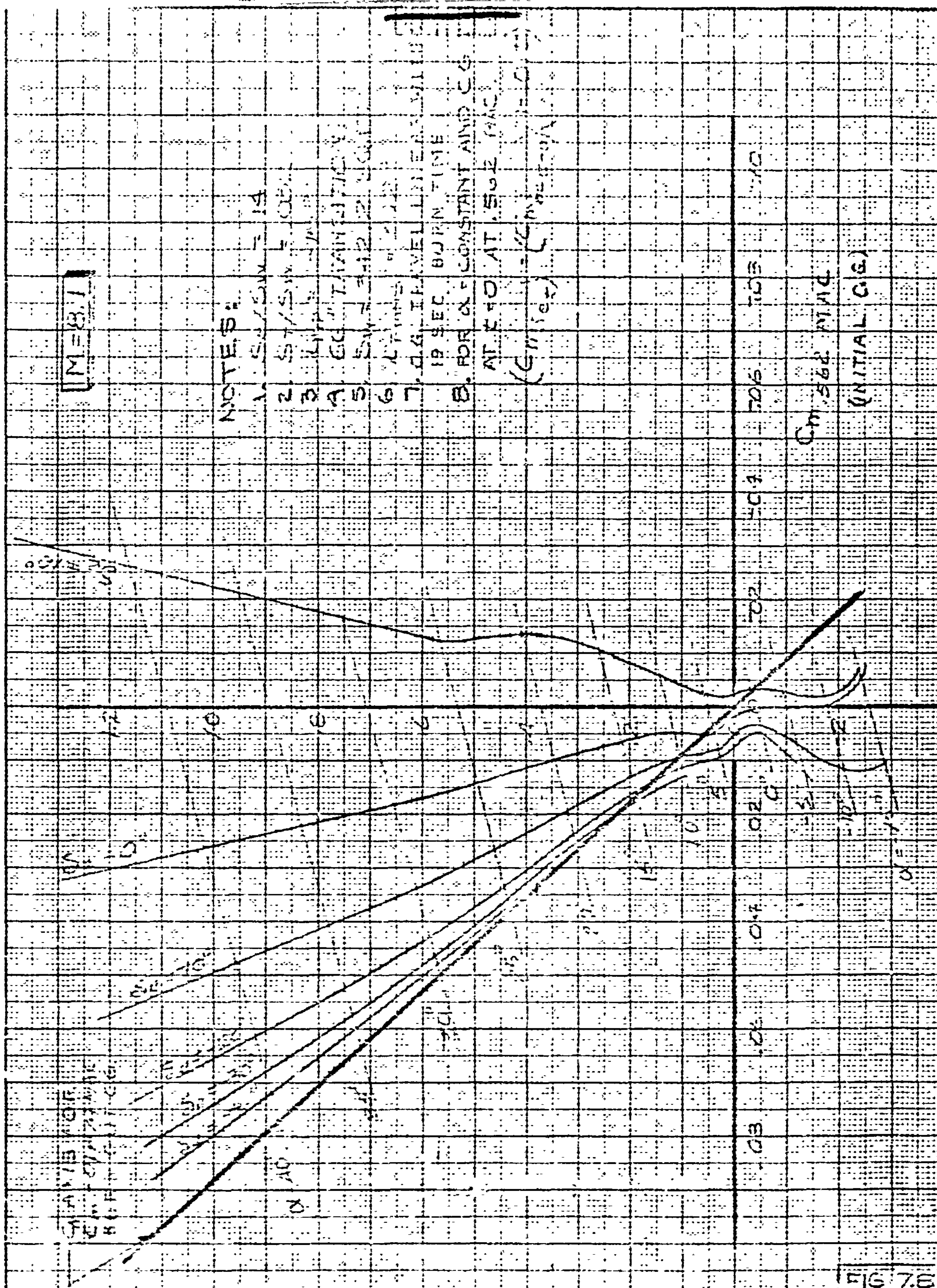


FIG 7.6

| CALC | KLA | 12-21-6? | REVISED | DATE | LONGITUDINAL STABILITY | 644-2035 |
|---|---|---|---|---|---|---|
| CHECK | | | | | TIPS RETRACTED-CG TRANSITION | D2-6174 |
| APR | | | | | | |
| APR | | | | | BOEING AIRPLANE COMPANY $M = 3.1$ | PAGE 7.12 |

NOTES:

1. C.G. TRAVEL LINEAR WITH 19 SEC. BURN TIME
2. $\Lambda_{TIPS} = -15°$ — EK' TRANSITION — $S_w = 343\ FT^2$
   $\Gamma_{TIPS} = .052$ — $\angle_{TRANS} = -5.2°$ — $b = 19.7\ FT$

## BODY AXIS

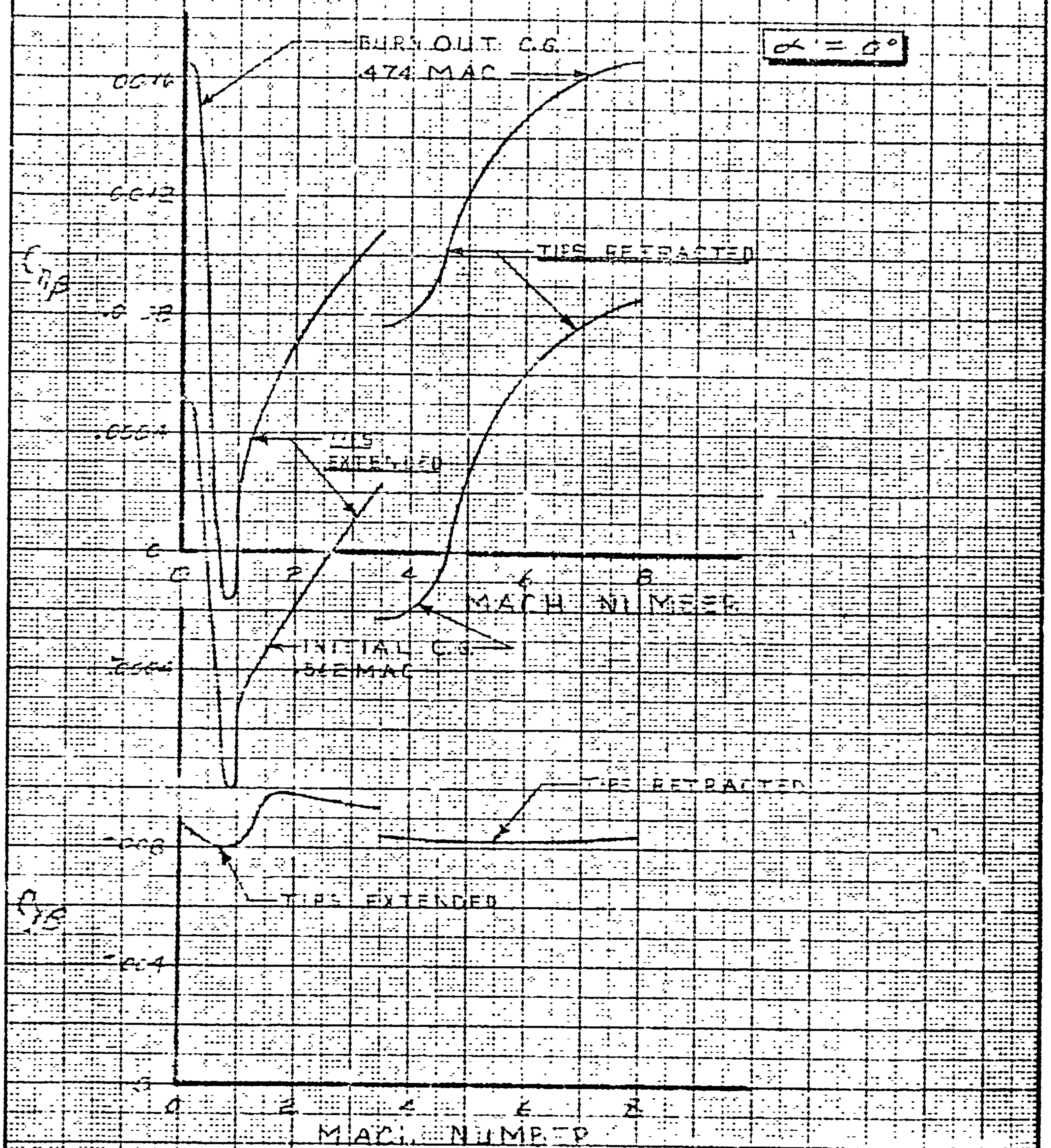


FIG 7

| CALC | K.R.W. | 5-31-0 | REVISED | DATE |
|---|---|---|---|---|
| CHECK | | | | |
| APR | | | | |
| APR | | | | |

DIRECTIONAL STABILITY — $\alpha = 0°$ — **190**

BOEING AIRPLANE COMPANY

D4-2035

D2-8174

PAGE 7.13

NOTES:

1. CG TRAVEL LINEAR WITH 19 SEC BURN TIME
2. $i_{T/R} = -15°$ 66" TRANSITION $S_w = 343\ FT^2$
   $S_{T_S}/S_W = .032$ $i_{TRANS} = 5.2°$ $D = 13.7\ FT$

BODY AXIS

$\alpha = 15°$

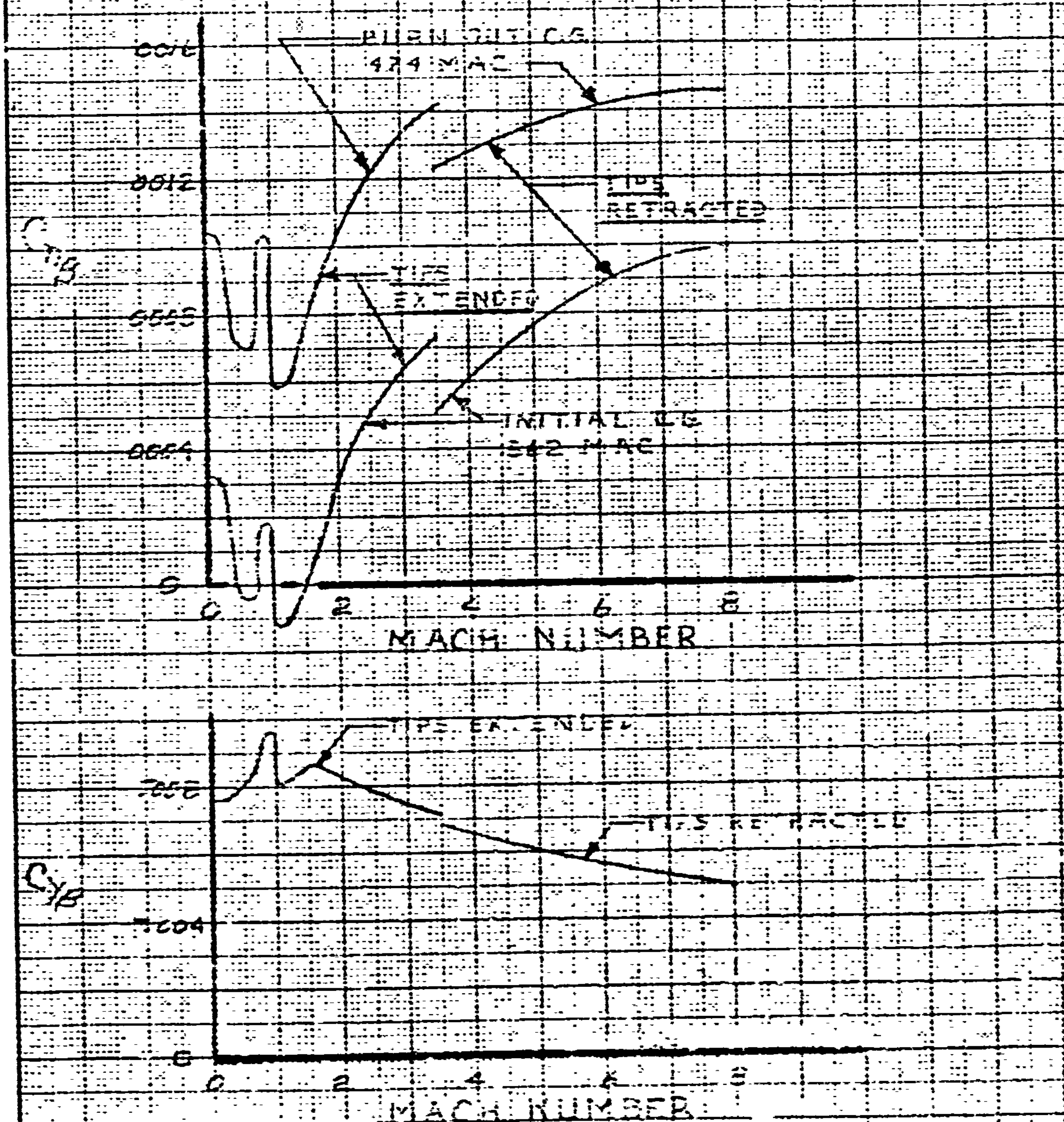


FIG 7.C

| | | | | | |
|---|---|---|---|---|---|
| CALC | KAH | 12-30-? | REVISED | DATE | DIRECTIONAL STABILITY |
| CHECK | | | | | $\alpha = 15°$ 191 |
| APR | | | | | BOEING AIRPLANE COMPANY |
| APR | | | | | |

244-2035

D2-8174

PAGE 714

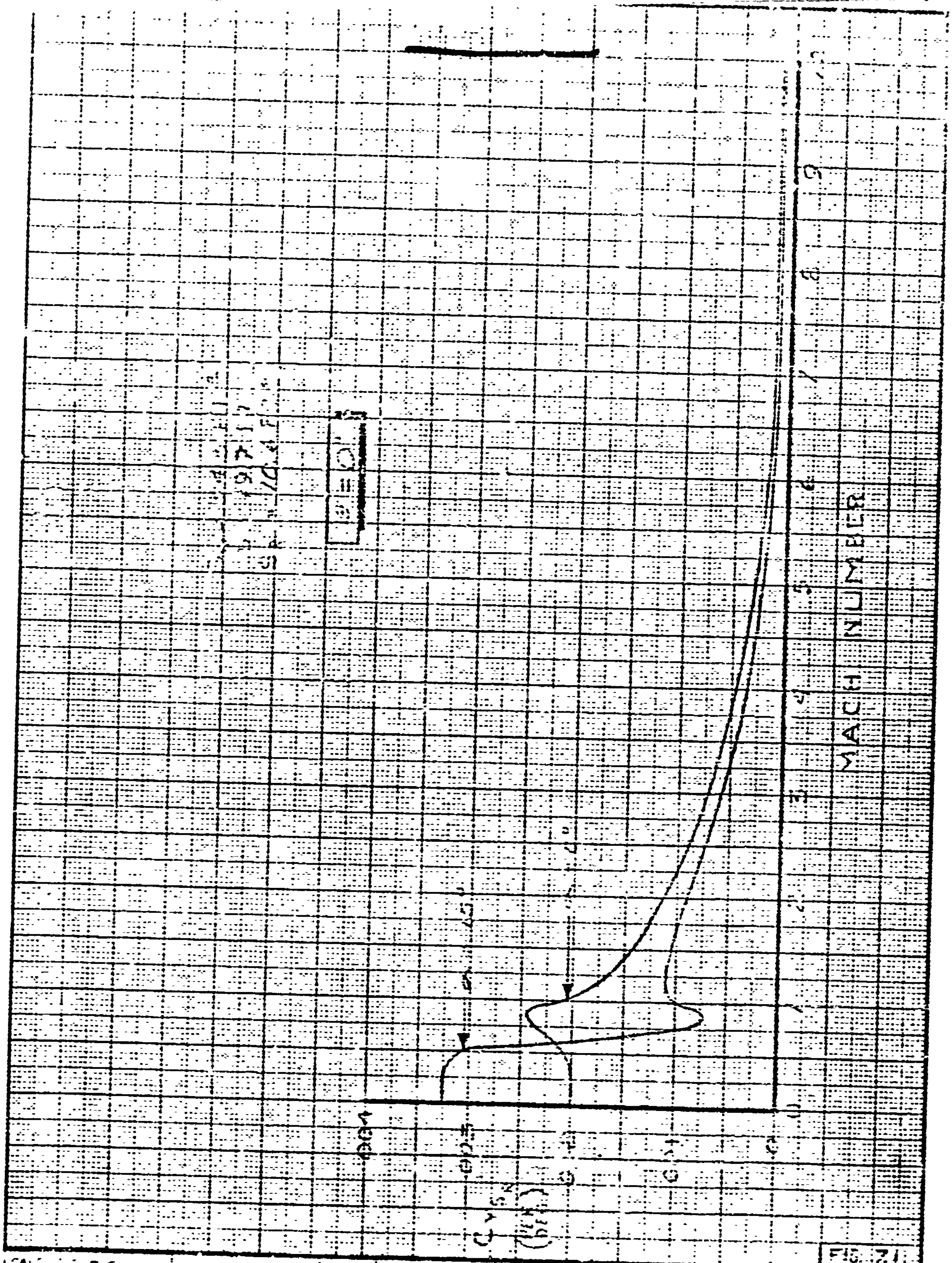


| CALC | | | REVISED | DATE |
|---|---|---|---|---|
| CHECK | | | | |
| APR | | | | |
| APR | | | | |

FIG. 7.1

# RUDDER EFFECTIVENESS

**192**

244-2035

D2-8174

BOEING AIRPLANE COMPANY

PAGE 7.15

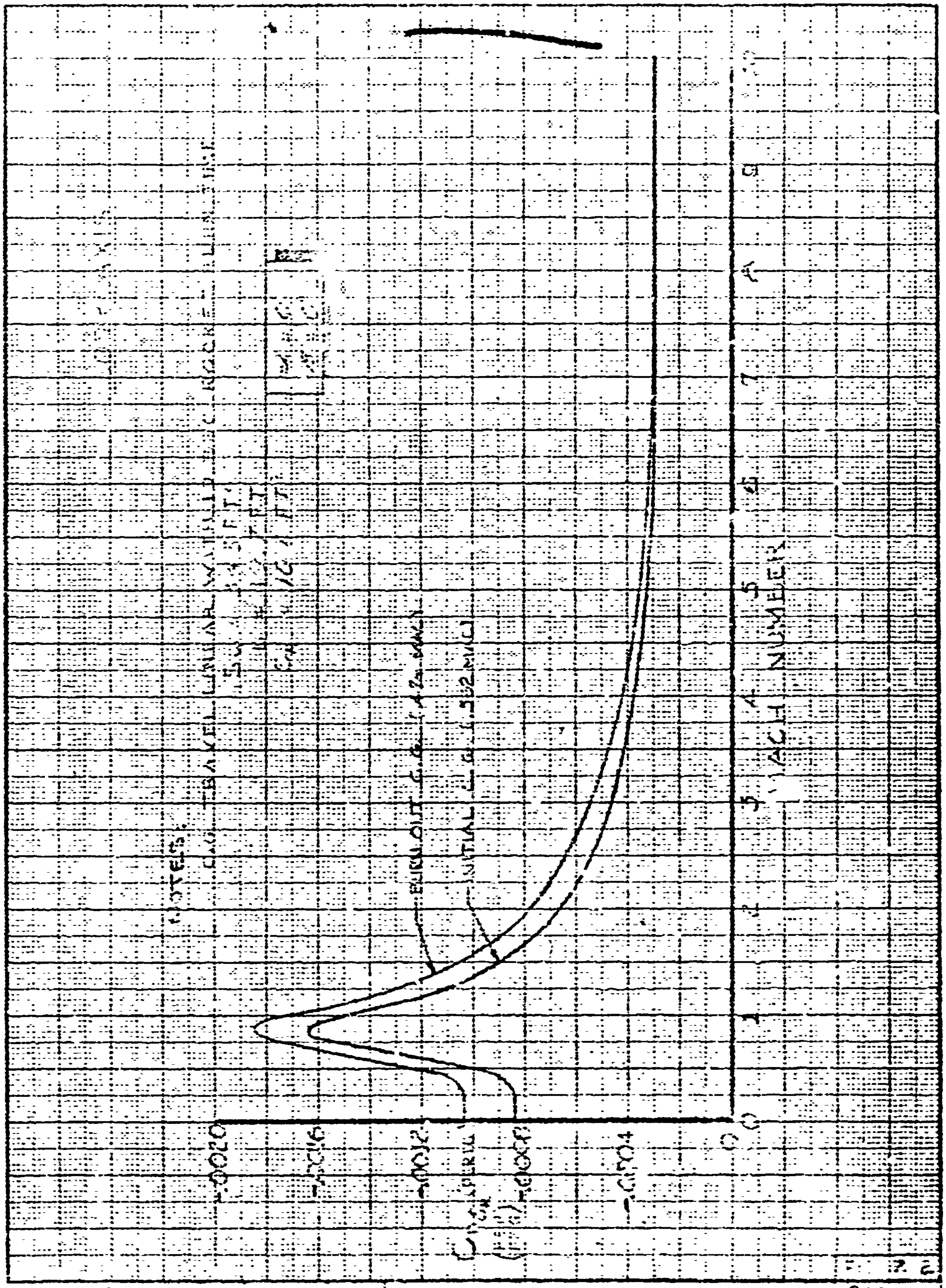


FIG. 7.2

| CALC | DEP | 12-23-? | REVISED | DATE |
|---|---|---|---|---|
| CHECK | | | | |
| APR | | | | |
| APR | | | | |

**RUDDER EFFECTIVENESS**

$\alpha = 0°$

193

844-2035

D2-8174

BOEING AIRPLANE COMPANY

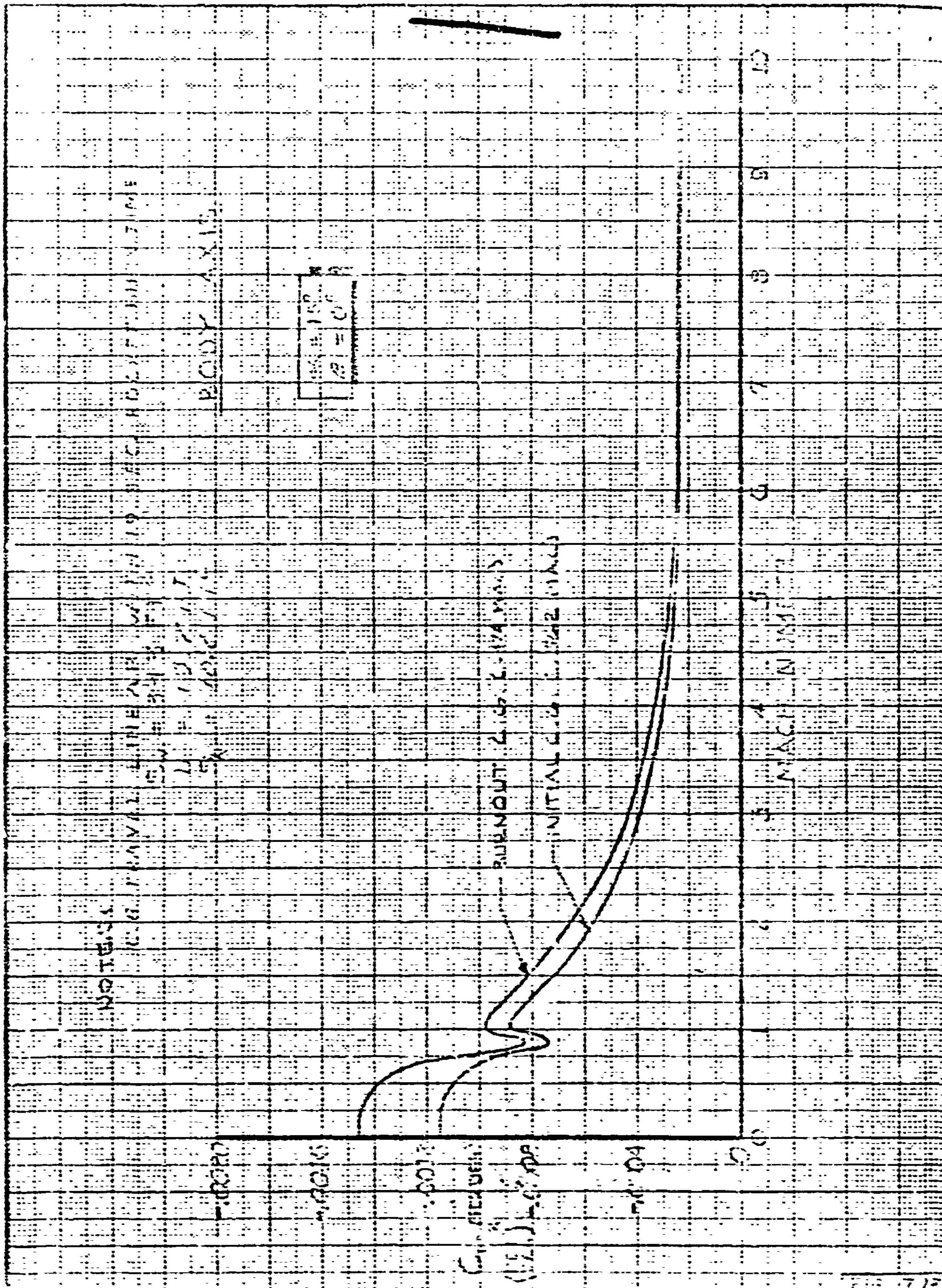


CALC
CHECK
APR
APR
REVISED
DATE

# RUDDER EFFECTIVENESS

$\alpha = 15°$

BOEING AIRPLANE COMPANY

D2-8174

PAGE 7.17